

# **Donor–Acceptor Stabilization of Compounds with Low Coordinate Group 13 and 14 Elements**

by  
**Sanjukta Pahar**

**10CC16A26009**

A thesis submitted to the  
Academy of Scientific & Innovative Research  
for the award of the degree of  
DOCTOR OF PHILOSOPHY  
in  
SCIENCE

Under the supervision of  
**Dr. Sakya Singha Sen**



**CSIR-National Chemical Laboratory, Pune**

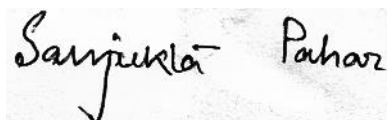


Academy of Scientific and Innovative Research  
AcSIR Headquarters, CSIR-HRDC campus  
Sector 19, Kamla Nehru Nagar,  
Ghaziabad, U.P. – 201 002, India

**January - 2022**

## Certificate

This is to certify that the work incorporated in this Ph.D. thesis entitled, “*Donor–Acceptor Stabilization of Compounds with Low Coordinate Group 13 and 14 Elements*” submitted by *Sanjukta Pahar* to the Academy of Scientific and Innovative Research (AcSIR) in fulfillment of the requirements for the award of the Degree of *the Doctor of Philosophy in Science*, embodies original research work carried out by the student. We, further certify that this work has not been submitted to any other University or Institution in part or full for the award of any degree or diploma. Research material(s) obtained from other source(s) and used in this research work has/have been duly acknowledged in the thesis. Image(s), illustration(s), figure(s), table(s) etc., used in the thesis from other source(s), have also been duly cited and acknowledged.



(Signature of Student)

Sanjukta Pahar

Date: 07-01-2022



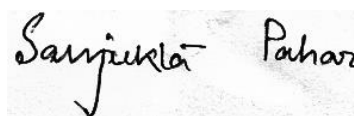
(Signature of Supervisor)

Dr. Sakya Singha Sen

Date: 07-01-2022

## STATEMENTS OF ACADEMIC INTEGRITY

I, Sanjukta Pahar, a Ph.D. student of the Academy of Scientific and Innovative Research (AcSIR) with Registration No. 10CC16A26009 hereby undertake that the thesis entitled “Donor–Acceptor Stabilization of Compounds with Low Coordinate Group 13 and 14 Elements” has been prepared by me and that the document reports original work carried out by me and is free of any plagiarism in compliance with the UGC Regulations on “*Promotion of Academic Integrity and Prevention of Plagiarism in Higher Educational Institutions (2018)*” and the CSIR Guidelines for “*Ethics in Research and in Governance (2020)*”.



**Signature of the Student**

Date: 07-01-2022

Place: Pune

---

It is hereby certified that the work done by the student, under my/our supervision, is plagiarism-free in accordance with the UGC Regulations on “*Promotion of Academic Integrity and Prevention of Plagiarism in Higher Educational Institutions (2018)*” and the CSIR Guidelines for “*Ethics in Research and in Governance (2020)*”.

NA

**Signature of the Co-supervisor (if any)**

Name:

Date:

Place:



**Signature of the Supervisor**

Name: Dr. Sakya Singha Sen

Date: 07-01-2022

Place: Pune

*This dissertation is dedicated to*  
*All my family members*

## Acknowledgement

*Ph.D. is a long journey; a unique and endeavor experience that takes you through the untraversed path, to overcome the final goal fixed in mind. Success in this journey is extensive and grueling, and it certainly would not have been possible without close association with many people. I am taking this opportunity to express my deepest gratitude to each and everyone who has helped and supported me throughout the course of my research journey both professionally and on a personal level. However, mentioning is not sufficient to thank them in the right way.*

*Much of my success in the PhD program would not have been made possible without the constant assistance, inspiring guidance, and tremendous support of **Dr. Sakya Singha Sen**. First of all, thank you for welcoming me into your research group under less typical circumstances. Secondly, thank you for the intellectual and moral support I received during the early stages of my carrier development. He has had the patience to allow me my space but the precognition to press me when necessary. His encouragement and confidence in me took me new hope, made me realize that doing Ph.D. is an exciting journey. I feel extremely privileged for the freedom rendered by him in the laboratory to fulfill my dream with proper planning and the final implementation. He has trained me a lot, not only in the research field but also about living a beautiful life which I never expected from a supervisor. I could never wish for a better supervisor, nor a truer friend, I'll miss our long conversation at our group party more than anything. And I will always remain a prodigious fan of his coolness, style, and excellent communication skills. Lastly, thank you for always being accommodating to my personal circumstances and professional needs.*

*I want to convey my sincere thanks to my Doctoral Advisory Committee members, **Dr. Benudhar Punji**, **Dr. T. Raja**, and **Dr. Mahesh Dharne** for their valuable suggestions and encouragement during my Ph.D. journey which helped me a lot to widen my research from various perspectives.*

*I am grateful to **Prof. Ashish Lele** (Director, CSIR-NCL), and **Prof. A. K. Nangia** (Former Director, CSIR-NCL), **Dr. D. Srinivas** (Former Head, Catalysis and Inorganic Chemistry Division), **Dr. C. S. Gopinath** (Former Head, Catalysis and Inorganic Chemistry Division), and **Dr. Shubhangi Umbarkar** (Head, Catalysis and Inorganic Chemistry Division), for*

giving me this opportunity and providing all necessary infrastructure and facilities to carry out my research work. I would like to acknowledge all the support from office staff of Catalysis and Inorganic Chemistry Division. I am also highly thankful to **DST-INSPIRE** for the financial assistance.

My sincere thanks to **Dr. Amitava Das, Dr. Sayam Sen Gupta, Dr. Rahul Banerjee, Dr. Sayan Bagchi, Dr. Samir Chikkali, Dr. E Balaraman, Dr. C. V. Ramana, Dr. B. L. V. Prasad, Dr. Paresh Dhepe, Dr. Santosh Babu, Dr. Pradip Maity, Dr. Utpal Das, Dr. Arup Kumar Rath, Dr. Janardan Kundu, Mrs. Kohle, Mr. Iyer, Mr. Purushothaman, Library staff, Student academic office staff, and all other scientists of NCL** for their motivation, constant encouragement, and support.

Additionally, I extend my thanks to our collaborators **Dr. Kumar Vanka** and his doctoral students **Dr. Tamal Da** and **Vipin** for their valuable suggestions and kind cooperation in theoretical calculations. My sincere thanks to **Dr. Rajesh Gonnade** and his group members **Dr. Ekta, Dr. Samir, Dr. Shridhar, Dr. Veer, Christy, Tabrez, Debjani and Bhupender**, for single-crystal X-ray diffraction measurements. **Mrs. Shantakumari** and her students for the help in HRMS analysis, and **Mrs. Ansanas** for elemental analysis. I would also like to thank **Dr. Sapna Ravindranathan, Dr. Udaya Kiran Mareli, and Dr. T. G. Ajithkumar** and their team **Dinesh, Satish, Meenakshi, Deepali**, for NMR facilities.

I want to express great appreciation to **Dr. D. S. Reddy** and his doctoral students **Dr. Satish sir, Dr. Santu Da, Dr. Paresh sir, Dr. Rahul sir, Dr. Gorakh Sir, Dr. Pronay, Akshay, Rahul, Suhag, Yash, Monika, Datta and Vishal** for their kind help and support.

I am highly grateful to **Dr. Shabana Khan and her research group** from IISER-Pune for their kind help at the different fragments of my research journey.

I am very much fortunate to work and spent most of my daytime with a fantastic and enthusiastic young research group of colleagues in the Sen Lab. It has been a great learning experience for me through our group seminars. It is my pleasure to thank all my past and present lab mates **Dr. Sandeep, Dr. Swamy, Dr. Milan, Gargi, Rohit, Kritika, Ajith, Vishal, Biplab, kajal, Dr. Moumita Di and Dr. Yuvaraj anna** for devoting their precious time, helping me with many valuable suggestions.

*Beyond the group, many well-wishers from CSIR-NCL made my journey more comfortable. I am thankful to **Dr. Debu da, Dr. Ashish, Dr. Rangrajan, Dr. Reddy, Dr. Anupam Da, Neha, Chandan, Dr. Abhijit Da, Dr. Koushik da, Dr. Jaganath Da, Dr. Siba Da, Dr. Vinod, Dr. Manoj, Dr. Garima, Dr. Tapas da, Dr. Deborin Da, Dr. Sushil, Samadhan, Srijan, Manish, Prem, Bharath, Pawan, Dharmendra, Viksit, Dr. Abdul, Nirsad, Ashish Da Naru, Shinjini, Rashmi, Dr. Meena, Moumita, Shibam, Rohit Sr., Kailash Pandhare, Sumanta, Govind, Chandu, Sonia, Dr. Manjur, Dr. Indra, Dr. Aslam sir, Dr. Rahul Jagtap, Dr. Satej Sir, Dr. Monalisa di, Dr. Arunava Da, Dr. Hridesh Da, Dr. Firoj Da, Sadhna, Dr. Shailaja, Subhrashis da, Dr. Subrata Da, Dr. Santi Da, Dr. Anup Da, Dr. Saikat Da, Dr. Chini Da, Dr. Pravat Da, Dr. Arijit Da, Dr. Arjun Da, Dr. Saibal Da, Dr. Mahitosh Da, Dr. Basudeb, Dr. Munmun Di, Dr. Bittu Da, Dr. Krishanu Da, Dr. Kheria Da, Dr. sujit Da, Dr. Shantanu Da, Dr. Atanu Da, Dr. Atreyee Di, Dr. Chayanika Di, Dr. Rupa, Dr. Piyali, Dr. Sutanu, Dr. Saikat Da, Dr. Shilpi Di, Dr. Ketan Bjaiya, Sushmita, Neha, Lavanya, Priya, Priyanka Walko, Priyanka Halder, Vinita, Mahesh Pol, Pinka, Singham, Vikash Chaturvedi, Ravi Ranjan, Himanshu, Akash, Dr. Neeta, Dr. Ravindar Phatke, Ruchi, Subhra Di, Priyanka Kataria, Suman devi, Dr. Ayesha, Dr. Vinita, Himadri, Koushik, Dr. Tamal, Rashid, Anirban, Sujata, Dr. Mahendar Power** from NCL for their kind help and support.*

*Personally, I am immensely thankful to all my teachers from my nursery grade level. No words are sufficient to acknowledge my prized friends out of NCL who have helped me at various stages of my work in NCL. I would like to extend my special thanks to all of my close friends **Brinta, Dr. Sutirtha, Sanchita, Akash, Saptam and Bani** for their kind support and love.*

*I am very much grateful to **Dr. Rebecca Melen** at Cardiff University and her research group for helping and supporting me to complete my dream internship project within a very short period of time with successful outcomes in a hard-hitting pandemic (Covid-2020) time.*

*My family is always a source of inspiration and great moral support for me in pursuing my educational journey. I owe a lot to my beloved parents and my uncles who encouraged and helped me at every stage of my personal and academic life and longed to see this achievement come true. My sincere thanks to my beloved family members, my grandma **Late Monorama Pahar (thamma)**, my father **Subrata Pahar (my Bapi)**, mother **Sova Pahar (Maa)**, my uncles **Somenath Pahar (Mej Ka)**, **Krishnandu Pahar (Chot)**, my aunties **Mithu Pahar, Tapasi Pahar**, my one and only brother **Dwaipayan Pahar (My babu)**, my sisters **Swastika Pahar***

*(Didi), Swagata Biswas (Puu darling), Jagrata Pahar, Sushreeta Baine, Namrata Biswas (Mistu), my brother-in-law Tuhin Chattopadhyay, for their endless love, support, and sacrifice. I am very much indebted to my whole family who supported me in every possible way to see the completion of this research work. I must thank my would-be better half **Mr. Abhishek Das**, with whom I am going to tie up my life, for supporting and encouraging me all the possible way for the last few months to finish up my long-awaited journey. I express my gratitude to all the family members of **'Das Family'** for understanding and supporting me. I owe to thank my best friend, critic, best gossip partner and scientific partner **Dr. Suvendu Karak** for his inspiration, understanding, support, love and for being with me in all the good and bad times of my Ph.D. His constant support and encouragement boosted up my confidence and made this possible.*

*I wish to thank the great scientific community whose achievements are a constant source of inspiration for me. Above all, I extend my gratitude's to the Almighty God for giving me the wisdom, health, and strength to undertake this research work and enabling me to its completion.*

*... Sanjukta*



## CONTENT OF THE THESIS

<b>Content</b>	<b>Page No.</b>
Abbreviations	i
General remarks	iv
Synopsis	v

### Chapter 1:

<b>Introduction</b>	<b>1-23</b>
1.1 General Introduction`	<b>2</b>
1.2 Stabilization of Heavier Low-valent Group 13 and 14 Compounds	<b>2</b>
1.3 Low-coordinate Group 13 and 14 compounds	<b>4</b>
1.4 Donor-acceptor concept	<b>5</b>
1.4.1 Donor-Acceptor Stabilization of Group 13 Complexes	<b>6</b>
1.4.2 Donor-Acceptor Stabilization of Heavier Group 14 Elements	<b>8</b>
1.5 Main group compounds as an alternative to the Transition metal-complex	<b>11</b>
1.5.1 Main group compounds in homogeneous catalysis	<b>12</b>
1.5.1.1 Hydroboration of carbonyl compounds and unsaturated C=C bonds	<b>13</b>
1.6 Aim and outline of the thesis	<b>15</b>
1.7 References	<b>17</b>

### Chapter 2:

<b>Access to Silicon(II)- and Germanium(II)-Indium Compounds</b>	<b>24-42</b>
2.1. Introduction	<b>25</b>
2.2. Results and discussion	<b>26</b>
2.2.1. Synthesis and characterization of complexes 2.1 and 2.2	<b>26</b>
2.2.2. Structural Elucidation of complex 2.1 and 2.2	<b>27</b>
2.2.3. Synthesis and characterization of complex 2.3 and 2.4	<b>29</b>

2.2.4. Structural Elucidation of complex 2.3 and 2.4	30
2.2.5. Theoretical Studies	32
2.3. Conclusions	36
2.4. References	37

**Chapter 3:**

<b>Access to Group 13 and 14 Compounds using Picolyl Functionalized <math>\beta</math>-diketiminato Ligand</b>	<b>43-61</b>
3.1: Introduction	44
3.2: Results and Discussions	45
3.2.1: Synthesis, characterization and structural elucidation of chlorogermylene (3.1)	45
3.2.2: Theoretical illumination of chlorogermylene (3.1)	46
3.2.3: Unsuccessful attempts to prepare germylium ylidene and germanium (II) hydrides	47
3.2.4: Synthesis, characterization and structural elucidation of PyPyr ligand supported chlorogermylene (3.2) and adduct (3.3)	48
3.2.5: Theoretical illumination of PyPyr ligand supported chlorogermylene (3.2)	50
3.2.6: Synthesis, characterization and structural elucidation of chlorostannylene (3.4) and analogous aluminium chloride compound (3.5)	52
3.2.7: Synthesis, characterization and structural elucidation of tin cation (3.6) with the reaction of SnCl <sub>2</sub> and 3.4	53
3.2.8: Synthesis, characterization and structural elucidation of analogous six membered alane compound (3.7)	55
3.2.9: Theoretical illumination of six membered dialane (3.7)	56
3.2.10: Synthesis, characterization and structural elucidation of methylpyridinato ligand supported dichlorosilane (3.8)	57
3.3: Conclusions	58
3.4: References	59

**Chapter 4:**

<b>Transmetallation involving Stannylene and First Row Transition Metals</b>	<b>62-72</b>
4.1: Introduction	<b>63</b>
4.2: Results and discussions	<b>64</b>
4.2.1: Synthesis, characterization and structural elucidation of nickel-chloride (4.1) and copper-chloride complex (4.2)	<b>64</b>
4.2.2: Synthesis, characterization and structural elucidation of monomeric nickel-hydride (4.3)	<b>67</b>
4.2.3: Synthesis, characterization and structural elucidation of cationic nickel complex (4.4)	<b>68</b>
4.3: Conclusions	<b>70</b>
4.4: References	<b>70</b>

**Chapter 5:**

<b>Pyridylpyrrolido Ligand Supported Germylene and Stannylene Chemistry</b>	<b>73-93</b>
5.1: Introduction	<b>74</b>
5.2: Results and Discussions	<b>75</b>
5.2.1: Synthesis, characterization and structural elucidation of compound 5.1 and 5.2	<b>76</b>
5.2.2: Alternative synthetic pathway to produce highly pure compound 5.1 in quantitative yield	<b>78</b>
5.2.3: Synthesis, characterization and structural elucidation of compound 5.3	<b>79</b>
5.2.4: Synthesis, characterization and structural elucidation of compound 5.4 and 5.5	<b>80</b>
5.2.5: Synthesis, characterization and structural elucidation of compound 5.6	<b>82</b>
5.2.6: Catalytic hydroboration studies using 5.5 as catalyst	<b>83</b>
5.3: Conclusions	<b>89</b>
5.6: References	<b>89</b>

---

Appendix: Experimental details, crystallographic data and spectral details	<b>94-204</b>
Abstract	<b>205</b>
List of publication(s) in SCI Journal(s)	<b>206</b>
List of papers with abstract presented (oral/poster) at national/international conferences/seminars with complete details	<b>207</b>
About the author	<b>209</b>
Published papers	<b>211</b>

## Abbreviations

### Units and standard terms

BDE	Bond Dissociation Energy
°C	Degree Centigrade
DFT	Density Functional Theory
mg	Milligram
h	Hour
Hz	Hertz
mL	Millilitre
min.	Minute
mmol	Millimole
NPA	Natural Population Analysis
ppm	Parts per million
%	Percentage
Mp	Melting Point
Calcd.	Calculated
CCDC	Cambridge Crystallographic Data Centre
CIF	Crystallographic Information file

### Chemical Notations

---

---

Ar	Aryl
MeCN	Acetonitrile
CDCl <sub>3</sub>	Deuterated chloroform
C <sub>6</sub> D <sub>6</sub>	Deuterated benzene
DMSO-d <sub>6</sub>	Deuterated dimethyl sulfoxide
Toluene-d <sub>8</sub>	Deuterated toluene
DCM	Dichloromethane
DMSO	Dimethyl sulfoxide
EtOH	Ethanol
Me	Methyl
Et	Ethyl
Dipp	Di-isopropylaniline
<sup>i</sup> Pr	Isopropyl
<sup>t</sup> Bu	Tertiary butyl
EtOAc	Ethyl Acetate
HBpin	Pinacolborane
MeOH	Methanol
Py	Pyridine
THF	Tetrahydrofuran
Et <sub>2</sub> O	Di-ethyl ether
TMSCN	Trimethylsilyl cyanide

---

<sup>n</sup> BuLi	<sup>n</sup> butyllithium
NHC	N-Heterocyclic carbene
NHSi	N-Heterocyclic silylene
IPr	1,3-bis(2,6-diisopropylphenyl)imidazol-2-ylidene


#### Other Notations

$\delta$	Chemical shift
<i>J</i>	Coupling constant in NMR
Equiv.	Equivalents
HRMS	High Resolution Mass Spectrometry
NMR	Nuclear Magnetic Resonance
RT	Room temperature
UV	Ultraviolet
XRD	X-Ray Diffraction

## General remarks

- All chemicals were purchased from commercial sources and used as received.
- All reactions were carried out under inert atmosphere following standard procedures using Schlenk techniques and glovebox.
- The solvent used were purified by an MBRAUN solvent purification system MBS-800 and further dried over activated molecular sieves prior to use.
- Column chromatography was performed on silica gel (100-200 mesh size).
- The preparation of sensitive NMR samples was carried out in a Glove box or under an inert atmosphere of argon applying standard Schlenk technique.
- Deuterated solvents for NMR spectroscopic analyses were used as received. All  $^1\text{H}$ ,  $^{13}\text{C}$ ,  $^{11}\text{B}$ ,  $^{19}\text{F}$ ,  $^{29}\text{Si}$  and  $^{119}\text{Sn}$  NMR analysis were obtained using a Bruker or JEOL 200 MHz, 400 MHz or 500 MHz spectrometers. Coupling constants were measured in Hertz. All chemical shifts are quoted in ppm, relative to TMS, using the residual solvent peak as a reference standard.
- HRMS spectra were recorded at UHPLC-MS (Q-exactive-Orbitrap Mass Spectrometer) using electron spray ionization [(ESI<sup>+</sup>, +/- 5kV), solvent medium: acetonitrile and methanol] technique and mass values are expressed as  $m/z$ . GC-HRMS (EI) was recorded in Agilent 7200 Accurate-mass-Q-TOF.
- LC-MS were obtained using a Q Exactive Thermo Scientific and an Agilent Technologies 6120.
- All the reported melting points are uncorrected and were recorded using Stuart SMP-30 melting point apparatus.
- Chemical nomenclature (IUPAC) and structures were generated using ChemDraw Professional 15.1.

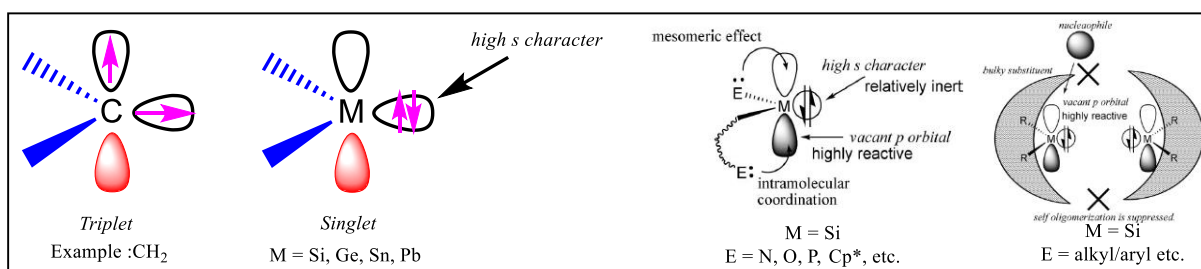


	<b>Synopsis of the Thesis to be submitted to the Academy of Scientific and Innovative Research for Award of the Degree of Doctor of Philosophy in Chemistry</b>
<b>Name of the Candidate</b>	<b>SANJUKTA PAHAR</b>
<b>Degree Enrollment No. and Date</b>	<b>PhD in Chemical Science (10CC16A26009) August 2016</b>
<b>Title of the Thesis</b>	<b>Donor–Acceptor Stabilization of Compounds with Low Coordinate Group 13 and 14 Elements</b>
<b>Research Supervisor</b>	<b>Dr. Sakya S. Sen (CSIR-NCL Pune)</b>

## Introduction

The *p*-block elements have grown its interest to chemists since the beginning of the discovery of periodic table. By 1869, of the 63 known elements by then, more than half of the 30 *p*-block elements had been discovered. However, research on synthesis and reactivity studies of low-valent and low-coordinated group 13 and 14 compounds have flourished in the last few couple of decades. Generally, low-valent main-group elements residing on higher than of the third row display abnormal physical and chemical properties. In contrast to methylene (CH<sub>2</sub>), heavier methylene analogues (SiH<sub>2</sub>, GeH<sub>2</sub>, SnH<sub>2</sub> and PbH<sub>2</sub>) have singlet ground state rather than triplet state (See in Scheme 1). The large energy gap and spatial difference between the *s*- and *p*- orbitals prevent the formation of hybrid orbitals.<sup>1</sup> After the report from Arduengo and his coworkers to crystallize N-heterocyclic carbene,<sup>2</sup> the heavier group 14 metallylenes discovered by taking the advantages of electronic and steric stabilization. In the case of electronic stabilization, the covalently bound ligands associated with donor atoms partly donate their electron density into a highly reactive vacant coordination site, and thereby minimizing the electrophilicity of a vacant orbital. In another case, the sterically bulky ligands attached to a central atom can shield the vacant coordination site from the outer nucleophilic attack or solvent molecules, and therefore, suppress the propensity of the polymerization and/or oligomerization of their corresponding monomer units. In order to stabilize low-coordinate metal centers, monodentate bulky ligands for example amides<sup>3</sup> and 2,6-terphenyls<sup>4-6</sup> have been successfully well discovered with many unusual bonding styles.<sup>7-9</sup> To deliberate greater stability to such low valent complexes, bulky bidentate N,N'-ligands such as  $\beta$ -diketiminates and the related amidinate, guanidinate and triazenide ligands have also been widely

explored due to their straight forward synthesis and versatility, by occupying a further coordination site on the metal, in favor of adapting the steric as well as electronic properties.<sup>10-13</sup>



**Scheme 1.** Outlook of molecular and electronic features and stabilization of metallocenes

### Statement of Problem

The importance of small molecules like  $H_2$ ,  $CO$ ,  $CO_2$ ,  $NH_3$  is that they are ubiquitous, relatively cheap, synthons for building more complex molecules, and produced in large scales in industrial processes. Most of the homogeneous catalytic cycles involve such small molecules. Therefore, it is deemed desirable to use them into syntheses of value-added chemical products. However, the activation of such relatively inert bonds usually requires a catalyst. The typical catalysts feature late transition metals due to their amenability to be in a variety of oxidation states, to coordinate to a substrate, and to be a good source/sink for electrons depending on the nature of the transition state. The most active transition metal catalysts are based on Pt, Pd, Rh, Ru, Ir, Os etc. However, the current trend in catalysis is to move to cheaper and greener alternatives because late transition metal-based catalysts are expensive as well as there are some concerns on the incorporation of such heavy metals into products. Main group elements, on the other hand, are cheap, more abundant, and have lesser issues regarding toxicity. Recently, the compounds with heavier low valent main group elements are slowly gaining foothold in transition metal free catalysis and they could show promising reactivity towards small molecules. The challenge is to induce the appropriate configuration on the metal centre to bind such small molecules, and eventually make them active for further reaction, ideally in a catalytic manner. Clearly, such questions require a concerted and holistic approach, including synthetic skills for ligand design and fabrication, an in-depth understanding of mechanistic and kinetic aspects of the interaction of small molecules with the activating entity.

## Objectives

We have aimed to develop new ligand systems to stabilize the low-valent main group compounds in low oxidation states and explore them as alternative resources to transition metal complexes for activation of small molecules as well as important organic transformations, and to evolve the new ways for the sustainable production of metal free catalytic systems. The objectives of my thesis is as follows:

1. Use of existing compounds with low valent group 14 elements as ligands
2. Design of new ligands and synthesis of new compounds with low valent group 14 elements
3. Transition metal free organic transformation

## Methodology

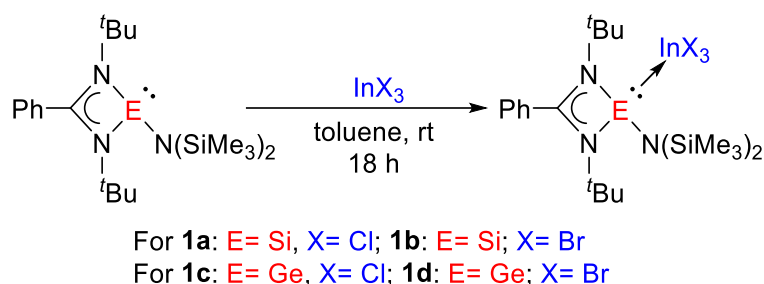
### ***Chapter I: General Introduction***

In this chapter, we have presented an overview of the elementary interest and challenging synthetic protocols regarding the development of the chemistry of low-valent main group compounds and the application in small molecule activation and catalysis. A wide-ranging introduction covering a brief explanation of important compounds in this area of research is described with the literature precedence. The objectives and the results presented in this thesis are outlined

### ***Chapter II: Silicon(II)- and Germanium(II)-Indium Compounds***

For the enrichment and understanding of main-group chemistry, the heavier congeners of carbenes have played a significant role in the formation stable Lewis adducts with group 13 elements such as boron, aluminum, and gallium. The investigation with indium and the understanding of such a stable silylene-indium complex has still remained elusive presumably due to the low solubility of the indium halides in majority of the organic solvents. Similarly, a germylene-indium complex is also unidentified till date. As the indium is enticing one of the most important dopant species for silicon crystals used in photovoltaics, so the use of indium compounds in electronics has fashioned renewed interest in the chemistry of silicon and indium. We have successfully prepared and characterized the first Silylene and Germylene complexes of Indium, by the reactions of amidinate ligand supported Silylene and Germylene with  $\text{InCl}_3$  and  $\text{InBr}_3$ , respectively (Scheme 2). The

solid-state molecular structures of **1a**, **1b**, **1c**, and **1d** were confirmed by single-crystal X-ray studies which established the monomeric nature of the adducts. The X-ray studies, in combination with the DFT calculations, recommend that the Si–In and the Ge–In bonds are of the classical donor–acceptor type.

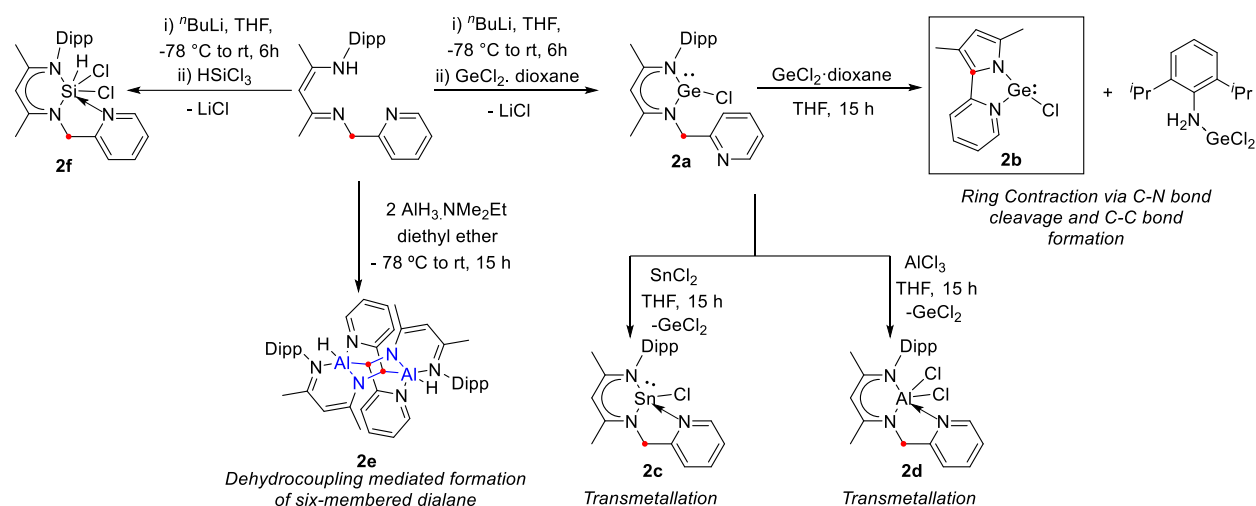


**Scheme 2.** Reactions of Si(II) & Ge(II) Amide with Indium Halides

### Chapter III: Access to Group 13 and 14 Compounds using Picolyl Functionalized $\beta$ -diketiminato Ligand

The symmetrical  $\beta$ -diketiminato ligand can provide adequate thermodynamic and/or kinetic effort to stabilize a large variety of transition metals and main group elements. The nacnac supported chlorogermylene,  $[\text{CH}\{(\text{CMe})(2,6\text{-}i\text{Pr}_2\text{C}_6\text{H}_3\text{N})\}_2]\text{GeCl}$ , has enjoyed an extensive devotion due to its usefulness as a synthon to synthesize a series of germanium compounds. Whereas a tridentate pendent picolyl functionalized nacnac framework is comparatively less well-explored system which has been used for the synthesis of iron, chromium, yttrium, and scandium complexes along with only one result with magnesium and calcium complexes. We have introduced and prepared a new six membered chlorogermylene (**2a**) bearing the unsymmetrical nacnac-based tridentate ligand moiety. The ligand scaffold proved to be surprisingly flexible and allowed for the isolation of structurally different compounds under otherwise identical conditions. We have also prepared a five-membered new pyridylpyrrolide germylene **2b** in presence of another equivalent of  $\text{GeCl}_2$  with **1**. On the other hand, **2a** undergoes an unusual transmetallation reaction generating **2c** and **2d** with  $\text{SnCl}_2$  and  $\text{AlCl}_3$  respectively. We have also described the synthesis of an unexpected six-membered dialane heterocycle **2e** resulting from the double dehydrocoupling of the ligand with  $\text{AlH}_3$ . The molecular structure of **2e** adopted to an analogue of cyclohexane, where two C–C bonds

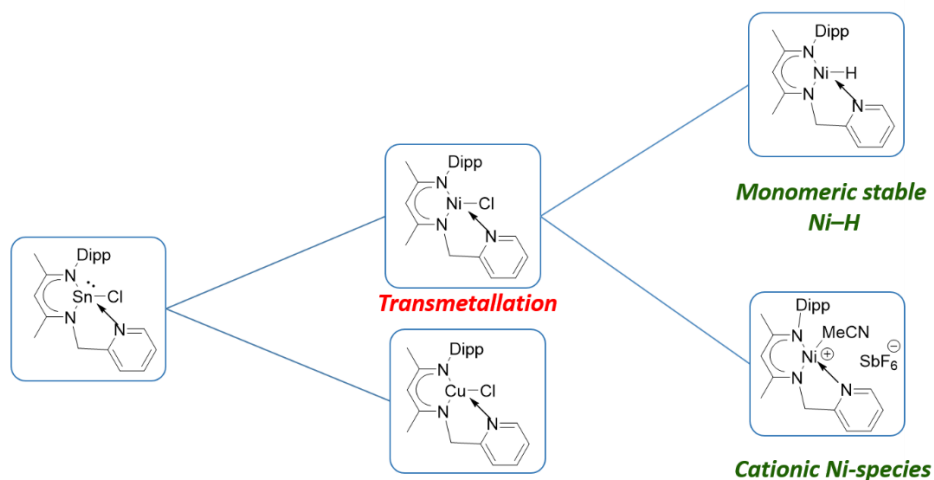
have been replaced by isoelectronic Al–N bonds. We have also successfully synthesized and characterized methylpyridinato  $\beta$ -Diketiminato ligand stabilized dichlorosilane (**2f**).



**Scheme 3.** Synthesis and reactivity studies of methyl-pyridiato nacnac ligand and analogous germylene **2a**

#### Chapter IV: Transmetalation involving Stannylene and First Row Transition Metals

Transmetalation is a special type of organometallic reaction involving the transfer of ligand from one metal to another. This method is commonly well explored for the preparation of a series of a transition metal compounds, whereas the transmetalation involving *p*-block elements are quite infrequent. Here in this chapter, we have extended the transmetalation chemistry from *p*- to *d*-block elements to synthesize nickel and copper halide complexes using new nacnac-based tridentate ligand scaffold having a pyridyl-methyl pendent group.



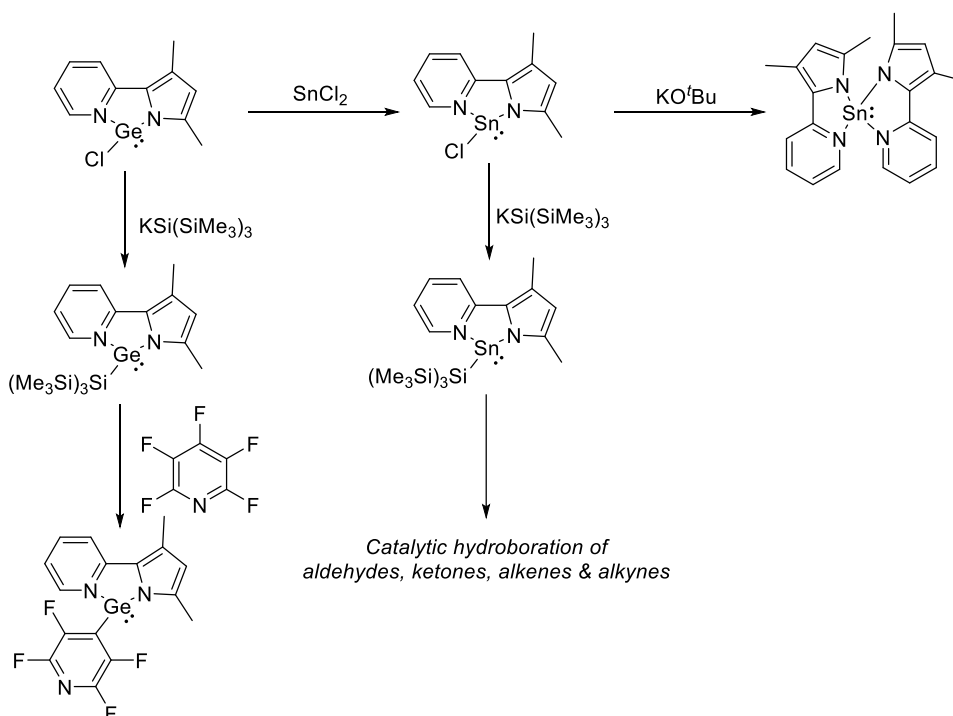
**Scheme 4.** Synthesis of methyl-pyridiato nacnac ligand supported nickel and copper halide complexes and synthetic protocol to prepare monomeric Ni-H and cationic Ni species

The nickel hydride complexes along with the nickel cations play a vital role in organometallic chemistry especially in the field of homogeneous catalysis. But the chemistry of nickel hydride complexes lagged way behind than that of many other metal hydride complexes, mainly due to the limited availability of well-defined ligand systems. We are able to synthesize and stabilize the challenging monomeric Nickel-hydride complex as well as the cationic nickel species containing non-coordinating anionic moiety. The catalytic application of using the hydride and cationic species is currently under progress.

#### **Chapter V: Pyridylpyrrolido Ligand Supported Germylene and Stannylene Chemistry**

The bidentate monoanionic bulky N,N'-ligands such as  $\beta$ -diketiminates, amidinates, guanidates, and recently two monoanionic ditopic ligands have been widely discovered to stabilize low-valent main-group elements, due to their straightforward synthesis. The fine tuning of the substituents around the metal and the occupation of a second coordination site to the metal produces the ligand scaffold much more attractive. Recently, the pyridylpyrrolido ligand, a very similar monoanionic bidentate ligand, had found extensive application in transition metal chemistry. We have introduced this ligand for the first time for the generation of pyridylpyrrolido ligand supported chlorogermylene (**2b**) (high yield synthesis) from which analogous chlorostannylene has been synthesized via transmetalation. Further we have also introduced the hypersilyl group in

pyridylpyrrolido germylene and stannylene to synthesized pyridylpyrrolido hypersilylmetallylene. Then we have revealed the fluoride affinity of the silicon atoms of the hypersilyl moiety for germylene. The reaction of hypersilylgermylene with pentafluoroarene cleaves the para-C–F bond of the fluoroarene ring and produce aryl germylene along with elimination of  $(\text{Me}_3\text{Si})_3\text{SiF}$ . The homoleptic tin complex has been formed on the treatment of chlorostannylene with KO'Bu in toluene. The catalytic hydroboration of aldehydes, ketones, alkenes and alkynes using hypersilyl substituted cost-effective tin(II) compounds has been explored as well.



**Scheme 5.** Synthesis and reactivity of Pypyr ligand supported Ge(II) and Sn (II) compounds

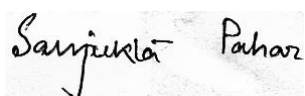
## Conclusions

In conclusion, we have prepared and characterized the first silylene and germylene complexes of indium, by the reactions of with  $\text{InCl}_3$  and  $\text{InBr}_3$ , respectively. We have introduced the flexible methylpyridinato ligand supported tridentate nacnac ligand for the preparation of germylenes and stannylenes and their unusual reactivities towards transmetallation has been performed. The transmetallation methodology has been extended further for the pyridylpyrrolido (Pypyr) ligand supported germylenes. The activation of C–F bond of the fluoroarene ring has been established

with the hypersilyl substituted germylene featuring Pypyr ligand. The hypersilyl substituted cost-effective tin(II) compound has been used for the exploration of catalytic hydroboration of not only for aldehydes, ketones, but for alkenes and alkynes, which was thus far not known.

### **Future Directions**

We have the tools to develop novel, more sustainable methods to harvest energy to satisfy growing demands, as well as methods to trap greenhouse gases such as CO<sub>2</sub> and transform them into useful products. While certain transition metals (TM) such as Fe, Co, and Ni are readily available and more benign than rare precious metals such as Ir, Rh, and Pt, lighter main group elements are relatively abundant and more cost effective. In addition, the removal of trace TMs in the agrochemical, pharmaceutical, and electronics industries is very costly and labour intensive, but must be carried out to a high standard based on regulations maintained by governing bodies on products for human consumption, and to meet the demands of modern-day electronics. Silicon, aluminum and several main group elements are the most abundant metal in the Earth's crust. Aluminium mostly exists in +3 oxidation state, and is typically combined with other elements forming extraordinarily stable minerals. Nevertheless, Al is the most widely produced non-ferrous metal and remains one of the cheapest metals to produce. The recycling process of Al requires nearly 5% of the energy input to obtain pure Al from natural sources and is thus extremely important on a sustainability front. As a result, high abundance and low cost, Al-based compounds are widespread in industry and academia. So, in future we can aim is to synthesize Al-containing catalyst to activate the thermodynamically stable and kinetically inert CO<sub>2</sub> molecules and simultaneous regeneration to value-added carbon products (i.e., ethanol, methanol, and various hydrocarbons). So, an efficient utilization of renewable carbon resources is helpful and crucial to maintain a long-term and sustainable development of our society.



Signature of Student



Signature of Supervisor



## Chapter 1: Introduction

### Abstract

This chapter illustrates an overview of the primary interest and challenging synthetic encounters regarding the development of the new ligand systems to stabilize the low-coordinated, low-valent main group compounds and explore them as alternative resources to transition metal complexes for the activation of small molecules as well as important organic transformations, and to evolve the new ways for the sustainable construction of metal-free catalytic systems. A general introduction covering a brief elucidation of the perception along with the important compounds in this area of research is discussed with the relevant literature precedence. The objectives and the results further presented in this thesis are outlined.

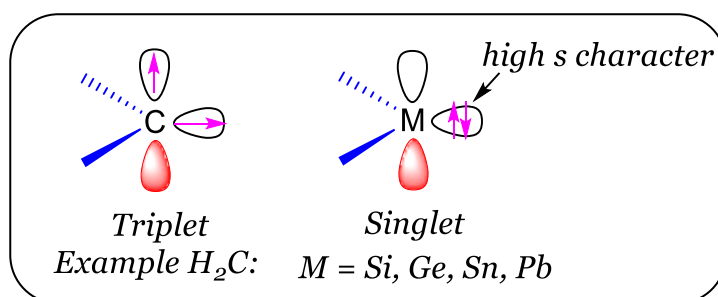
## 1.1 General Introduction

Interest in low-valent, low-coordinate or multiply bonded main group chemistry has experienced a significant surge since the last quarter of the twentieth. The activation of small molecules is considered as one of the key steps during a catalytic cycle with transition metals. As a result, transition metals serve as an active catalyst for a variety of homogeneous and heterogeneous transformations. On the contrary, it was long believed that main group compounds cannot act as efficient catalysts because of their incompetence to activate small molecules. However, recently a large number of main group compounds with low-valent elements are capable of activating small molecules as well as a variety of Group 14 hydrides have shown to behave like transition metals. This resurgence has been developed by designing new tunable ligand and innovative synthetic methodologies that have permitted the synthesis and isolation of novel main group complexes that were previously too reactive to handle.<sup>1-6</sup> All these discoveries that directed to this enormous revolution mainly originated from a simple desire to synthesize main-group compounds that were unknown as stable species. These introduced one or more of the following: (1) formation of multiple bonds between heavier main-group elements such as Al, Si, P or their heavier congeners;<sup>7</sup> (2) stable low-valent derivatives with open coordination sites;<sup>8-10</sup> (3) molecules containing quasi-open coordination sites which can form frustrated Lewis pairs;<sup>11</sup> (4) stable paramagnetic compounds with unpaired electrons centered on the heavier main group (that is, radicals);<sup>12-14</sup> or (5) stable singlet diradicaloid electronic configurations.<sup>2</sup> The isolation of all such compounds is still challenging due to their unstable existence.<sup>15,16</sup> The desirable goal is to utilize main group complexes, that could replace transition metal complexes, due to the environmental issues and scarcity of the late transition metals.<sup>17</sup> This thesis mainly has focused on the stabilization of low-coordinate group 13 and 14 compounds using the donor-acceptor concept and their utilization towards catalysis.

## 1.2 Stabilization of Heavier Low-valent Group 13 and 14 Compounds

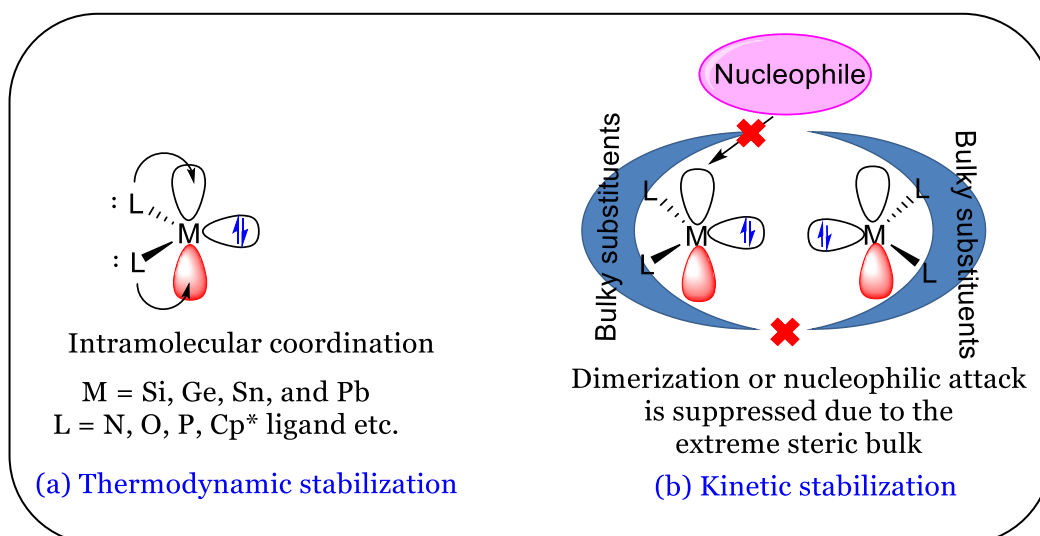
The attempts to prepare methylene carbene ( $\text{CH}_2$ ), the simplest members of a molecular family, as an isolable species still continues to attract considerable attention.<sup>18</sup> However, the isolation of the  $\text{CH}_2$  moiety was difficult in the bulk phase.<sup>19</sup> Nonetheless, the synthesis of methylene functionality

stabilized through other substrates was accomplished using phosphorus- ( $R_3P=CH_2$ ) and numerous metal-supported ( $L_xM=CH_2$ ;  $L =$  ligands) reagents.<sup>20</sup> The stability of the heavier methylene congeners,  $H_2E$ : ( $E = Si-Pb$ ) increases while going down the group due to the inert pair effect.<sup>21</sup> Although dichloroplumbylene ( $PbCl_2$ ) and dichlorostannylene ( $SnCl_2$ ) can be considered as very stable ionic compounds at room temperature, they also exist as ion pairs form or in polymeric form in solution as well as in the solid-state. The dichlorogermylene,  $GeCl_2 \cdot dioxane$ <sup>22</sup> can be isolated as a Lewis adduct, whereas the compounds of divalent silicon are scarcely isolable without using the advantage of both electronic and steric protection.<sup>23</sup>



**Fig. 1.1:** Differences between the ground states of carbenes and metallylenes

Unlike the triplet state of methylene, the heavier carbene congeners feature a singlet state as they have a large energy gap and the spatial difference between the  $s$ - and  $p$ - orbitals, which prevent forming a hybrid orbital (Figure 1.1). The extremely high reactivity has been described due to the presence of their vacant  $p$ -orbitals. As a consequence, they have the tendency to dimerization. In order to stabilize them, the protection of the highly reactive vacant  $p$ -orbital is required by introducing both the electronic and steric supported ligand backbone. These strategies are described in Figure 1.2. For the need of thermodynamic stabilization, the hetero donor atom (such as N, O, S) can be introduced to bind with the central atom and can donate its electron density to the empty  $p$ -orbital in order to stabilize the system.<sup>24</sup>

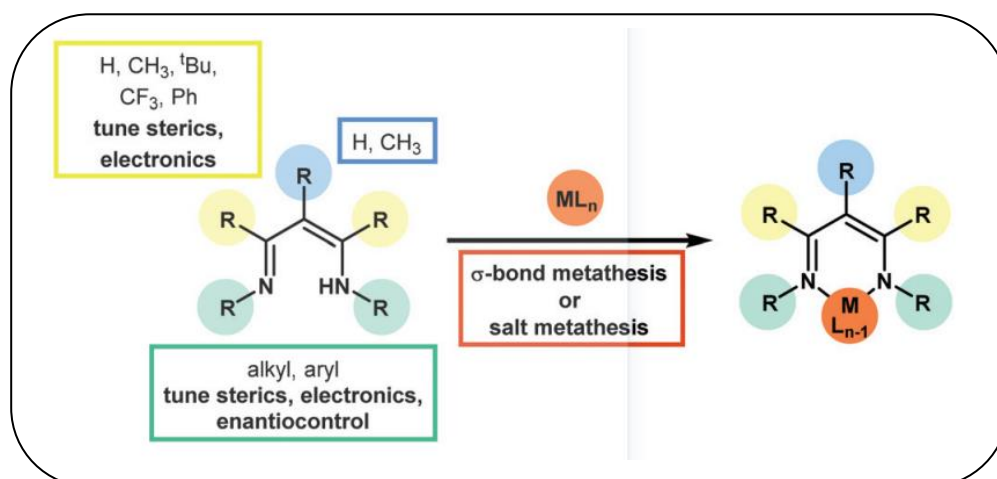


**Fig. 1.2:** (a) Thermodynamic stabilization and (b) kinetic stabilization of metallylenes

### 1.3 Low-coordinate Group 13 and 14 compounds

The coordination number of an atom can be defined as the sum of the number of other atoms to which it is bonded in any way. Compounds in which an element has a lower-than its usual coordination number often exhibit considerably different chemical and physical properties from those in which the element has an unusual or higher coordination number. These changes sometimes render such low-coordinate compounds appropriate for catalysis and as precursors for realizing unusual compounds. The neutral uncomplexed group 13 compounds (known as ‘triel’) are generally shown their coordination number 3 as they are stable in trivalent state, but due to their electron-deficient nature the coordination numbers of 4, 5, 6, and higher are also exhibited for both neutral and anionic species. Theoretically, many low-valent compounds could be possible to prepare using the metathesis method using the metal salt of the desired substituent with a low-valent element halide. However, in practice, monovalent halide salts are only commercially accessible for thallium and indium. Although the metastable univalent halides for aluminum and gallium are possible to prepare but they are metastable in nature. Similarly, neutral group 14 elements (known as ‘tetrel’) are holding four electrons in the valence shell. Exploiting the catenation property, the carbon can form a long chain or structures by forming covalent bonds with other carbon atoms, but silicon can only form from disilanes with only one silicon center and the property is diminishing while going down the group. Hence, carbon is capable to form longer *p-p* sigma bonded chains than its heavier analogues, which could be able to bond via higher valence

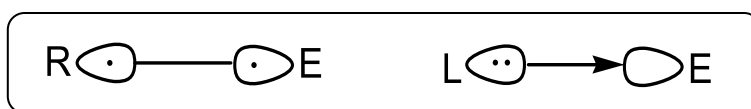
shell orbitals. But the isolation of the first stable double bond containing heavier group 14 elements containing Si=C,<sup>25</sup> and Si=Si,<sup>26</sup> resulted in remarkable progress in the chemistry of unsaturated compounds of heavier elements. The low-coordinate, low-valent groups 13 and 14 compounds can only be stabilized by introducing ligands that coordinate to the metal element through at least one nitrogen atom. The monoanionic bidentate nitrogen-based analogs of the  $\beta$ -diketonate ligand are one of the richest and most well-investigated ligands, which is often referred to as ‘nacnac’ ligands. The ready tuning of the steric properties through the N-alkyl/aryl substituents over the ligand backbone as well as the strongly electron-donation behavior of these systems allowed to stabilize the complexes kinetically and thermodynamically (Figure 1.3). Using all these tunable properties a wide range of recent landmark discoveries have been reported with *s*-, *p*-, *d*-, and *f*-blocks elements featuring nacnac supporting frame-works.<sup>27,28</sup>



**Fig. 1.3:** The utility of the  $\beta$ -diketiminato ligand scaffold by tuning its steric and electronic parameters<sup>28d</sup> (Adopted from *Dalton Trans.*, 2017, **46**, 4483–4498)

#### 1.4 Donor-acceptor concept

The IUPAC definition of a donor-acceptor bond (or dative) is "The coordination bond formed upon the interaction between molecular species, one of which serves as a donor and the other as an acceptor of the electron pair to be shared in the complex formed". However, it was Arne Haaland, who has given salient characteristics of a dative bond: (a) it is weak, (b) longer than a typical single bond, (c) small degree of charge transfer and most importantly (d) difference in energy between the homolytic and heterolytic bond dissociations.<sup>29a</sup>



**Fig. 1.4:** Representation of covalent/electron-sharing bonding (left) and donor-acceptor bonding (right)

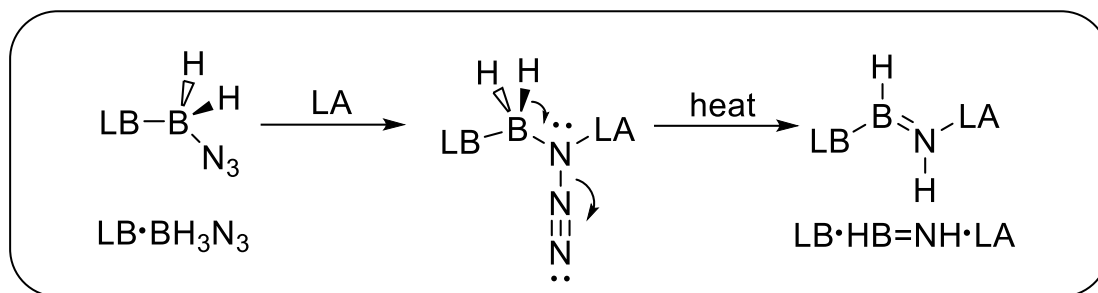
Donor–acceptor (D-A) complexes with low-valent main group elements are currently a very active area as it has offered an unrivaled opportunity to bring together the disciplines of synthetic chemistry and theoretical research. The chemical bonding in transition metal complexes has been extensively discussed based on Ligand→TM  $\sigma$ -donation and TM→Ligand  $\pi$  backdonation [Dewar-Chatt-Duncanson (DCD) model] and sometimes Ligand→TM  $\pi$  donation and TM→Ligand  $\sigma$ -backdonation (Reverse DCD Model). However, the bonding in main group chemistry is generally explained by sharing of electrons between two hybrid orbitals with some exceptions like adduct formation between group 13 acids and group 15 bases, which are rationalized in terms of D-A interaction. The characteristic feature of the D-A complexes with low-valent main group elements is the presence of dative bonds L→E (E=main group element) instead of covalent (electron sharing) bonds R–E (Figure 1.4). Moreover, an electronically rich structure intermediate between the coordinate and the sigma sharing bond may exist, for example, when a N-C=N ligand is involved that has an allyl-anion-like  $\pi$  framework, which can accommodate only four electrons, but it has five, two from each nitrogen and one from carbon. This features an extra electron without increasing the charge at the coordinating atom. Pinpointing the birth of D-A complexes of main group elements is a very challenging task, but it would be safe to comment that the advent of NHCs as ligands kick-started the low coordinate main group D-A compounds. The primary role of NHCs is to donate electron density to the low-lying LUMO of the main group elements, which would otherwise be involved in molecular decomposition.

#### 1.4.1 Donor-Acceptor Stabilization of Group 13 Complexes

The mixed hydride complexes can perform an important role as intermediates in the production of several semiconducting materials and they are promising as hydrogen storage materials and can be precursors to inorganic polymers. The  $H_2E-E'H_2$  species are the most unstable in their free state under ambient conditions and are susceptible to oligomerization or polymerization due to the presence of highly active electron pair (HOMO) and low-lying LUMO within the same molecule (i.e. dual Lewis acid-base character) (Scheme 1.1).



was able to prepare the Lewis acid (LA) assisted elimination of  $N_2$  followed by H migration from B to N of  $LB \cdot BH_2N_3$  afforded a donor-acceptor complex of  $HB=NH$  in the form of  $LB \cdot HB=NH \cdot LA$  (Scheme 1.2).<sup>33</sup>

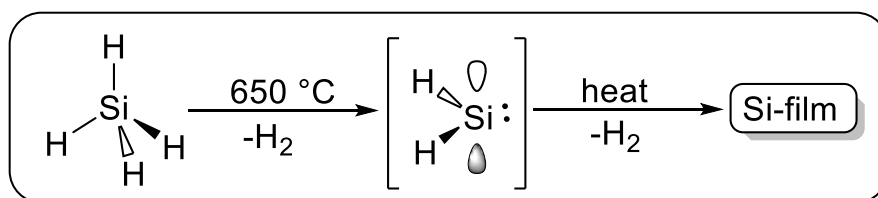


**Scheme 1.2** Lewis acid-assisted  $N_2$  elimination from an azidoborane adduct to form a stable  $HB=NH$  complex

A similar unsaturated mixed group 13/15 hydride,  $HGa=NH$ , will also convert into gallium nitride ( $GaN$ ), a highly valued material for its blue luminescent and semiconducting properties.<sup>34</sup> A similar donor-acceptor stabilization strategy via Lewis acid-assisted  $N_2$  elimination was also employed as shown in Scheme 1.2 to isolate a  $HGa=NH$  donor-acceptor complex.

#### 1.4.2 Donor-Acceptor Stabilization of Heavier Group 14 Elements

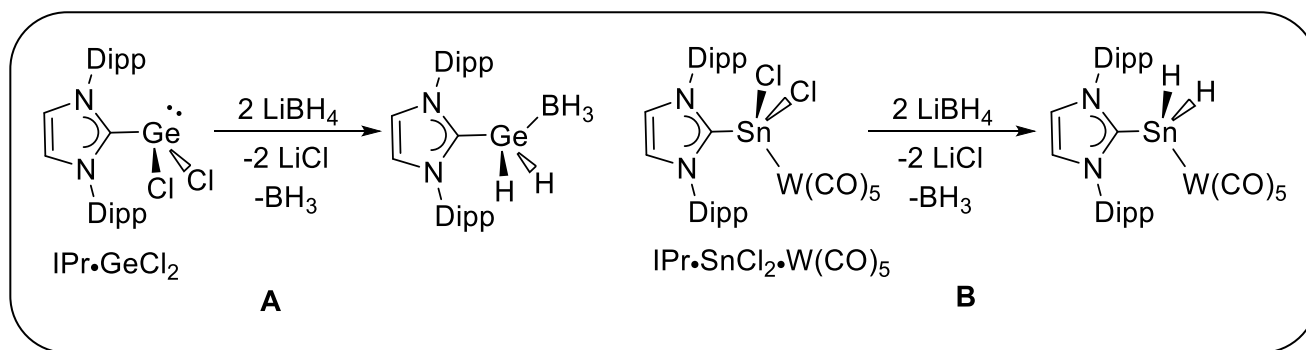
The research group of Rivard extensively worked on the isolation of reactive Group 14 hydrides using donor-acceptor protocol, a vital portion for the elevation of the contemporary donor-acceptor chemistry.<sup>35</sup> The interest in group 14 hydrides stems from their possible occurrence during the formation of some bulk semiconducting materials. For example, during the chemical vapour deposition (CVD) technique of semiconducting silicon films,  $SiH_2$  was obtained as an intermediate at very high temperatures ( $>550$  °C), (Scheme 1.3).<sup>36</sup>



**Scheme 1.3**  $SiH_2$  is an intermediate present during the synthesis of Si-film from  $SiH_4$  via high-temperature CVD methods

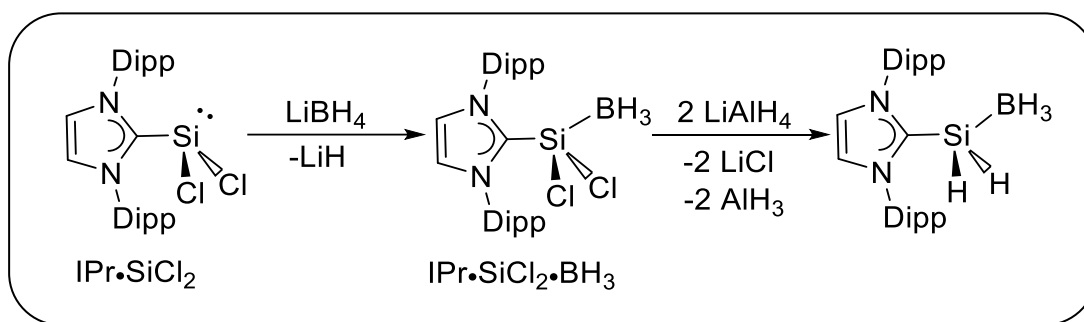


The group 14 dihydrides are generally very unstable at room temperature in their free state;<sup>37</sup> however, with the partnership with the Lewis acid and Lewis bases they can be stabilized in the form of donor-acceptor complexes  $LB \cdot EH_2 \cdot LA$ . The first example was reported in 2009, where a  $GeH_2$  unit was stabilized using IPr as a Lewis base and  $BH_3$  as a Lewis acid.<sup>38</sup> The reaction of  $IPr \cdot GeCl_2$  with two equivalents of  $LiBH_4$  afforded the stable donor-acceptor complex  $IPr \cdot GeH_2 \cdot BH_3$  (Scheme 1.4 A), where  $LiBH_4$  provides the H as well as the Lewis acidic  $BH_3$  group to stabilize the moiety. In the dihydride compound, the N-heterocyclic carbene IPr donates a pair of an electron into the vacant  $p$  orbital of the Ge, whereas the lone pair residing on the  $GeH_2$  unit binds to the Lewis acidic  $BH_3$  group; hence, a push-pull interaction permits the isolation of the reactive  $GeH_2$  moiety under ambient reaction condition.



**Scheme 1.4** Synthesis of donor-acceptor complexes of  $GeH_2$  (A),  $SnH_2$  (B)

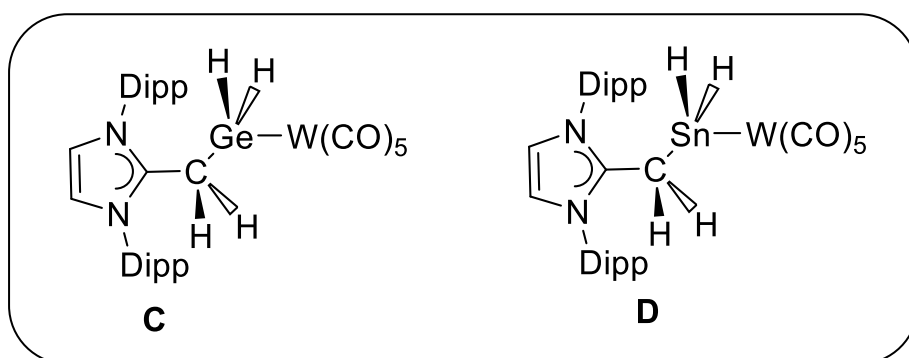
A similar method was attempted for the isolation of a  $SnH_2$  complex. The reaction of  $IPr \cdot SnCl_2$  with  $LiBH_4$  only offered  $IPr \cdot BH_3$  as a soluble product, along with the formation of metallic tin as black insoluble precipitate. Later, the addition of the highly Lewis acidic  $W(CO)_5$  unit allowed the isolation of the  $SnH_2$  donor-acceptor complex  $IPr \cdot SnH_2 \cdot W(CO)_5$  (Scheme 1.4 B)<sup>39</sup> via the treatment of  $IPr \cdot SnCl_2 \cdot W(CO)_5$  with  $LiBH_4$ . This donor-acceptor stabilization strategy was also further expanded to include an example of a  $SiH_2$  adduct,  $IPr \cdot SiH_2 \cdot BH_3$  as stated below (Scheme 1.5).<sup>40</sup>



### Scheme 1.5 Synthesis of donor-acceptor complexes of SiH<sub>2</sub>

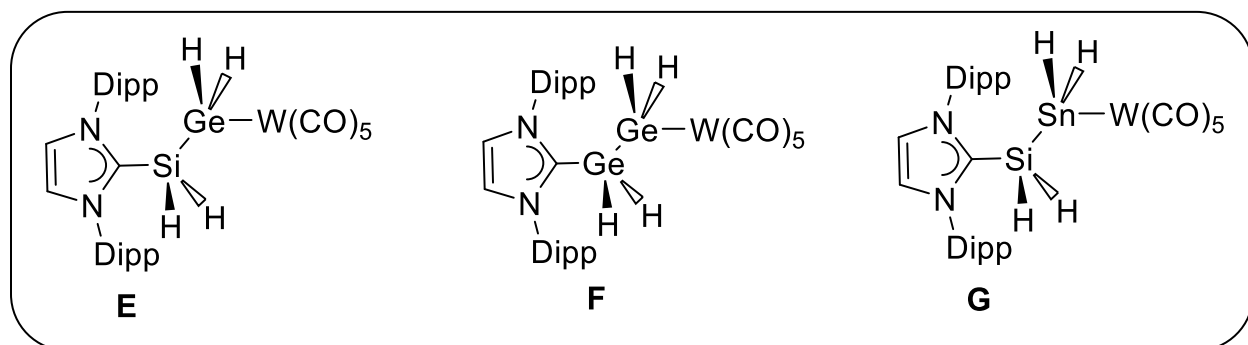
The research group of Marks also contributed to the synthesis of organogermylene and stannylene complexes through donor-acceptor studies.<sup>41</sup> The small free stannylene fragment SnMe<sub>2</sub> is highly unstable<sup>42</sup> and procedures oligomeric species [SnMe<sub>2</sub>]<sub>x</sub> spontaneously, which is connected by intrachain Sn–Sn  $\sigma$ -bonds.<sup>43</sup> Marks has reported a compound THF·SnMe<sub>2</sub>·Fe(CO)<sub>4</sub>, where the SnMe<sub>2</sub> unit can be observed as both an electron-pair donor (Lewis base) as well as an electron pair acceptor (Lewis acid) which supports the classical dative bonding modes: THF:→Sn and Sn:→Fe.<sup>44</sup>

Very recently, N-heterocyclic olefins known as NHOs, such as IPr=CH<sub>2</sub> have been employed as Lewis bases by the group of Rivard for the stabilization of GeH<sub>2</sub> and SnH<sub>2</sub> units. Due to the existence of a highly polarized exocyclic double bond in the NHOs, a significant amount of negative charge is located at the terminal carbon of IPr=CH<sub>2</sub>. Therefore, the strong donor ability of IPr=CH<sub>2</sub> was used to capture GeH<sub>2</sub> and SnH<sub>2</sub> units by the formation of IPrCH<sub>2</sub>·GeH<sub>2</sub>·W(CO)<sub>5</sub> (**C**) and IPrCH<sub>2</sub>·SnH<sub>2</sub>·W(CO)<sub>5</sub> (**D**), respectively (Figure 1.6).<sup>45</sup>



**Fig. 1.6:** Donor-acceptor stabilization of GeH<sub>2</sub> (**C**) and SnH<sub>2</sub> (**D**) complexes with IPr=CH<sub>2</sub>

A similar combination of LA/LB was also observed to isolate the heavier inorganic ethylene analogs H<sub>2</sub>Si–GeH<sub>2</sub>, H<sub>2</sub>Ge–GeH<sub>2</sub> and H<sub>2</sub>Si–SnH<sub>2</sub> in the form of the stable donor-acceptor complexes IPr·H<sub>2</sub>Si–GeH<sub>2</sub>·W(CO)<sub>5</sub> (**E**), IPr·H<sub>2</sub>Ge–GeH<sub>2</sub>·W(CO)<sub>5</sub> (**F**), IPr·H<sub>2</sub>Si–SnH<sub>2</sub>·W(CO)<sub>5</sub> (**G**), respectively (Figure 1.7).<sup>46</sup>

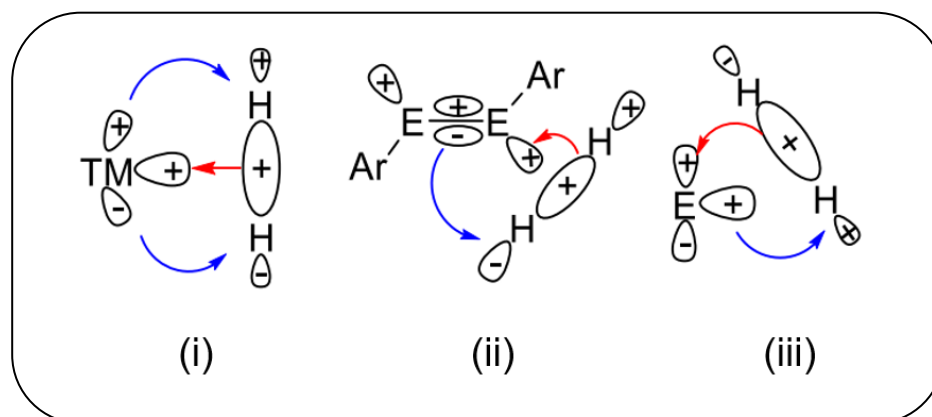


**Fig. 1.7:** Donor-acceptor stabilization of  $\text{H}_2\text{Si-GeH}_2$  (E),  $\text{H}_2\text{Ge-GeH}_2$  (F) and  $\text{H}_2\text{Si-SnH}_2$  (G) complexes

### 1.5 Main group compounds as an alternative to the Transition metal-complex

The catalytic reactions have been considered as the exclusive domain for the transition metals due to their ability to change of variable oxidation state, which was allowed them to go for oxidative addition and reductive elimination. However, there has been substantial progress in stabilizing main group *p*-block elements in their low oxidation states with the idea of mimicking “transition-metal like” chemistry with them.<sup>47</sup> The non-toxicity, environmentally benignity, and sustainability have led to the main group compounds as feasible replacements to the transition metal catalysts.

Remarkable development has been identified in the field of low valent main-group compounds, such as B(I),<sup>48</sup> Al(I),<sup>49</sup> Si(0),<sup>50-52</sup> and Ge(0)<sup>53-55</sup> in the form of multiple bonded species, carbenoids, and donor stabilized (e.g. carbene, imine, phosphine) atoms.<sup>9,56-59</sup> All those highly reactive species have revealed few common characteristics with the transition-metal complexes with small energy-separated frontier orbitals (Figure 1.8).<sup>17</sup> As a result, many of them display very interesting and unusual reactivity towards small molecules such as  $\text{H}_2$ ,  $\text{NH}_3$ , etc.

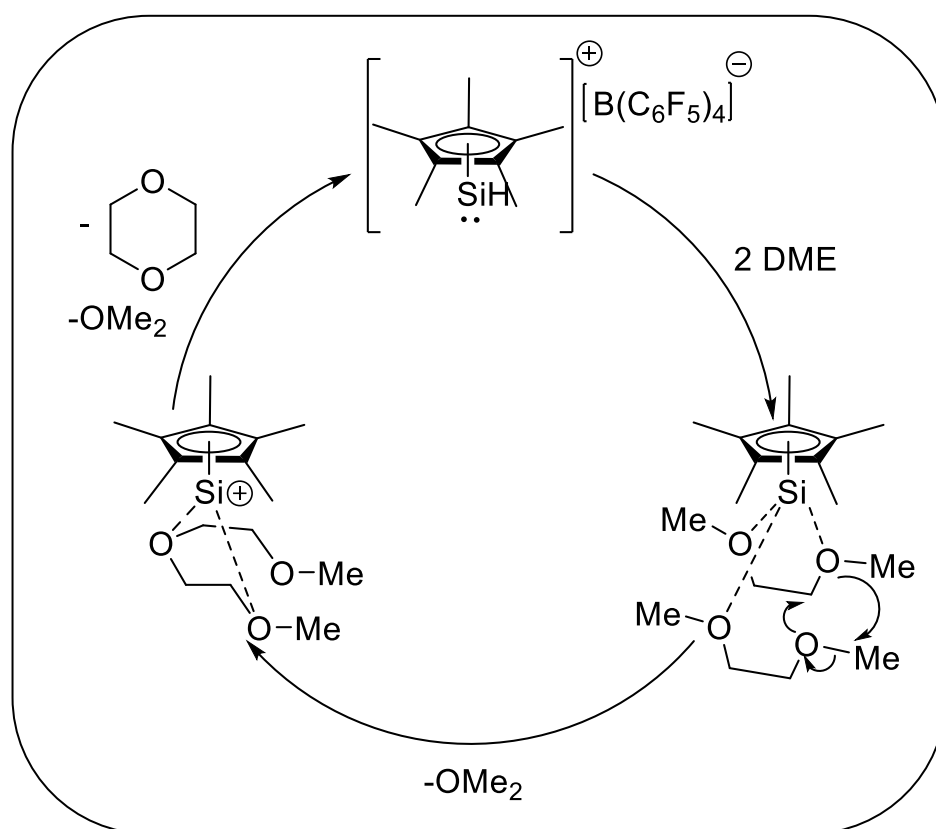


**Fig 1.8:** Frontier orbital interaction of dihydrogen with (i) transition metals, (ii) main group multiple bonds, and (iii) singlet main group species e.g. carbenes, tetrylenes<sup>17</sup> (Adopted from *Nature*, 2010, **463**, 171–177)

### 1.5.1 Main group compounds in homogeneous catalysis

Transition metal catalysts are very successful for the conversion of numerous organic transformations into value-added products with stereo-, regio- and chemoselectivity. However, the toxicity, the increasing cost, relatively low abundance, and recent trends to fulfill the goal of “cheap metals for noble tasks” have essentially urged for the development of alternative methods. Earlier the main group elements were found with limited applications to some Lewis acid catalysis. Recently there is a continuous global effort of using the *s*- and *p*-block elements of the periodic table for molecular catalysis.<sup>58, 60-63</sup> In 2007, the report on the heterolytic dihydrogen activation by the ‘frustrated’ Lewis pairs (FLPs) by the group of Stephan has shown outstanding advancement in catalytic processes.<sup>64</sup> Along with that many single-site catalysts based on cheap and abundant *s*- and *p*- block elements have already been investigated.

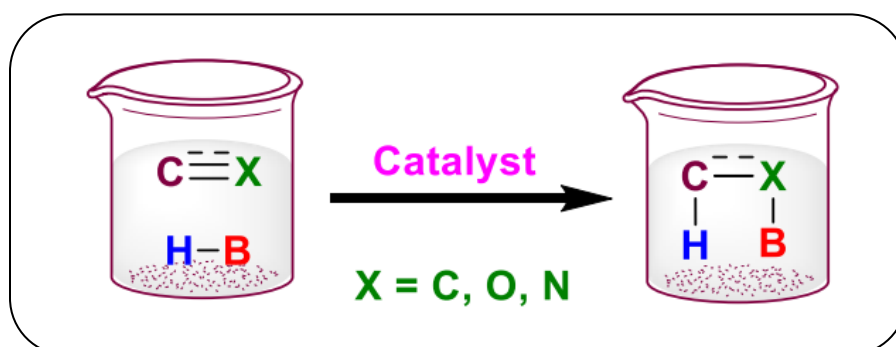
In this shed of light, the significant work by the group of Roesky and Baceiredo on the hydrosilylation of olefins and conversion of CO<sub>2</sub> to methanol stoichiometrically by using Nacnac Si(II)<sup>60</sup> and Ge(II)<sup>65a</sup> hydrides, respectively have unlocked a new path for the study and application of the low valent main group compounds in molecular catalysis. Recently, the catalytic conversion of 1,2-dimethoxyethane (DME) into 1,4-dioxane and dimethyl ether has been reported by a low valent Si(II) cation (Scheme 1.6).<sup>65b</sup> The proposed catalytic cycle for the conversion of the DME displays that two DME molecules coordinate weakly along with the association of four centers to the silicon atom of the cation. This activated state undergoes a rearrangement in the ether frame diglyme and is finally degraded to dimethyl ether and 1,4-dioxane to regenerate the catalyst.



**Scheme 1.6** Si(II) cation catalyzed conversion of DME to 1,4-dioxane

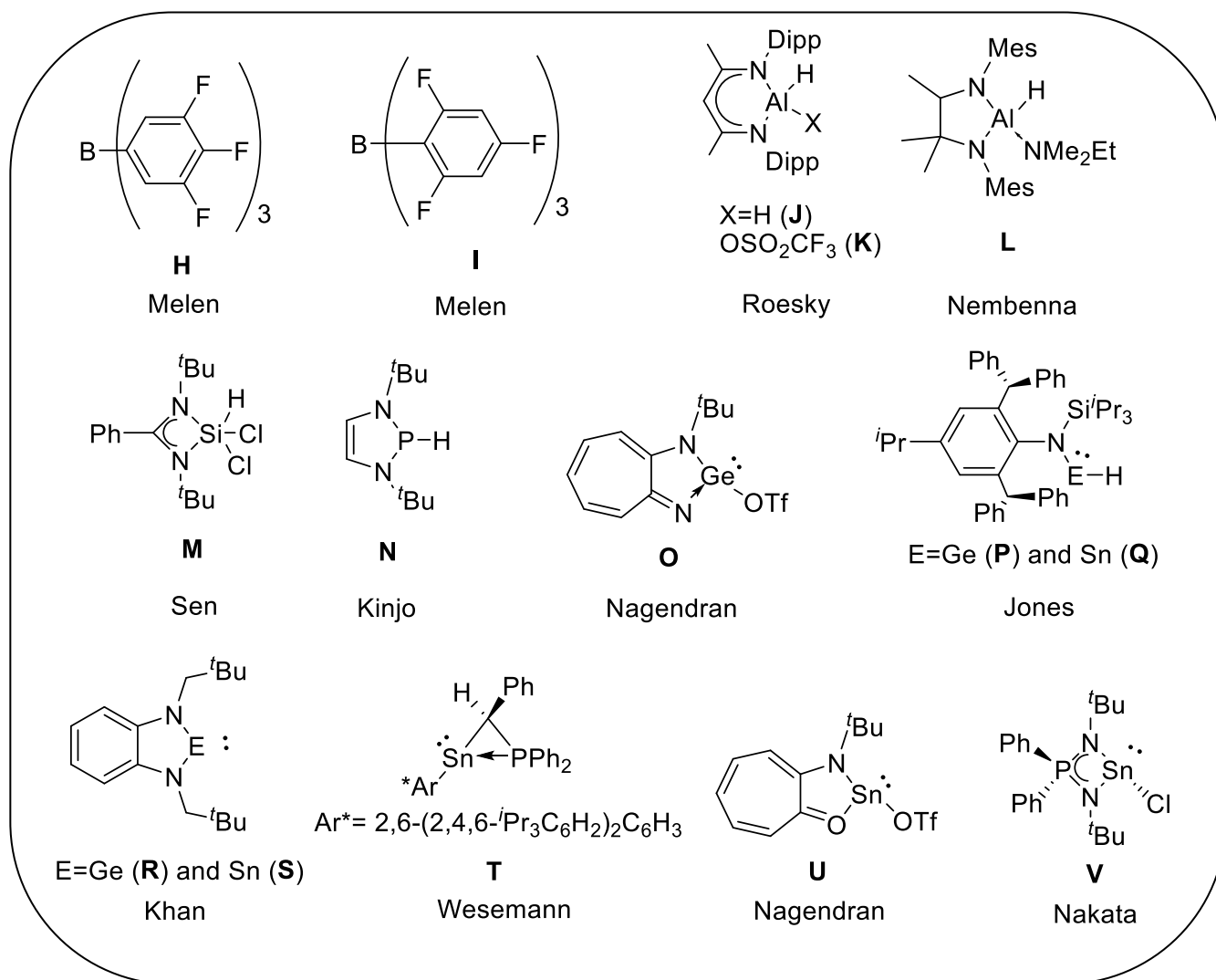
### 1.5.1.1 Hydroboration of carbonyl compounds and unsaturated C=C bonds

Hydroboration is an important transformation for the reduction of carbonyl compounds to alcohols (Scheme 1.7). Although several transition metal catalysts have been reported in the literature,<sup>66</sup> but a metal-free oxazaborolidine was established as an enantioselective hydroboration catalyst by the group of Corey and coworkers in 1987.<sup>67</sup> Later on, in 2004, an enantioselective reduction of ketones using a chiral Ga complex has been described by the group of Woodward.<sup>68</sup> Subsequently, a flurry of research activity on the carbonyl hydroboration has been reported by using compounds with the *p*-block element (such as P, Al, Ge, Sn, Pb, etc.) as single-site catalysts (Chart 1).<sup>69-74</sup>



### Scheme 1.7 Hydroboration of unsaturated compounds with HBpin

Hydroboration of carbon-carbon double or triple bonds can lead to the formation of alkenylboronic acid derivatives, including vinylboronates, which are commonly suitable in various cross-coupling reactions. There is an exponential growth on alkene and alkyne hydroboration using *p*-block compounds mainly containing the B,<sup>75</sup> Al,<sup>76</sup> and Si.<sup>77</sup> Surprisingly, there are only few reports on tin catalyzed hydroboration, thanks to the groups of Jones,<sup>78</sup> Wesemann,<sup>79</sup> Nagendran,<sup>80</sup> Khan,<sup>81</sup> and recently by Nakata (Chart 1).<sup>82</sup>



**Chart 1.** Selected examples of hydroboration catalysts with *p*-block elements

## 1.6 Aim and outline of the thesis

The syntheses of the low-coordinate and low valent heavier group 14 compounds are an emerging domain due to their unique reactive properties. Unlike saturated compounds, the central atom in these compounds possesses a vacant orbital along with a pair of electrons in their valence shell or an open coordination site. In order to explore such compounds, the selection of a suitable ligand is definitely an art in main group chemistry because utilizing bulky ligands, with appropriate steric and electronic effects, is an essential feature to stabilize main-group complexes. Several ligands have already been found to be very efficient in this perspective and reported by different research groups.

Eventually, exploitation of the main group elements towards small molecule activation to molecular catalysis established the recent ongoing quest for using them as alternatives to the traditional transition metals. However, such studies are still in the early times due to the paucity of well-established main-group compounds.

The introduction portion of the thesis has pronounced that, with proper kinetic and/or thermodynamic support, synthetic chemists have overcome the challenges associated with the stabilization of low-coordinate and low valent group 13 and 14 compounds. A wide range of literature surveys have been studied on the recent development with the donor-acceptor concept and briefly described the synthesis, stabilization, and their utilization towards small molecule activation and/or catalysis by using appropriate donor-acceptor or LA/LB amalgamations.

The main aim of the thesis is to further extend our knowledge on the synthesis, and reactivity of low-coordinated aluminum, silicon, germanium, and tin chemistry and also the application of earth-abundant, cheap or readily accessible tin compounds in homogeneous catalysis, primarily on hydroboration of unsaturated compounds. All the final compounds have been prepared and characterized by multinuclear NMR spectroscopy, single-crystal X-ray diffraction, and HRMS spectrometry. The following chapters will cover all these aspects of the thesis.

**Chapter 2** accounts for the synthesis and characterization of the first silylene complexes of indium by the reactions of  $[\text{PhC}(\text{N}^t\text{Bu})_2\text{SiN}(\text{SiMe}_3)_2]$  with  $\text{InCl}_3$  and  $\text{InBr}_3$ , respectively. The methodology has been further extended to prepare the first germylene complexes of indium using analogous

amidinate ligand stabilized low-valent germylene moiety. All the donor-acceptor complexes described in this chapter have been authenticated by single-crystal X-ray studies, which established the monomeric nature of these adducts. Finally, the DFT calculations in combination with the X-ray studies, suggest that the Si–In and the Ge–In bonds are of the classical donor–acceptor type in nature.

**Chapter 3** illustrates the preparation of a new chlorogermylene and dichlorosilane bearing nacnac-based tridentate ligand containing a pyridyl-methyl group. The ligand scaffold demonstrated very surprising flexibility and allowed for the isolation of structurally different compounds. The six-membered germylene can be smoothly converted into a five-membered pyridylpyrrolide germylene in the presence of another equivalent of GeCl<sub>2</sub>·dioxane under ambient reaction conditions. The analogous reaction with SnCl<sub>2</sub> or AlCl<sub>3</sub> resulted in unusual transmetallation reaction. The synthesis and molecular structure of an unexpected six-membered dialane heterocycle, an analogue of cyclohexane, has been prepared through double-dehydrocoupling by the treatment of the ligand with AlH<sub>3</sub>. All the isolated compounds have been characterized by single-crystal X-ray studies and spectroscopically.

**Chapter 4** represents the extension of the transmetallation chemistry from *p*- to *d*-block elements. The nickel and copper halide complexes have been prepared using a new nacnac-based tridentate ligand supported chlorostannylene featuring a pyridyl-methyl pendent group. The catalytically active stable nickel-hydride complex has been synthesized with the treatment of K-selectride as H-source. Furthermore, a stable tri-coordinated cationic nickel complex has also been realized with a weakly coordinating SbF<sub>6</sub><sup>-</sup> anion.

**Chapter 5** delineates a series of low-valent monomeric germanium and tin compounds featuring a pyridylpyrrolide ligand. The uncommon transmetallation chemistry, taking place between two elements of the same group, has been expanded further using pyridylpyrrolide ligand to prepare the stannylene compound from the corresponding germylene. Whereas the preparation of stannylene through a direct lithiation method led to the activation of the ortho C–H bond of the pyridine ring and functionalized with a <sup>t</sup>Bu moiety. We have introduced the hypersilyl group in the germylene and stannylene moiety using nucleophilic substitution reactions with KSi(SiMe<sub>3</sub>)<sub>3</sub>. The reaction of hypersilyl group substituted germylene with C<sub>5</sub>F<sub>5</sub>N afforded a tetrafluoropyridyl



germylene via the elimination of  $(\text{Me}_3\text{Si})_3\text{SiF}$  through the C–F bond activation of  $\text{C}_5\text{F}_5\text{N}$ . Finally, the hypersilyl stannylene has been explored as an effective catalyst for the hydroboration of aldehydes, ketones, alkenes, and alkynes.

### 1.7 Reference:

1. P. P. Power, *Chem. Rev.*, 2003, **103**, 789–810.
2. F. Breher, *Coord. Chem. Rev.*, 2007, **251**, 1007–1043.
3. P. P. Power, *Organometallics*, 2007, **26**, 4362–4372.
4. E. Rivard and P. P. Power, *Inorg. Chem.*, 2007, **46**, 10047–10064.
5. S. Nagendran and H. W. Roesky, *Organometallics*, 2008, **27**, 457–492.
6. M. Asay, C. Jones and M. Driess, *Chem. Rev.*, 2011, **111**, 354–396.
7. P. P. Power, *Chem. Rev.*, 1999, **99**, 3463–3503.
8. P. P. Gaspar and R. West, *Silylene Chemistry of Organic Silicon Compounds 2, Part 3* (eds Rappoport, Z. & Apeloig, Y.), 1998, 2463–2568 (Wiley).
9. Y. Mizuhata, T. Sasamori and N. Tokitoh, *Chem. Rev.*, 2009, **109**, 3479–3511.
10. G. Linti and H. Schnöckel, *Coord. Chem. Rev.*, 2000, **206–207**, 285–319.
11. D.W. Stephan, *Dalton Trans.*, 2009, 3129–3136.
12. P. P. Power, *Chem. Rev.*, 2003, **103**, 739–809.
13. R. G. Hicks, *Org. Mol. Biochem.*, 2007, **5**, 1321–1338.
14. V. Ya. Lee, M. Nakamoto and A. Sekiguchi, *Chem. Lett.*, 2008, **37**, 128–133.
15. W. E. Dasent, *Nonexistent Compounds* (Marcel Dekker, 1965).
16. M. J. Taylor, *Metal-to-Metal Bonded States* (Academic, 1975).
17. P. P. Power, *Nature*, 2010, **463**, 171–177.
18. For selected review articles, see: (a) H. Tomioka, *Acc.Chem. Res.*, 1997, **30**, 315–321; (b) D. Bourissou, O. Guerret, F. P. Gabbaï and G. Bertrand, *Chem. Rev.*, 2000, **100**, 39–92.
19. W. Sander, G. Bucher and S. Wierlacher, *Chem. Rev.*, 1993, **93**, 1583–1621.
20. (a) F. N. Tebbe, G. W. Parshall and G. S. Reddy, *J. Am. Chem. Soc.*, 1978, **100**, 3611–3613; (b) P. Schwab, M. B. France, J. W. Ziller and R. H. Grubbs, *Angew. Chem., Int. Ed. Engl.*, 1995, **34**, 2039–2041; (c) R. R. Schrock, *J. Am. Chem. Soc.*, 1975, **97**, 6577–6578. For selected work involving  $\text{L}_x\text{M}-\text{ER}_2$  complexes (E = Si, Ge and Sn), see: (d) D. G.

- Gusev, F.-G. Fontaine, A. J. Lough and D. Zargarian, *Angew. Chem., Int. Ed.*, 2003, **42**, 216–219; (e) R. G. Waterman, P. G. Hayes and T. D. Tilley, *Acc. Chem. Res.*, 2007, **40**, 712–719; (f) C. Zybilla and G. Müller, *Angew. Chem., Int. Ed. Engl.*, 1987, **26**, 669–670.
21. R. S. Drago, *J. Phys. Chem.*, 1958, **62**, 353–357.
22. (a) T. Fjeldberg, A. Haaland, B. E. R. Schilling, M. F. Lappert and A. J. J. Thorne, *Chem. Soc., Dalton Trans.*, 1986, 1551; (b) P. T. Matsunaga, J. Kouvetakis and T. L. Groy, *Inorg. Chem.*, 1995, **34**, 5103–5104.
23. (a) W. W. du Mont, T. Gust, E. Seppälä and C. J. Wismach, *Organomet. Chem.*, 2004, **689**, 1331–1336. (b) A. Rizzo, C. Puzzarini, S. Coriani and J. J. Gauss, *Chem. Phys.*, 2006, **124**, 034108-1–034108-16; (c) W. W. du Mont, T. Gust, E. Seppälä, C. Wismach, P. G. Jones, L. Ernst, J. Grunenberg and H. C. Marsmann, *Angew. Chem., Int. Ed.*, 2002, **41**, 3829–3832.
24. (a) M. J. Weidenbruch, *Organomet. Chem.*, 2002, **646**, 39–52; (b) Y. Mizuhata, T. Sasamori and N. Tokitoh, *Chem. Rev.*, 2009, **109**, 3479–3511;
25. M. Weidenbruch, *Organometallics*, 2003, **22**, 4348–4360.
26. A. G. Brook, F. Abdesaken, G. Gutekunst, and R. K. Kallury, *J. Chem. Soc., Chem. Commun.*, 1981, 191–192.
27. R. West, M. J. Fink, and J. Michl, *Science*, 1981, **214**, 1343–1344.
28. See, for example: (a) M. S. Hill, P. B. Hitchcock and R. Pongtavornpinyo, *Science*, 2006, **311**, 1904–1907; (b) S. P. Green, C. Jones and A. Stasch, *Science*, 2007, **318**, 1754–1757; (c) M. M. Rodriguez, E. Bill, W. W. Brennessel and P. L. Holland, *Science*, 2011, **334**, 780–783; (d) R. L. Webster, *Dalton Trans.*, 2017, **46**, 4483–4498.
29. (a) A. Haaland, *Angew. Chem. Int. Ed. Engl.* 1989, **28**, 992–1007; (b) M. Asay, C. Jones and M. Driess, *Chem. Rev.*, 2011, **111**, 354–396; (c) Y. Tsai, *Coord. Chem. Rev.*, 2012, **256**, 722–758; (d) C. Chen, S. M. Bellows and P. L. Holland, *Dalton Trans.*, 2015, **44**, 16654–16670; (e) C. Camp and J. Arnold, *Dalton Trans.*, 2016, **45**, 14462–14498; (f) M. Shimoi, S.-ichiro Nagai, M. Ichikawa, Y. Kawano, K. Katoh, M. Uruichi and H. Ogino, *J. Am. Chem. Soc.*, 1999, **121**, 11704–11712.
30. (a) U. Vogel, A. Y. Timoshkin and M. Scheer, *Angew. Chem. Int. Ed.*, 2001, **40**, 4409–4412; (b) U. Vogel, P. Hoemensch, K. -Ch. Schwan, A. Y. Timoshkin and M. Scheer,

- Chem. Eur. J.*, 2003, **9**, 515–519; (c) K. -Ch. Schwan, A. Y. Timoshkin, M. Zabel and M. Scheer, *Chem. Eur. J.*, 2006, **12**, 4900–4908; (d) M. Bodensteiner, U. Vogel, A. Y. Timoshkin and M. Scheer, *Angew. Chem. Int. Ed.*, 2009, **48**, 4629–4633; (e) M. Bodensteiner, A. Y. Timoshkin, E. V. Peresyphkina, U. Vogel and M. Scheer, *Chem. –Eur. J.*, 2013, **19**, 957–963; (f) C. Marquardt, A. Adolf, A. Stauber, M. Bodensteiner, A. V. Virovets, A. Y. Timoshkin and M. Scheer, *Chem. –Eur. J.*, 2013, **19**, 11887–11891; (g) C. Marquardt, C. Thoms, A. Stauber, G. Balázs, M. Bodensteiner and M. Scheer, *Angew. Chem. Int. Ed.*, 2014, **53**, 3727–3730; (h) C. Marquardt, T. Jurca, K.-C. Schwan, A. Stauber, A. V. Virovets, G. R. Whittell, I. Manners and M. Scheer, *Angew. Chem. Int. Ed.*, 2015, **54**, 13782–13786.
31. A. C. Malcolm, K. J. Sabourin, R. McDonald, M. J. Ferguson and E. Rivard, *Inorg. Chem.*, 2012, **51**, 12905–12916.
32. (a) E. R. Lory and R. F. Porter, *J. Am. Chem. Soc.*, 1973, **95**, 1766–1770; (b) Y. Kawashima, K. Kawaguchi and E. J. Hirota. *Chem. Phys.*, 1987, **87**, 6331–6333; (c) C. A. Thompson and L. Andrews, *J. Am. Chem. Soc.*, 1995, **117**, 10125–10126; (d) F. Zhang, P. Maksyutenko, R. I. Kaiser, A. M. Mebel, A. Gregusova, S. A. Perera and R. J. Bartlett, *J. Phys. Chem. A*, 2010, **114**, 12148–12154.
33. For selected computational studies on HBNH, see: (a) N. C. Baird and R. K. Datta, *Inorg. Chem.*, 1972, **11**, 17–19; (b) M. H. Matus, D. J. Grant, M. T. Nguyen and D. A. Dixon, *J. Phys. Chem. C*, 2009, **113**, 16553–16560; (c) R. Sundaram, S. Scheiner, A. K. Roy and T. J. Kar, *Phys. Chem. C*, 2015, **119**, 3253–3259.
34. (a) A. K. Swarnakar, C. Hering-Junghans, K. Nagata, M. J. Ferguson, R. McDonald, N. Tokitoh and E. Rivard, *Angew. Chem. Int. Ed.*, 2015, **54**, 10666–10669; (b) A. K. Swarnakar, C. Hering-Junghans, M. J. Ferguson, R. McDonald and E. Rivard, *Chem. Sci.*, 2017, **8**, 2337–2343.
35. E. Rivard, *Dalton Trans.*, 2014, **43**, 8577–8586.
36. (a) E. Rivard, *Chem. Soc. Rev.*, 2016, **45**, 989–1003. (b) J. M. Jasinski and S. M. Gates, *Acc. Chem. Res.*, 1991, **24**, 9–15.

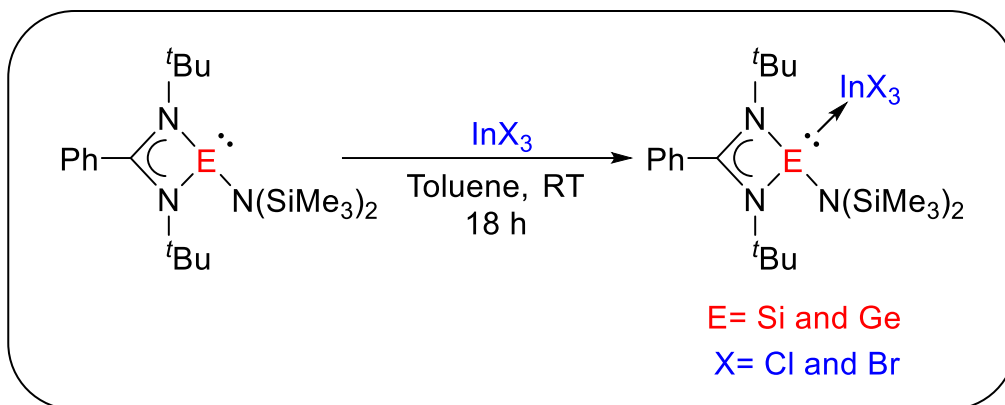
37. (a) X. Wang, L. Andrews and G. P. Kushto, *J. Phys. Chem. A*, 2002, **106**, 5809–5816; (b) T. C. Smith, D. J. Clouthier, W. Sha and A. G. Adam, *J. Chem. Phys.*, 2000, **113**, 9567–9576.
38. K. C. Thimer, S. M. I. Al-Rafia, M. J. Ferguson, R. McDonald and E. Rivard, *Chem. Commun.*, 2009, 7119–7121.
39. (a) S. M. I. Al-Rafia, A. C. Malcolm, S. K. Liew, M. J. Ferguson and E. Rivard, *J. Am. Chem. Soc.*, 2011, **133**, 777–779;
40. S. M. I. Al-Rafia, A. C. Malcolm, R. McDonald, M. J. Ferguson and E. Rivard, *Chem. Commun.*, 2012, **48**, 1308–1310.
41. (a) T. J. Marks, *J. Am. Chem. Soc.*, 1971, **93**, 7090–7091; (b) T. J. Marks and A. R. Newman, *J. Am. Chem. Soc.*, 1973, **95**, 769–773; (c) G. W. Grynkewich, B. Y. K. Ho, T. J. Marks, D. J. Tomaja and J. J. Zuckerman, *Inorg. Chem.*, 1973, **12**, 2522–2525. For reviews on divalent tetrel (:ER<sub>2</sub>) coordination chemistry, see: (d) W. Petz, *Chem. Rev.*, 1986, **86**, 1019–1047; (e) M. S. Holt, W. L. Wilson and J. H. Nelson, *Chem. Rev.*, 1989, **89**, 11–49.
42. R. Becerra, P. P. Gaspar, C. R. Harrington, W. J. Leigh, I. Vargas-Baca, R. Walsh and D. Zhou, *J. Am. Chem. Soc.*, 2005, **127**, 17469–17478.
43. (a) K.-H. Scherping and W. P. Neumann, *Organometallics*, 1982, **1**, 1017–1020; (b) B. Watta, W. P. Neumann and J. Sauer, *Organometallics*, 1985, **4**, 1954–1957. For stable examples of diorganostannylenes, see: (c) T. Fjeldberg, A. Haaland, B. E. R. Schilling, M. F. Lappert and A. J. Thorne, *J. Chem. Soc., Dalton Trans.*, 1986, 1551–1556; (d) G. H. Spikes, Y. Peng, J. C. Fettinger and P. P. Power, *Z. Anorg. Allg. Chem.*, 2006, **632**, 1005–1010.
44. For discussions on dative bonding in the main group, see: (a) A. Haaland, *Angew. Chem., Int. Ed. Engl.*, 1989, **28**, 992–1007; (b) D. Himmel, I. Krossing and A. Schnepf, *Angew. Chem., Int. Ed.*, 2014, **53**, 370–374.
45. S. M. I. Al-Rafia, M. J. Ferguson and E. Rivard, *Inorg. Chem.*, 2011, **50**, 10543–10545.
46. (a) S. M. I. Al-Rafia, M. R. Momeni, M. J. Ferguson, R. McDonald, A. Brown and E. Rivard, *Organometallics*, 2013, **32**, 6658–6665; (b) S. M. I. Al-Rafia, A. C. Malcolm, R. McDonald, M. J. Ferguson and E. Rivard, *Angew. Chem. Int. Ed.*, 2011, **50**, 8354–8357.

- 
47. C. L. B. Macdonald and B. D. Ellis, *In The Encyclopedia of Inorganic Chemistry, 2nd edition*; R. B. King, editor, John Wiley & Sons.: Chichester, U.K., 2005.
48. R. Kinjo, B. Donnadieu, M. A. Celik, G. Frenking and G. Bertrand, *Science*, 2011, **333**, 610–613.
49. C. Cui, H. W. Roesky, H.-G. Schmidt, M. Noltemeyer, H. Hao and F. Cimpoesu, *Angew. Chem. Int. Ed.*, 2000, **39**, 4274–4276.
50. K. C. Mondal, H. W. Roesky, M. C. Schwarzer, G. Frenking, B. Niepötter, H. Wolf, R. Herbst-Irmer and D. Stalke, *Angew. Chem. Int. Ed.*, 2013, **52**, 2963–2967.
51. Y. Xiong, S. Yao, S. Inoue, J. D. Epping and M. Driess, *Angew. Chem. Int. Ed.*, 2013, **52**, 7147–7150.
52. Y. Xiong, S. Yao, G. Tan, S. Inoue and M. Driess, *J. Am. Chem. Soc.*, 2013, **135**, 5004–5007.
53. Y. Li, K. C. Mondal, H. W. Roesky, H. Zhu, P. Stollberg, R. Herbst-Irmer, D. Stalke and D. M. Andrada, *J. Am. Chem. Soc.*, 2013, **135**, 12422–12428.
54. T. Chu, L. Belding, A. van der Est, T. Dudding, I. Korobkov and G. I. Nikonov, *Angew. Chem. Int. Ed.*, 2014, **53**, 2711–2715.
55. M. Driess and H. Grützmacher, *Angew. Chem. Int. Ed. Engl.*, 1996, **35**, 828–856.
56. R. C. Fischer and P. P. Power, *Chem. Rev.*, 2010, **110**, 3877–3923.
57. D. Martin, M. Soleilhavoup and G. Bertrand, *Chem. Sci.*, 2011, **2**, 389–399.
58. P. P. Power, *Acc. Chem. Res.*, 2011, **44**, 627–637.
59. (a) R. Becerra, J. P. Cannady and R. J. Walsh, *Phys. Chem. A*, 2002, **106**, 4922–4927. (b) R. Becerra, J. P. Cannady and R. Walsh, *J. Phys. Chem. A*, 2003, **107**, 9588–9593. (c) R. Becerra, J. P. Cannady and R. Walsh, *J. Phys. Chem. A*, 2006, **110**, 6680–6686.
60. R. Rodriguez, D. Gau, Y. Contie, T. Kato, N. Saffon-Merceron and A. Baceiredo, *Angew. Chem. Int. Ed.*, 2011, **50**, 11492–11495.
61. (a) P. P. Power, *Chem. Rec.*, 2011, **12**, 238–255. (b) T. Chivers and J. Konu, *Inorg. Chem.*, 2009, **30**, 131–176.
62. S. Yao, Y. Xiong and M. Driess, *Organometallics*, 2011, **30**, 1748–1767.
63. D. W. Stephan, *Org. Biomol. Chem.*, 2008, **6**, 1535–1539.
64. D. W. Stephan, *J. Am. Chem. Soc.*, 2015, **137**, 10018–10032.
-

65. (a) A. Jana, G. Tavcar, H. W. Roesky and M. John, *Dalton Trans.*, 2010, **39**, 9487–9489; (b) K. Les c yńska, A. Mix, R. J. F. Berger, B. Rummel, B. Neumann, H. -G. Stammler and P. Jutzi, *Angew. Chem. Int. Ed.*, 2011, **50**, 6843–6846.
66. (a) K. Oshima, T. Ohmura and M. Suginome, *J. Am. Chem. Soc.*, 2012, **134**, 3699–3702; (b) J. Cid, J. J. Carbo and E. Fernandez, *Chem. – Eur. J.*, 2012, **18**, 1512–1521; (c) S. M. Smith and J. M. Takacs, *Org. Lett.*, 2010, **12**, 4612–4615; (d) S. M. Smith and J. M. Takacs, *J. Am. Chem. Soc.*, 2010, **132**, 1740–1741; (e) C. J. Lata and C. M. Crudden, *J. Am. Chem. Soc.*, 2010, **132**, 131–137; (f) B. Nguyen and J. M. Brown, *Adv. Synth. Catal.*, 2009, **351**, 1333–1343.
67. E. J. Corey, R. K. Bakshi and S. Shibata, *J. Am. Chem. Soc.*, 1987, **109**, 5551–5553.
68. A. J. Blake, A. Cunningham, A. Ford, S. J. Teat and S. Woodward, *Chem. Eur. J.*, 2000, **6**, 3586–3594.
69. (a) T. J. Hadlington, M. Hermann, G. Frenking and C. Jones, *J. Am. Chem. Soc.*, 2014, **136**, 3028–3031. (b) J. Schneider, C. P. Sindlinger, S. M. Freitag, H. Schubert and L. Wesemann, *Angew. Chem. Int. Ed.*, 2017, **56**, 333–337. (c) Y. Wu, C. Shan, Y. Sun, P. Chen, J. Ying, J. Zhu, L(Luo). Liu and Y. Zhao, *Chem. Commun.*, 2016, **52**, 13799–13802.
70. C.-C. Chong, H. Hirao and R. Kinjo, *Angew. Chem. Int. Ed.*, 2015, **54**, 190–194.
71. Z. Yang, M. Zhong, X. Ma, S. De, C. Anusha, P. Parameswaran and H. W. Roesky, *Angew. Chem. Int. Ed.*, 2015, **54**, 10225–10229.
72. (a) V. K. Jakhar, M. K. Barman and S. Nembenna, *Org. Lett.*, 2016, **18**, 4710–4713. (b) J. R. Lawson, L. C. Wilkins and R. L. Melen, *Chem. - Eur. J.*, 2017, **23**, 10997–11000.
73. (a) C. Weetman, M. D. Anker, M. Arrowsmith, M. S. Hill, G. Kociok-Köhn, D. J. Liptrot and M. F. Mahon, *Chem. Sci.*, 2016, **7**, 628–641. (b) C. Weetman, M. S. Hill and M. F. Mahon, *Chem. Commun.*, 2015, **51**, 14477–14480.
74. (a) M.-A. Courtemanche, M.-A. Légaré, L. Maron and F.-G. Fontaine, *J. Am. Chem. Soc.*, 2013, **135**, 9326–9329. (b) D. Franz, L. Sirtl, A. Pöthig and S. Inoue, *Z. Anorg. Allg. Chem.*, 2016, **642**, 1245–1250. (c) J. L. Lortie, T. Dudding, B. M. Gabidullin and G. I. Nikonov, *ACS Catal.*, 2017, **7**, 8454–8459.
75. (a) J. R. Lawson, L. C. Wilkins and R. L. Melen, *Chem. - Eur. J.*, 2017, **23**, 10997–11000. (b) J. L. Carden, L. J. Gierlichs, D. F. Wass, D. L. Browne and R. L. Melen, *Chem.*

- Commun.*, 2019, **55**, 318–321. (c) J. S. McGough, S. M. Butler, I. A. Cade and M. J. Ingleson, *Chem. Sci.*, 2016, **7**, 3384–3389. (d) M. Fleige, J. Möbus, T. vom Stein, F. Glorius and D. W. Stephan, *Chem. Commun.*, 2016, **52**, 10830–10833. (e) Q. Yin, S. Kemper, H. F. T. Klare and M. Oestreich, *Chem. - Eur. J.*, 2016, **22**, 13840–13844. (f) A. Prokofjevs, A. Boussonihre, L. Li, H. Bonin, E. Lacite, D. P. Curran and E. Vedejs, *J. Am. Chem. Soc.*, 2012, **134**, 12281–12288.
76. (a) Z. Yang, M. Zhong, X. Ma, K. Nijesh, S. De, P. Parameswaran and H. W. Roesky, *J. Am. Chem. Soc.*, 2016, **138**, 2548–2551. (b) A. Bismuto, S. P. Thomas and M. J. Cowley, *Angew. Chem. Int. Ed.*, 2016, **55**, 15356–15359. (c) A. Bismuto, M. J. Cowley and S. P. Thomas, *ACS Catal.*, 2018, **8**, 2001–2005.
77. (a) M. K. Bisai, S. Pahar, T. Das, K. Vanka and S. S. Sen, *Dalton Trans.*, 2017, **46**, 2420–2424. (b) T. J. Hadlington, M. Hermann, G. Frenking and C. Jones, *J. Am. Chem. Soc.*, 2014, **136**, 3028–3031; (c) C. C. Chong, H. Hirao and R. Kinjo, *Angew. Chem. Int. Ed.*, 2015, **54**, 190–194.
78. A. Jana, H. W. Roesky, C. Schulzke, A. Döring, T. Beck, A. Pal and R. Herbst-Irmer, *Inorg. Chem.*, 2009, **48**, 193–197.
79. M. L. Shegavi and S. K. Bose, *Catal. Sci. Technol.*, 2019, **9**, 3307–3336.
80. M. K. Sharma, M. Ansari, P. Mahawar, G. Rajaraman and S. Nagendran, *Dalton Trans.*, 2019, **48**, 664–672.
81. R. Dasgupta, S. Das, S. Hiwase, S. Pati and S. Khan, *Organometallics*, 2019, **38**, 1429–1435.
82. K. Nakaya, S. Takahashi, A. Ishii, K. Boonpalit, P. Surawatanawong and N. Nakata, *Dalton Trans.*, 2021, **50**, 14810–14819.

## Chapter 2: Access to Silicon(II)– and Germanium(II)–Indium Compounds



### Abstract:

In spite of the amazing behaviour of N-heterocyclic silylene to perform as a Lewis base and form stable Lewis adducts with group 13 elements such as boron, aluminum, and gallium, there has been no such analogous investigation with indium and the realization of a stable silylene–indium complex has still remained elusive. Similarly, a germylene–indium complex is also presently unknown. We pronounce herein the reactions of  $[\text{PhC}(\text{N}^t\text{Bu})_2\text{SiN}(\text{SiMe}_3)_2]$  (**1a**) and  $[\text{PhC}(\text{N}^t\text{Bu})_2\text{GeN}(\text{SiMe}_3)_2]$  (**1b**) with  $\text{InCl}_3$  and  $\text{InBr}_3$  that have brought out the first silylene–indium complexes,  $[\text{PhC}(\text{N}^t\text{Bu})_2\text{Si}\{\text{N}(\text{SiMe}_3)_2\} \rightarrow \text{InCl}_3]$  (**2.1**) and  $[\text{PhC}(\text{N}^t\text{Bu})_2\text{Si}\{\text{N}(\text{SiMe}_3)_2\} \rightarrow \text{InBr}_3]$  (**2.2**), as well as the first germylene–indium complexes,  $[\text{PhC}(\text{N}^t\text{Bu})_2\text{Ge}\{\text{N}(\text{SiMe}_3)_2\} \rightarrow \text{InCl}_3]$  (**2.3**) and  $[\text{PhC}(\text{N}^t\text{Bu})_2\text{Ge}\{\text{N}(\text{SiMe}_3)_2\} \rightarrow \text{InBr}_3]$  (**2.4**). The solid-state molecular structures of all species have been authenticated by single-crystal X-ray diffraction studies. Note that **2.3** and **2.4** are the first structurally characterized organometallic compounds that feature a Ge–In single bond (apart from the compounds in Zintl phases). Theoretical calculations reveal that the Si(II)→In bonds in **2.1** and **2.2** and the Ge(II)→In bonds in **2.3** and **2.4** are dative in nature.



## 2.1. Introduction

The concept of chemical bonding is primarily described as the combination of a Lewis base and a Lewis acid, forming a Lewis adduct, has celebrated its centenary anniversary<sup>1</sup> and is still mounting stronger day by day. With the progress of stable N-heterocyclic carbenes (NHCs) and their higher homologues, N-heterocyclic silylenes (NHSis), we have entered into a new era of neutral Lewis bases. The realization of NHC and NHSi complexes of main-group elements has seen a flurry of research activity into their bonding properties and reactivity in recent years.<sup>2,3</sup> However, there are a few main-group halides for which the coordination chemistry of NHC and NHSi either has been explored only recently or has not been developed at all. Indium halide is one of the prominent example of such a halide. In fact, the organometallic chemistry of indium is, by far, significantly less developed in comparison to its lighter congeners such as boron, aluminum, and gallium. This is partially due to the low solubility of indium halides in a majority of organic solvents. Nevertheless, on adoption of a salt elimination methodology between  $\text{InCl}_3$  and lithiated ligands, quite a few indium derivatives have been isolated.<sup>4</sup> Very recently, Braunschweig and co-workers reported the formation of a metal-only Lewis pair (MOLP)<sup>5</sup> between indium halides and electron-rich coordinatively unsaturated zerovalent platinum compounds.<sup>6</sup> They have also demonstrated that a dynamic equilibrium exists between MOLPs and their oxidative addition products.<sup>6</sup> The N-heterocyclic carbene (NHC) chemistry of indium has also come to the fore in recent years. The advances made in this field have mainly come from the group of Jones and co-workers, who isolated the coordination complexes between NHC and indium halides.<sup>7a,b</sup> Subsequently, their trimethyl complexes with NHCs have also been realized.<sup>7c</sup> Detailed quantum mechanical calculations on the structures and stabilities of NHC–indium adducts have also been reported in literature.<sup>8</sup>

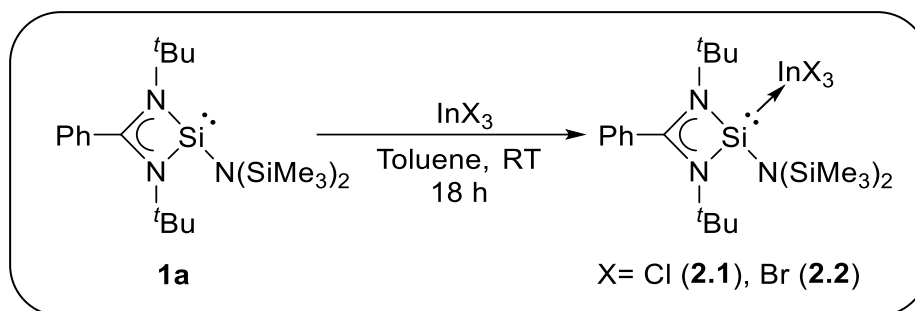
The use of indium compounds in electronics (indium is becoming one of the most important dopant species for silicon crystals used in photovoltaics, for instance)<sup>9</sup> has provided renewed interest in the chemistry of silicon and indium chemistry. Early works by Götze,<sup>10</sup> Cowley,<sup>11</sup> Weidlein,<sup>12</sup> and, to a large extent, by Wiberg<sup>13</sup> have led to the isolation of a variety of silyl–indium compounds, where the formal oxidation state of silicon is +4. However, in recent years, attention has shifted to silicon compounds, where the formal oxidation state of silicon is +2, popularly known as

silylenes.<sup>14</sup> Illustrations of carbonyl-free silylene complexes of 3d transition metals in the formal oxidation state +2 are now too frequent to be comprehensively listed, thanks to extensive investigations by the groups of H. Roesky, P. Roesky, Stalke, Driess, Tacke, Inoue, Khan, and many others.<sup>15–26</sup> The coverage of the s and p blocks is also expanding and is supplemented by examples of bonding to *s*-/*p*-block Lewis acids such as boron,<sup>27</sup> aluminum,<sup>27</sup> calcium,<sup>28</sup> germanium,<sup>29</sup> tin,<sup>30</sup> and lead.<sup>30</sup> However, when it comes to indium, there has only been one reaction reported between a Si(II) compound and an indium derivative. Jutzi and co-workers reported the reaction of decamethylsilicocene with InMe<sub>3</sub> that led to the disilyl indium compound [Cp\*<sub>2</sub>Si(Me)]<sub>2</sub>InMe in place of a stable silylene–indium adduct, resulting from the insertion of the silylene moiety into the two In–C bonds.<sup>31</sup> Therefore, a typical silylene–indium adduct is still inaccessible. In light of the extensive coordination chemistry of [PhC(N<sup>t</sup>Bu)<sub>2</sub>SiN(SiMe<sub>3</sub>)<sub>2</sub>] (**1a**)<sup>32</sup> toward main group halides, we have investigated the reactions of **1a** with indium halides. The reaction scope has also been extended to the analogous Ge(II) amide [PhC(N<sup>t</sup>Bu)<sub>2</sub>GeN(SiMe<sub>3</sub>)<sub>2</sub>] (**1b**)<sup>33</sup> with indium halides as, to the best of our knowledge, no compound with a Ge–In single bond has been structurally characterized. The report of a Ge–In single bond has only been found in Zintl compounds such as La<sub>3</sub>In<sub>4</sub>Ge and La<sub>3</sub>InGe.<sup>34</sup> In this chapter, we have discussed the first silylene–indium and germylene–indium complexes and their isolation, structural elucidation, and bonding properties.

## 2.2. Results and discussion

### 2.2.1. Synthesis and characterization of complexes **2.1** and **2.2**

The preparation of the complexes **2.1** and **2.2** involves one-pot reaction of **1a** with an equimolar amount of InCl<sub>3</sub> or InBr<sub>3</sub> in toluene, and monomeric compounds of composition [PhC(N<sup>t</sup>Bu)<sub>2</sub>Si{N(SiMe<sub>3</sub>)<sub>2</sub>}→InCl<sub>3</sub>] (**2.1**) and [PhC(N<sup>t</sup>Bu)<sub>2</sub>Si{N(SiMe<sub>3</sub>)<sub>2</sub>}→InBr<sub>3</sub>] (**2.2**) (Scheme 2.1) were obtained as colorless precipitates. The removal of toluene and subsequent workup in THF resulted in the colorless crystals of **2.1** and **2.2**.

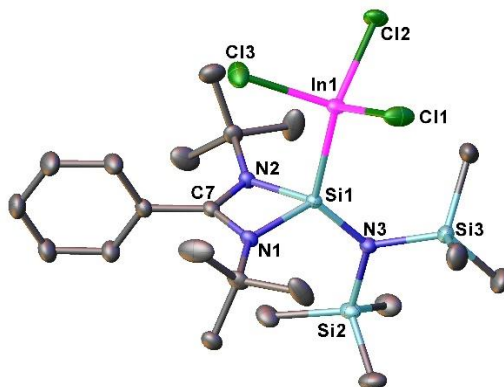


**Scheme 2.1:** Reactions of Si(II) amide with indium halides

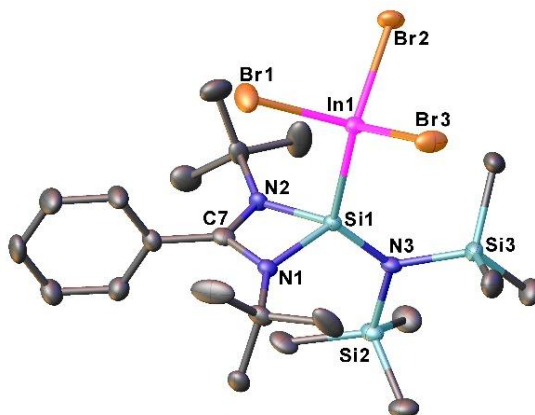
As per our anticipation, the adducts are insoluble in most of solvents and marginally soluble in THF and  $\text{CHCl}_3$ . Moreover, they show a tendency toward decomposition, resulting in a grayish precipitate, which is most probably elemental indium. The partial solubility of the adducts in  $\text{CDCl}_3$  allowed us to record the  $^1\text{H}$  NMR spectra. The  $^1\text{H}$  NMR spectra of **2.1** and **2.2** show typical signals for the  $^t\text{Bu}$  protons in the amidinate ligand ( $\delta$  1.42 (**2.1**) and 1.35 (**2.2**) ppm). We could not obtain any resonance in the solution-state  $^{29}\text{Si}$  NMR spectrum presumably due to the low solubility of the adducts and gradual decomposition towards elemental indium. However, in the solid state, the  $^{29}\text{Si}$  NMR chemical shift of **2.2** appears at  $\delta$  -31.7 ppm, while **2.1** shows a broad signal ranging from -54.4 to -84.3 ppm, which are in good accordance with silylene adducts previously reported by Khan, Tacke, and others.<sup>25,26,27a</sup> The appearance of two signals for the trimethylsilyl groups in  $^1\text{H}$  (**2.1**,  $\delta$  0.56 and 0.65 ppm; **2.2**, 0.50 and 0.60 ppm) as well as  $^{29}\text{Si}$  NMR of **2.1** and **2.2** indicates that they are not equivalent, resulting from the hindered rotation due to the presence of the bulky substituents around the Si(II) atom. The molecular ion peaks were observed with the highest relative intensity in the ESI-MS spectrum at  $m/z$  676.1 (**2.1**) and 784.9 (**2.2**).

### 2.2.2. Structural Elucidation of complex **2.1** and **2.2**

The molecular structures of compounds **2.1** and **2.2** are depicted in Figures 2.1 and 2.2, respectively. The selected bond lengths of **2.1** and **2.2** are given in Table 2.1. Both crystallize in the monoclinic space group  $P2_1/n$ .<sup>35</sup> The structural parameters of **2.1** and **2.2** are very much alike, and the noticeable alterations of the bond lengths and angles are attributed to the halide atoms being different. The Si(II) atoms in **2.1** and **2.2** are four coordinated and exhibit a slightly distorted tetrahedral geometry.



**Fig. 2.1:** Molecular structure of **2.1**. Anisotropic displacement parameters are depicted at the 50% probability level. Hydrogen atoms are omitted for clarity. Selected bond lengths and angles are given in Table 2.1.



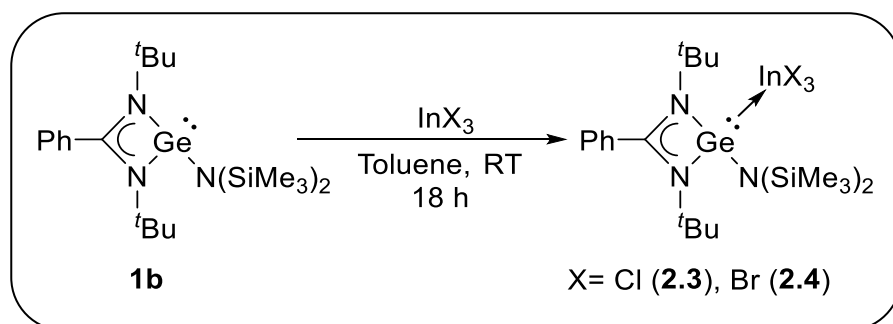
**Fig. 2.2:** Molecular structure of **2.2**. Anisotropic displacement parameters are depicted at the 50% probability level. Hydrogen atoms are omitted for clarity. Selected bond lengths and angles are given in Table 2.1.

The Si–N(SiMe<sub>3</sub>)<sub>2</sub> bond distances in **2.1** and **2.2** are 1.6946(16) and 1.697(4) Å, respectively, which are shorter than that in the parent silylene **1a** (1.769(7) Å). The respective Si(II)–In bond lengths in **2.1** and **2.2** are 2.5804(5) and 2.5840(12) Å, respectively, which are marginally longer than the sum of their covalent radii (2.55 Å). Although, to the best of our knowledge, Si(II)–In bond lengths have not been reported previously, the value is very close to that in the doubly chloride bridged complex [{(Me<sub>3</sub>Si)<sub>3</sub>Si}<sub>2</sub>In(μ-Cl)<sub>2</sub>Li(thf)<sub>2</sub>] (2.591(7) Å) reported by Cowley and coworkers,<sup>11</sup> but substantially shorter than those in the previously reported complexes In<sub>8</sub>(Si<sup>*i*</sup>Bu<sub>3</sub>)<sub>6</sub>

(2.615(1)–2.683(1) Å)<sup>13b</sup> and  $\text{In}_{12}(\text{Si}^t\text{Bu}_3)_8$  (2.668(3)–2.685(3) Å).<sup>13c</sup> The geometry around the indium atom in **2.1** and **2.2** is distorted tetrahedral. The average In–Cl distance observed in **2.1** is 2.3869 Å, which is marginally longer than the average In–Cl bond length in  $\text{IMes}\cdot\text{InCl}_3$  (2.352 Å).<sup>6</sup> Similarly, the average In–Br bond length (2.5206 Å) is slightly longer than that in Jones'  $[\text{InBr}_3\{\text{CN}(^i\text{Pr})\text{C}_2\text{Me}_2\text{N}(^i\text{Pr})\}]$  (2.500 Å).<sup>5</sup>

### 2.2.3. Synthesis and characterization of complex **2.3** and **2.4**

To the best of our knowledge, structural authentication of a compound with a Ge–In single bond has no precedence (apart from those in Zintl phases). Rösch et al. reported that  $\text{In}(\text{GeEt}_3)_3$  could not be isolated as a pure compound, and no other preparative details are available.<sup>36</sup> It was characterized only by IR spectroscopy.<sup>37</sup> Using the same synthetic strategy similar to silylene–indium complexes, the germylene–indium complexes,  $[\text{PhC}(\text{N}^t\text{Bu})_2\text{Ge}\{\text{N}(\text{SiMe}_3)_2\}\rightarrow\text{InCl}_3]$  (**2.3**) and  $[\text{PhC}(\text{N}^t\text{Bu})_2\text{Ge}\{\text{N}(\text{SiMe}_3)_2\}\rightarrow\text{InBr}_3]$  (**2.4**), were prepared from **1b** utilizing 1:1 mixture of indium halides in toluene (Scheme 2.2). Filtration of the solvent and further recrystallization at  $-35\text{ }^\circ\text{C}$  in a freezer, afforded the desired complexes in good yield. The single-crystal X-ray studies confirm the identity of **2.3** and **2.4**, which are the first structurally authenticated compounds having a Ge–In single bond (Figures 2.3 and 2.4).



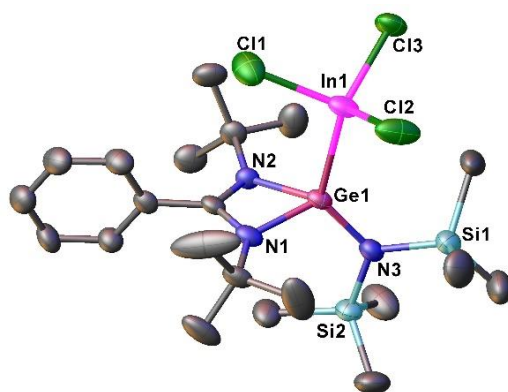
**Scheme 2.2:** Reactions of Ge(II) Amide with Indium Halides

The germylene–indium complexes **2.3** and **2.4** are insoluble in most of organic solvents and partially soluble in THF and  $\text{CHCl}_3$  akin to the silylene–indium complexes. They also have a tendency to decompose towards elemental indium. The  $^1\text{H}$  NMR spectra of **2.3** and **2.4** show typical signals for the tBu protons in the amidinate ligand ( $\delta$  1.23 (**2.3**), and 1.24 (**2.4**) ppm). On other hand, both **2.3** and **2.4** display two signals for the  $\text{SiMe}_3$  moieties in their respective  $^1\text{H}$  NMR spectra (**2.3**,  $\delta$  0.43 and 0.62 ppm; **2.4**,  $\delta$  0.42 and 0.63 ppm), representing that they are not

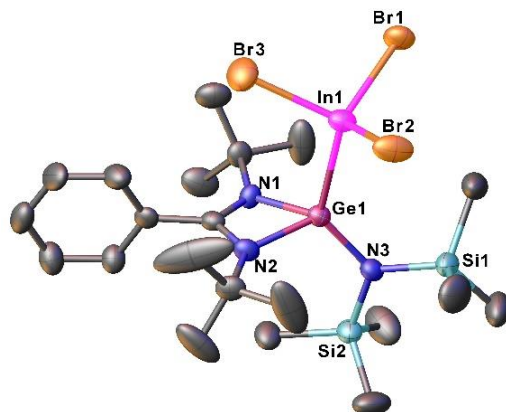
equivalent. The molecular ion peaks were observed in the ESI-MS spectrum at  $m/z$  700.0 (**2.3**), and 830.9 (**2.4**) with the highest relative intensity.

#### 2.2.4. Structural Elucidation of complex **2.3** and **2.4**

The molecular structure of **2.3** and **2.4** are shown in figures 2.3 and 2.4. Both **2.3** and **2.4** crystallize in the monoclinic space group  $P2_1/n$ . The structural features of **2.3** and **2.4** are very similar to those of **2.1** and **2.2**. Both Ge atoms in **2.3** and **2.4** are four-coordinated and adopt a distorted-tetrahedral geometry. The Ge–In bonds were determined to be 2.6167(6) (**2.3**) and 2.6241(6) (**2.4**) Å, which are shorter than the sum of the germanium and indium covalent radii (2.72 Å)<sup>38a</sup> and expectedly longer than those reported for [(<sup>t</sup>Bu<sub>2</sub>MeSi)<sub>2</sub>GeInGe(SiMe<sup>t</sup>Bu<sub>2</sub>)<sub>2</sub>][Li(thf)<sub>4</sub>] (2.5453(4) and 2.5387(4) Å), where the Ge–In bonds possess some double bond character.<sup>38b</sup> The Ge–N<sub>amidinate</sub> bond lengths are comparable to those in **1b** and previously reported amidinato germylene chloride [PhC(N<sup>t</sup>Bu)<sub>2</sub>GeCl].<sup>39</sup> The geometry of the In atoms in **2.3** and **2.4** is close to tetrahedral, as observed from the mean Ge–In–Cl (111.5°) and Ge–In–Br (111.29°) bond angles. The In–Cl and In–Br bonds in **2.3** and **2.4** are comparable to those of **2.1** and **2.2**, respectively.



**Fig. 2.3:** Molecular structure of **2.3**. Anisotropic displacement parameters are depicted at the 50% probability level. Hydrogen atoms are omitted for clarity. Selected bond lengths and angles are given in Table 2.1.



**Fig. 2.4:** Molecular structure of **2.4**. Anisotropic displacement parameters are depicted at the 50% probability level. Hydrogen atoms are omitted for clarity. Selected bond lengths and angles are given in Table 2.1.

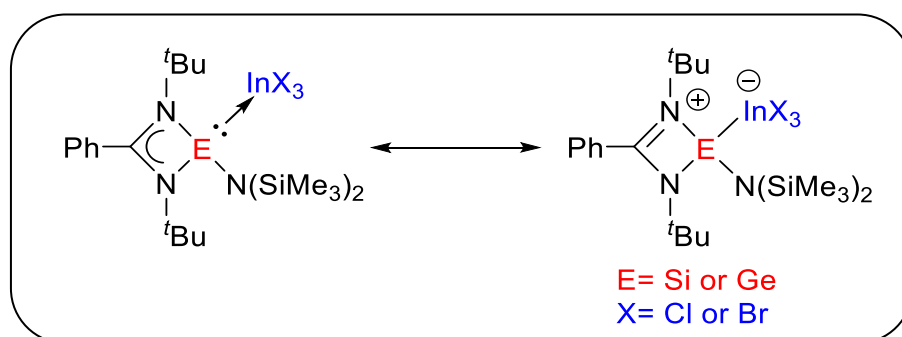
Parameters	<b>2.1</b>	<b>2.2</b>	<b>2.3</b>	<b>2.4</b>
Si–In	2.5804(5) Å	2.5804(12) Å	-	-
Ge–In	-	-	2.6167(6) Å	2.6241(6) Å
In–Cl	2.3806(5), 2.3845(5), 2.3977(6) Å	-	2.3567(14), 2.3611(15), 2.3609(16) Å	-
In–Br		2.5278(6), 2.5174(5), 2.5167(5) Å		2.4932(17), 2.5019(8), 2.5011(6) Å
Si–N(SiMe <sub>3</sub> ) <sub>2</sub>	1.6946(16) Å	1.697(4) Å		
Ge–N(SiMe <sub>3</sub> ) <sub>2</sub>			1.811(4) Å	1.814(4) Å
∠Si–In–Cl	119.566(17), 117.018(18), 105.085(17)°	-	-	-
∠Si–In–Br	-	105.90(3), 117.70(3), 118.42(3)°	-	-
∠Ge–In–Cl	-	-	115.37(4), 113.48(4), 105.26(4)°	-
∠Ge–In–Br	-	-	-	116.35(2), 106.11(2), 111.41(2)°
∠In–Si–N(SiMe <sub>3</sub> ) <sub>2</sub>	124.43(6)°	124.27(13)°	-	-

$\angle \text{In-Ge-N}(\text{SiMe}_3)_2$	-	-	128.79(13) $^\circ$	128.49 (13) $^\circ$
--	---	---	---------------------	----------------------

**Table 2.1:** Structural parameters of **2.1**, **2.2**, **2.3**, and **2.4**.

### 2.2.5. Theoretical Studies

As silylene- and germylene-indium complexes have not been reported in the literature before, we were intrigued to gain insight into the nature of the Si-In and Ge-In bonds in these complexes. The classical dative bonding concept in main-group compounds has recently fashioned passionate debate in the recent literature.<sup>40-42</sup> In order to gain more insight into the bonding in silylene-indium and germylene-indium complexes, density functional theory (DFT) calculations have been performed with the aid of the Turbomole 7.1 suite of programs,<sup>43</sup> using the PBE functional.<sup>44</sup> The def-TZVP<sup>45</sup> basis set has been employed. The resolution of identity (RI),<sup>46</sup> along with the multipole accelerated resolution of identity (marij)<sup>47</sup> calculations have been hired for an accurate and effectual treatment of the electronic Coulomb term in the DFT calculations. The values stated are  $\Delta G$  values, with zero-point energy corrections, internal energy and entropic contributions encompassed through frequency calculations on the optimized minima, with the temperature fixed at 298.15 K. Harmonic frequency calculations were performed for all stationary points to confirm them as local minima or transition state structures. The NBO<sup>48</sup> analysis (single point calculations done using the final geometry obtained at PBE/def-TZVP level of theory as described above) in this study has been performed with density functional theory, with the aid of Gaussian 9.0,<sup>49</sup> using the PBE functional and the def2-TZVP<sup>50</sup> basis set. The Si-In or Ge-In bond can be interpreted either as a classical donor-acceptor bond between the In(III) species and a silylene or germylene or as an ion pair consisting of a silyl or germyl cation with a Si-In or Ge-In single bond (see Figure 2.5).





**Fig. 2.5.** Possible bonding interpretation for the complexes **2.1–2.4**.

We have chosen as a standard tris(trimethylsilyl)indium species  $\text{In}(\text{SiMe}_3)_3$  (**1c**),<sup>10</sup> a molecule with a Si–In single bond. We have also performed calculations on the model silylene–indium compound with a three-coordinate silicon center bearing a Si–In bond such as the diaminosilylene–indium complexes  $(\text{Me}_2\text{N})_2\text{Si}:\rightarrow\text{InX}_3$  (X = Cl (**1d**), Br (**1e**)). The nature of the Si–In bond has been analyzed on the basis of four parameters: (a) bond dissociation energy (BDE), (b) shared electron number (SEN), which is an indicator of covalent bond strength, (c) Wiberg bond index (WBI), and (d) bond length. The results of the calculations are shown in Table 2.2. A dative bond can be distinguished from an electron-sharing bond by the nature of dissociation of the bond. The former favors heterolytic dissociation while the latter prefers homolytic dissociation.<sup>40</sup> Calculations suggest that both **2.1** and **2.2** prefer heterolytic cleavage (BDEs of 42.2 and 38.7 kcal/mol, respectively) over homolytic cleavage (BDEs of 122.1 and 117.3 kcal/mol, respectively), similar to those in **1d** and **1e** (heterolytic cleavage (BDEs of 23.7 and 21.7 kcal/mol respectively) vs homolytic cleavage (BDEs of 134.0 and 130.7 kcal/mol respectively)), while the standard molecule **1c**, with a Si–In single bond, prefers homolytic cleavage (BDE of 46.0 kcal/mol) over heterolytic cleavage (BDE of 149.9 kcal/mol). This indicates dative bond character in the Si–In bond in complexes **2.1** and **2.2**. Even though the Si–In bond lengths in **2.1**, **2.2**, and **1c** do not show significant differences, both SEN and WBI values obtained from calculations for **2.1** and **2.2** are less than the values obtained for **1c** (see Table 2.2) but are in good agreement with those obtained for **1d** and **1e**, indicating the dative bond character of the Si–In bond in **2.1** and **2.2**.

	<b>2.1</b>	<b>2.2</b>	<b>2.3</b>	<b>2.4</b>	<b>1c</b>	<b>1d</b>	<b>1e</b>
BDE for homolytic cleavage ( $\Delta G$ in kcal/mol)	122.1	117.3	124.3	120.3	46.0	134.0	130.7
BDE for heterolytic cleavage ( $\Delta G$ in kcal/mol)	42.2	38.7	29.8	27.1	149.9	23.7	21.7
SEN (In-A)	0.995	0.984	1.005	0.991	1.217	0.981	0.987
WBI (In-A)	0.739	0.745	0.671	0.675	0.823	0.677	0.691
In-A (Å)	2.63	2.64	2.67	2.69	2.64	2.68	2.68

**Table 2.2.** Bond Dissociation Energies (BDEs), Shared Electron Numbers (SENs), Wiberg Bond Indices (WBIs), and Bond Distances for Complexes **2.1–2.4** and **1c–1e**

Natural bond orbital (NBO) analysis has also been done in order to obtain more evidence for the dative bond character of the Si–In bond in complexes **2.1** and **2.2**. The general NBO criterion to distinguish a dative bond from a covalent bond is the change in the formal charge on the atoms. The calculated atomic charges  $Q_A(\text{dat})$  and  $Q_B(\text{dat})$  for a dative-bonded pair deviate markedly from the charges ( $Q_A(\text{sep})$  and  $Q_B(\text{sep})$ ) in the dissociated species by about equal and opposite amounts for A and B.<sup>42</sup> In complex **2.2**, the charge differences ( $\Delta Q$ ) calculated (see Table 2.3) as described above are  $-0.369$  for In and  $+0.400$  for Si. A similar trend is seen in complex **2.1**, with a charge difference of  $-0.381$  for In and of  $+0.376$  for Si. These data are in good agreement with those obtained for **1d** and **1e**. However, such a trend is not observed in the standard molecule **1c**, due to its covalent bond character. All of these results clearly indicate that the bond between Si and In is a classical donor–acceptor bond.

Charge	2.1		2.2		2.3		2.4	
	Si	In	Si	In	Ge	In	Ge	In
Q(dat)	1.495	1.010	1.519	0.774	1.338	1.046	1.356	0.804
Q(sep)	1.119	1.391	1.119	1.143	1.088	1.391	1.088	1.143
$\Delta Q(Q(\text{dat}) - Q(\text{sep}))$	0.376	-0.381	0.400	-0.369	0.250	-0.345	0.268	-0.339

Charge	1c		1d		1e	
	Si	In	Si	In	Si	In
Q(dat)	1.015	0.400	1.337	1.003	1.359	0.750
Q(sep)	1.204	0.369	1.001	1.391	1.001	1.143
$\Delta Q(Q(\text{dat}) - Q(\text{sep}))$	-0.189	0.031	0.336	-0.388	0.358	-0.393

**Table 2.3.** Natural Charges for Si, Ge, and In Atoms in Complexes **2.1–2.4** and **1c–1e** and the Corresponding Separated Fragments

To the best of our knowledge, there is no compound reported so far with a Ge–In single bond. It is therefore not possible to directly compare the SEN, WBI and bond length values of the complexes **2.3** and **2.4** (provided in Table 2.2) with a standard molecule. However, calculations suggest that both **2.3** and **2.4** prefer heterolytic cleavage (BDEs of 29.8 kcal/mol and 27.1 kcal/mol respectively) over homolytic cleavage (BDEs of 124.3 kcal/mol and 120.3 kcal/mol respectively), which indicates the dative bond character of the Ge–In bond in the complexes **2.3** and **2.4**. The NBO analysis, done and discussed earlier for complexes **2.1** and **2.2**, was also conducted for complexes **2.3** and **2.4**. It was found that the charge difference ( $\Delta Q$ ) is +0.268 for Ge and -0.339 for In complex **2.4** (see Table 2.3). The same trend is found in the case of complex **2.3** as well: a charge difference of +0.250 for Ge and -0.345 for In. These results suggest that the Ge–In bond in **2.3** and **2.4** is a classical donor acceptor bond.

In order to understand the influence of solvent effects, we have performed solvent phase calculations as well. All the calculations pronounced here have been performed again with the inclusion of COSMO,<sup>51</sup> with toluene ( $\epsilon = 2.374$ ) taken as the solvent. Even though the exact values obtained from these calculations are changed due to the effect of the solvent, the trends in the values as well as the conclusions are still the same as in the case of the gas phase calculations (see Table 2.4 and 2.5). Hence, the conclusions reached with regard to the nature of the bonding in the silicon and germanium complexes are not altered when solvent effects are taken into account.

	<b>2.1</b>	<b>2.2</b>	<b>2.3</b>	<b>2.4</b>	<b>1c</b>	<b>1d</b>	<b>1e</b>
BDE for homolytic cleavage ( $\Delta G$ in kcal/mol)	87.9	84.8	89.1	86.2	45.6	93.4	91.1
BDE for heterolytic cleavage ( $\Delta G$ in kcal/mol)	42.2	39.7	30.0	27.7	102.1	24.7	23.0
SEN (In-A)	1.005	0.992	1.033	1.018	1.215	1.026	1.027
WBI (In-A)	0.758	0.761	0.695	0.697	0.823	0.717	0.726
In-A (Å)	2.62	2.63	2.66	2.67	2.64	2.66	2.66

**Table 2.4.** The bond dissociation energies (BDE), shared electron number (SEN), Wiberg bond indices (WBI), and bond distances for complexes **2.1–2.4** and **1c–1e** obtained, after the inclusion of solvent effects with COSMO.

Charge	2.1		2.2		2.3		2.4	
	Si	In	Si	In	Ge	In	Ge	In
Q(dat)	1.510	1.001	1.533	0.773	1.351	1.038	1.370	0.801
Q(sep)	1.105	1.426	1.105	1.178	1.080	1.426	1.080	1.178
$\Delta Q(Q(\text{dat}) - Q(\text{sep}))$	0.405	-0.425	0.428	-0.405	0.271	-0.388	0.290	-0.377

Charge	1c		1d		1e	
	Si	In	Si	In	Si	In
Q(dat)	1.010	0.414	1.360	0.986	1.381	0.741
Q(sep)	1.199	0.369	0.981	1.426	0.981	1.178
$\Delta Q(Q(\text{dat}) - Q(\text{sep}))$	-0.189	0.045	0.379	-0.440	0.400	-0.437

**Table 2.5.** The natural charge for Si, Ge, and In atoms in the complexes **2.1–2.4** and **1c–1e** and the corresponding separated fragments obtained after the inclusion of solvent effects with COSMO.

### 2.3. Conclusions

At the beginning of this chapter, we pointed out that there is no silylene or germylene is reported to form adduct with indium halides. In this chapter, we have shown the preparation and characterization of the first silylene complexes of indium **2.1** and **2.2**, by the reactions of  $[\text{PhC}(\text{N}^t\text{Bu})_2\text{SiN}(\text{SiMe}_3)_2]$  (**1a**) with  $\text{InCl}_3$  and  $\text{InBr}_3$ , respectively. The methodology has been extended to prepare the first germylene complexes of indium, **2.3** and **2.4**. The constitutions of **2.1–2.4** were authenticated by single-crystal X-ray studies, which confirmed the monomeric nature of these adducts. The X-ray studies, in combination with DFT calculations, suggest that the Si–In and the Ge–In bonds are of the donor–acceptor type. Overall, this study underpins the high

synthetic potential of the donor-stabilized silylenes and germylenes for the preparation of novel higher-coordinate tetrel(II) compounds.

## 2.4. References

1. G. N. Lewis, *J. Am. Chem. Soc.*, 1916, **38**, 762–785.
2. Selected examples of carbene-supported main-group compounds: (a) D. Bourissou, O. Guerret, F. P. Gabbaï and G. Bertrand, *Chem. Rev.*, 2000, **100**, 39–91. (b) Y. Wang, Y. Xie, P. Wei, R. B. King, H. F. Schaefer III; P. V. R. Schleyer and G. H. Robinson, *Science*, 2008, **321**, 1069–1071. (c) R. S. Ghadwal, H. W. Roesky, S. Merkel, J. Henn and D. Stalke, *Angew. Chem., Int. Ed.*, 2009, **48**, 5683–5686. (d) A. C. Filippou, O. Chernov and G. Schnakenburg, *Angew. Chem., Int. Ed.*, 2009, **48**, 5687–5690. (e) S. M. I. Al-Rafia, A. C. Malcom, R. McDonald, M. J. Ferguson and E. Rivard, *Angew. Chem., Int. Ed.*, 2011, **50**, 8354–8357. (f) H. Braunschweig, R. D. Dewhurst, K. Hammond, J. Mies, K. Radacki and A. Vargas, *Science*, 2012, **336**, 1420–1422. (g) K. C. Mondal, H. W. Roesky, M. C. Schwarzer, G. Frenking, B. Niepötter, H. Wolf, R. Herbst-Irmer and D. Stalke, *Angew. Chem., Int. Ed.*, 2013, **52**, 2963–2967. (h) K. C. Mondal, H. W. Roesky, M. C. Schwarzer, G. Frenking, I. Tkach, H. Wolf, D. Kratzert, R. Herbst-Irmer, B. Niepötter and D. Stalke, *Angew. Chem., Int. Ed.*, 2013, **52**, 1801–1805. (i) Y. Xiong, S. Yao, S. Inoue, J. D. Epping and M. Driess, *Angew. Chem., Int. Ed.*, 2013, **52**, 7147–7150.
3. L. Alvarez-Rodriguez, J. A. Cabeza, P. Garcia-Alvarez and D. Polo, *Coord. Chem. Rev.*, 2015, **300**, 1–28.
4. (a) F. W. B. Einstein, M. M. Gilbert and D. G. Tuck, *Inorg. Chem.*, 1972, **11**, 2832–2836. (b) O. T. Beachley Jr., R. Blom, M. R. Churchill, K. Faegri Jr., J. C. Fettinger, J. C. Pazik and L. Victoriano, *Organometallics*, 1989, **8**, 346–356. (c) A. L. Hawley, C. A. Ohlin, L. Fohlmeister and A. Stasch, *Chem. - Eur. J.*, 2017, **23**, 447–455. (d) B. Prashanth, D. Bawari and S. Singh, *ChemistrySelect*, 2017, **2**, 2039–2043.
5. Selected references on MOLP: (a) H. Braunschweig, K. Gruss and K. Radacki, *Angew. Chem., Int. Ed.*, 2007, **46**, 7782–7784. (b) H. Braunschweig, K. Gruss and K. Radacki, *Inorg. Chem.*, 2008, **47**, 8595–8597. (c) F. Hupp, M. Ma, F. Kroll, J. O. C. Jimenez-Halla,

- R. D. Dewhurst, K. Radacki, A. Stasch, C. Jones and H. Braunschweig, *Chem. - Eur. J.*, 2014, **20**, 16888–16898. (d) H. Braunschweig, M. A. Celik, R. D. Dewhurst, M. Heid, F. Hupp and S. S. Sen, *Chem. Sci.*, 2015, **6**, 425–435. (e) J. Bauer, H. Braunschweig and R. D. Dewhurst, *Chem. Rev.*, 2012, **112**, 4329–4346. (f) H. Braunschweig, P. Cogswell and K. Schwab, *Coord. Chem. Rev.*, 2011, **255**, 101–117.
6. R. Bertermann, J. Böhnke, H. Braunschweig, R. D. Dewhurst, T. Kupfer, J. H. Muessig, L. Pentecost, K. Radacki, S. S. Sen and A. Vargas, *J. Am. Chem. Soc.*, 2016, **138**, 16140–16147.
7. (a) S. J. Black, D. E. Hibbs, M. B. Hursthouse, C. Jones, K. M. A. Malik and N. A. Smithies, *J. Chem. Soc., Dalton Trans.*, 1997, 4313–4320. (b) C. D. Abernethy, M. L. Cole and C. Jones, *Organometallics*, 2000, **19**, 4852–4857. (c) M. M. Wu, A. M. Gill, L. Yunpeng, L. Yongxin, R. Ganguly, L. Falivene and F. García, *Dalton Trans.*, 2017, **46**, 854–864.
8. N. Holzmann, A. Stasch and C. Jones, *Chem. - Eur. J.*, 2011, **17**, 13517–13525.
9. S. Z. Karazhanov, *J. Appl. Phys.*, 2001, **89**, 4030–4036.
10. H. Bürger and U. Götze, *Angew. Chem., Int. Ed. Engl.*, 1969, **8**, 140–141.
11. A. M. Arif, A. H. Cowley, T. M. Elkins and R. A. Jones, *J. Chem. Soc., Chem. Commun.*, 1986, 1776–1777.
12. R. Wochele, W. Schwarz, K. W. Klinkhammer, K. Locke and J. Weidlein, *Z. Anorg. Allg. Chem.*, 2000, **626**, 1963–1973.
13. (a) N. Wiberg, K. Amelunxen, H. Nöth, M. Schmidt and H. Schwenk, *Angew. Chem., Int. Ed. Engl.*, 1996, **35**, 65–67. (b) N. Wiberg, T. Blank, A. Purath, G. Stösser and H. Schnöckel, *Angew. Chem., Int. Ed.*, 1999, **38**, 2563–2565. (c) N. Wiberg, T. Blank, H. Nöth and W. Ponikvar, *Angew. Chem., Int. Ed.*, 1999, **38**, 839–841.
14. For reviews on silicon(II) compounds, please see: (a) M. Haaf, T. A. Schmedake and R. West, *Acc. Chem. Res.*, 2000, **33**, 704–714. (b) S. Nagendran and H. W. Roesky, *Organometallics*, 2008, **27**, 457–492. (c) Y. Mizuhata, T. Sasamori and N. Tokitoh, *Chem. Rev.*, 2009, **109**, 3479–3511. (d) S. K. Mandal and H. W. Roesky, *Chem. Commun.*, 2010, **46**, 6016–6041. (e) S. Yao, Y. Xiong and M. Driess, *Organometallics*, 2011, **30**, 1748–1767. (f) M. Asay, C. Jones and M. Driess, *Chem. Rev.*, 2011, **111**, 354–396. (g) S.

- S. Sen, S. Khan, S. Nagendran and H. W. Roesky, *Acc. Chem. Res.*, 2012, **45**, 578–587. (h) S. S. Sen, S. Khan, P. P. Samuel and H. W. Roesky, *Chem. Sci.*, 2012, **3**, 659–682. (i) R. S. Ghadwal, R. Azhakar and H. W. Roesky, *Acc. Chem. Res.*, 2013, **46**, 444–456. (j) H. W. Roesky, *J. Organomet. Chem.*, 2013, **730**, 57–62. (k) S. Yadav, S. Saha and S. S. Sen, *ChemCatChem*, 2016, **8**, 486–501 and references therein.
15. J. A. Baus, F. M. Muck, H. Schneider and R. Tacke, *Chem. - Eur. J.*, 2017, **23**, 296–303.
16. F. M. Muck, J. A. Baus, A. Ulmer, C. Burschka and R. Tacke, *Eur. J. Inorg. Chem.*, 2016, **2016**, 1660–1670.
17. (a) D. Gallego, A. Breck, E. Irran, F. Meier, M. Kaupp, M. Driess and J. F. Hartwig, *J. Am. Chem. Soc.*, 2013, **135**, 15617–15626. (b) N. C. Breit, T. Szilvási, T. Suzuki, D. Gallego and S. Inoue, *J. Am. Chem. Soc.*, 2013, **135**, 17958–17968. (c) W. Wang, S. Inoue, S. Yao and M. Driess, *J. Am. Chem. Soc.*, 2010, **132**, 15890–15892. (d) G. Tan, S. Enthaler, S. Inoue, B. Blom and M. Driess, *Angew. Chem., Int. Ed.*, 2015, **54**, 2214–2218.
18. (a) D. Gallego, S. Inoue, B. Blom and M. Driess, *Organometallics*, 2014, **33**, 6885–6897. (b) B. Blom, S. Enthaler, S. Inoue, E. Irran and M. Driess, *J. Am. Chem. Soc.*, 2013, **135**, 6703–6713.
19. W. Wang, S. Inoue, S. Enthaler and M. Driess, *Angew. Chem., Int. Ed.*, 2012, **51**, 6167–6171.
20. R. Azhakar, R. S. Ghadwal, H. W. Roesky, J. Hey, L. Krause and D. Stalke, *Dalton Trans.*, 2013, **42**, 10277–10281.
21. (a) S. Schäfer, R. Köppe, M. T. Gamer and P. W. Roesky, *Chem. Commun.*, 2014, **50**, 11401–11403. (b) S. Schäfer, R. Köppe and P. W. Roesky, *Chem. - Eur. J.*, 2016, **22**, 7127–7133.
22. S. Yadav, E. Sangtani, D. Dhawan, R. G. Gonnade, D. Ghosh and S. S. Sen, *Dalton Trans.*, 2017, **46**, 11418–11424.
23. S. Khan, S. Pal, N. Kathewad, P. Parameswaran, S. De and I. Purushothaman, *Chem. Commun.*, 2016, **52**, 3880–3882.
24. N. Parvin, S. Pal, S. Khan, S. Das, S. K. Pati and H. W. Roesky, *Inorg. Chem.*, 2017, **56**, 1706–1712.

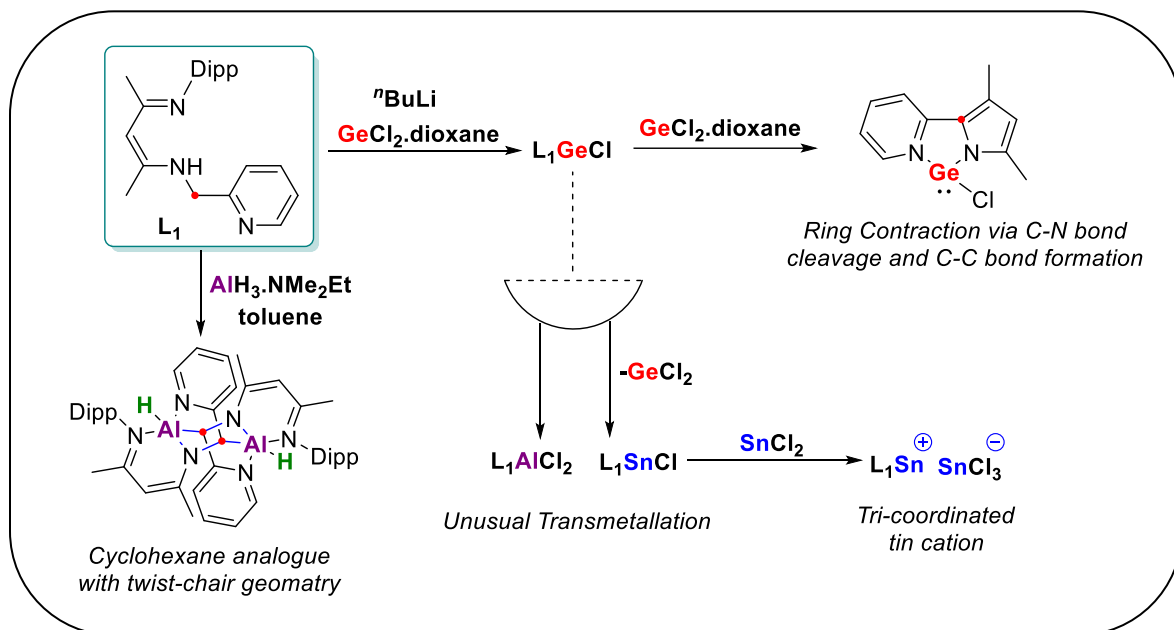
- 
25. S. Khan, S. K. Ahirwar, S. Pal, N. Parvin and N. Kathewad, *Organometallics*, 2015, **34**, 5401–5406.
26. N. Parvin, R. Dasgupta, S. Pal, S. S. Sen and S. Khan, *Dalton Trans.*, 2017, **46**, 6528–6532.
27. (a) F. M. Mück, J. A. Baus, R. Bertermann, C. Burschka and R. Tacke, *Organometallics*, 2016, **35**, 2583–2588. (b) K. Junold, J. A. Baus, C. Burschka, C. Fonseca Guerra, F. M. Bickelhaupt and R. Tacke, *Chem. -Eur. J.*, 2014, **20**, 12411–12415. (c) R. S. Ghadwal, H. W. Roesky, S. Merkel and D. Stalke, *Chem. -Eur. J.*, 2010, **16**, 85–88.
28. B. Blom, G. Klatt, D. Gallego, G. Tan and M. Driess, *Dalton Trans.*, 2015, **44**, 639–644.
29. S.-P. Chia, H.-W. Xi, Y. Li, K. H. Lim and C.-W. So, *Angew. Chem., Int. Ed.*, 2013, **52**, 6298–6301.
30. Y.-L. Shan, B.-X. Leong, H.-W. Xi, R. Ganguly, Y. Li, K. H. Lim and C.-W. So, *Dalton Trans.* 2017, **46**, 3642–3648.
31. T. Kühler, P. Jutzi, A. Stammler and H.-G. Stammler, *Chem. Commun.*, 2001, 539–540.
32. S. S. Sen, J. Hey, R. Herbst-Irmer, H. W. Roesky and D. Stalke, *J. Am. Chem. Soc.*, 2011, **133**, 12311–12316.
33. P. P. Samuel, A. P. Singh, S. P. Sarish, J. Matussek, I. Objartel, H. W. Roesky and D. Stalke, *Inorg. Chem.*, 2013, **52**, 1544–1549.
34. A. M. Guloy and J. D. Corbett, *Inorg. Chem.*, 1996, **35**, 2616–2622.
35. (a) T. Kottke and D. Stalke, *J. Appl. Crystallogr.*, 1993, **26**, 615–619. (b) D. Stalke, *Chem. Soc. Rev.*, 1998, **27**, 171–178. (c) T. Schulz, K. Meindl, D. Leusser, D. Stern, J. Graf, C. Michaelson, M. Ruf, G. M. Sheldrick and D. Stalke, *J. Appl. Crystallogr.*, 2009, **42**, 885–891. (d) L. Krause, R. Herbst-Irmer, G. M. Sheldrick and D. Stalke, *J. Appl. Crystallogr.* 2015, **48**, 3–10. (e) L. Krause, R. Herbst-Irmer and D. Stalke, *J. Appl. Crystallogr.*, 2015, **48**, 1907–1913.
36. L. Rösch, Formation of the Ge–In Bond. In *Inorganic Reactions and Methods: The Formation of Bonds to C, Si, Ge, Sn, Pb (Part 2)*; J. J. Zuckerman and A. P. Hagen, *Eds.*; Wiley: Hoboken, NJ, USA, 1989; Vol. **10**.
37. N. S. Vyazankin, G. A. Razuvaev and O. A. Kruglaya, *Organomet. Chem. Rev. A*, 1968, **3**, 323.



- 
38. (a) J. Emsley, *The Elements, 3rd ed.*; Oxford University Press: Oxford, U.K., 1998. (b) N. Nakata, R. Izumi, V. Y. Lee, M. Ichinohe and A. Sekiguchi, *Chem. Lett.*, 2008, **37**, 1146–1147.
39. S. Nagendran, S. S. Sen, H. W. Roesky, D. Koley, H. Grubmüller, A. Pal and R. Herbst-Irmer, *Organometallics*, 2008, **27**, 5459–5463.
40. D. Himmel, I. Krossing and A. Schnepf, *Angew. Chem., Int. Ed.*, 2014, **53**, 370–374.
41. G. Frenking, *Angew. Chem., Int. Ed.*, 2014, **53**, 6040–6046.
42. D. Himmel, I. Krossing and A. Schnepf, *Angew. Chem., Int. Ed.*, 2014, **53**, 6047–6048.
43. R. Ahlrichs, M. Bär, M. Häser, H. Horn and C. Kölmel, *Chem. Phys. Lett.*, 1989, **162**, 165–169.
44. J. P. Perdew, K. Burke and M. Ernzerhof, *Phys. Rev. Lett.*, 1996, **77**, 3865–3868.
45. K. Eichkorn, F. Weigend, O. Treutler and R. Ahlrichs, *Theor. Chem. Acc.*, 1997, **97**, 119–124.
46. K. Eichkorn, O. Treutler, H. Öhm, M. Häser and R. Ahlrichs, *Chem. Phys. Lett.*, 1995, **240**, 283–289.
47. M. Sierka, A. Hogekamp and R. Ahlrichs, *J. Chem. Phys.*, 2003, **118**, 9136–9148.
48. A. E. Reed, R. B. Weinstock and F. Weinhold, *J. Chem. Phys.*, 1985, **83**, 735–746.
49. Gaussian 09, Revision A.01, M. J. Frisch, G. W. Trucks, H. B. Schlegel, G. E. Scuseria, M. A. Robb, J.R. Cheeseman, G. Scalmani, V. Barone, B. Mennucci, G. A. Petersson, H. Nakatsuji, M. Caricato, X. Li, H. P. Hratchian, A. F. Izmaylov, J. Bloino, G. Zheng, J. L. Sonnenberg, M. Hada, M. Ehara, K. Toyota, R. Fukuda, J. Hasegawa, M. Ishida, T. Nakajima, Y. Honda, O. Kitao, H. Nakai, T. Vreven, J. J. A. Montgomery, J. E. Peralta, F. Ogliaro, M. Bearpark, J. J. Heyd, E. Brothers, K. N. Kudin, V. N. Staroverov, R. Kobayashi, J. Normand, K. Raghavachari, A. Rendell, J. C. Burant, S. S. Iyengar, J. Tomasi, M. Cossi, N. Rega, J. M. Millam, M. Klene, J. E. Knox, J. B. Cross, V. Bakken, C. Adamo, J. Jaramillo, R. Gomperts, R. E. Stratmann, O. Yazyev, A. J. Austin, R. Cammi, C. Pomelli, J. W. Ochterski, R. L. Martin, K. Morokuma, V. G. Zakrzewski, G. A. Voth, P. Salvador, J. J. Dannenberg, S. Dapprich, A. D. Daniels, O. Farkas, J. B. Foresman, J. V. Ortiz, J. Cioslowski and D. J. Fox, *Gaussian Inc., Wallingford CT*, 2009.

50. (a) F. Weigend and R. Ahlrichs, *Phys. Chem. Chem. Phys.*, 2005, **7**, 3297-3305. (b) F. Weigend, *Phys. Chem. Chem. Phys.*, 2006, **8**, 1057-1065.
51. A. Klamt and G. Schüürmann, *J. Chem. Soc., Perkin Trans. 2.*, 1993, **5**, 799–805.

## Chapter 3: Access to Group 13 and 14 Compounds using Picolyl Functionalized $\beta$ -diketiminato Ligand



### Abstract:

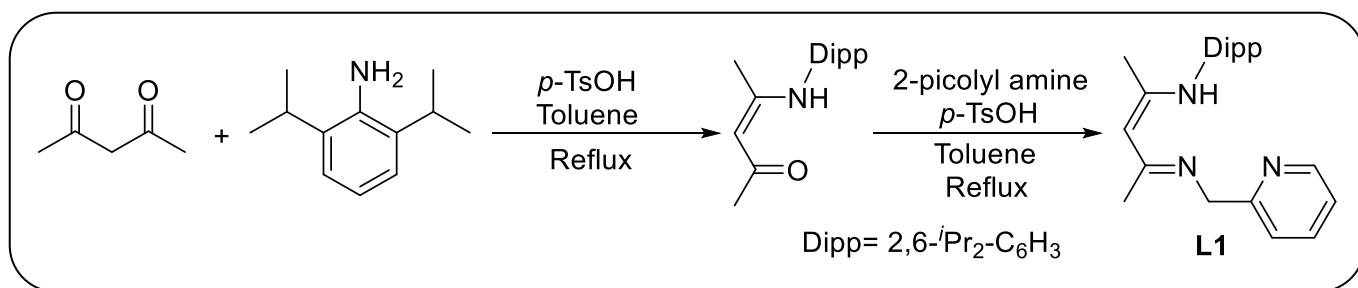
In this chapter, we have employed a nacnac-based tridentate ligand containing a picolyl group (**L1**) to isolate chlorogermylene (**3.1**). The reaction of **3.1** with another equivalent of  $\text{GeCl}_2 \cdot \text{dioxane}$  surprisingly gave pyridylpyrrolide-based chlorogermylene (**3.2**) via C–N bond cleavage and C–C coupling, while with  $\text{SnCl}_2$  and  $\text{AlCl}_3$ , it afforded the respective transmetalated products, **3.4** and **3.5**. However, the transmetalated product stannylene (**3.4**) afforded a tri-coordinated tin cation (**3.6**) in presence of another equivalent of  $\text{SnCl}_2$ . In order to prepare **L1** supported alane, the treatment of **L1** in presence of  $\text{AlH}_3 \cdot \text{NMe}_2\text{Et}$  led to the formation of an unusual cyclohexane type six-membered dialane heterocycle (**3.7**). We have also prepared and structurally characterized the analogous dichlorosilane compound (**3.8**).

### 3.1: Introduction

A significant number of isolable tetrylenes i.e. the heavier congeners of carbenes are currently known in literature. They have quickly established their appreciation from laboratory curiosities to valuable ligands in metal-mediated homogeneous catalysis. Stabilization of such sub valent compounds is frequently achieved by the engagement of sterically bulky and electron-rich ancillary ligands; the most common of them is the chelating mono-anionic  $\beta$ -diketiminate (or “nacnac”) ligand family,  $[\text{HC}\{\text{(R)C(R')N}\}_2]^-$ .<sup>2</sup> The nacnac supported chlorogermylene,  $[\text{CH}\{\text{(CMe)}_2, 6\text{-}^i\text{Pr}_2\text{C}_6\text{H}_3\text{N}\}_2]\text{GeCl}$  (**A**),<sup>1</sup> from the Roesky group, has enjoyed substantial attention due to its utility as a synthon to prepare a series of germanium compounds.<sup>2</sup> **A** was a promising precursor to furnish more exotic molecular species through (i) hydride-for-halide exchange, leading to a robust Ge(II) hydride complex<sup>2d</sup>; (ii) one-electron reduction, giving a remarkable two-coordinate germanium centered radical,<sup>3</sup> (iii) dehydrohalogenation leading to reactive germylene species, and most recently, (iv) salt metathesis. A less well-developed ligand system is a nacnac framework containing a picolyl functionality (**L1**). The pendant pyridine moiety on one of the nitrogen atoms can provide additional support sterically as well as extra electronic stabilization to the metal center. This tridentate ligand has been reported for the synthesis of iron, chromium, yttrium, and scandium complexes.<sup>4,5</sup> Recently, we have described magnesium and calcium complexes using this ligand and demonstrated their usefulness as catalysts for the hydroboration of aldehydes and ketones.<sup>6</sup> Hence, the choice of ligand has the potential to provide intramolecular stabilization to the electron-deficient germylium-ylidenes. A further impetus comes from the recent report on pyridine functionalized silane, which shows unprecedented binding properties with Rh and Ir.<sup>7</sup> To our surprise, we did not obtain any germylium-ylidene species, but the presence of the picolyl functionality in **L1** promoted several unusual alternate reactivity such as smooth ring contraction via C–N bond cleavage, facile dehydrocoupling, transmetallation and a six membered Al-heterocycle formation, which are not observed for the traditional nacnac-based systems. The work is another testimony to the fact that small variations in the ligand system can yield unprecedented outcomes.<sup>8</sup>

### 3.2: Results and Discussions

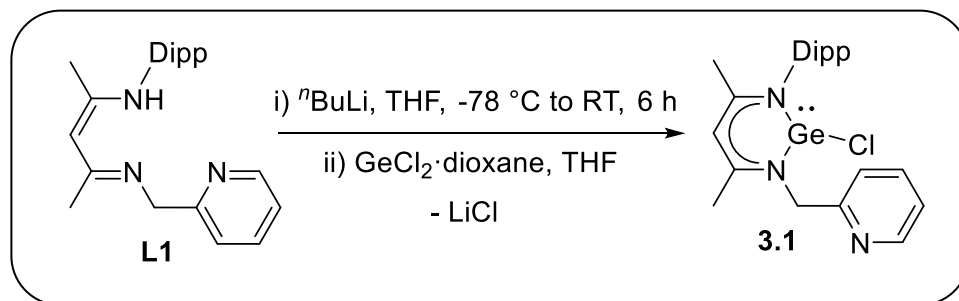
The ligand (**L1**) was synthesized following the literature procedures given by Chen and coworkers.<sup>7</sup> Initially, 2-((2,6-Diisopropylphenyl)imido)-2-penten-4-one was prepared by using the condensation method of acetylacetone with 2,6-diisopropylaniline in presence of catalytic amount of *p*-toluenesulfonic acid. Subsequently, this freshly prepared product was treated with 2-picoyl amine again in the presence of a catalytic amount of *p*-toluenesulfonic acid in toluene and refluxed for 12 h using a dean-stark apparatus, to afford the desired ligand precursor **L1** in 61% yield (Scheme 3.1). It was further crystallized in hexane solution and the pure crystals were characterized by NMR (<sup>1</sup>H and <sup>13</sup>C) and mass spectrometry.



**Scheme 3.1:** Synthesis of ligand (**L1**)

#### 3.2.1: Synthesis, characterization and structural elucidation of chlorogermylene (3.1)

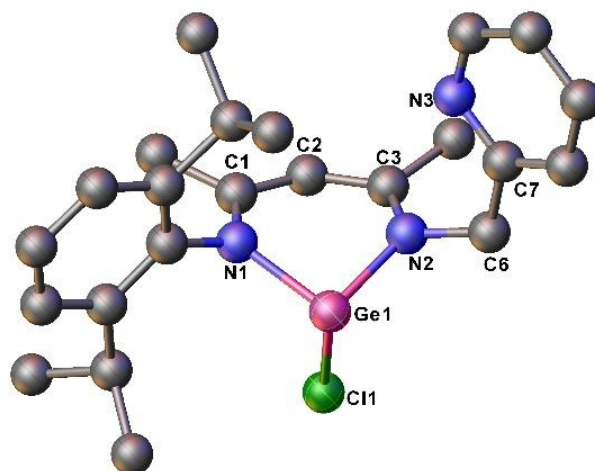
Using <sup>n</sup>BuLi in THF at room temperature led to the formation of the lithium salt of the ligand via the deprotonation of the same. Subsequently the reaction with GeCl<sub>2</sub>·dioxane afforded the desired germylene monochloride (**3.1**) as a bright yellow solid (Scheme 3.2).



**Scheme 3.2:** Synthesis of germylene monochloride (**3.1**)

The compound **3.1** was confirmed by multinuclear NMR spectroscopy. The <sup>1</sup>H NMR spectrum indicates complete deprotonation of the ligand with the disappearance of the N–H resonance. **3.1**

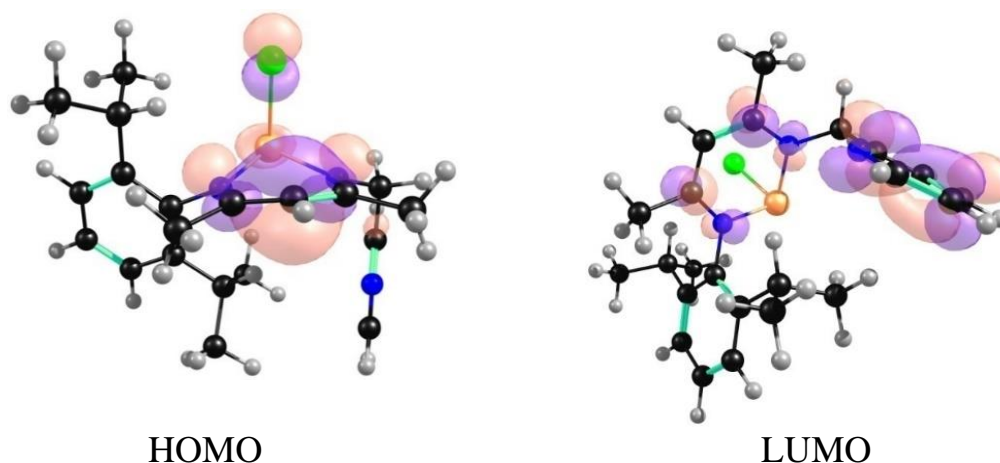
clearly shows two sets of doublets for the two isopropyl groups, one septet, and two singlets for the methyl groups in the  $^1\text{H}$  NMR spectrum. Single crystals were grown from the concentrated toluene solution of **3.1** at  $-4\text{ }^\circ\text{C}$ . The solid state molecular structural data revealed that, belying expectations, the Ge atom is tri-coordinated (Figure 3.1) and displays a distorted trigonal-pyramidal geometry, and that the pyridine-N does not coordinate to the Ge center. The significant bond lengths are Ge1–Cl1 = 2.3523(5), Ge1–N1 1.9539(15), Ge1–N2 1.9591(16), Å.



**Fig. 3.1:** Molecular structure of **3.1** with anisotropic displacement parameters depicted at the 50% probability level. Hydrogen atoms are not shown for clarity. Selected bond lengths (Å) and bond angles (1): Ge1–N1 1.9539(15), Ge1–N2 1.9591(16), Ge1–Cl1 2.3523(5); N1–Ge1–N2 90.67(6), N1–Ge1–Cl1 94.13(5), N2–Ge1–Cl1 92.30(5).

### 3.2.2: Theoretical illumination of chlorogermylene (**3.1**)

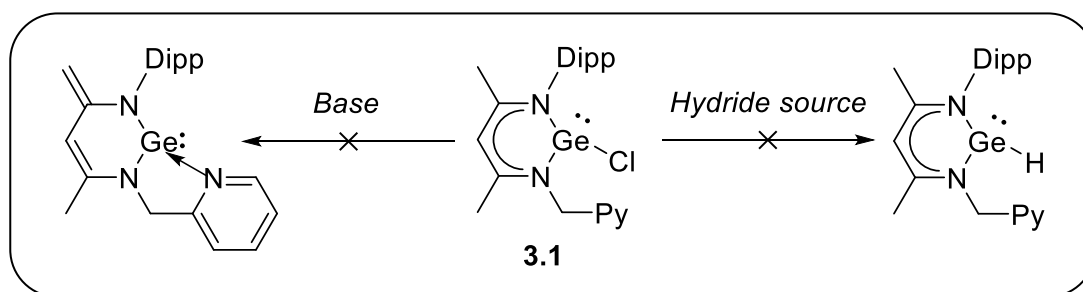
Calculations with density functional theory (DFT) show that the HOMO is located at the Ge center and throughout the six-membered nacrane ring, while the LUMO is spread over the pyridine ring (Figure 3.2). The HOMO–LUMO energy gap for **3.1** has been premeditated to be 6.48 eV, at the PBE/TZVP/M06-2X/6-311+G(d) level of theory (for further computational details, please see the experimental section).



**Fig. 3.2:** HOMO and LUMO of Compound **3.1**. HOMO-LUMO energy gap is 6.48 eV

### 3.2.3: Unsuccessful attempts to prepare germylium ylidene and germanium (II) hydrides

Further to access the germylium ylidene through the base-assisted dehydrochlorination via monodeprotonation from a methyl group on the backbone of the  $\beta$ -diketiminato ligand instead of a nucleophilic Cl/N(SiMe<sub>3</sub>)<sub>2</sub> substitution at germanium, we have employed several bases like LiN(SiMe<sub>3</sub>)<sub>2</sub>, KN(SiMe<sub>3</sub>)<sub>2</sub>, KNSi(SiMe<sub>3</sub>)<sub>3</sub>, KO<sup>t</sup>Bu, DBU, triethylamine as well as with the I<sup>t</sup>Bu (1,3-di-tert-butyl-1H-imidazol-3-ium-2-ide) carbene with **3.1** (Scheme 3.3). But we were exclusively ended up with the ligand moiety for each and every attempts. However, we have observed a sudden colour change of yellow to green at low temp (-40 °C) with the addition of LDA (Lithium diisopropylamide). But the establishment of the new complex was unsuccessful due to the sensitivity because the color of the reaction mixture did not sustain at room temperature and even in NMR tube and we have obtained the spectrum of free ligand (**L1**).



**Scheme 3.3:** Unsuccessful attempts to prepare germylium ylidene and germanium (II) hydrides

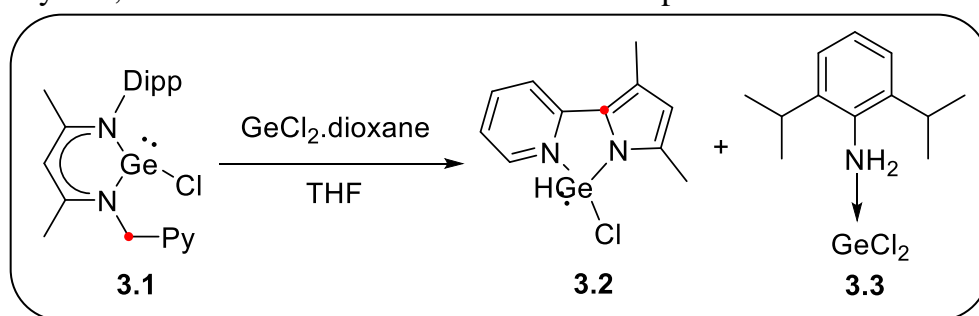
Additionally, to get the germanium (II) hydrides, we have treated the complex **3.1** with several well-known hydride sources like K-Selectride, L-Selectride, phenylsilane, tributyltin hydride, NaH, LiAlH<sub>4</sub> etc (Scheme 3.3). Unfortunately, we were unsuccessful to achieve the expected germanium (II) hydride after several efforts. To check the robustness of Ge–Cl bond of complex **3.1**, we have also performed a reaction with methyl lithium with the expectation of receiving the metathesis reaction with compound **3.1**, without any success. Roesky and co-workers, have reported a new method to produce the germanium (II) hydride by adding NaBH<sub>4</sub> followed by the addition of PMe<sub>3</sub>,<sup>2f</sup> where the free Lewis base PMe<sub>3</sub> has been used to remove the Lewis acids of these adducts resulting as Me<sub>3</sub>P·BH<sub>3</sub> adduct by releasing germanium (II) hydride. Following the same practice, we have also treated compound **3.1** with NaBH<sub>4</sub>. Although, the color has been changed from yellow to fluorescent green, we were unable to get the structural endorsement of the formation of our expected hydride from the reaction mixture. To know the activity of the pair of electrons residing on Ge center of complex **3.1**, we have gone through a reaction with BH<sub>3</sub>·SMe<sub>2</sub>, giving the same color change from yellow to fluorescent green and further ineffectual to afford any conclusive results.

#### **3.2.4: Synthesis, characterization and structural elucidation of PyPyr ligand supported chlorogermylene (3.2) and adduct (3.3)**

After many abortive attempts to get the expected compounds, we sought to prepare the corresponding germylium ylidene by abstracting the chloride using another equivalent of GeCl<sub>2</sub>·dioxane. Surprisingly, the addition of another equivalent of GeCl<sub>2</sub>·dioxane to a THF solution of **3.1** led to the cleavage of the C–N bond next to the Ge-heteroatom bond and afforded a new chlorogermylene (**3.2**) supported by the pyridylpyrrolide ligand, along with the formation of a DippNH<sub>2</sub>·GeCl<sub>2</sub> adduct (**3.3**) (Scheme 3.4), instead of affording any Ge<sup>II</sup>→Ge<sup>II</sup> donor–acceptor compound.<sup>9</sup> X-ray diffraction analysis of the crystals obtained from the fractional crystallization of the reaction mixture confirmed the formation of **3.2** and **3.3**. Nucleophilic attack on the nacnac β-carbon and the subsequent ring contraction reaction has been recently reported, but it usually entails a strong reductant like alkali metals or the Mg(I) dimer,<sup>10</sup> except for the report from Cui and coworkers, who demonstrated the ring contraction upon reacting a β-diketiminato Al(I) compound,

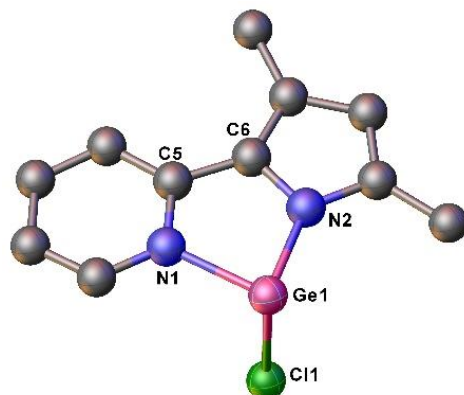


$[\text{HC}\{(\text{C}'\text{Bu})_2(\text{NAr})_2\}]\text{Al}$  with an N-heterocyclic carbene (NHC).<sup>11</sup> Interestingly, pyridylpyrrolide (PyPyr) ligands have recently witnessed extensive activity in transition metal chemistry due to their *push-pull effect* (pyrrolide  $\pi$  orbitals serve as donors, while pyridine  $\pi^*$  orbitals as acceptors).<sup>12</sup> In order to learn about the main group metal-ligand interaction with the pyrrole  $\pi$ -system, Stalke and coworkers recently reported Ge–Pb compounds using a 2,5-bis-{(pyrrolidino)-methyl}-pyrrole pincer ligand.<sup>13</sup> However, there is no such literature present about the study of only the PyPyr moiety as a ligand for any heavier main group element. Our strategy serendipitously offers a new access to PyPyr chlorogermylene, which we will discuss in details in chapter 5.



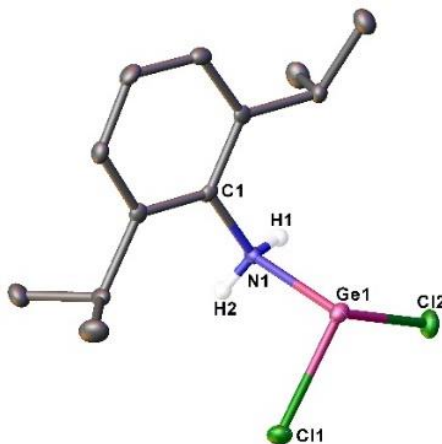
**Scheme 3.4:** Reaction of complex **3.1** with  $\text{GeCl}_2$ .dioxane

The single crystal X-ray structure of **3.2** has been derived from X-ray diffraction data (Figure 3.3). The germanium atom is tri-coordinated, with a longer Ge–N bond (2.0401(14) Å) to the pyridine nitrogen and a short Ge–N bond to the pyrrole (1.9408(15) Å) nitrogen atom. The C–C bond lengths in the pyrrole ring are very close, with a slight increase in the C6–C7 bond length (1.408(3) Å). The small N1–Ge1–N2 bite angle of 79.77(1)° is comparable with the one reported with the late transition metal complexes supported by PyPyr.<sup>10</sup> The two methyl groups attached with the pyrrole ring exhibit two significant singlets at  $\delta$  2.40 and 2.34 ppm in the  $^1\text{H}$  NMR spectrum.



**Fig. 3.3:** Molecular structure of **3.2** with anisotropic displacement parameters depicted at the 50% probability level. Hydrogen atoms are not shown for clarity. Selected bond lengths (Å) and bond angles (°): Ge1–N2 1.9408(15), Ge1–N1 2.0401(14), Ge1–Cl1 2.3141(4), N2–C8 1.366(2), N2–C5 1.384(2), N1–C1 1.348(2), N1–C4 1.367(2); N2–Ge1–N1 79.77(6), N2–Ge1–Cl1 95.75(4), N1–Ge1–Cl1 91.61(4).

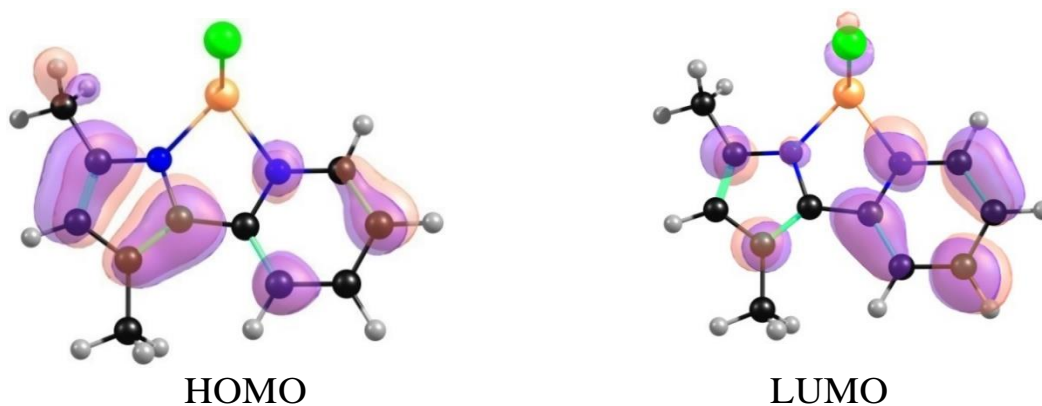
The solid-state molecular structure of **3.3** is given in Figure 3.4, which shows a Ge–N dative bond of 2.1674(14) Å, substantially longer than that in DMAP→GeCl<sub>2</sub> adduct (2.028(2) Å) reported by Rivard and coworkers.<sup>14</sup>



**Fig. 3.4:** Molecular structure of compound **3.3** with anisotropic displacement parameters depicted at the 50% probability level. Hydrogen atoms are not shown for clarity. Selected bond lengths (Å) and bond angles (°): Cl1–Ge1 2.2744(4), Cl2–Ge1 2.2793(4), Ge1–N1 2.1674(14); N1–Ge1–Cl1 90.63(4), N1–Ge1–Cl2 90.78(4), Cl1–Ge1–Cl2 95.903(16).

### 3.2.5: Theoretical illumination of PyPyr ligand supported chlorogermylene (3.2)

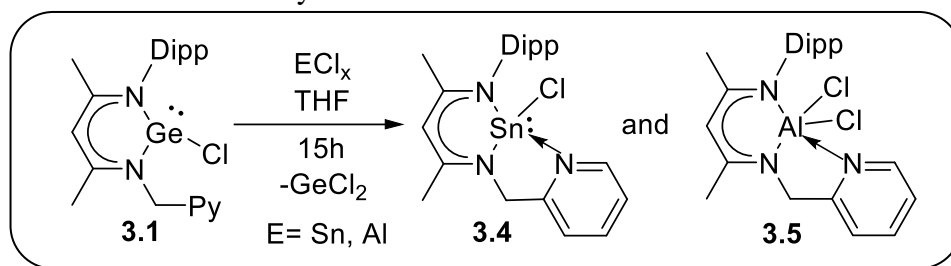
In order to find out the nature of metal ligand interaction in the tri-coordinated germanium compound **3.2**, we have further completed natural bond orbital (NBO) analysis. The NBO analysis of **3.2** revealed that the contribution of the 4d orbital of the Ge centre towards the bonding is very trivial: the natural occupation in the 4d shell of the Ge centre is equal to 0.01 (See the experimental section for details, Page: 161). For the charge transfer from the ligands to the metal ion, a stabilizing electronic effect is accountable for the formation of chemical bonds. This is evidenced by the NBO charge of 1.08 on the Ge atom. The leading ionic character of the Ge–ligand bond is also evident in the localized Lewis-like description of the bonding design. In the Lewis structure of **3.2**, no other localized electron pair for bonding between the Ge and the coordinated ligands was observed. From the NBO data, the “non-Lewis” occupancy suggests that large charge-transfer interactions take place, where the ligand lone-pair orbital efficiently donates its electron density to an unoccupied orbital residing on the metal. From the NBO analysis, the second order perturbation energy for the Ge centre with the surrounding ligands extends between 61.8 kcal/mol and 178.6 kcal/mol. The interaction energies of the Ge centre with the two-nitrogen donor and one chloride donor ligands are 61.8 kcal/mol, 84.0 kcal/mol and 178.6 kcal/mol respectively. Consistent with the structural data, the pyrrole nitrogen interacts more strongly (84.0 kcal/mol) than the pyridine nitrogen (61.8 kcal/mol). The DFT calculations also reveal that in **3.2** both the HOMO and LUMO are localized over the five and six membered rings and both of them have pi symmetry in nature (Figure 3.5). The HOMO–LUMO energy gap has been determined to be 5.48 eV (for more details please see the experimental section, Page: 161).



**Fig. 3.5:** HOMO and LUMO of Compound **3.2**. HOMO-LUMO energy gap is 5.48 eV

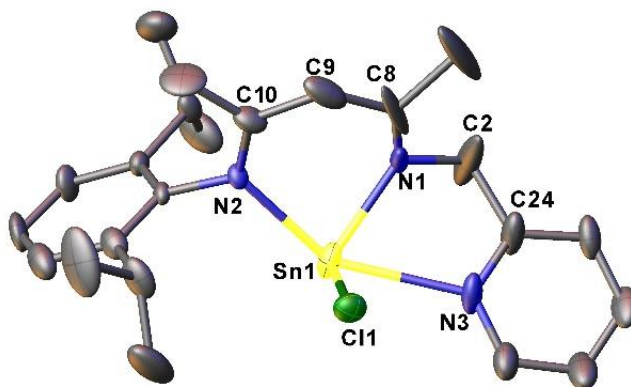
### 3.2.6: Synthesis, characterization and structural elucidation of chlorostannylene (**3.4**) and analogous aluminium chloride compound (**3.5**)

In order to substantiate the formation of C–C coupled product **3.2**, the reaction of **3.1** with other Lewis acids like SnCl<sub>2</sub> and AlCl<sub>3</sub> was performed. The reaction of **3.1** with SnCl<sub>2</sub> and AlCl<sub>3</sub> led to the transmetallated products, **3.4** and **3.5** respectively along with the extrusion of GeCl<sub>2</sub> (Scheme 3.5). Not only the examples are scant for the transmetallation between two p-block elements,<sup>15</sup> the extrusion of GeCl<sub>2</sub> is also not very common.<sup>16</sup>

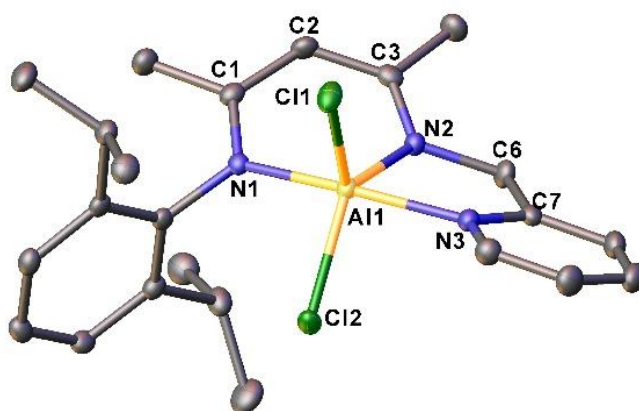


**Scheme 3.5:** Reaction of complex **3.1** with SnCl<sub>2</sub> and AlCl<sub>3</sub>

Compounds **3.4** and **3.5** were further characterized by Single crystal X-ray studies. The structural data reveal that the pyridine moiety coordinates to both the tin and aluminum center in compounds **3.4** and **3.5** (Figure 3.6 and 3.7 for **3.4** and **3.5** respectively), possibly due to the higher Lewis acidity of tin and aluminium in comparison to germanium. Compound **3.4** crystallizes in triclinic symmetry with *P*-1 space group whereas **3.5** crystallizes in monoclinic *P*2<sub>1</sub>/*c* space group. The Sn–N<sub>pyridine</sub> bond [2.559(7) Å] is significantly longer than the Sn–N<sub>ligands</sub> bond lengths (2.290(4) and 2.138(8) Å). Similarly, The Al–N<sub>ligands</sub> bonds (1.9092(15) and 1.9783(15) Å) are substantially shorter than the Al–N<sub>pyridine</sub> bond length [2.0641(15) Å]. The Sn atom in **3.4** adopts a distorted square planar geometry. The Al atom in **3.5** exhibits a distorted trigonal bipyramidal polyhedron with N1 and N3 at the apical positions and N2, Cl1 and Cl2 are in the equatorial positions. The <sup>119</sup>Sn for compound **3.4** was observed at -301.83 ppm. The molecular ion peaks were detected with the highest relative intensity at *m/z* 504.0860 for **3.4** and 446.2590 for **3.5**.



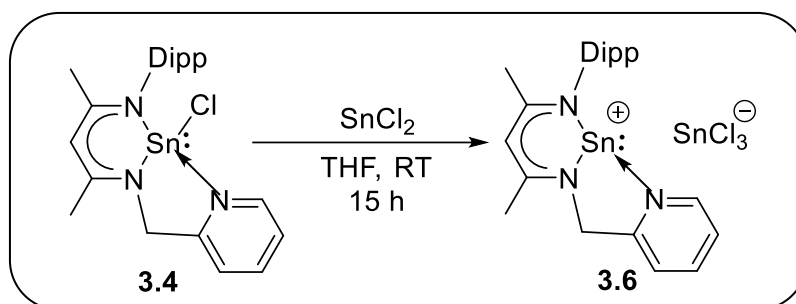
**Fig. 3.6:** Molecular structure of **3.4** with anisotropic displacement parameters depicted at the 50% probability level. Hydrogen atoms are not shown for clarity. Selected bond lengths (Å) and bond angles (°): Sn1–Cl1 2.465(2), Sn1–N2 2.290(4), Sn1–N1 2.138(8), Sn1–N3 2.559(7); N2–Sn1–N1 81.5(2), N1–Sn1–N3 68.3(2), N2–Sn1–N3 146.9(2), N2–Sn1–Cl1 90.1(1), N3–Sn1–Cl1 80.5(2), N1–Sn1–Cl1 96.8(2).



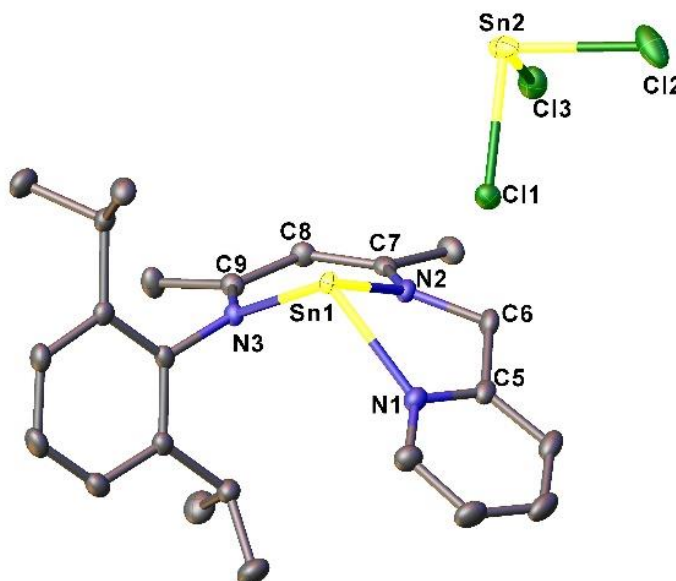
**Fig. 3.7:** Molecular structure of **3.5** with anisotropic displacement parameters depicted at the 50% probability level. Hydrogen atoms are not shown for clarity. Selected bond lengths (Å) and bond angles (°): Al1–N2 1.9092(15), Al1–N1 1.9783(15), Al1–N3 2.0641(15); N2–Al1–N1 91.38(6), N2–Al1–N3 79.76(6), N1–Al1–N3 168.78(6), N2–Al1–Cl1 113.79(5), N1–Al1–Cl1 98.79(4), N3–Al1–Cl1 91.13(4), N2–Al1–Cl2 130.01(5), N1–Al1–Cl2 93.66(5), N3–Al1–Cl2 86.92(4), Cl1–Al1–Cl2 114.44(3).

### 3.2.7: Synthesis, characterization and structural elucidation of tin cation (**3.6**) with the reaction of SnCl<sub>2</sub> and **3.4**

The addition of another equivalent of  $\text{SnCl}_2$  to **3.4** in THF led to a stannylum cation **3.6** instead of affording any Sn(II)–Sn(II) donor–acceptor compound (Scheme 3.6).<sup>17</sup> Colorless single crystals of **3.6** suitable for X-ray diffraction studies were grown from the saturated toluene solution at  $-30^\circ\text{C}$  in a freezer. The molecular structure of **3.6** is shown in Figure 3.8 along with the important bond lengths and angles. **3.6** crystallizes in the monoclinic space group,  $P2_1/n$ . The pyridine moiety coordinated to the tin center to stabilize the cationic tin species. The  $^{119}\text{Sn}$  NMR shows peak at  $-148.61$  and  $-374.01$  ppm for the tri substituted tin cation and  $\text{SnCl}_3^-$ , respectively.



**Scheme 3.6:** Synthesis of tri-coordinated cation tin compound **3.6**

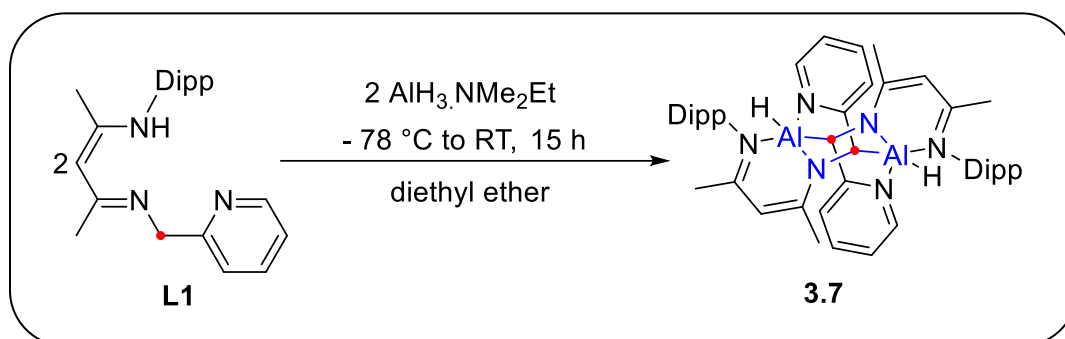


**Fig. 3.8.** Molecular structure of **3.6** with anisotropic displacement parameters depicted at the 50% probability level. Hydrogen atoms are not shown for clarity. Selected bond lengths (Å) and bond angles (1): Sn2–C11 2.5053(8), Sn2–C13 2.4947(7), Sn2–C12 2.4855(7), Sn1–

N1 2.370(2), Sn1–N2 2.184(2), Sn1–N3 2.231(2); N2–Sn1–N1 70.60(6), N1–Sn1–N3 106.20(6), N2–Sn1–N3 80.36(6).

### 3.2.8: Synthesis, characterization and structural elucidation of analogous six membered alane compound (3.7)

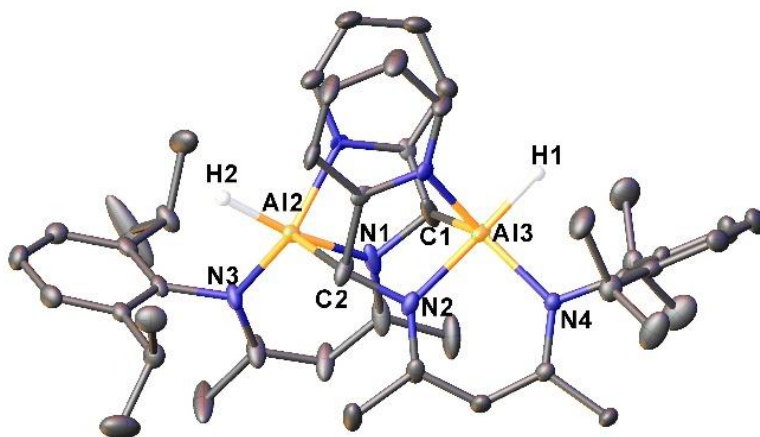
Soluble aluminum hydride compounds have been extensively studied in recent years as the catalysts for the hydroboration of alkynes, aldehydes, ketones, esters, carbodimides, etc.<sup>18</sup> In order to prepare the analogous aluminum hydride from **3.5**, we have treated compound **3.5** with several hydrogenating agents such as PhSiH<sub>3</sub>, Et<sub>3</sub>SiH, L-selectride etc. without any success. Hence, we sought to prepare the aluminum hydride using a dehydrocoupling method by reacting the ligand with the alane. Surprisingly, the reaction of **L1** with AlH<sub>3</sub>·NMe<sub>2</sub>Et at room temperature led to the formation of an unusual six-membered ring alane compound (**3.7**) consisting of two aluminum, two nitrogen and two carbon atoms (Scheme 3.7). Compounds containing an Al<sub>n</sub>C<sub>n</sub>N<sub>n</sub> framework are rare,<sup>19</sup> but recently a unique Al<sub>2</sub>Si<sub>4</sub> heterocycle has been reported by Roesky, Stalke, Koley and coworkers.<sup>20</sup>



**Scheme 3.7:** Dehydrocoupling mediated formation of six-membered dialane (**3.7**)

The formation of **3.7** was made possible by the double dehydrocoupling between alane and N–H of the ligand. The molecular structure of **3.7** is shown in Figure 3.9. The core structure of **3.7** is a tricyclo compound consisting of a six-membered Al<sub>2</sub>C<sub>2</sub>N<sub>2</sub> ring and two five-membered AlC<sub>2</sub>N<sub>2</sub> rings (Figure 3.9). The six-membered ring is centrosymmetric adopting a twisted chair conformation. The geometry of each Al atom can be viewed as trigonal bipyramidal. The two Al–N bond distances in the six-membered ring are 1.9801(17) and 1.9750(16) Å. The two Al–C bond distances are 2.1542(18) and 2.1733(19) Å, which are longer than the Al(III)–C bonds in the dimer of Me<sub>3</sub>Al (2.145(7) and 2.146(8) Å),<sup>21</sup> presumably due to the higher coordination number

in **3.7**. The Al–H bond lengths are 1.56(2) and 1.55(2) Å. After crystallization, compound **3.7** is not properly soluble in most of the common deuterated solvents, so we are unable to record meaningful solution state spectroscopic data. The  $^{27}\text{Al}$  ( $I=5/2$ ) NMR of **3.7** displays a sharp resonance at 38.9 ppm, which is in agreement with the presence of a penta-coordinated Al center.<sup>22</sup> In the IR spectrum, two sharp bands at 1693 and 1743  $\text{cm}^{-1}$  were noticed, which can be attributed to the stretching frequency of the two Al–H bond.



**Fig. 3.9:** Molecular structure of **3.7** with anisotropic displacement parameters depicted at the 50% probability level. Hydrogen atoms (apart from those bound to Al) are not shown for clarity. Selected bond lengths (Å) and bond angles (1): Al2–N1 1.9801(17), Al2–C2 2.1542(18), Al2–H2 1.56(2), Al3–N2 1.9750(16), Al3–C1 2.1733(19), Al3–H1 1.55(2); N1–Al2–C2 90.44(7), N2–Al3–C1 90.02(7), C1–N1–Al2 110.80(14), C2–N2–Al3 110.90(12), N1–C1–Al3 113.05(12), N2–C2–Al2 113.14(11).

### 3.2.9: Theoretical illumination of six membered dialane (**3.7**)

To get insight into the nature of metal ligand interaction of compound **3.7**, we have performed NBO analysis. For the penta-coordinated metal complex, there are two possibilities: either the metal centre is  $sp^3d$  hybridized; i.e. the metal  $d$  orbital is required to participate in bonding, or the charge transfer from the ligand to the metal is predominant. But the role of the  $d$  orbitals in the bonding pattern of penta-coordinated compounds is very unlikely in case of second-row non-metals, due to the large promotion energies involved. Previous investigation on the penta-coordinate aluminum complex also pointed towards the exclusion of the  $d$  orbital in the bonding.<sup>23</sup>

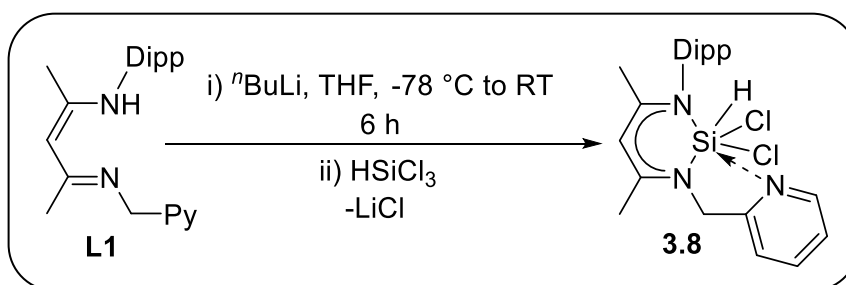


From the NBO second order perturbation energy data, the values are high ( $> 50.0$  kcal/mol). This, along with the results obtained from the WBI and NLMO bond order analysis, suggests that the covalent bonding of the Al with the coordinated ligand is weak. Only in the case of Al–H does the bond order ( $\sim 0.7$ ) indicate covalency. Most of the bonding is ionic in nature.

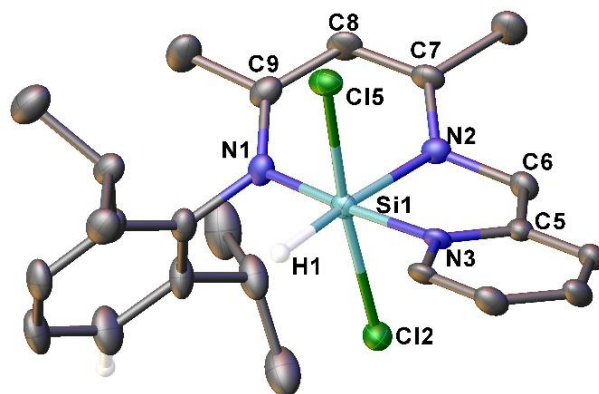
### 3.2.10: Synthesis, characterization and structural elucidation of methylpyridinato ligand supported dichlorosilane (**3.8**)

The chemistry of divalent silicon compounds, known as silylenes, is rapidly developing.<sup>24</sup> Although methylene ( $\text{H}_2\text{C}:$ ) is stable in its triplet state, silylene ( $\text{H}_2\text{Si}:$ ) or other heavier tetrylenes  $\text{H}_2\text{M}:$  (where  $\text{M} = \text{Ge}, \text{Sn}$  and  $\text{Pb}$ ) feature a singlet ground state due to the large energy gap and spatial difference between their  $s$ - and  $p$ - orbitals. The first breakthrough in the chemistry of stable Si(II) compounds was reported by Jutzi and coworkers<sup>25</sup> with the isolation of a silicocene, while Denk and coworkers<sup>26</sup> isolated the first N-heterocyclic silylene (NHSi) with the delicate balance of appropriate electronic and steric stabilization. With the success of stabilizing Ge(II) and Sn(II) compounds using **L1**, we embarked into stabilizing the more challenging Si(II) compound.

For this purpose, we have treated **L1** with  $n\text{BuLi}$  in THF and subsequently equimolar amount of trichlorosilane ( $\text{HSiCl}_3$ ) was added at low temperature (Scheme 3.8). The removal of THF and followed by workup in toluene resulted the yellow crystals of **3.8**. The proton of the Si–H moiety shows a sharp singlet at 5.67 ppm in the  $^1\text{H}$  NMR spectrum of **3.8**. Single crystal X-ray diffraction analysis confirmed the formation of **3.8**. It crystallizes in the monoclinic space group  $P-1$  and adopts a distorted octahedral geometry around the silicon center (Figure 3.10). The Si–H bond length is 1.42(5) Å and the bond length for both the two axial Si–Cl are almost equal (2.281(2) Å and 2.276(1) Å). The Si–N bond attached with the pyridine ring (1.933 Å) is longer than the other two Si–N (1.861 Å and 1.859 Å) of the ligand indicating that the former is a dative bond whether the latter is a covalent one. We have tried to generate the Si(II) compound from **3.8**, but no success has been hitherto achieved.



**Scheme 3.8:** Synthesis of methylpyridinato ligand supported dichlorosilane (**3.8**)



**Fig. 3.10.** Molecular structure of **3.8** with anisotropic displacement parameters depicted at the 50% probability level. Hydrogen atoms are not shown for clarity. Selected bond lengths (Å) and bond angles (1): Si1–H1 1.42(5), Si1–Cl2 2.281(2), Si1–Cl5 2.276(1), Si1–N1 1.861(3), Si1–N2 1.859(4), Si1–N3 1.936(3); N2–Si1–N1 92.3(2), N1–Si1–N3 175.1(2), N2–Si1–N3 82.9(2), Cl2–Si1–Cl5 171.51(7), Cl2–Si1–H1 89.0(2), Cl5–Si1–H1 91.0(2).

### 3.3: Conclusions

In conclusion, we have prepared a new chlorogermylene (**3.1**) featuring a nacnac-based tridentate ligand with a pendent pyridyl-methyl group. The ligand scaffold proved to be surprisingly flexible and allowed for the isolation of structurally different compounds under identical reaction conditions. We have shown that the six-membered germylene **3.1** can be smoothly converted into a five-membered germylene **3.2** in the presence of another equivalent of  $\text{GeCl}_2 \cdot \text{dioxane}$ . On the other hand, **3.1** goes through an easy but rare transmetallation reaction with  $\text{SnCl}_2$  as well as with  $\text{AlCl}_3$ . We have also prepared and structurally characterized a stable tri-coordinated cationic tin compound (**3.6**) containing  $\text{SnCl}_3^-$  as a counter anion upon reacting stannylene **3.4** with another

equivalent of  $\text{SnCl}_2$ . An unexpected six-membered dialane complex (**3.7**) has also been prepared through a double dehydrocoupling of ligand with  $\text{AlH}_3$ . **3.7** can be viewed as an analogue of cyclohexane, where two C–C bonds have been replaced by isoelectronic Al–N bonds. The analogous chemistry has also been extended for the preparation of dichlorosilane compound (**3.8**), which may serve as a precursor for the generation of analogous chlorosilylene.

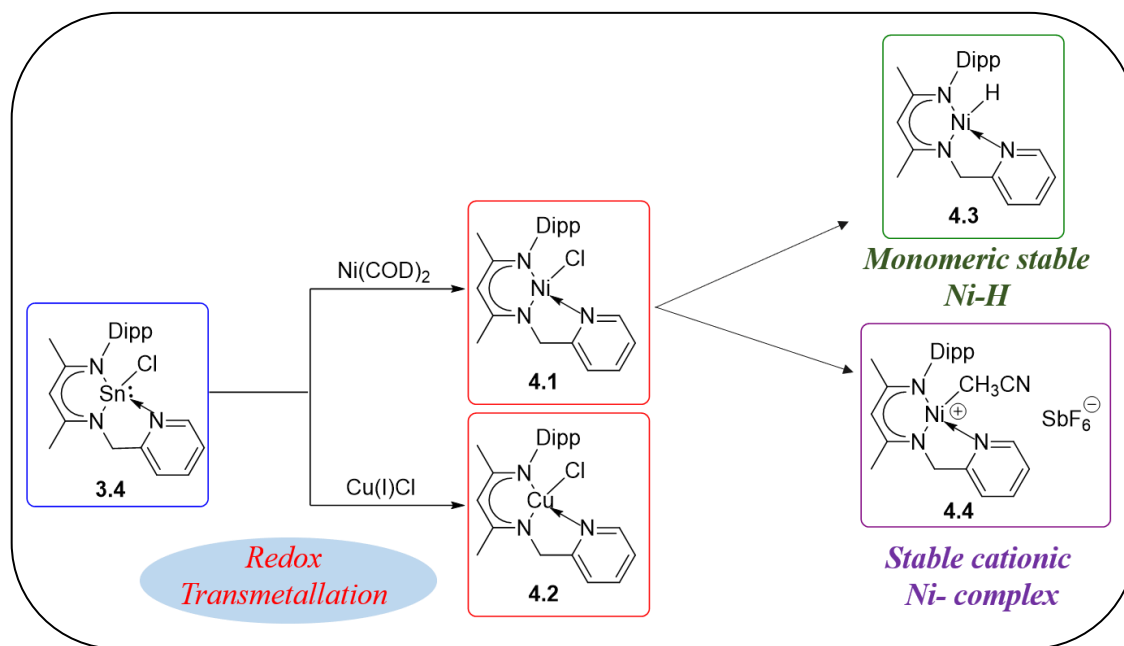
### 3.4: References

1. Y. Ding, H. W. Roesky, M. Noltemeyer and H.-G. Schmidt, *Organometallics*, 2001, **20**, 1190–1194.
2. For selected reference: (a) L. W. Pineda, V. Jancik, H. W. Roesky, D. Neculai and A. M. Neculai, *Angew. Chem., Int. Ed.*, 2004, **43**, 1419–1421. (b) L. W. Pineda, V. Jancik, K. Starke, R. B. Oswald and H. W. Roesky, *Angew. Chem., Int. Ed.*, 2006, **45**, 2602–2605. (c) M. Driess, S. Yao, M. Brym and C. van Wüllen, *Angew. Chem., Int. Ed.*, 2006, **45**, 4349–4352. (d) A. Jana, D. Ghoshal, H. W. Roesky, I. Objartel, G. Schwab and D. Stalke, *J. Am. Chem. Soc.*, 2009, **131**, 1288–1293. (e) S. P. Sarish, S. S. Sen, H. W. Roesky, I. Objartel and D. Stalke, *Chem. Commun.*, 2011, **47**, 7206–7208. (f) Y. Ding, H. Hao, H. W. Roesky, M. Noltemeyer and H. G. Schmidt, *Organometallics*, 2001, **20**, 4806–4811.
3. W. D. Woodul, E. Carter, R. Müller, A. F. Richards, A. Stasch, M. Kaupp, D. M. Murphy and M. Driess, C. Jones, *J. Am. Chem. Soc.* 2011, **133**, 10074–10077.
4. (a) L. Bourget-Marle, M. F. Lappert and J. R. Severn, *Chem. Rev.*, 2002, **102**, 3031–3066. (b) C. Camp and J. Arnold, *Dalton Trans.*, 2016, **45**, 14462–14498.
5. X. Xu, Y. Chen, G. Zou and J. Sun, *Dalton Trans.*, 2010, **39**, 3952–3958.
6. S. Yadav, R. Dixit, M. K. Bisai, K. Vanka and S. S. Sen, *Organometallics*, 2018, **37**, 4576–4584.
7. F. Kaiser, R. M. Reich, E. Rivard and F. E. Kühn, *Organometallics*, 2018, **37**, 136–144.
8. T. Kunz, C. Schrenk and A. Schnepf, *Inorg. Chem.*, 2020, **59**, 6279–6286.
9. (a) Z. Yang, X. Ma, R. B. Oswald, H. W. Roesky, C. Cui, H. Schmidt and M. Noltemeyer, *Angew. Chem., Int. Ed.*, 2006, **45**, 2277–2280. (b) S.-P. Chia, H.-W. Xi, Y. Li, K. H. Lim and C.-W. So, *Angew. Chem., Int. Ed.*, 2013, **52**, 6298–6301.

- 
10. (a) S. L. Choong, C. Schenk, A. Stasch, D. Dange and C. Jones, *Chem. Commun.*, 2012, **48**, 2504–2506. (b) W. D. Woodful, A. F. Richards, A. Stasch, M. Driess and C. Jones, *Organometallics*, 2010, **29**, 3655–3660.
11. J. Li, X. Li, W. Huang, H. Hu, J. Zhang and C. Cui, *Chem. Eur. J.*, 2012, **18**, 15263–15266.
12. For selected references: (a) J. L. McBee, J. Escalada and T. D. Tilley, *J. Am. Chem. Soc.*, 2009, **131**, 12703–12713. (b) J. L. McBee and T. D. Tilley, *Organometallics*, 2009, **28**, 3947–3952. (c) D. Pucci, I. Aiello, A. Aprea, A. Bellusci, A. Crispini, M. Ghedini, *Chem. Commun.*, 2009, 1550–1552. (d) A. T. Luedtke and K. I. Goldberg, *Inorg. Chem.* 2007, **46**, 8496–8498. (e) J. A. Flores, J. G. Andino, N. P. Tsvetkov, M. Pink, R. J. Wolfe, A. R. Head, D. L. Lichtenberger, J. Massa and K. G. Caulton, *Inorg. Chem.*, 2011, **50**, 8121–8131.
13. C. Maaß, D. M. Andrada, R. A. Mata, R. Herbst-Irmer and D. Stalke, *Inorg. Chem.*, 2013, **52**, 9539–9548.
14. A. K. Swarnakar, S. M. McDonald, K. C. Deutsch, P. Choi, M. J. Ferguson, R. McDonald and E. Rivard, *Inorg. Chem.*, 2014, **53**, 8662–8671.
15. (a) M. Olaru, R. Kather, E. Hupf, E. Lork, S. Mebs and J. Beckmann, *Angew. Chem., Int. Ed.*, 2018, **57**, 5917–5920. (b) M. Olaru, S. Krupke, E. Lork, S. Mebs and J. Beckmann, *Dalton Trans.*, 2019, **48**, 5585–5594.
16. B. Raghavendra, K. Bakthavachalam, T. Das, T. Roisnel, S. S. Sen, K. Vanka and S. Ghosh, *J. Organometal. Chem.*, 2020, **911**, 121142 (1-8).
17. Krebs, K. M.; Maudrich, J.-J.; Wesemann, L. *Dalton Trans.*, **2016**, 45, 8081–8088
18. (a) W. Li, X. Ma, M. G. Walawalkar, Z. Yang and H. W. Roesky, *Coord. Chem. Rev.*, 2017, **350**, 14–29. (b) M. L. Shegavi and S. K. Bose, *Catal. Sci. Technol.*, 2019, **9**, 3307–3336. (c) N. Sarkar, S. Bera and S. Nembenna, *J. Org. Chem.*, 2020, **85**, 4999–5009.
19. (a) W. Zheng, A. Stasch, J. Prust, H. W. Roesky, F. Cimpoesu, M. Noltemeyer and H.-G. Schmidt, *Angew. Chem., Int. Ed.*, 2001, **40**, 3461–3464. (b) K. J. Blakeney, P. D. Martin and C. H. Winter, *Organometallics*, 2020, **39**, 1006–1013.
-

- 
20. J. Li, M. Zhong, H. Keil, H. Zhu, R. Herbst-Irmer, D. Stalke, S. De, D. Koley and H. W. Roesky, *Chem. Commun.*, 2019, **55**, 2360-2363.
21. G. S. McGrady, J. S. Turner, R. M. Ibberson and M. Prager, *Organometallics*, 2000, **19**, 4398-4401.
22. R. Mondol and E. Otten, *Inorg. Chem.*, 2019, **58**, 6344–6355.
23. S. Milione, G. Milano and L. Cavallo, *Organometallics*, 2012, **31**, 8498–8504.
24. (a) Y. Mizuhata, T. Sasamori and N. Tokitoh, *Chem. Rev.*, 2009, **109**, 3479–3511. (b) M. Asay, C. Jones and M. Driess, *Chem. Rev.*, 2011, **111**, 354–396.
25. P. Jutzi, D. Kanne and C. Krüger, *Angew. Chem. Int. Ed.*, 1986, **25**, 164–164.
26. M. Denk, R. Lennon, R. Hayashi, R. West, A. V. Belyakov, H. P. Verne, A. Haaland, M. Wagner and N. Metzler, *J. Am. Chem. Soc.*, 1994, **116**, 2691–2692.

## Chapter 4: Transmetallation involving Stannylene and First Row Transition Metals

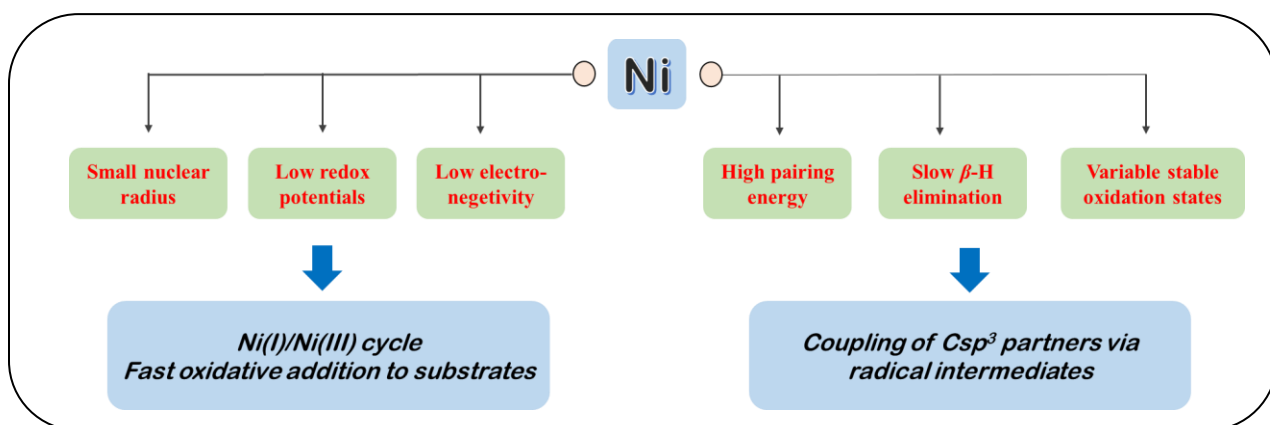


### Abstract

In this chapter, we have extended the transmetallation methodology for the preparation of first-row transition metal complexes such as nickel and copper chloride complexes from a compound with a low-valent tin atom which is quite unusual. As the nickel complexes play a vibrant role in organometallic chemistry, especially in the field of homogeneous catalysis, we have synthesized and stabilized the monomeric nickel-hydride complex as well as the cationic nickel species containing non-coordinating anionic fragment.

## 4.1: Introduction

Transmetalation is a special type of organometallic reaction involving the transfer of ligand from one metal to another. This methodology is commonly well explored for the preparation of a series of transition metal compounds. The development of new transition metal catalysts is of wide interest in synthetic methodology.<sup>1</sup> As the first-row transition metals like manganese, iron, and nickel are very much abundant on earth, their utilization in catalysis has engrossed extensive consideration for the environmental friendly organic synthesis.<sup>2</sup> The chemistry of nickel complexes and their use in homogeneous catalysis has been under progress for the last two decades. In the field of transition metal catalysis, nickel might look like just the underprivileged younger sibling of palladium and platinum. The palladium-catalyzed cross-coupling reactions have already been huge success and finally, it was honored with the prestigious Nobel Prize in Chemistry in 2010. Nickel has been placed just above palladium in the periodic table and it is expected accomplish many of the identical elementary reactions as a group 10 metal like palladium or platinum.<sup>3</sup> As a result, nickel is often considered as an inexpensive alternative to precious metal catalysts, exclusively for cross-coupling reactions. But nickel complexes display some diverse reactive properties from other group 10 metals such as small nuclear radius, low electronegativity, high pairing energy, both high- and low-spin configurations, variable stable oxidation states ranging from Ni(0) to Ni(IV) and low redox potentials (Figure 4.1).<sup>4</sup> All these distinct properties allow Ni catalysts to accommodate and stabilize paramagnetic intermediates along with the access to radical pathways and can easily undergo slow  $\beta$ -H elimination.<sup>4</sup> Many new nickel complexes have already been reported designing multiple novel ligand systems. The catalytic behaviors represent the unique characteristics that distinguish nickel from the previously reported palladium complexes.



**Fig. 4.1:** Valuable assets of Ni<sup>4</sup> (adapted from *Acc. Chem. Res.*, 2020, **53**, 4, 906–919)

The recent fascination about nickel chemistry deals with the preparation and stabilization of low-coordinate nickel complexes as they are highly reactive than others. The high flexibility towards exogenous ligand binding accounts for a high multiplicity of conversions within the coordination sphere of the metal. In this context, metal-hydride entities are of particular interest, firstly, due to their behavior hanging on the residual ligand sphere, and secondly, they can act as the most capable initiators for the most of the different transformations. A lot of attractive chemistry has been found featuring the combination of hydride with nickel using a few amiable ligand scaffolds.<sup>5</sup> However, the chemistry of nickel hydride complexes lagged way behind that of many other metal hydride complexes, mainly due to the limited availability of well-defined ligand systems. As the  $\beta$ -diketiminato ligand has displayed a very versatile tunability in the past for both the main group and transition metal chemistry,<sup>6</sup> so (i) it could be useful for the preparation of coordinatively unsaturated complexes, (ii) it might stabilize the high as well as the low oxidation states of the central metal, and (iii) after complexation, it can show interesting reactivities.<sup>7</sup> Herein, we have modified the traditional symmetrical nacnac ligand system by introducing a methylpyridinato moiety to generate an unsymmetrical ligand scaffold featuring additional donor support for the stabilization of low-coordinated nickel and copper complexes preparing from chlorostannylene analogue (**3.4**) using the transmetallation method. Afterwards, we have prepared challenging monomeric nickel-hydride complex as well as the cationic nickel species containing non-coordinating anionic moiety.

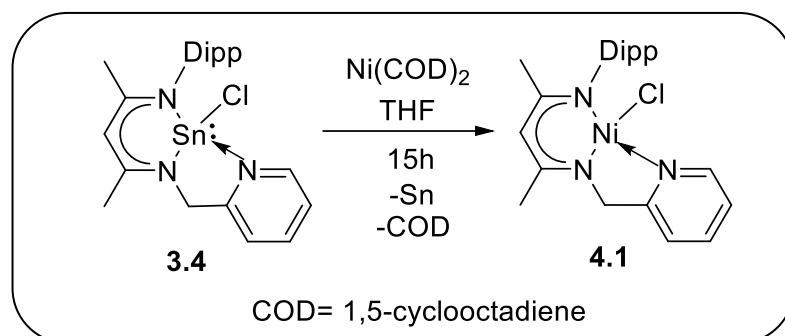
## 4.2: Results and discussions

### 4.2.1: Synthesis, characterization and structural elucidation of nickel-chloride (**4.1**) and copper-chloride complex (**4.2**)

Considering the clean and high yield transformations between two *p*-block elements using transmetallation, we have further extended the transmetallation method towards *p*- to *d*-block elements and afforded analogous nickel (**4.1**) and copper (**4.2**) complexes. The equimolar amount of stannylene **3.4** with Ni(COD)<sub>2</sub> in THF surprisingly led to the formation of the nickel-chloride (**4.1**), presumably with the removal of metallic tin as a precipitate. In this reaction, the oxidation

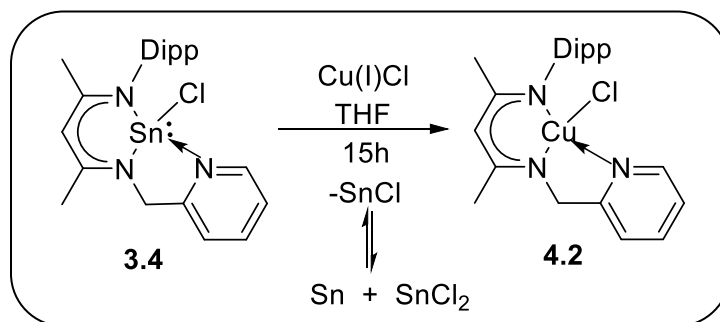


number of the nickel has been changed from 0 to +2 and the vice-versa is true for the central Sn atom; overall it can be described as a redox transmetallation. The removal of solvent and subsequent workup in THF led to the formation of **4.1** with 92 % yield.



**Scheme 4.1:** Synthesis of low-coordinated nickel-chloride (**4.1**) using redox-transmetallation methodology

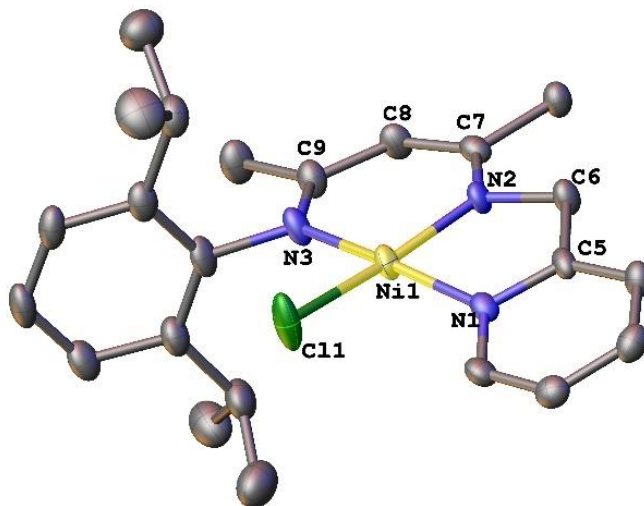
Utilizing a similar reaction methodology, stannylyene **3.4** has been further treated with an equimolar amount of Cu(I)Cl, which afforded the redox transmetallated Cu(II) complex. Filtration of the THF solution from the reaction mixture and storing the concentrated resulting solution at  $-30\text{ }^{\circ}\text{C}$  in a freezer afforded the complex **4.2** in good yield.



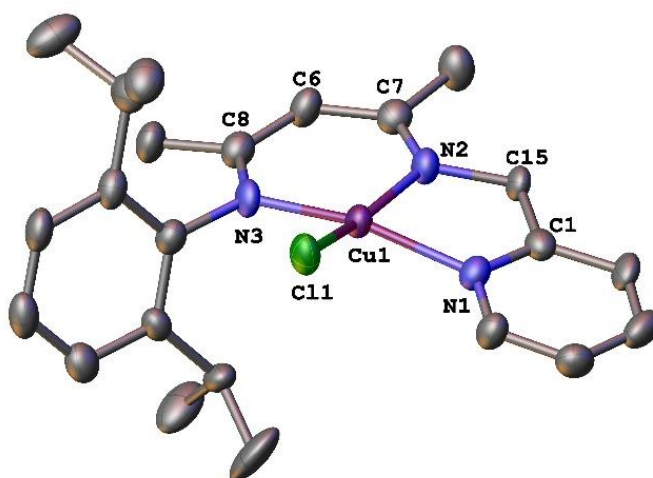
**Scheme 4.2:** Synthesis of **4.2** from chlorostannylyene (**3.4**) via transmetallation methodology

Compound **4.1** was characterized by multinuclear NMR spectroscopy. It clearly shows doublets for two sets of the isopropyl groups, one septet, and two singlets for the methyl groups in the  $^1\text{H}$  NMR spectrum, whereas no NMR peak has been observed for complex **4.2** because of the paramagnetic nature of the central Cu center. Single crystals of **4.1** and **4.2** were grown in a day from the concentrated THF solution at  $-30\text{ }^{\circ}\text{C}$  in a freezer. The solid-state molecular structures of **4.1** and **4.2** are shown in Figures 4.2 and 4.3 respectively along with the important bond lengths

and angles. **4.1** crystallizes in the monoclinic space group  $P-1$ , whereas **4.2** crystallizes in  $P2_1/n$ . Both the crystal structure reveals that both Ni and Cu center is tetra-coordinated, adopting distorted square-planar geometry.



**Fig. 4.2:** Molecular structure of **4.1** with anisotropic displacement parameters depicted at the 50% probability level. Hydrogen atoms are not shown for clarity. Selected bond lengths (Å) and bond angles (°): Ni1–C11 2.194(1), Ni1–N2 1.860(4), Ni1–N1 1.944(3), Ni1–N3 1.906(3); N1–Ni1–C11 90.08(2), N1–Ni1–N2 83.98(2), N2–Ni1–N3 94.09(4), N3–Ni1–C11 92.88(1).

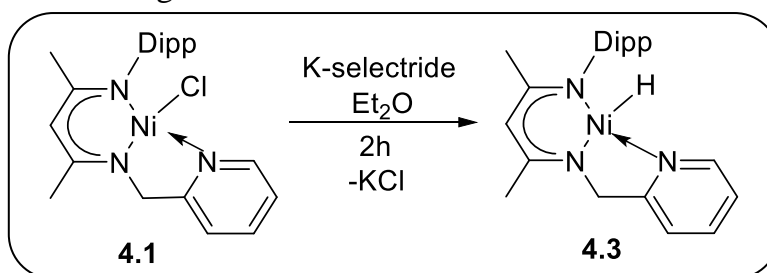


**Fig. 4.3:** Molecular structure of **4.2** with anisotropic displacement parameters depicted at the 50% probability level. Hydrogen atoms are not shown for clarity. Selected bond lengths

(Å) and bond angles (°): Cu1–Cl1 2.263(2), Cu1–N1 2.023(7), Cu1–N2 1.934(6), Cu1–N3 1.948(7); N1–Cu1–N2 82.3(3), N2–Cu1–N3 94.3(3), N1–Cu1–Cl1 91.5(2), N3–Cu1–Cl1 96.6(2).

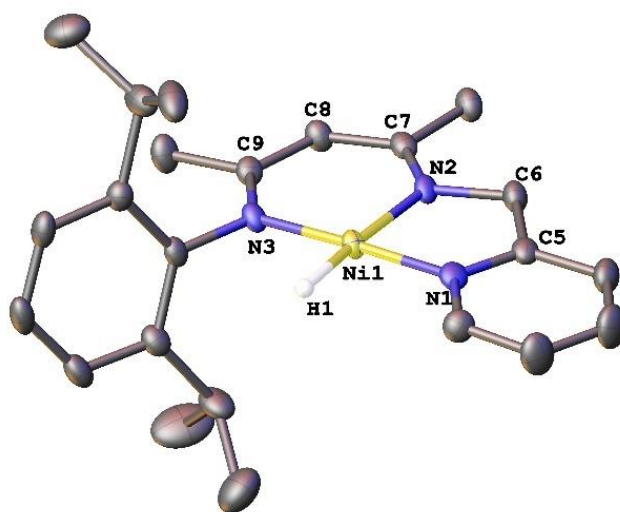
#### 4.2.2: Synthesis, characterization and structural elucidation of monomeric nickel-hydride (4.3)

The nickel hydride complexes are considered as very highly reactive systems that are extensively used in academic and industrial laboratories, primarily in the pitch of homogeneous catalysis for the conversion of several organic or inorganic substrates and in the electrolytic generation of H<sub>2</sub>.<sup>9</sup> Although the chemistry of nickel-hydride complexes was hindered largely due to the limited accessibility of suitably designed systems. Early attempts to stabilize and isolate nickel hydride complexes using several well-established protocols for palladium and platinum analogues often failed, which was defined as the low thermal stability for the nickel hydride complexes.<sup>9,10</sup> Later on, the exploration of new ligand systems has led to the discovery of nickel hydrides. Nickel-halide complexes are represented as suitable starting material for the synthesis of the respective hydride derivative by its reaction with KHBET<sub>3</sub> or by salt metathesis with other metal hydrides. Adding K-selectride (potassium tri-sec-butylborohydride) to a solution of compound **4.1** in di-ethyl ether immediately led to a colour change from black to red and subsequent workup after 2h afforded the stable monomeric nickel-hydride complex **4.3** as red crystals (Scheme 4.3). It must be noted here that, the symmetrical nacnac supported first isolable low-coordinated nickel hydride complex was dimeric and readily eliminated H<sub>2</sub> in presence of external donors or on heating.<sup>5</sup>



**Scheme 4.3:** Preparation of stable monomeric nickel-hydride (**4.3**)

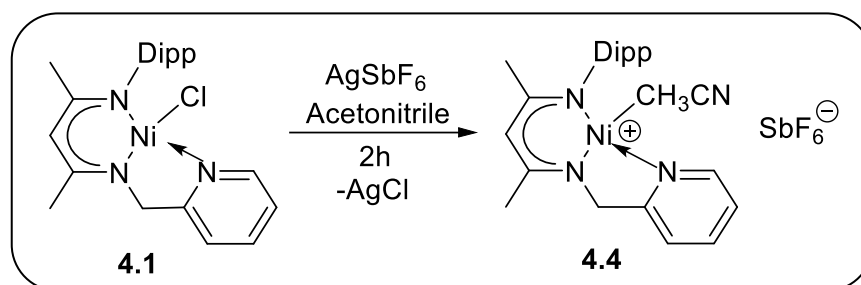
Compound **4.3** was characterized by NMR spectroscopy displaying the significant peak of nickel-hydride at -22.6 ppm along with the resonances of two sets of doublets for the isopropyl groups, one septet, and two singlets for the methyl groups in the  $^1\text{H}$  NMR spectrum. Red crystals suitable for X-ray diffraction studies were obtained by the slow evaporation of the di-ethyl ether solvent. Complex **4.3** has been crystallized in monoclinic, space group  $P2_1/n$  adopting a distorted square-planer geometry. The observed Ni–H distance (1.50(1) Å) is comparable to the previously reported Ni–H distances (e.g., 1.49(5), 1.43(5), and 1.505(20) Å).<sup>11,12</sup>



**Fig. 4.4:** Molecular structure of **4.3** with anisotropic displacement parameters depicted at the 50% probability level. Hydrogen atoms are not shown for clarity. Selected bond lengths (Å) and bond angles (°): Ni1–H1 1.520(1), Ni1–N2 1.939(2), Ni1–N1 1.859(2), Ni1–N3 1.826(2); N1–Ni1–H1 87.21(2), N1–Ni1–N2 87.35(8), N2–Ni1–N3 93.62(8), N3–Ni1–H1 91.86(1).

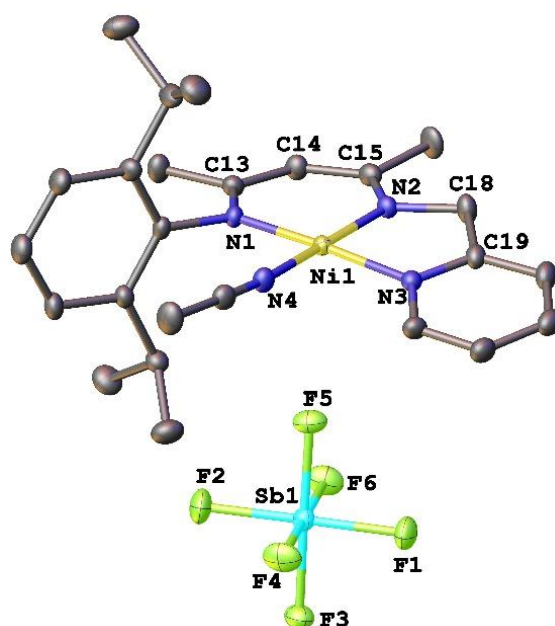
#### 4.2.3: Synthesis, characterization and structural elucidation of cationic nickel complex (**4.4**)

A series of cationic nickel complexes have already been reported for the C–C cross-coupling reactions,<sup>13,15</sup> polymerization of styrene,<sup>14</sup> amination of aryl halides,<sup>16</sup> and Suzuki<sup>17,18</sup> and Kumada reactions.<sup>19</sup> With this backdrop, we have also prepared a cationic nickel complex featuring methylpyridinato nacnac ligand by abstracting the chloride from **4.1** (Scheme 4.4). Treating **4.1** with an equimolar amount of  $\text{AgSbF}_6$  led to the formation of **4.4** stabilized via coordination by a solvent molecule (acetonitrile) with a high yield.



**Scheme 4.4:** Preparation of a stable cationic nickel complex (**4.4**)

Compound **4.4** was further characterized by single-crystal X-ray studies and NMR spectroscopy. The structural data reveal that solvent molecule (acetonitrile) coordinates to the nickel center presumably to attenuate its electrophilic nature. Compound **4.4** crystallizes in the monoclinic symmetry with  $P2_1/n$  space group. The solvent coordinated tetra-coordinated nickel center adopts a distorted square-planar geometry with a non-coordinating  $\text{SbF}_6^-$  anionic fragment (Figure 4.5). The  $\text{Ni-N}_{\text{pyridine}}$  bond [1.919(4) Å] is observed as significantly longer than the  $\text{Ni-N}_{\text{ligands}}$  bond lengths [1.893(4) and 1.844(3) Å].



**Fig. 4.5:** Molecular structure of **4.4** with anisotropic displacement parameters depicted at the 50% probability level. Hydrogen atoms are not shown for clarity. Selected bond lengths (Å) and bond angles (°):  $\text{Ni1-N1}$  1.893(4),  $\text{Ni1-N2}$  1.844(3),  $\text{Ni1-N3}$  1.919(4),  $\text{Ni1-N4}$  1.889(4);  $\text{N1-Ni1-N2}$  94.8(2),  $\text{N1-Ni1-N4}$  90.6(2),  $\text{N2-Ni1-N3}$  84.6(2),  $\text{N3-Ni1-N4}$  90.3(2).

### 4.3: Conclusions

The past two decades have seen spectacular progress in the chemistry of nickel complexes with a catalogue of discovery and application of several nickel-hydride and cationic nickel species. We have introduced and explored the unusual reactivities of several main group and first-row transition metal complexes containing the methyl-pyridyl group supported unsymmetrical ncnac ligand scaffold. We are able to prepare monomeric nickel-chloride and copper-chloride using a redox-transmetallation methodology from a stannylene compound. In a subsequent reaction with K-selectride, the chloride ligand is replaced with a hydride moiety, leading to the formation of a monomeric nickel-hydride complex. Further, we have prepared the cationic nickel species comprising a non-coordinating anionic moiety.

### 4.4: References

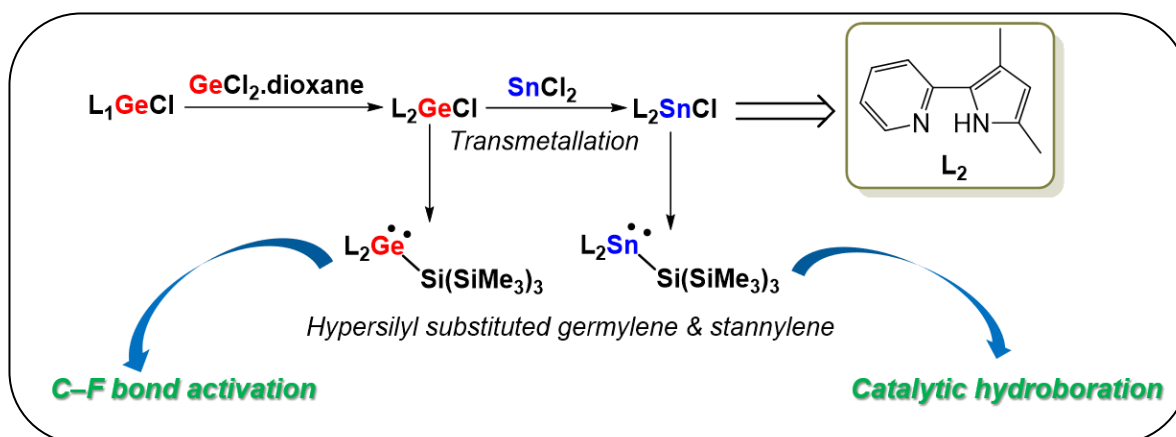
1. X. Wu and A. V. Gordon, *Eur. J. Org. Chem.*, **2009**, 503–509.
2. T. Nishimura, Y. Ando, H. Shinokubo, and Yoshihiro Miyake, *Chem. Lett.*, 2021, **50**, 1049–1052.
3. S. Z. Tasker<sup>1</sup>, E. A. Standley and T. F. Jamison, *Nature*, 2014, **509**, 299–309.
4. J. Diccianni, Q. Lin and T. Diao, *Acc. Chem. Res.*, 2020, **53**, 4, 906–919.
5. S. Pfirrmann, C. Limberg and B. Ziemer, *Dalton Trans.*, 2008, 6689–6691.
6. L. Bourget-Merle, M. F. Lappert and J. R. Severn, *Chem. Rev.*, 2002, **102**, 3031–3065.
7. (a) Y.-C. Tsai, P.-Y. Wang, S.-A. Chen and J.-M. Chen, *J. Am. Chem. Soc.*, 2007, **129**, 8066–8067; (b) W. H. Monillas, G. P. A. Yap, L. A. MacAdams and K. H. Theopold, *J. Am. Chem. Soc.*, 2007, **129**, 8090–8091; (c) J. M. Smith, R. L. Lachicotte, K. A. Pittard, T. R. Cundari, G. Lukat-Rodgers, K. R. Rodgers and P. L. Holland, *J. Am. Chem. Soc.*, 2001, **123**, 9222–9223; (d) G. Bai and D. W. Stephan, *Angew. Chem. Int. Ed.*, 2007, **46**, 1856–1859; (e) N. W. Aboeella, E. A. Lewis, A. M. Reynolds, W. W. Brennessel, C. J. Cramer and W. B. Tolman, *J. Am. Chem. Soc.*, 2002, **124**, 10660–10661; (f) D. J. E. Spencer, N. W. Aboeella, A. M. Reynolds, P. L. Holland and W. B. Tolman, *J. Am. Chem. Soc.*, 2002, **124**, 2108–2109.
8. H. Gehring, R. Metzinger, C. Herwig, J. Intemann, S. Harder and C. Limberg, *Chem. Eur. J.*, 2013, **19**, 1629–1636.

9. M. L. H. Green, C. N. Street and G. Wilkinson, *Z. Naturforsch., B: J. Chem. Sci.*, 1959, **14**, 738.
10. E. H. Brooks and F. Glockling, *J. Chem. Soc. A*, 1967, 1030–1034.
11. S. Pfirrmann, C. Limberg, C. Herwig, C. Knispel, B. Braun, E. Bill and R. Stösser, *J. Am. Chem. Soc.*, 2010, **132**, 13684–13691.
12. J. Breitenfeld, R. Scopelliti and X. Hu, *Organometallics*, 2012, **31**, 2128–2136.
13. (a) Z. Xi, X. Zhang, W. Chen, S. Fu and D. Wang, *Organometallics*, 2007, **26**, 6636–6642; (b) K. Inamoto, J.-i. Kuroda, T. Sakamoto and K. Hiroya, *Synthesis*, 2007, 2853–2866.
14. W. Buchowicz, A. Koziol, L. B. Jerzykiewicz, T. Lis, S. Pasykiewicz, A. Pecherzewska and A. Pietrzykowski, *J. Mol. Catal. A*, 2006, **257**, 118–123.
15. M. Moreno-Mañas, M. Pérez and R. Pleixats, *J. Org. Chem.* 1996, **61**, 2346–2351.
16. (a) K. Matsubara, K. Ueno, Y. Koga and K. Hara, *J. Org. Chem.*, 2007, **72**, 5069–5076; (b) R. A. Kelly III, N. M. Scott, S. Díez-Gonzalez, E. D. Stevens and S. P. Nolan, *Organometallics*, 2005, **24**, 3442–3447.
17. V. Ritleng, A. M. Oerel and M. J. Chetcuti, *Dalton Trans.*, 2010, **39**, 8153–8160.
18. (a) K. Inamoto, J.-i. Kuroda, E. Kwon, K. Hiroya and T. Doi, *J. Organomet. Chem.*, 2009, **694**, 389–396; (b) J.-i. Kuroda, K. Inamoto, K. Hiroya and T. Doi, *Eur. J. Org. Chem.*, 2009, 2251–2261; (c) Y. Zhou, Z. Xi, W. Chen and D. Wang, *Organometallics*, 2008, **27**, 5911–5920; (d) C.-Y. Liao, K.-T. Chan, Y.-C. Chang, C.-Y. Chen, C.-Y. Tu, C.-H. Hu and H. M. Lee, *Organometallics*, 2007, **26**, 5826–5833; (e) C.-C. Lee, W.-C. Ke, K.-T. Chan, C.-L. Lai, C.-H. Hu and H. M. Lee, *Chem. Eur. J*, 2007, **13**, 582–591; (f) K. Inamoto, J.-i. Kuroda, K. Hiroya, Y. Noda, M. Watanabe and T. Sakamoto, *Organometallics*, 2006, **25**, 3095–3098; (g) P. L. Chiu, C.-L. Lai, C.-F. Chang, C.-H. Hu and H. M. Lee, *Organometallics*, 2005, **24**, 6169–6178; (h) D. S. McGuinness, K. J. Cavell, B. W. Skelton and A. H. White, *Organometallics*, 1999, **18**, 1596–1605.
19. (a) A. Liu, X. Zhang and W. Chen, *Organometallics*, 2009, **28**, 4868–4871; (b) J. Berding, M. Lutz, A. L. Spek and E. Bouwman, *Organometallics*, 2009, **28**, 1845–1854; (c) S. Gu and W. Chen, *Organometallics*, 2009, **28**, 909–914; (d) Z. Xi, B. Liu and W.

Chen, *J. Org. Chem.*, 2008, **73**, 3954–3957; (e) K. Matsubara, K. Ueno and Y. Shibata, *Organometallics*, 2006, **25**, 3422–3427.



## Chapter 5: Pyridylpyrrolido Ligand Supported Germylene and Stannylene Chemistry

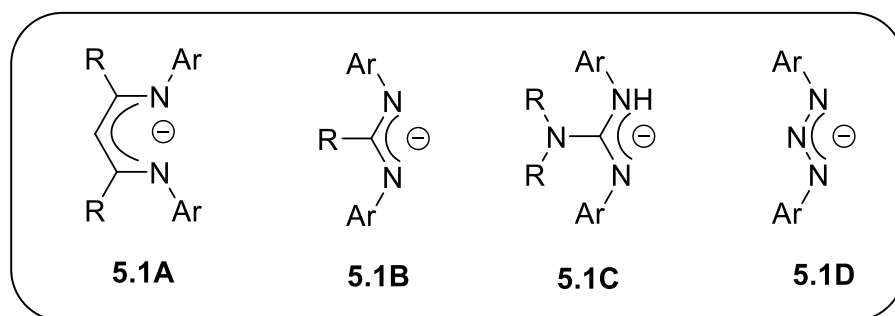


### Abstract:

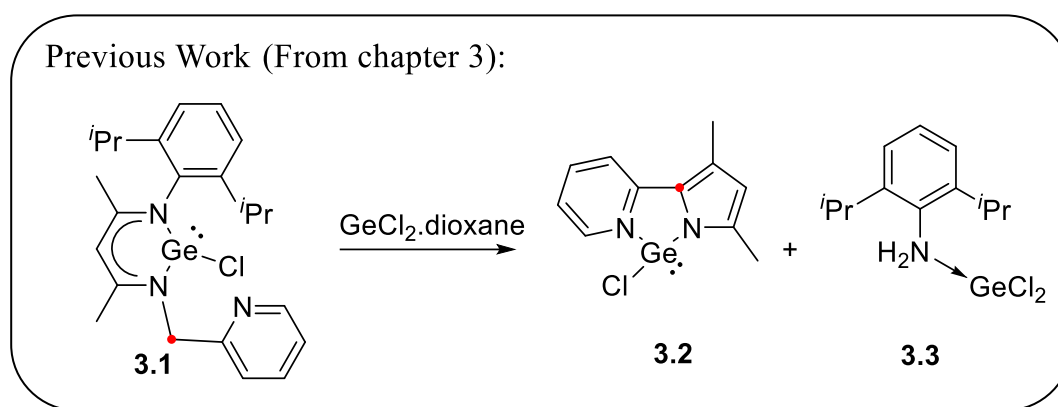
In this chapter, we will discuss about the high scale synthesis of the chlorogermylene (**3.2**), along with the preparation of a sequences of new germynes and stannylens starting from **3.2**. The transmetallation reaction between **3.2** and  $SnCl_2$  led to the formation of analogous chlorostannylene (**5.1**) with simultaneous removal of  $GeCl_2$ . This transmetallation between two elements from the same group is very scarce till date. The attempt to prepare **5.1** via lithiation method, led to the formation of **5.2** as an unexpected side product, where the ortho C–H bond of the pyridine ring was activated and functionalized with a  $nBu$  moiety. Subsequently, **3.2** and **5.1** were used as precursors to give germylene (**5.4**) and stannylene (**5.5**) containing tris(trimethylsilyl)silyl (hypersilyl) moieties. Utilizing the affection between fluoride and silicon atom, we have prepared tetrafluoropyridyl germylene (**5.6**) by treating **5.4** with  $C_5F_5N$  along with the simultaneous elimination of  $(Me_3Si)_3SiF$ . As there is a insufficiency of Sn(II) compound as single-site catalysts, we have also explored the hydroboration of aldehydes, ketones, alkenes and alkynes using **5.5** as a catalyst. All the compounds have been successfully characterized by single-crystal X-ray as well as by state-of-the spectroscopic art.

## 5.1: Introduction

For the enrichment and understanding of main-group chemistry, heavier congeners of carbenes have played a substantial role along with the development of new sterically demanding monoanionic ligand scaffold. To stabilize compounds with low-valent main-group elements, bidentate monoanionic bulky N,N'-ligands (Fig 5.1) such as  $\beta$ -diketiminates (**5.1A**), amidinates (**5.1B**), guanidinate (**5.1C**), triazenide (**5.1D**), and recently monoanionic ditopic ligands have been widely explored due to their straightforward synthesis, possibility for a fine-tuning of the substituents, and occupying a second coordination site on the metal.<sup>1-5</sup> A very similar monoanionic bidentate ligand, the pyridylpyrrolide ligand (PyPyr), had found widespread application in transition metal chemistry apparently due to its push-pull nature. Special thanks to the pioneering work done by the groups of Tilley, Goldberg, Pucci, Carty, Caulton and others.<sup>6-10</sup> The DFT calculations on N-methyl pyridyl-pyrrolide indicate that the HOMO is primarily located on the pyrrolide site, while the LUMO is on pyridyl moiety.<sup>11</sup> However, the chemistry of this ligand with main group elements has not been widely explored till date. This is somewhat surprising because the pyrrolide ligand is electron rich and the adjacent pyridyl motif may provide additional stability through donation. Recently, we have accessed a pyridylpyrrolido germylene (**3.2**)<sup>12</sup> serendipitously from a picolyl functionalized  $\beta$ -diketiminato chlorogermylene (Scheme 5.1). However, the yield of the germylene was less than 50%. In this chapter, we have discussed a high yield preparation of **3.2** and its further reactivity studies. The corresponding stannylenes chemistry has also been studied.



**Fig 5.1:** Examples of monoanionic bidentate N,N'-ligands

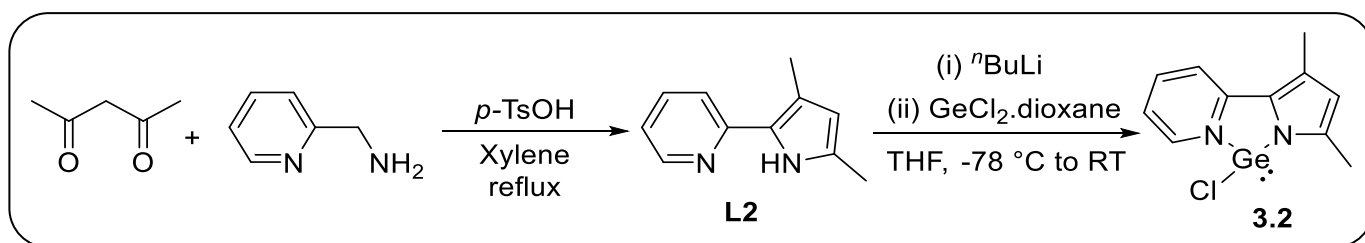


**Scheme 5.1:** Rearrangement of picolyl substituted  $\beta$ -diketiminato chlorogermylene (**3.1**) to PyPyrchlorgermylene (**3.2**) upon addition of GeCl<sub>2</sub>·dioxane.<sup>12</sup>

The synthesis of tetrylene derivatives with electropositive hypersilyl moiety has been presently undergoing a rapid development in the field of low-valent main-group chemistry. The use of hypersilyl group in compounds with main-group elements was dated back in 1981, when Brook exposed that the photolysis of an acylsilane offered the discovery to the first well-characterized compound with a Si=C double bond.<sup>13</sup> The advantages of the hypersilyl group are not only deals with the good  $\sigma$ -donation or noticeable steric bulk, but the viable readiness of the precursors and prospect of further functionalization due to the presence of the SiMe<sub>3</sub> moieties. Subsequently, a significant research effort has been dedicated to using hypersilyl moiety as a stabilizer for novel compounds with low-valent main-group elements with key contributions coming from the groups of Stalke,<sup>14</sup> Inoue,<sup>15</sup> Aldridge,<sup>16</sup> Rivard,<sup>17</sup> Leszczyńska,<sup>18</sup> Castel,<sup>19</sup> Marschner, Baumgartner, and others.<sup>20</sup> Recently we have also reported benz-amidinato silylene,<sup>21</sup> germylene,<sup>22</sup> stannylene<sup>23</sup> with hypersilyl moiety and studied their reactivities.<sup>21,23-25</sup> Here, we have synthesized similar hypersilyl moiety substituted germylene and stannylene featuring PyPyr ligand scaffold and studied their reactivity studies. Finally, the catalytic utility of a PyPyr-based hypersilyl stannylene towards hydroboration of aldehydes, ketones, alkenes and alkynes, has also been examined.

## 5.2: Results and Discussions

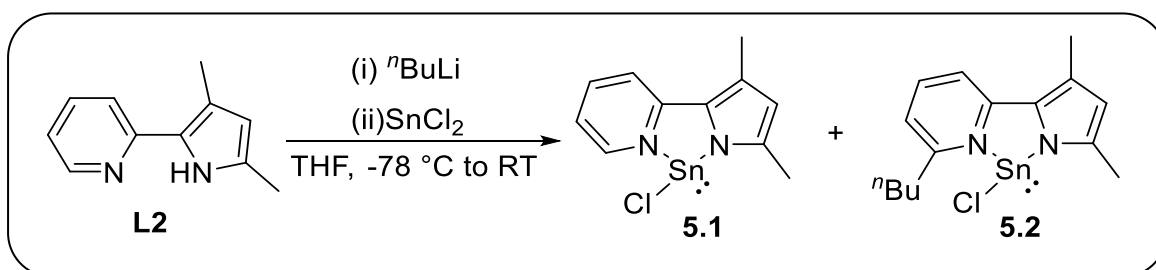
The high yield synthesis of the PyPyr-based chlorogermylene (93 %) employed in the study and depicted in Scheme 5.2. The pyridylpyrrole ligand was prepared according to a reported literature procedure<sup>26</sup> and the previously described chlorogermylene **3.2** was prepared by treating the ligand with <sup>n</sup>BuLi and GeCl<sub>2</sub>·dioxane subsequently to get quantitative yield (Scheme 5.2).



**Scheme 5.2:** High yield synthesis of **3.2**

### 5.2.1: Synthesis, characterization and structural elucidation of compound **5.1** and **5.2**

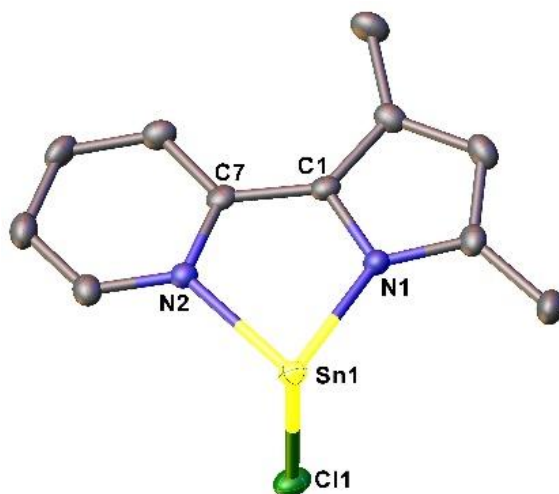
With the success of the high yield synthesis of **3.2**, our next attempt was to prepare the analogous stannylene. However, along with the generation of our desired stannylene (**5.1**), the reaction led to the formation of another stannylene (**5.2**), where the ortho C–H bond of the pyridine ring was activated and further functionalized with a <sup>n</sup>Bu moiety (Scheme 5.3). Such direct alkylation of the of pyridine or the selective functionalization of the ortho C–H bond of the of pyridine ring was described using excess <sup>t</sup>BuLi with controlled reaction condition in very low temperature.<sup>27</sup> We were unable to prepare compound **5.2** in a suitable reaction condition that can permit the complete spectroscopic characterization even after using two equivalents of <sup>n</sup>BuLi and we have always obtained the formation of mixture of **5.1** and **5.2**. Hence, the identification of compound **5.2** was only supported by the solid-state single-crystal X-ray structure and HRMS data. The purity of **5.1** was finally achieved by lithiating PyPyr ligand with Li(HMDS) with successive addition of 1 equiv of SnCl<sub>2</sub>.<sup>28b</sup>



**Scheme 5.3:** Synthesis of **5.1** and **5.2**

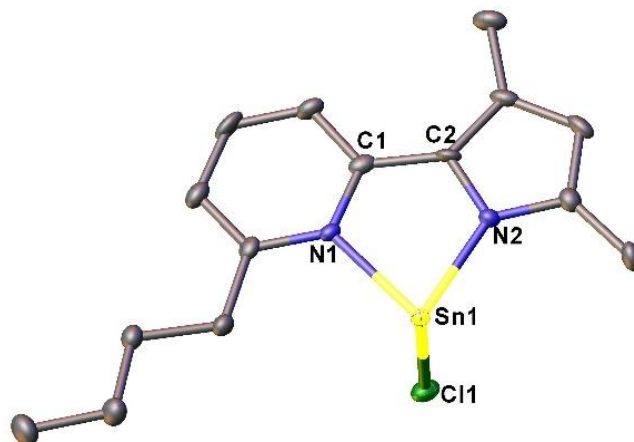
The solid-state structure of **5.1** has been derived from single crystal X-ray diffraction study (Fig. 5.2). **5.1** crystallizes in the triclinic space group *P*-1. The tin atom is tri-coordinated and comprises a short Sn1–N1 bond to the pyrrole (2.15(2) Å) and a longer Sn1–N2 bond (2.25(1) Å) to the

pyridine nitrogen atom. The two methyl groups attached with the pyrrole ring exhibit two singlets at  $\delta$  2.30 and 2.36 ppm in the  $^1\text{H}$  NMR spectrum, while the  $^{119}\text{Sn}$  NMR resonates at -151.86 ppm. The Sn-Cl bond length is 2.48(1) Å, which is in good agreement with the previously reported other chlorostannylenes by the groups of Roesky, Stalke, Jones, Nakata, Nagendran, and others.<sup>28</sup>



**Fig. 5.2:** The molecular structure of **5.1**. Anisotropic displacement parameters are depicted at the 50% probability level. Selected bond lengths [Å] and angles [°]: Sn1–N1 2.15(2), Sn1–N2 2.25(1), and Sn1–Cl1 2.48(1); N1–Sn1–N2 74.5(1), N1–Sn1–Cl1 93.6(1), and N2–Sn1–Cl1 90.16(9).

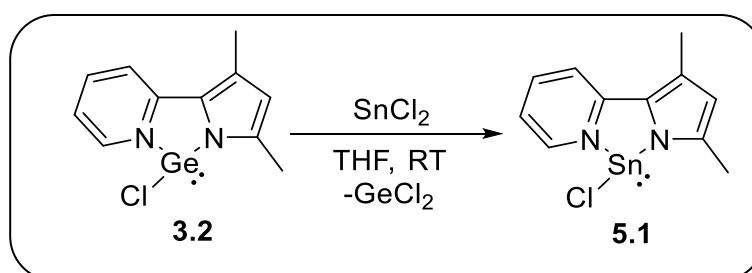
Suitable crystals of **5.2** for the X-ray structural analysis were obtained from the concentrated toluene solution at  $-30$  °C along with the crystals of compound **5.1**. Single crystal X-ray study of **5.2** reveals that the pyridine moiety contains the  $^n\text{Bu}$  group at the *ortho* position of pyridine N (Fig. 5.3). The tri-coordinated tin(II) chloride contains of a longer Sn1–N1 bond (2.251(3) Å) to the pyridine nitrogen atom and a relatively shorter Sn1–N2 bond (2.132(3) Å) to the pyrrole nitrogen atom. The Sn-Cl bond (2.3523(5) Å) in **5.2** is substantially shorter than that of **5.1**. The molecular ion peak of **5.2** was observed with the highest relative intensity in the HRMS spectrum at  $m/z$  383.0331.



**Fig. 5.3:** The molecular structure of **5.2**. Anisotropic displacement parameters are depicted at the 50% probability level. Selected bond lengths [ $\text{\AA}$ ] and angles [ $^\circ$ ]: Sn1–N1 2.251(3), Sn1–N2 2.132(3), and Sn1–Cl1 2.3523 (5); N1–Sn1–N2 74.7(1), N1–Sn1–Cl1 88.29(8), and N2–Sn1–Cl1 93.63 (9).

### 5.2.2: Alternative synthetic pathway to produce highly pure compound **5.1** in quantitative yield

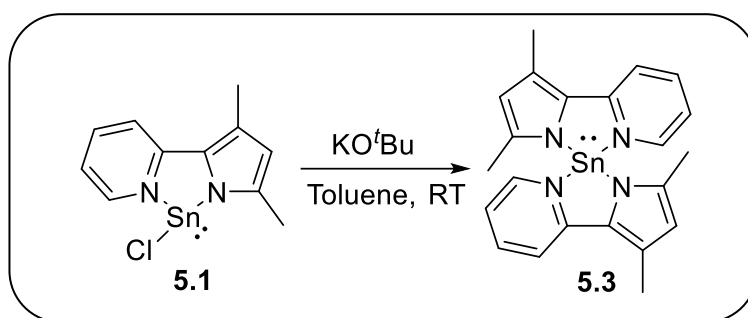
The reaction of equimolar amount of  $\text{SnCl}_2$  with **3.2** in THF led to the clean formation of **5.1** with concomitant removal of  $\text{GeCl}_2$  (Scheme 5.4) in quantitative yield. There are limited examples of the transmetallation between two *p*-block elements<sup>12,29</sup> and it is a very rare transmetallation between two *p*-block elements from the same group. The concentrated THF solution of **5.1** afforded the pale-yellow crystals suitable for single-crystal X-ray analysis after storing at  $-30\text{ }^\circ\text{C}$  in a freezer. The formation of **5.1** was further confirmed by comparing the spectroscopic data as well as the unit cell value of a single crystal with the previously obtained sample.



**Scheme 5.4:** Alternative synthesis of chlorostannylene (**5.1**) using transmetallation methodology

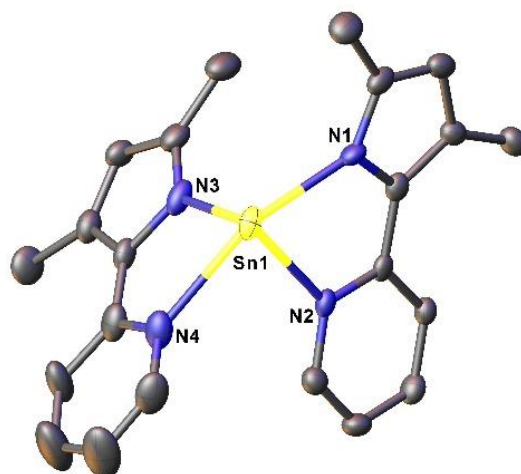
### 5.2.3: Synthesis, characterization and structural elucidation of compound 5.3

A homoleptic tin compound (**5.3**) was formed by treating **5.1** with equimolar amount of KO<sup>t</sup>Bu in toluene (Scheme 5.5). Compound **5.3** was characterized by <sup>1</sup>H, <sup>13</sup>C NMR spectroscopy, HRMS and X-ray structural analysis. However, after numerous attempts, we were unsuccessful to record the <sup>119</sup>Sn NMR spectrum due to the low solubility of **5.3**.



**Scheme 5.5:** Synthesis of homoleptic tin compound (**5.3**)

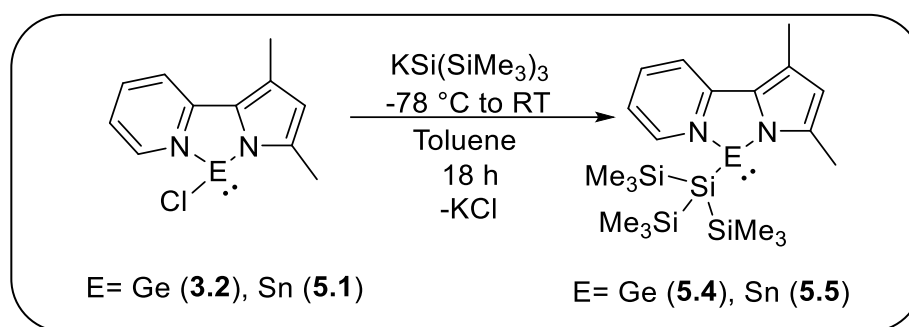
The <sup>1</sup>H NMR spectrum displays two singlets at  $\delta$  2.27 and 2.34 ppm, which was attributed to the methyl groups attached to the pyrrole ring. The air-sensitive yellow crystals suitable for X-ray analysis were obtained from the toluene solution of **5.3** at  $-30$  °C in a freezer. Compound **5.3** crystallizes in the triclinic space group *P*-1 (Figure 5.4). The coordination geometry around the Sn atom can be depicted as distorted sawhorse-like structure. The Sn1–N bonds with the pyrrole rings (2.197 (3) and 2.281 (4) Å) are moderately shorter than the Sn1–N bonds (2.355(4) and 2.432 (5) Å) to the pyridine nitrogen atoms.



**Fig. 5.4:** The molecular structure of **5.3**. Anisotropic displacement parameters are depicted at the 50% probability level. Selected bond lengths [ $\text{\AA}$ ] and angles [ $^\circ$ ]: Sn1–N1 2.281(4), Sn1–N2 2.355(4), Sn1–N3 2.197(3), and Sn1–N4 2.432(5); N1–Sn1–N2 70.0(1), N1–Sn1–N3 91.9(1), N2–Sn1–N4 80.1(1), and N3–Sn1–N4 71.1(1).

#### 5.2.4: Synthesis, characterization and structural elucidation of compound **5.4** and **5.5**

The treatment of **3.2** and **5.1** with  $\text{KSi}(\text{SiMe}_3)_3$  in toluene at room temperature smoothly afforded the hypersilyl substituted germylene (**5.4**) and stannylene (**5.5**) derivatives (Scheme 5.6). The red and orange crystals of **5.4** and **5.5** were isolated respectively, from the concentrated toluene solution at low temperature ( $-20\text{ }^\circ\text{C}$ ) within 3-4 days. The  $^1\text{H}$  NMR spectra of **5.4** and **5.5** display a resonance at 0.27 and 0.29 ppm respectively for the three  $\text{SiMe}_3$  groups. The two methyl groups attached to the pyrrole moiety show singlets at  $\delta$  2.30 and 2.36 ppm for the **5.4**, whereas the same have been observed at  $\delta$  2.36 and 2.39 ppm for **5.5**. We could not observe any resonance in the solution-state  $^{29}\text{Si}$  NMR (for **5.4** and **5.5**) as well as  $^{119}\text{Sn}$  NMR (for **5.5**) spectrum due to the gradual decomposition of both the compounds to the free ligand moiety. However, the  $^{29}\text{Si}$  NMR chemical shift of **5.4** appears at  $\delta$  -105.84 ( $\text{Si}(\text{SiMe}_3)_3$ ), -8.27 ( $\text{Si}(\text{SiMe}_3)_3$ ) ppm, while **5.5** shows signals at  $\delta$  -99.86 ( $\text{Si}(\text{SiMe}_3)_3$ ), -6.28 ( $\text{Si}(\text{SiMe}_3)_3$ ) ppm in the solid state.

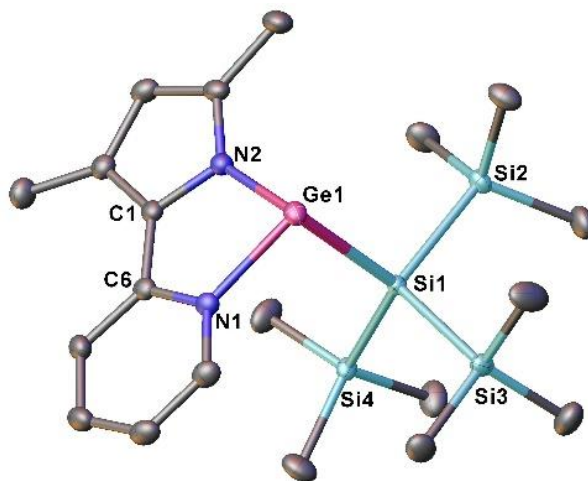


**Scheme 5.6:** Synthesis of hypersilyl substituted germylene (**5.4**) and stannylene (**5.5**)

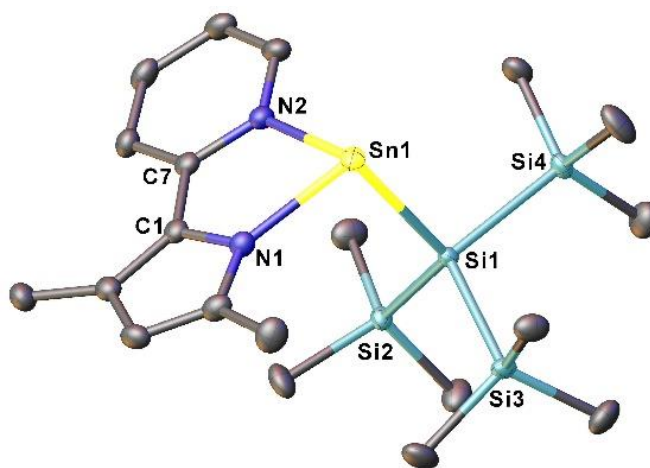
The molecular structures of **5.4** and **5.5** are represented in Figure 5.5 and Figure 5.6, respectively with important bond lengths and angles. The central Ge(II) and Sn(II) atoms in **5.4** and **5.5** are tri-coordinated and display a distorted trigonal-pyramidal geometry with a M–Si bond. The Ge–Si bond length in **5.4** (2.4900(4)  $\text{\AA}$ ) is shorter than that the reported bonds for other hypersilylgermylenes, such as  $[\text{PhC}(\text{NSiMe}_3)_2\text{GeSi}(\text{SiMe}_3)_3]$  (2.525(1)



Å),<sup>19a</sup> and  $[\text{PhC}(\text{N}^i\text{Bu})_2\text{GeSi}(\text{SiMe}_3)_3]$  (2.5216(5) Å).<sup>22</sup> The Sn–Si bond length in **5.5** (2.6675(8) Å) is in good indenture with the earlier reported Sn–Si bonds in the dimeric bis(hypersilyl)stannylene  $[\text{Sn}\{\text{Si}(\text{SiMe}_3)_3\}_2]_2$  (2.6667(11) Å).<sup>30</sup>



**Fig. 5.5:** The molecular structure of **5.4**. Anisotropic displacement parameters are depicted at the 50% probability level. Selected bond lengths [Å] and angles [°]: Ge1–Si1 2.4900(4), Si1–Si2 2.3488(5), Ge1–N1 2.039 (1), and Ge1–N2 1.973(1); N1–Ge1–N2 79.54(5), N1–Ge1–Si1 94.66(3), and N2–Ge1–Si1 99.65(3).

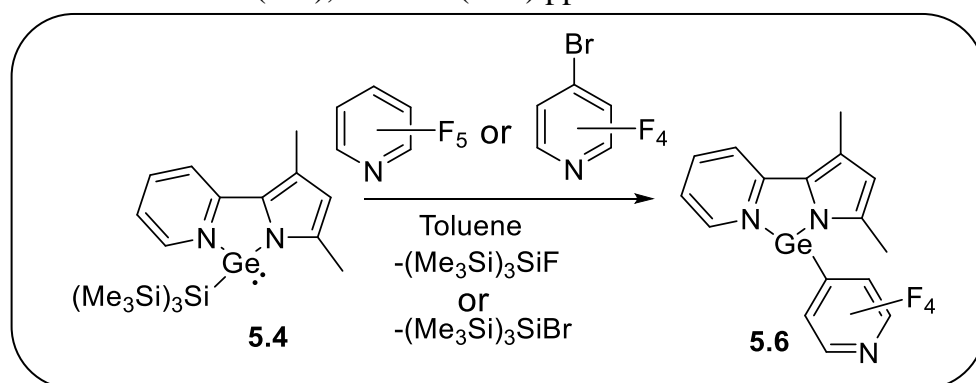


**Fig. 5.6:** The molecular structure of **5.5**. Anisotropic displacement parameters are depicted at the 50% probability level. Selected bond lengths [Å] and angles [°]: Sn1–Si1 2.6675(8), Si1–Si2

2.347(1), Sn1–N1 2.170(2), and Sn1–N2 2.251(1); N1–Sn1–N2 74.09(5), N1–Sn1–Si1 97.64(4), and N2–Sn1–Si1 93.98(4).

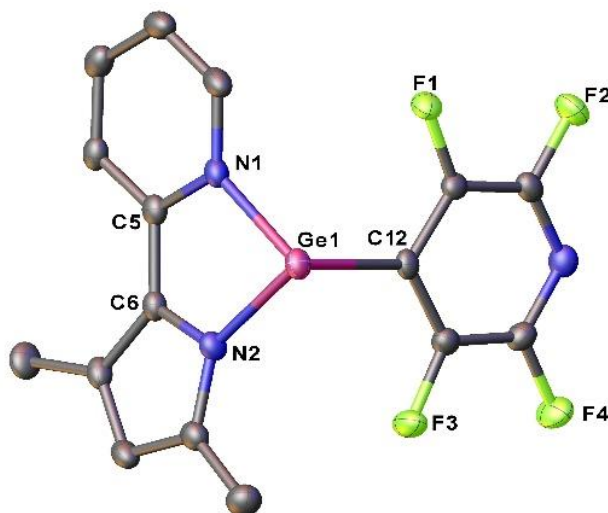
### 5.2.5: Synthesis, characterization and structural elucidation of compound 5.6

Due to our current interest towards understanding of the C–F bond activation by carbenes and its heavier analogues,<sup>31-35</sup> the reactivity of hypersilyl germylene, **5.4** with pentafluoropyridine has been explored. The strong affinity of silicon towards fluorine led to the elimination of  $(\text{Me}_3\text{Si})_3\text{SiF}$ , which was efficiently noticed at -255 ppm in the  $^{19}\text{F}$  NMR and afforded tetrafluoroaryl germylene, **5.6** (Scheme 5.7) (See the experimental section for the NMR of the reaction mixture). The  $^{19}\text{F}$  NMR spectrum of **5.6** displays two sharp resonances at -94.48 (*o*-F), -134.17 (*m*-F) ppm.



**Scheme 5.7:** Formation of perfluoroaryl germylene (**5.6**) from **5.4**

To further investigate about the C–F bond activation, the analogous reaction was performed with 4-Bromo-2,3,5,6-tetrafluoropyridine with **5.4**. To our surprise, instead of activating any C–F bond, the C–Br bond at the *para* position of the compound gets activated and produced compound **5.6**. The constitution of **5.6** was endorsed by single crystal X-ray diffraction studies, which is exemplified in Figure 5.7. The geometry around the Ge(II) center is distorted trigonal-pyramidal with Ge(II)–C bond of 2.072(2) Å, which is comparable well with the previously reported Ge–C bond length.<sup>22,36</sup>

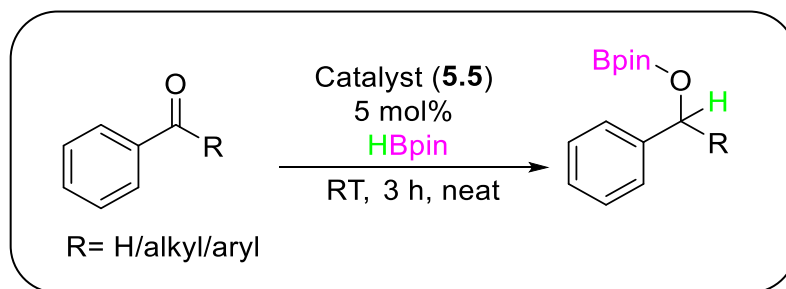


**Fig. 5.7:** The molecular structure of **5.6**. Anisotropic displacement parameters are depicted at the 50% probability level. Selected bond lengths [Å] and angles [°]: Ge1–N1 2.050(1), Ge1–N2 1.956(2), Ge1–C12 2.072(2), N3–C16 1.310(3), N3–C14 1.312(3), C16–F4 1.344(3), C14–F2 1.342(2); N1–Ge1–N2 79.82(7), N1–Ge1–C12 91.37(7), and N2–Ge1–C12 93.69(7).

### 5.2.6: Catalytic hydroboration studies using **5.5** as catalyst

One of the most important homogeneously catalyzed reactions is the accumulation of a B–H bond over the C=C, C=O, and C=N bonds i.e. the catalytic hydroboration. It is a powerful synthetic method for the bulk production of organoboron compounds.<sup>37</sup> Group 4 metallocenes<sup>38</sup> and precious metal compounds, mainly the organometallic rhodium and iridium complexes<sup>29</sup> are well-known catalysts for hydroboration reactions. Recently, there is a trend towards the investigation of catalysts with main group elements as viable replacements to transition metal catalysts, due to environmental concerns, inadequate global abundance, and the high cost of traditional transition metal catalysts.<sup>40-43</sup> A large number of research groups including ourselves have started utilizing compounds with *s*- and *p*-block elements as single site catalysts for the catalytic hydroboration of aldehydes and ketones. Here, we have explored the catalytic hydroboration of a series of aldehydes, ketones, alkynes, and alkenes with hypersilyl substituted stannylene **5.5**. These studies concentrated on stannylene systems, due to the low cost of tin compared to germanium and the very limited focus on using tin(II) compounds as catalysts or pre-catalysts for hydroboration of organic substrates. Although the number of publications are exponentially swelling on hydroboration using *p*-block compounds,<sup>44</sup> to the best of our knowledge there are very few reports

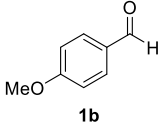
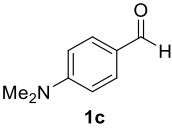
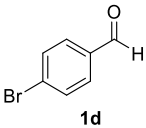
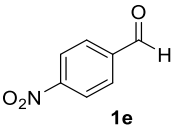
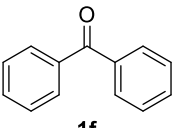
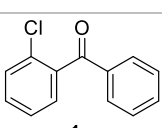
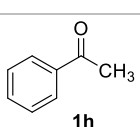
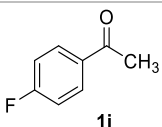
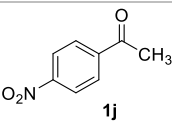
on tin catalyzed hydroboration by the groups of Jones,<sup>45</sup> Wesemann,<sup>46</sup> Nagendran,<sup>28c</sup> Khan,<sup>47</sup> and recently by Nakata.<sup>48</sup> However, all these examples are limited to only aldehydes and ketones. Our primary study on the catalytic application using **5.1**, **5.3**, and **5.5** revealed that they can catalyze benzaldehyde hydroboration with pinacolborane (HBpin) under mild conditions; however, the activities of **5.5** emerges as the best compared to **5.1** and **5.3**. (See Table 5.1, entries 1–3).



**Scheme 5.8:** Hydroboration of aldehydes and ketones catalyzed by **5.5**

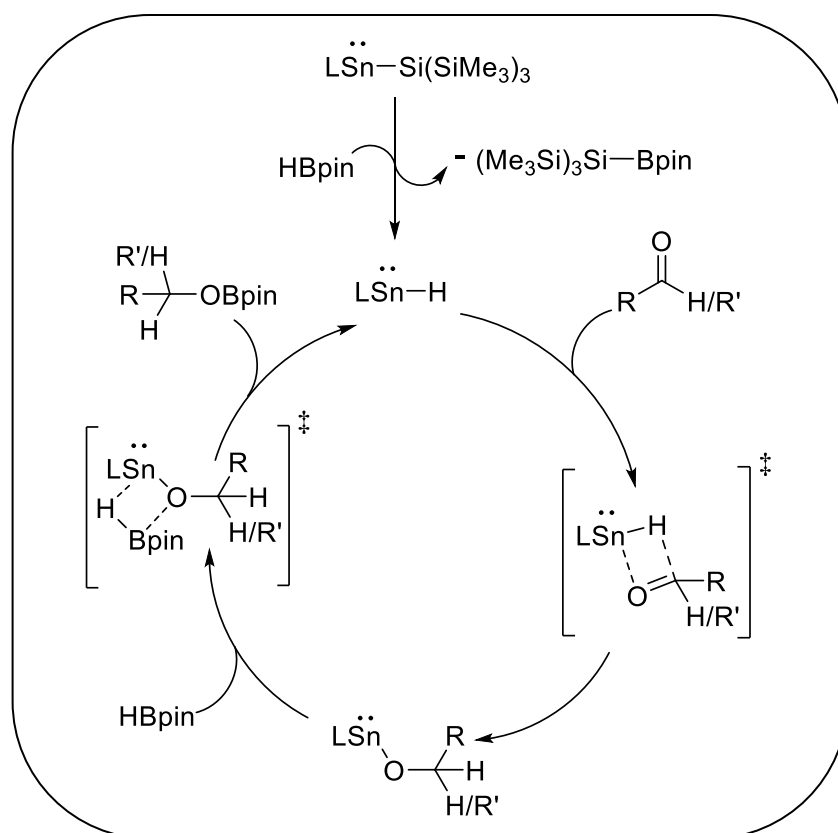
In the presence of only 5 mol% of catalyst **5.5**, the reduction of both benzaldehyde and acetophenone was completed in 3 hours at room temperature (Scheme 5.8). It was observed that the electron-withdrawing groups such as *para*-F (Table 5.1, entry 11), *para*-Br (Table 5.1, entry 6) and *ortho*-Cl (Table 5.1, entry 9) and electron-donating groups such as *p*-OMe (Table 5.1, entry 4) and *p*-NMe<sub>2</sub> (Table 5.1, entry 5) have very little effect on the reactivity and have afforded the corresponding boronate esters in moderate to good yields. However, the reaction was sluggish for NO<sub>2</sub> substituted benzaldehyde and acetophenone (Table 5.1, entries 7 and 12).

Entry	Substrates	Time/temperature	Yield (%)
1	 1a	3h/RT	97
2	 1a	3h/ RT	87 <sup>a</sup> 75 <sup>b</sup>
3	 1a	3h/ RT	67 <sup>c</sup> 68 <sup>d</sup>

4	 <b>1b</b>	3h/RT	98
5	 <b>1c</b>	3h/RT	86
6	 <b>1d</b>	3h/RT	96
7	 <b>1e</b>	3h/RT	72
8	 <b>1f</b>	3h/RT	99
9	 <b>1g</b>	3h/RT	98
10	 <b>1h</b>	3h/RT	99
11	 <b>1i</b>	3h/RT	80
12	 <b>1j</b>	3h/RT	42

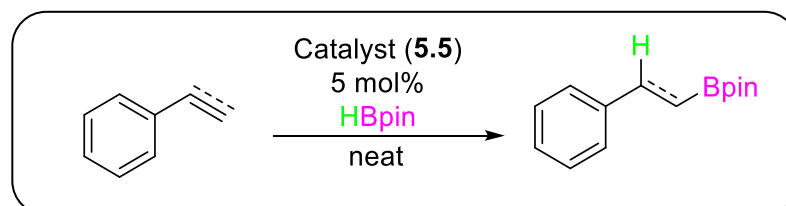
**Table 5.1:** All reactions were carried out under neat conditions at room temperature using 1 equiv. of HBpin. Yields were determined by the  $^1\text{H}$  NMR integration relative to mesitylene (1 equiv.) as an internal standard and the identity of the product was confirmed by  $\text{RCH}_2\text{OBpin}$  or  $\text{RR}_1\text{CHOBpin}$  resonances. <sup>a</sup>Catalyst: 5 mol% **5.1**. <sup>b</sup>Catalyst: 10 mol% **5.1**. <sup>c</sup>Catalyst: 5 mol% **5.3**. <sup>d</sup>Catalyst: 10 mol% **5.3**.

In order to investigate the mechanistic details, several control experiments were carried out. We did not observe any product formation between the reaction of **5.5** with aldehydes or ketones.<sup>45</sup> However, the treatment of **5.5** with HBpin presumably led to the formation of an unstable Sn(II) hydride compound. Although the  $^1\text{H}$  NMR spectrum is inconclusive, but the  $^{119}\text{Sn}$  NMR spectrum of the reaction mixture displays a doublet at 509.9 ppm with  $^1J_{\text{Sn-H}} = 38.81$  Hz, which is in good agreement with the previously reported  $[\{\text{HC}(\text{CMeNAr})_2\}]\text{SnH}$  (45 Hz) (Ar = 2,6-*i*-Pr<sub>2</sub>C<sub>6</sub>H<sub>3</sub>).<sup>49</sup> The corresponding  $^{11}\text{B}$  NMR spectrum of the reaction mixture shows resonance at 21.7 ppm, reflecting a three-coordinated boron center.<sup>50</sup> The B–H proton is also not observed, and this disappearance points towards the formation of the PyPyrSn(II) hydride. So, we hypothesize that the PyPyrSn(II) hydride reacts with aldehydes/ketones to form the corresponding metallalkoxides, which subsequently react with another molecule of HBpin to regenerate the hydride and form borate esters (Scheme 5.9). The tentative mechanistic cycle is as given below:

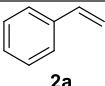
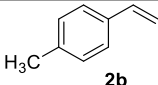
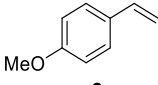
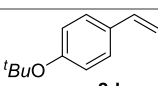
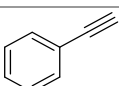
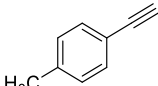
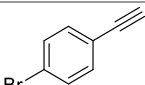
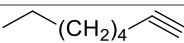


**Scheme 5.9:** The plausible mechanism of the catalytic hydroboration

Subsequently, the catalytic hydroboration has been further extended for styrene and phenylacetylene (Scheme 5.10). The catalytic activity of **5.5** was found to be inferior for alkene (Table 5.2, entry 1) than that of alkyne (Table 5.2, entry 5). In fact, substituted alkenes and alkynes reacted slothfully to procedure hydroborated products, giving very moderate yields. The intramolecularly base stabilized nature of **5.5** and the non-polar nature of alkenes and alkynes can be attributed to the sluggish nature of the hydroboration.



**Scheme 5.10:** Hydroboration of alkenes and alkynes catalyzed by **5.5**

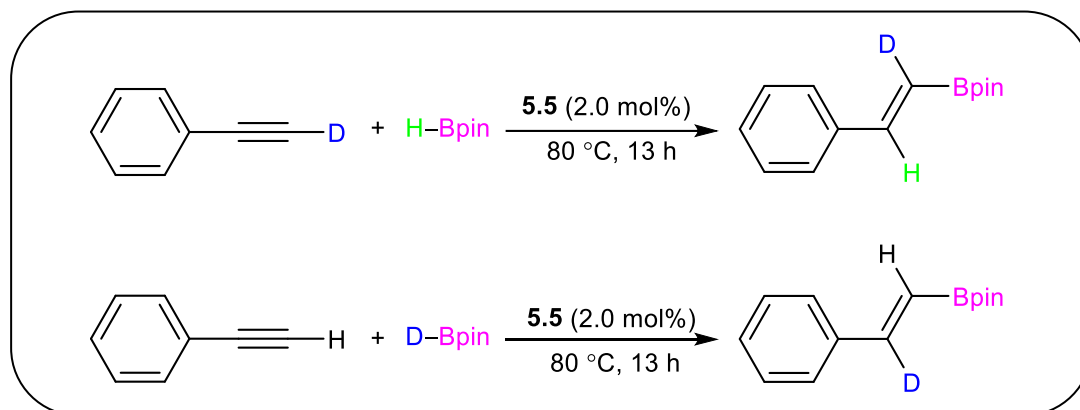
Entry	Substrates	Time/temperature	Yield (%)
1	 2a	13h/100 °C	64
2	 2b	13h/100 °C	53
3	 2c	13h/100 °C	62
4	 2d	13h/100 °C	42
5	 3a	13h/80 °C	74
6	 3b	13h/80 °C	58
7	 3c	13h/80 °C	34
8	 3d	13h/80 °C	58

**Table 5.2:** Hydroboration of alkenes and alkynes catalyzed by **5.5**. Yields were determined by  $^1\text{H}$  NMR integration relative to mesitylene (1 equiv.)

To explicate the regioselectivity of the products, a catalytic reaction using  $\text{PhC}\equiv\text{CD}$  and HBpin has been performed, where the resonance at 6.26 ppm in the  $^2\text{H}$  NMR spectrum has been observed. The *cis* arrangement of the deuterium and phenyl group has been established from the NMR studies. On the other hand, the product generated from the catalytic reaction of  $\text{PhC}\equiv\text{CH}$



with DBpin exhibits resonance at 6.57 ppm in the  $^2\text{H}$  NMR spectrum, indicating the *cis* orientation of deuterium and the Bpin moiety (see Scheme 5.11). These results are in good agreement with previously reported works on alkyne hydroboration by us<sup>51</sup> as well as by others.<sup>52</sup>



**Scheme 5.11:** Deuterium labelling experiment: hydroboration of phenylacetylene-D with HBpin (above) and hydroboration of phenylacetylene with DBpin (below)

### 5.3: Conclusions

In summary, we have synthesized a series of low-valent monomeric germanium (**3.2**) and tin (**5.1**) compounds containing pyridylpyrrolide ligand. Exploiting the advantage of nucleophilic substitution reactions using  $\text{KSi}(\text{SiMe}_3)_3$ , we have synthesized hypersilyl germylene (**5.4**) and stannylene (**5.5**). The reaction of **5.4** with  $\text{C}_5\text{F}_5\text{N}$  led to the formation of a tetrafluoropyridyl germylene (**5.6**) via concomitant elimination of  $(\text{Me}_3\text{Si})_3\text{SiF}$  through the C–F bond activation of  $\text{C}_5\text{F}_5\text{N}$ . Lastly, we have used hypersilyl stannylene, **5.5** as an efficient catalyst for the hydroboration of aldehydes, ketones, alkenes, and alkynes in mild reaction condition. Although the catalyst is competent for aldehydes and ketones, but the reduction of alkenes and alkynes was little bit sluggish.

### 5.4: References

1. L. Bourget-Merle, M. F. Lappert and J. R. Severn, *Chem. Rev.*, 2002, **102**, 3031–3066.
2. C. Camp and J. Arnold, *Dalton Trans.*, 2016, **45**, 14462–14498.
3. M. Asay, C. Jones and M. Driess, *Chem. Rev.*, 2010, **111**, 354–396.

4. (a) I. Koehne, N. Graw, T. Teuteberg, R. Herbst-Irmer and D. Stalke, *Inorg. Chem.*, 2017, **56**, 14968–14978. (b) I. Koehne, S. Bachmann, T. Niklas, R. Herbst-Irmer and D. Stalke, *Chem. Eur. J.*, 2017, **23**, 13141–13149.
5. R. Kretschmer, *Chem. Eur. J.*, 2020, **26**, 2099–2119.
6. J. L. McBee and T. D. Tilley, *Organometallics*, 2009, **28**, 3947–3952
7. A. T. Luedtke and K. I. Goldberg, *Inorg. Chem.*, 2007, **46**, 8496-8498.
8. D. Pucci, I. Aiello, A. Aprea, A. Bellusci, A. Crispini and M. Ghedini, *Chem. Commun.*, 2009, 1550-1552.
9. J.-L. Chen, C.-H. Lin, J.-H. Chen, Y. Chi, Y.-C. Chiu, P.-T. Chou, C.-H. Lai, G. Lee and A. J. Carty, *Inorg. Chem.*, 2008, **47**, 5154–5161.
10. J. A. Flores, J. G. Andino, N. P. Tsvetkov, M. Pink, R. J. Wolfe, A. R. Head, D. L. Lichtenberger, J. Massa and K. G. Caulton, *Inorg. Chem.*, 2011, **50**, 8121–8131.
11. K. Searles, A. K. Das, R. W. Buell, M. Pink, C.-H. Chen, K. Pal, D. G. Morgan, D. J. Mindiola and K. G. Caulton, *Inorg. Chem.*, 2013, **52**, 5611–5619.
12. S. Pahar, V. S. V. S. N. Swamy, T. Das, R. G. Gonnade, K. Vanka and S. S. Sen, *Chem. Commun.*, 2020, **56**, 11871–11874.
13. A. G. Brook, F. Abdesaken, B. Gutekunst, G. Gutekunst and R. K. Kallury, *Chem. Commun.* 1981, 191–192.
14. A. Heine and D. Stalke, *Angew. Chem., Int. Ed. Engl.*, 1994, **33**, 113-115.
15. (a) D. Wendel, A. Porzelt, F. A. D. Herz, D. Sarkar, C. Jandl, S. Inoue and B. Rieger, *J. Am. Chem. Soc.*, 2017, **139**, 8134–8137. (b) D. Wendel, T. Szilvási, C. Jandl, S. Inoue and B. Rieger, *J. Am. Chem. Soc.*, 2017, **139**, 9156–9159.
16. A. V. Protchenko, A. D. Schwarz, M. P. Blake, C. Jones, N. Kaltsoyannis, P. Mountford and S. Aldridge, *Angew. Chem., Int. Ed.*, 2013, **52**, 568–571.
17. M. M. D. Roy, M. I. J. Ferguson, R. McDonald, Y. Zhou and E. Rivard, *Chem. Sci.*, 2019, **10**, 6476–6481.
18. K. I. Leszczyńska, P. Deglmann, C. Präsang, V. Huch, M. Zimmer, D. Schweinfurth and D. Scheschkewitz, *Dalton Trans.*, 2020, **49**, 13218–13225.

- 
19. (a) D. Matioszek, N. Katir, S. Ladeira and A. Castel, *Organometallics*, 2011, **30**, 2230–2235. (b) N. Katir, D. Matioszek, S. Ladeira, J. Escudié and A. Castel, *Angew. Chem., Int. Ed.*, 2011, **50**, 5352–5355.
20. (a) H. Arp, J. Baumgartner, C. Marschner and T. Müller, *J. Am. Chem. Soc.*, 2011, **133**, 5632–5635. (b) H. Arp, C. Marschner, J. Baumgartner, P. Zark and T. Müller, *J. Am. Chem. Soc.*, 2013, **135**, 7949–7959. (c) H. Arp, J. Baumgartner and C. Marschner, *J. Am. Chem. Soc.*, 2012, **134**, 6409–6415.
21. M. K. Bisai, V. S. V. S. N. Swamy, T. Das, K. Vanka, R. G. Gonnade and S. S. Sen, *Inorg. Chem.*, 2019, **58**, 10536–10542.
22. M. K. Bisai, V. S. Ajithkumar, R. G. Gonnade and S. S. Sen, *Organometallics*, 2021, **40**, 2651–2657.
23. M. K. Bisai, V. S. V. S. N. Swamy, K. V. Raj, K. Vanka and S. S. Sen, *Inorg. Chem.*, 2021, **60**, 1654–1663.
24. M. K. Bisai, T. Das, K. Vanka, R. G. Gonnade and S. S. Sen, *Angew. Chem., Int. Ed.*, 2021, **60**, 20706–20710.
25. M. K. Bisai, V. Sharma, R. G. Gonnade and S. S. Sen, *Organometallics*, 2021, **40**, 2133–2138.
26. J. J. Klappa, A. E. Rich and K. McNeill, *Org. Lett.*, 2002, **4**, 435–437.
27. F. V. Scalzi and N. F. Golob, *J. Org. Chem.*, 1971, **36**, 2541–2542.
28. (a) S. S. Sen, M. P. Kritzler-Kosch, S. Nagendran, H. W. Roesky, T. Beck, A. Pal and R. Herbst-Irmer, *Eur. J. Inorg. Chem.*, 2010, 5304–5311. (b) C. Maaß, D. M. Andrada, R. A. Mata, R. Herbst-Irmer and D. Stalke, *Inorg. Chem.*, 2013, **52**, 9539–9548. (c) M. K. Sharma, M. Ansari, P. Mahawar, G. Rajaraman and S. Nagendran, *Dalton Trans.*, 2019, **48**, 664–672. (d) T. Chlupatý, Z. Padělková, F. DeProft, R. Willem and A. Růžička, *Organometallics*, 2012, **31**, 2203–2211. (e) C. Jones, R. P. Rose and A. Stasch, *Dalton Trans.*, 2008, 2871–2878. (f) N. Nakata, N. Hosoda, S. Takahashi and A. Ishii, *Dalton Trans.*, 2018, **47**, 481–490.
29. (a) M. Olaru, R. Kather, E. Hupf, E. Lork, S. Mebs and J. Beckmann, *Angew. Chem., Int. Ed.*, 2018, **57**, 5917–5920. (b) M. Olaru, S. Krupke, E. Lork, S. Mebs and J. Beckmann, *Dalton Trans.*, 2019, **48**, 5585–5594.
-

- 
30. K. W. Klinkhammer and W. Schwarz, *Angew. Chem., Int. Ed. Engl.*, 1995, **34**, 1334–1336
31. M. Pait, G. Kundu, S. Tothadi, S. Karak, S. Jain, K. Vanka and S. S. Sen, *Angew. Chem., Int. Ed.*, 2019, **58**, 2804–2808.
32. G. Kundu, S. De, S. Tothadi, A. Das, D. Koley and S. S. Sen, *Chem. Eur. J.*, 2019, **25**, 16533–16537.
33. G. Kundu, V. S. Ajithkumar, M. K. Bisai, S. Tothadi, T. Das, K. Vanka and S. S. Sen, *Chem. Commun.*, 2021, **57**, 4428–4431.
34. V. S. V. S. N. Swamy, N. Parvin, K. V. Raj, K. Vanka and S. S. Sen, *Chem. Commun.*, 2017, **53**, 9850–9853.
35. S. S. Sen and H. W. Roesky, *Chem. Commun.*, 2018, **54**, 5046–5057.
36. A. Jana, H. W. Roesky, C. Schulzke, A. Döring, T. Beck, A. Pal and R. Herbst-Irmer, *Inorg. Chem.*, 2009, **48**, 193–197.
37. For selected reviews on main group compound catalyzed hydroboration, please see: (a) C. C. Chong and R. Kinjo, *ACS Catal.*, 2015, **5**, 3238–3259. (b) G. I. Nikonov, *ACS Catal.* 2017, **7**, 7257–7266. (c) D. Mukherjee and J. Okuda, *Angew. Chem. Int. Ed.* 2018, **57**, 1458–1473.
38. (a) X. He and J. F. Hartwig, *J. Am. Chem. Soc.*, 1996, **118**, 1696–1702. (b) J. F. Hartwig and C. N. Muhoro, *Organometallics*, 2000, **19**, 30–38.
39. (a) K. Oshima, T. Ohmura and M. Suginome, *J. Am. Chem. Soc.*, 2012, **134**, 3699–3702. (b) J. Cid, J. J. Carbo and E. Fernandez, *Chem. - Eur. J.*, 2012, **18**, 1512–1521. (c) S. M. Smith and J. M. Takacs, *Org. Lett.*, 2010, **12**, 4612–4615. (d) S. M. Smith and J. M. Takacs, *J. Am. Chem. Soc.*, 2010, **132**, 1740–1741. (e) C. J. Lata and C. M. Crudden, *J. Am. Chem. Soc.*, 2010, **132**, 131–137. (f) B. Nguyen and J. M. Brown, *Adv. Synth. Catal.*, 2009, **351**, 1333–1343.
40. S. Yadav, S. Saha and S. S. Sen, *ChemCatChem*, 2016, **7**, 486–501.
41. C. C. Chong and R. Kinjo, *ACS Catal.*, 2015, **5**, 3238–3259.
42. For catalysis with alkaline earth metal, please see: (a) T. E. Stennett and S. Harder, *Chem. Soc. Rev.*, 2016, **45**, 1112–1128. (b) M. S. Hill, D. J. Liptrot and C. Weetman,
-

- Chem. Soc. Rev.*, 2016, **45**, 972–988. (c) S. Harder, *Chem. Rev.*, 2010, **110**, 3852–3876.
43. (a) Q.-L. Zhou, *Angew. Chem., Int. Ed.*, 2016, **55**, 5352–5353. (b) S. Bagherzadeh and N. P. Mankad, *Chem. Commun.*, 2016, **35**, 3844–3846. (c) D. Mukherjee, H. Osseili, T. P. Spaniol and J. Okuda, *J. Am. Chem. Soc.*, 2016, **138**, 10790–10793. (d) S. C. Sau, R. Bhattacharjee, P. K. Vardhanapu, G. Vijaykumar, A. Datta and S. K. Mandal, *Angew. Chem. Int. Ed.*, 2016, **55**, 15147–15151.
44. M. L. Shegavi and S. K. Bose, *Catal. Sci. Technol.*, 2019, **9**, 3307–3336.
45. T. J. Hadlington, M. Hermann, G. Frenking and C. Jones, *J. Am. Chem. Soc.*, 2014, **136**, 3028–3031.
46. J. Schneider, C. P. Sindlinger, S. M. Freitag, H. Schubert and L. Wesemann, *Angew. Chem., Int. Ed.*, 2017, **56**, 333–337.
47. R. Dasgupta, S. Das, S. Hiwase, S. Pati and S. Khan, *Organometallics*, 2019, **38**, 1429–1435.
48. K. Nakaya, S. Takahashi, A. Ishii, K. Boonpalit, P. Surawatanawong and N. Nakata, *Dalton Trans.*, 2021, **50**, 14810–14819.
49. A. Jana, H. W. Roesky, C. Schulzke and A. Döring, *Angew. Chem., Int. Ed.*, 2009, **48**, 1106–1109.
50. M. K. Bisai, T. Das, K. Vanka and S. S. Sen, *Chem. Commun.*, 2018, **54**, 6843–6846.
51. M. K. Bisai, S. Yadav, T. Das, K. Vanka and S. S. Sen, *Chem. Commun.*, 2019, **55**, 11711–11714.
52. S. Mandal, P. K. Verma and K. Geetharani, *Chem. Commun.*, 2018, **54**, 13690–13693.

**Appendix: Experimental details, crystallographic data and spectral details**

<b>6.1: Chapter 2 experimental details and crystallographic data</b>
6.1.1. Synthesis and experimental details of compounds 2.1–2.4
6.1.1.1. Synthesis of $[\text{PhC}(\text{N}^t\text{Bu})_2\text{Si}\{\text{N}(\text{SiMe}_3)_2\}\rightarrow\text{InCl}_3]$ (2.1)
6.1.1.2. Synthesis of $[\text{PhC}(\text{N}^t\text{Bu})_2\text{Si}\{\text{N}(\text{SiMe}_3)_2\}\rightarrow\text{InBr}_3]$ (2.2)
6.1.1.3. Synthesis of $[\text{PhC}(\text{N}^t\text{Bu})_2\text{Ge}\{\text{N}(\text{SiMe}_3)_2\}\rightarrow\text{InCl}_3]$ (2.3)
6.1.1.4. Synthesis of $[\text{PhC}(\text{N}^t\text{Bu})_2\text{Ge}\{\text{N}(\text{SiMe}_3)_2\}\rightarrow\text{InBr}_3]$ (2.4)
6.1.2. Crystal structure determination of complexes 2.1–2.4
6.1.3. Details of the DFT Calculations

<b>6.2: Chapter 3 experimental details, crystallographic data and details of theoretical calculations</b>
6.2.1. Synthesis and experimental details of compounds 3.1-3.8
6.2.1.1. Synthesis and characterization of compound 3.1
6.2.1.2. Synthesis and characterization of compound 3.2 and 3.3
6.2.1.3. Synthesis and characterization of compound 3.4
6.2.1.4. Synthesis and characterization of compound 3.5
6.2.1.5. Synthesis and characterization of compound 3.6
6.2.1.6. Synthesis and characterization of compound 3.7
6.2.1.7. Synthesis and characterization of compound 3.8
6.2.2. Crystallographic data for the structural analysis of compounds 3.1-3.8
6.2.3. Details of theoretical calculations

<b>6.3: Chapter 4 experimental details and crystallographic data</b>
6.3.1. Synthesis and experimental details of compounds 4.1–4.4
6.3.1.1. Synthesis of compound 4.1
6.3.1.2. Synthesis of compound 4.2

6.3.1.3. Synthesis of compound 4.3
6.3.1.4. Synthesis of compound 4.4
6.3.2. Crystallographic data for the structural analysis of compounds 4.1-4.4

<b>6.4: Chapter 5 experimental details, crystallographic data and General procedure for catalytic hydroboration</b>
---

6.4.1. Synthesis and experimental details of Ligand L2 and compounds 5.1-5.6
6.4.1.1. Synthesis and experimental details of ligand (L2): (3,5-dimethyl-2-(2-pyridyl)pyrrole)
6.4.1.2. High yield synthesis of compound 3.2
6.4.1.3. Synthesis and characterization of compound 5.1
6.4.1.4. Synthesis and characterization of compound 5.2
6.4.1.5. Synthesis and characterization of compound 5.3
6.4.1.6. Synthesis and characterization of compound 5.4
6.4.1.7. Synthesis and characterization of compound 5.5
6.4.1.8. Synthesis and characterization of compound 5.6
6.4.2. Crystallographic data for the structural analysis of compounds 5.1-5.6
6.4.3. General procedure for catalytic hydroboration
6.4.3.1. Spectroscopic data for hydroborated products
6.4.3.2. Regioselectivity studies
6.4.3.3. Mechanistic studies

<b>6.5: References</b>
------------------------

---

## 6.1: Chapter 2 experimental details and crystallographic data

### 6.1.1. Synthesis and experimental details of compounds 2.1–2.4

#### 6.1.1.1. Synthesis of [PhC(N<sup>t</sup>Bu)<sub>2</sub>Si{N(SiMe<sub>3</sub>)<sub>2</sub>}→InCl<sub>3</sub>] (2.1)

Toluene (20 mL) was added to a mixture of **1a** (0.419 g, 1 mmol) and InCl<sub>3</sub> (0.221 g, 1 mmol) at ambient temperature. The solution turned yellow to colorless with the formation of a white precipitate, and the resulting suspension was stirred for 12 h. The supernatant solvent was removed by using cannula filtration, and the precipitate obtained was dried under vacuum and was further dissolved in 10 mL of THF. Then the solution was supersaturated and kept at –35 °C to give single crystals of **2.1** suitable for X-ray analysis.

**Yield:** 0.519 g (79.0%).

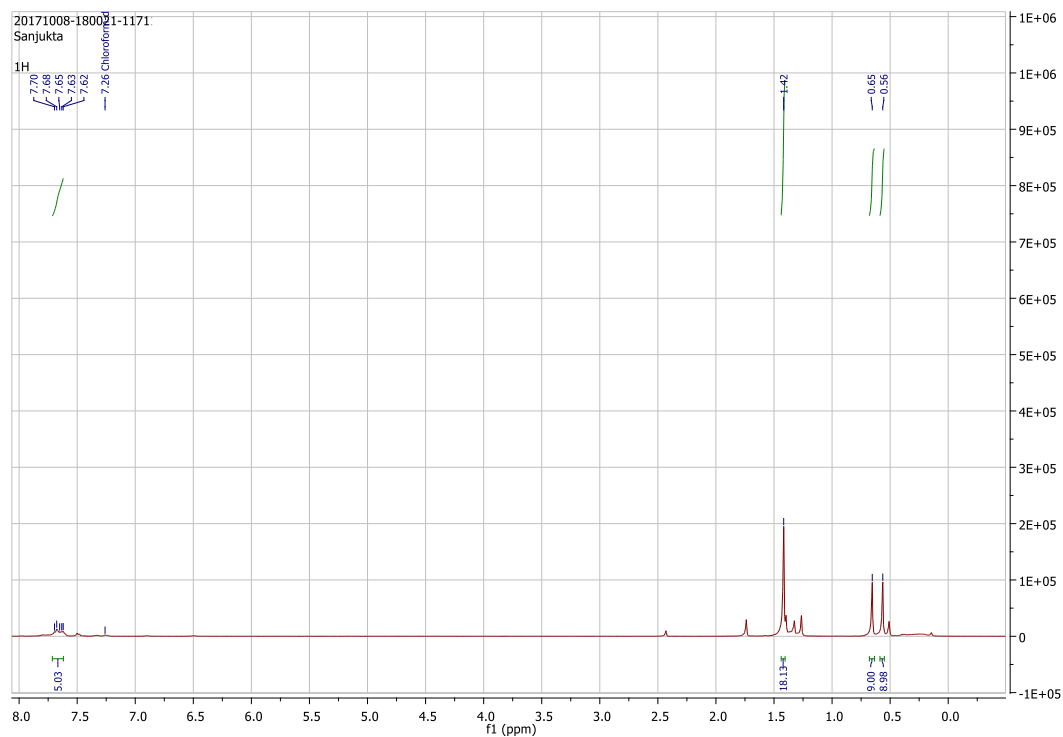
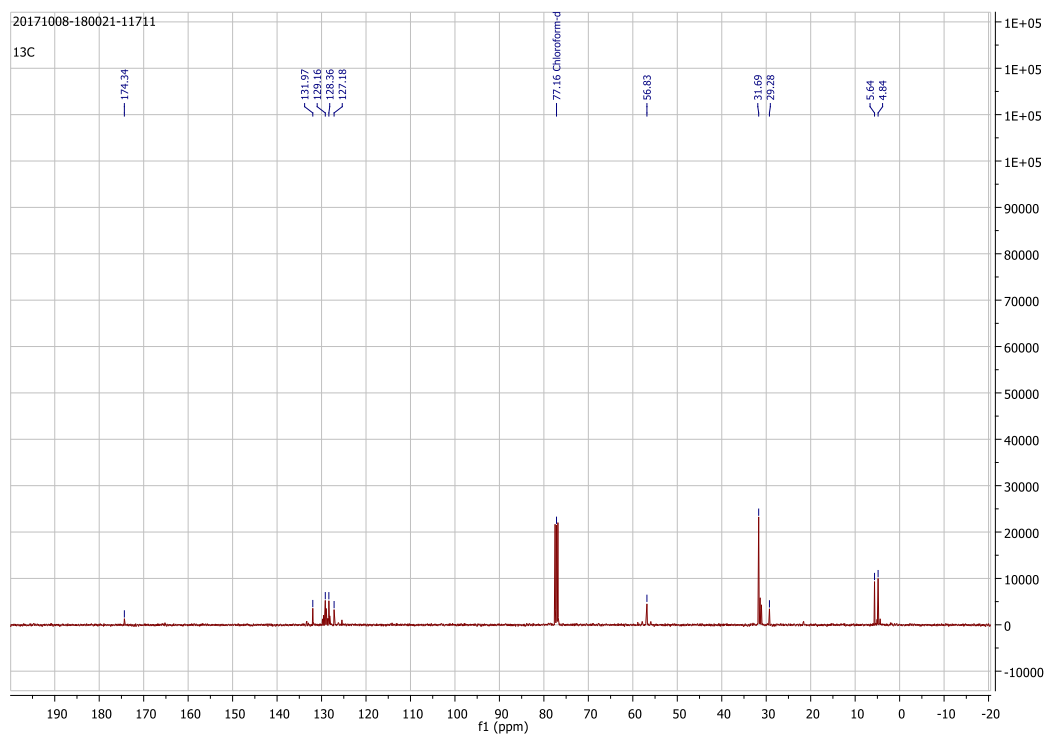
**Mp:** 176.8 °C.

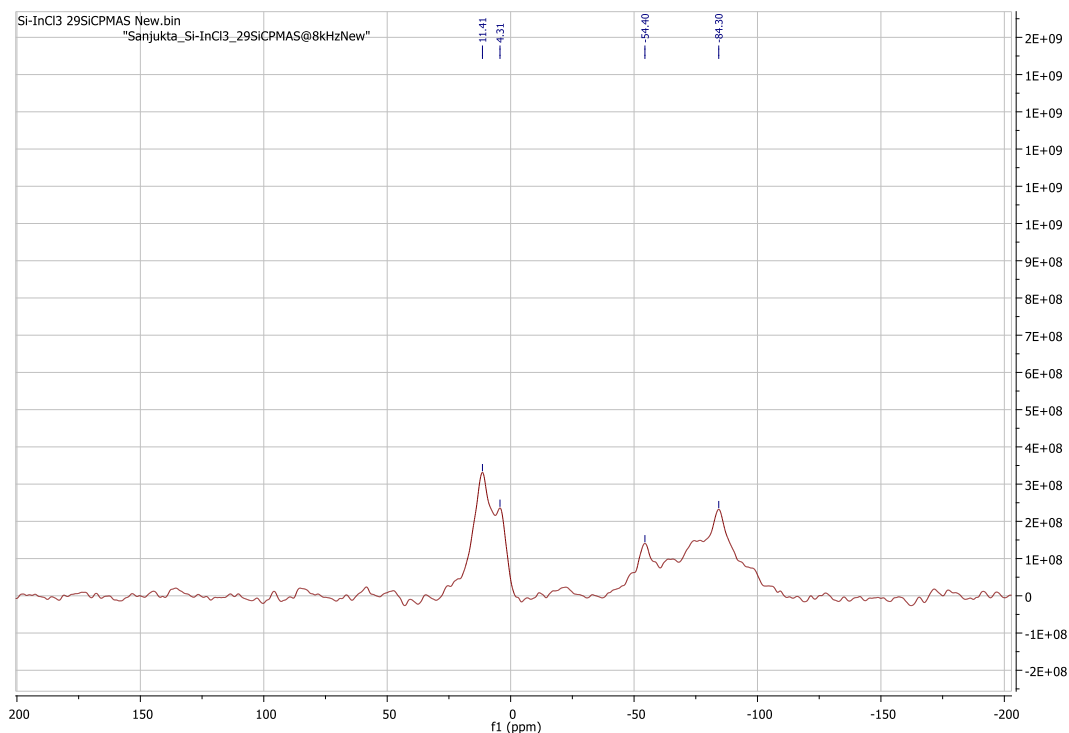
**NMR:** <sup>1</sup>H NMR (400 MHz, CDCl<sub>3</sub>, 298 K): δ 7.70–7.62 (m, 5 H), 1.42 (s, 18 H), 0.65 (s, 9 H), 0.56 (s, 9H) ppm. <sup>13</sup>CNMR (400 MHz, CDCl<sub>3</sub>, 298 K): δ 174.34, 131.97, 129.16, 128.36, 127.18, 56.83, 31.69, 29.28, 5.64, 4.84 ppm. <sup>29</sup>Si CP/MAS NMR (298 K): δ 11.4 (SiMe<sub>3</sub>), 4.3 (SiMe<sub>3</sub>), –54.4 to –84.3 (SiN(SiMe<sub>3</sub>)<sub>2</sub>).

**HRMS:** Calcd: 676.0761, found: 676.0833.

#### a) <sup>1</sup>H NMR of compound 2.1:

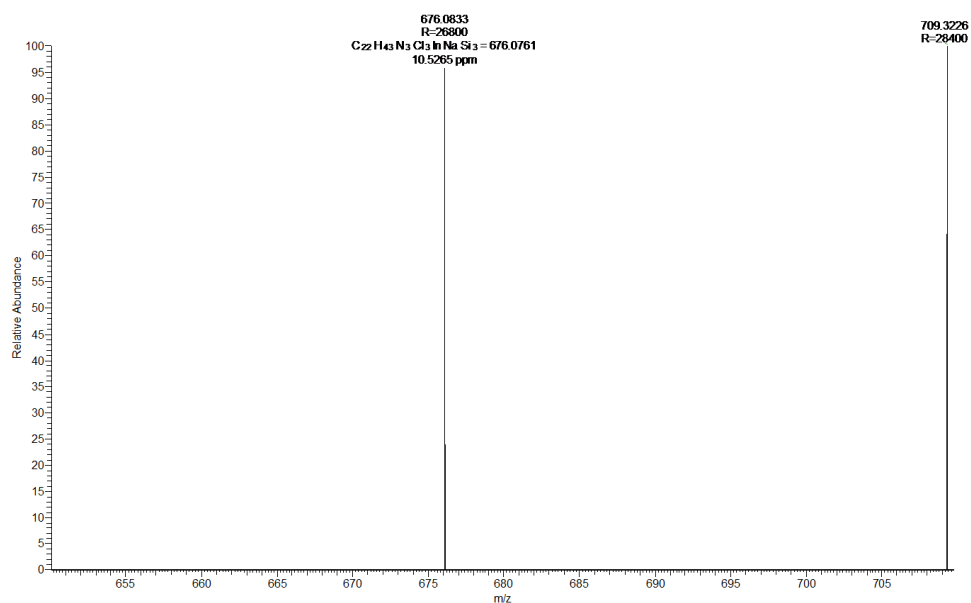


**b)  $^{13}\text{C}$  NMR of compound 2.1:****c) Solid-state  $^{29}\text{Si}$  NMR of compound 2.1:**



#### d) HRMS data of compound 2.1:

SP:2 #810 RT: 3.62 AV: 1 NL: 1.50E5  
T: FTMS + p ESI Fullms [100.0000-1500.0000]



#### 6.1.1.2. Synthesis of [PhC(N<sup>t</sup>Bu)<sub>2</sub>Si{N(SiMe<sub>3</sub>)<sub>2</sub>}→InBr<sub>3</sub>] (2.2)

Toluene (20 mL) was added to a mixture of **1a** (0.419 g, 1 mmol) and InBr<sub>3</sub> (0.354 g, 1 mmol) at ambient temperature. The solution turned yellow to pale orange with the formation of an orange

precipitate, and the resulting suspension was stirred for 12 h. The supernatant solvent was removed by using cannula filtration, and the precipitate obtained was dried under vacuum; subsequently, 10 mL of THF was added to the precipitate. The solution was kept at  $-35\text{ }^{\circ}\text{C}$  in a freezer to get single crystals of **2.2** suitable for X-ray analysis.

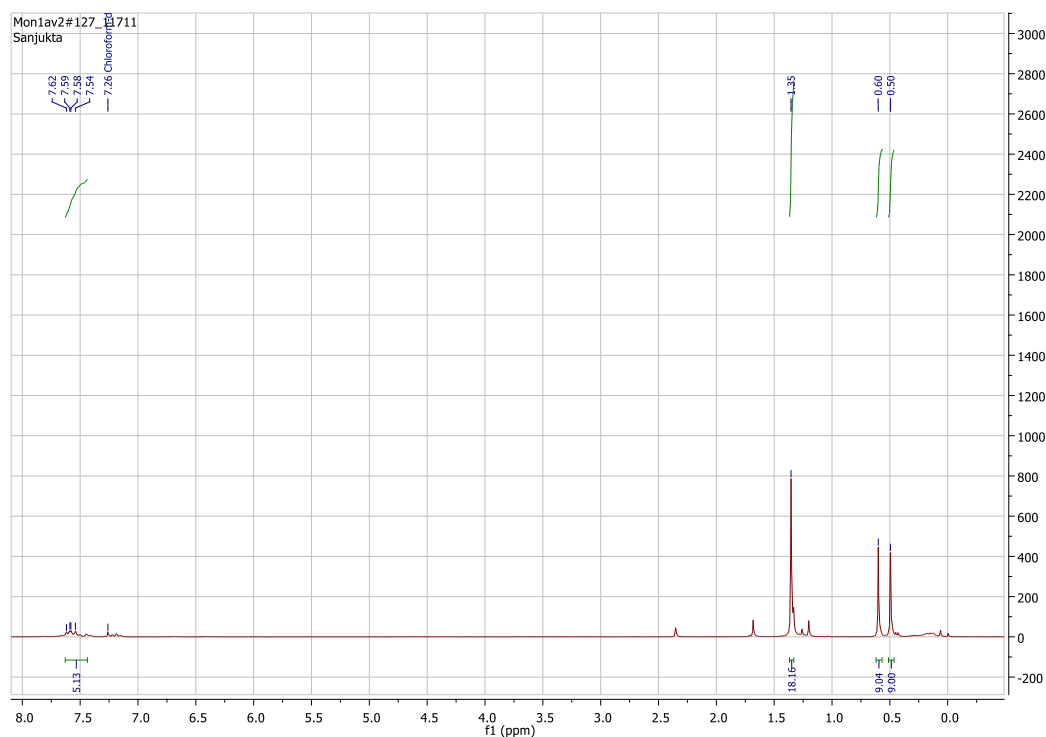
**Yield:** 0.583 g (74%).

**Mp:** 175.9  $^{\circ}\text{C}$ .

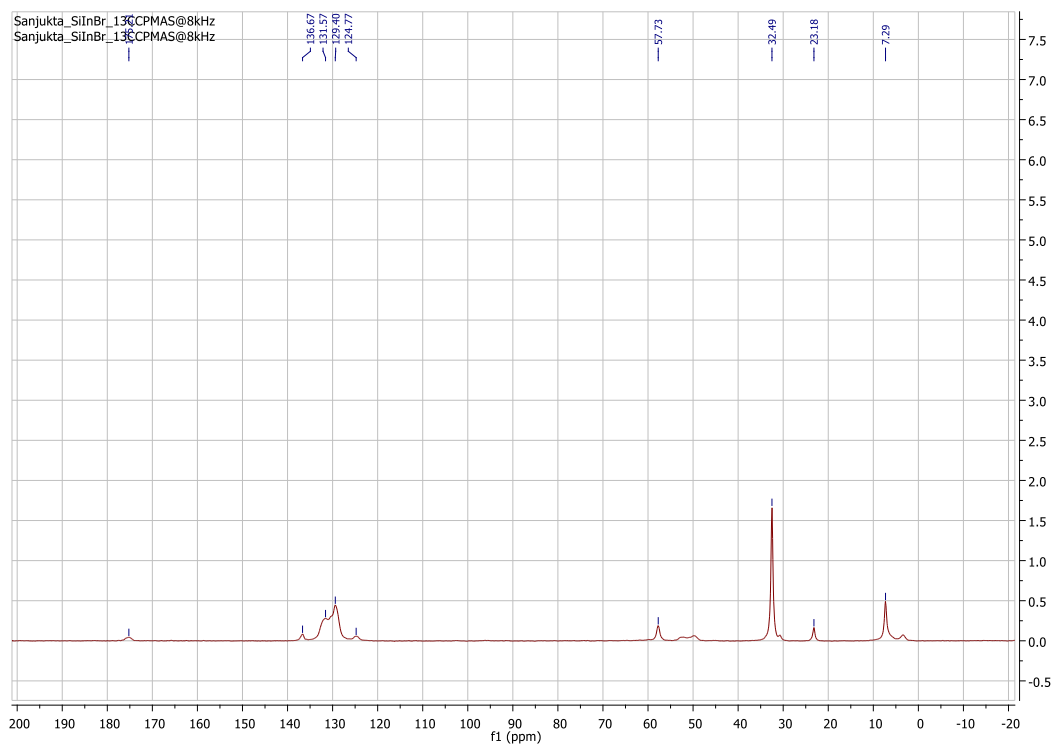
**NMR:**  $^1\text{H}$  NMR (400 MHz,  $\text{CDCl}_3$ , 298 K):  $\delta$  7.62–7.54 (m, 5 H), 1.35 (s, 18 H), 0.60 (s, 9 H), 0.50 (s, 9 H) ppm.  $^{13}\text{C}$  solid state NMR (298 K):  $\delta$  175.21, 136.67, 131.57, 129.4, 124.77, 57.73, 32.49, 23.18, 7.29 ppm.  $^{29}\text{Si}$  CP/MAS NMR (298 K):  $\delta$  14.1 ( $\text{SiMe}_3$ ), 10.9 ( $\text{SiMe}_3$ ),  $-31.7$  ( $\text{SiN}(\text{SiMe}_3)_2$ ).

**HRMS:** Calcd: 784.9348, found 784.9966.

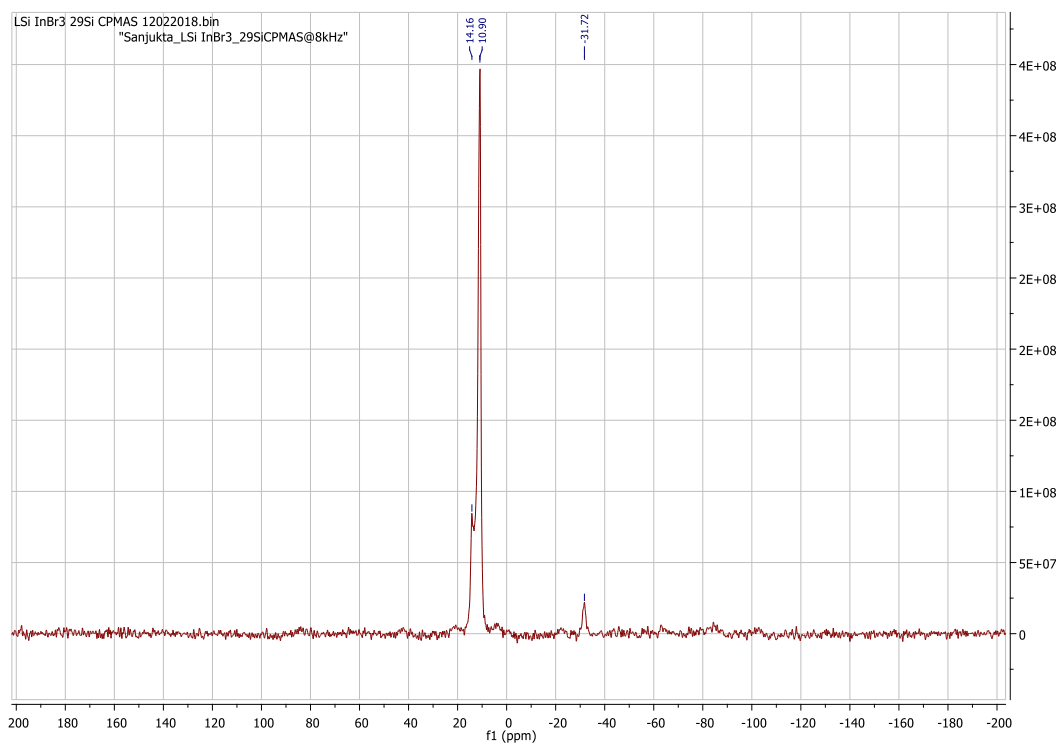
**a)  $^1\text{H}$  NMR of compound 2.2:**



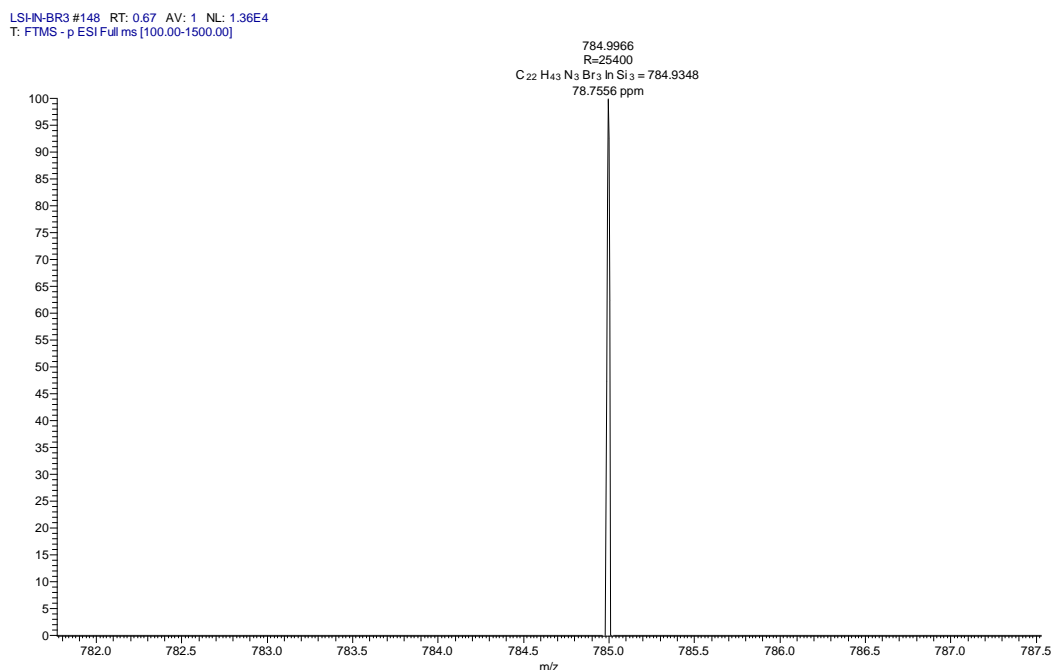
**b) Solid-state  $^{13}\text{C}$  NMR of compound 2.2:**



c) Solid-state  $^{29}\text{Si}$  NMR of compound 2.2:



d) HRMS data of compound 2.2:



### 6.1.1.3. Synthesis of [PhC(N<sup>t</sup>Bu)<sub>2</sub>Ge{N(SiMe<sub>3</sub>)<sub>2</sub>}→InCl<sub>3</sub>] (2.3)

To a mixture of **1b** (0.465 g, 1 mmol) and InCl<sub>3</sub> (0.221 g, 1 mmol) in a Schlenk flask was added toluene (20 mL) at ambient temperature. The solution turned colorless with concomitant formation of a white precipitate. The resulting suspension was stirred for 12 h. The reaction mixture was filtered, and the filtrate was concentrated and kept at −35 °C in a freezer to afford a white crystals of **2.3** suitable for X-ray analysis.

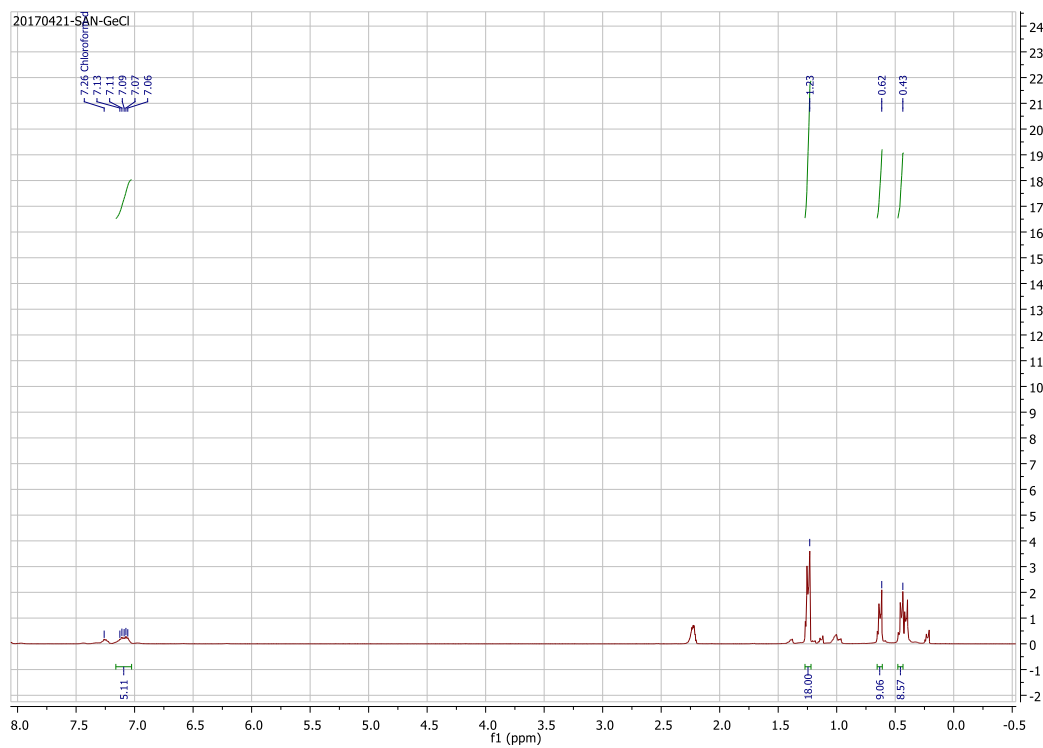
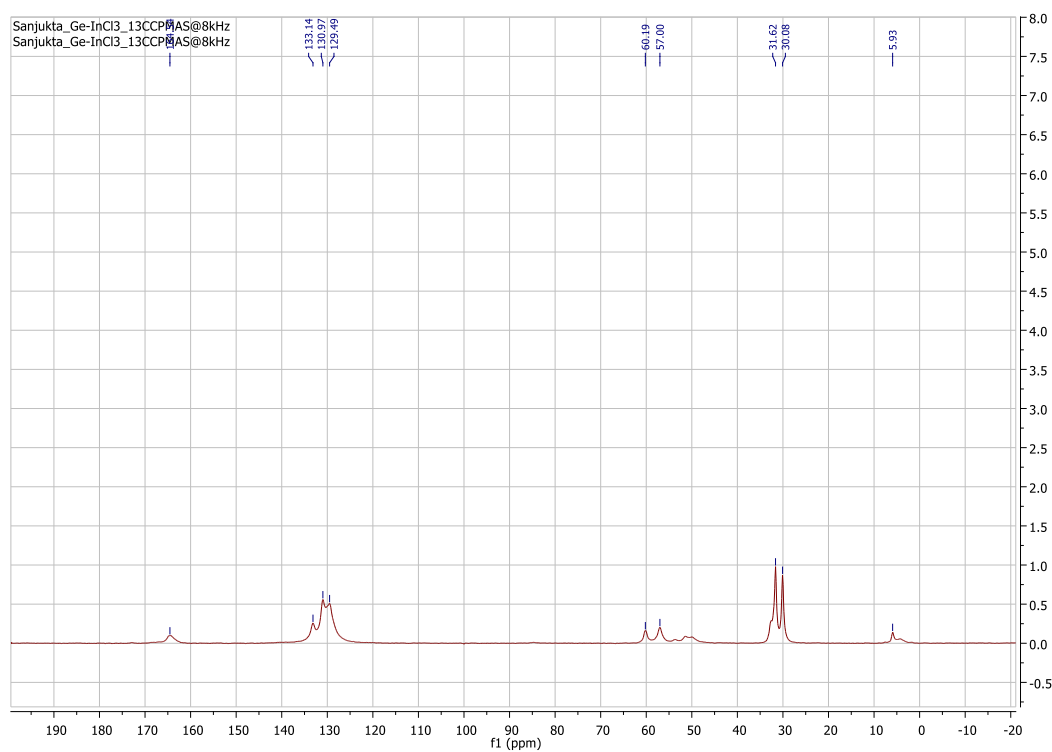
**Yield:** 0.450 g (64%).

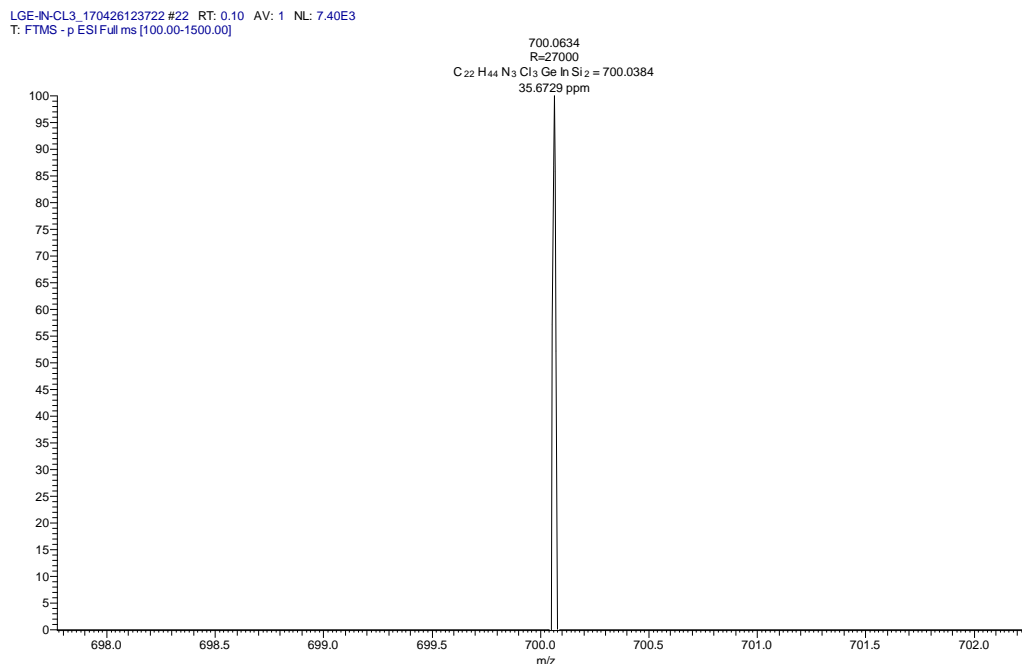
**Mp:** 136.9 °C.

**NMR:** <sup>1</sup>H NMR (400 MHz, CDCl<sub>3</sub>, 298 K): δ 7.13–7.06 (m, 5 H), 1.23 (s, 18 H), 0.62 (s, 9 H), 0.43 (s, 9 H) ppm. <sup>13</sup>C solid state NMR (298 K): δ 164.54, 133.14, 130.97, 129.49, 60.19, 57.0, 31.62, 30.08, 5.93 ppm.

**HRMS:** Calcd: 700.0384, found 700.0634.

#### a) <sup>1</sup>H NMR of compound 2.3:

**b) Solid-state  $^{13}\text{C}$  NMR of compound 2.3:****c) HRMS data of compound 2.3:**



#### 6.1.1.4. Synthesis of [PhC(N<sup>t</sup>Bu)<sub>2</sub>Ge{N(SiMe<sub>3</sub>)<sub>2</sub>}→InBr<sub>3</sub>] (2.4)

A mixture of **1b** (0.465 g, 1 mmol) and InBr<sub>3</sub> (0.354g, 1 mmol) was placed in a Schlenk flask, and toluene (20 mL) was added to it at ambient temperature. The solution turned colorless with simultaneous formation of a white precipitate. The reaction mixture was filtered after 12 h, and the filtrate was kept at -35 °C in a freezer to afford a white crystal of **2.4** suitable for X-ray analysis.

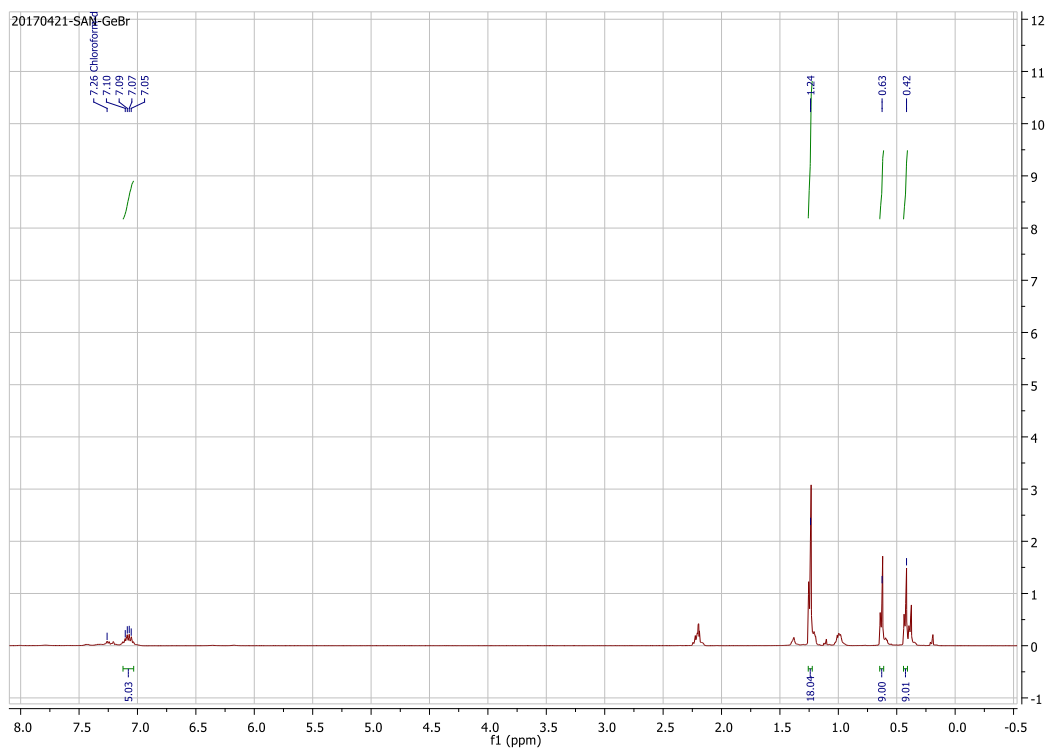
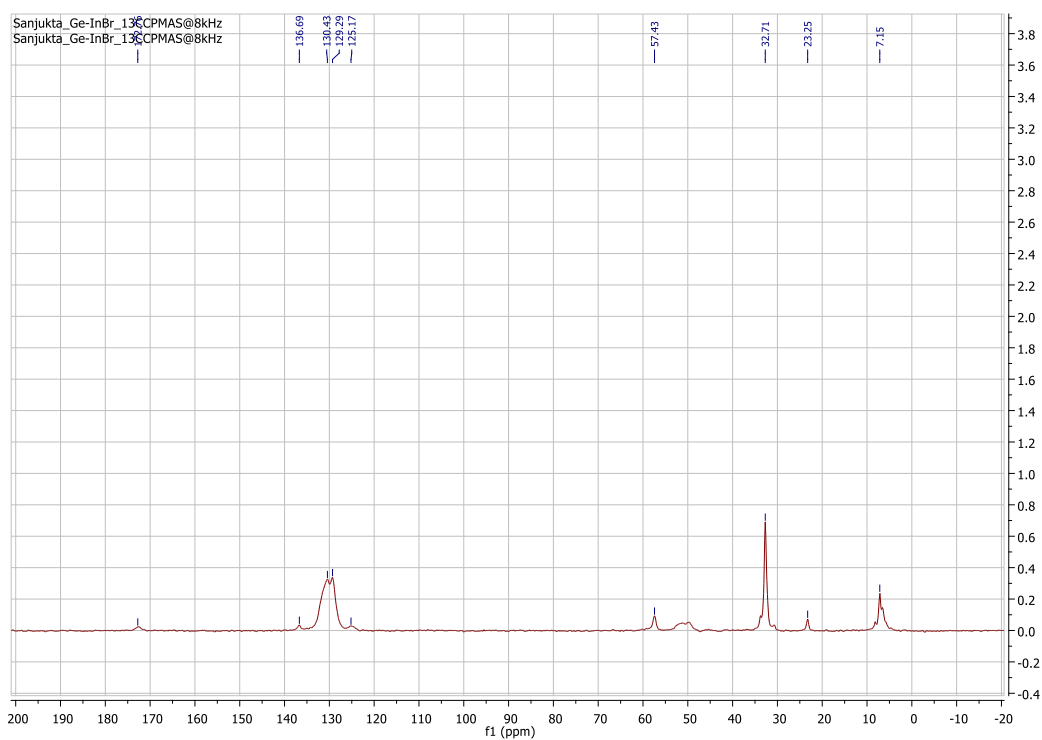
**Yield:** 0.598 g (72%).

**Mp:** 162.8 °C.

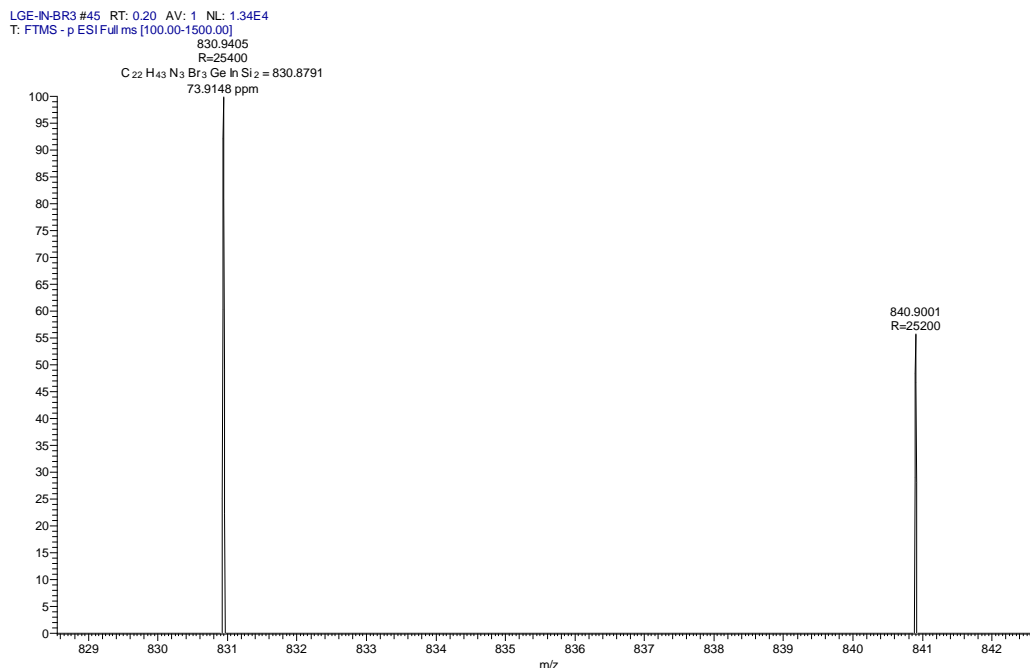
**NMR:** <sup>1</sup>H NMR (400 MHz, CDCl<sub>3</sub>, 298 K): δ 7.10–7.05 (m, 5 H), 1.24 (s, 18 H), 0.63 (s, 9 H), 0.42 (s, 9H) ppm. <sup>13</sup>C solid state NMR (298 K): δ 172.75, 136.69, 130.43, 129.29, 125.17, 57.43, 32.71, 23.25, 7.15 ppm.

**HRMS:** Calcd: 830.8791, found 830.9405.

##### a) <sup>1</sup>H NMR of compound 2.4:

**b) Solid-state  $^{13}\text{C}$  NMR of compound 2.4:****c) HRMS data of compound 2.4:**





### 6.1.2. Crystal structure determination of complexes 2.1–2.4

A good-quality single crystal was hand-picked under a polarized optical microscope and then mounted in the diffractometer. The data collection was done at 100–150 K. The crystals were mounted on a Super Nova Dual source X-ray diffractometer system (Agilent Technologies) equipped with a CCD area detector and operated at 250W power (50 kV, 0.8 mA) to generate Mo K $\alpha$  radiation ( $\lambda = 0.71073 \text{ \AA}$ ) and Cu K $\alpha$  radiation ( $\lambda = 1.54178 \text{ \AA}$ ) at 100–150 K. Initial scans of each specimen were performed to obtain preliminary unit cell parameters and to assess the mosaicity (breadth of spots between frames) of the crystal to select the required frame width for data collection. The CrysAlisPro program software suite was employed to carry out overlapping  $\phi$  and  $\omega$  scans at detector ( $2\theta$ ) settings ( $2\theta = 28^\circ$ ). Following data collection, reflections were sampled from all regions of the Ewald sphere to redetermine unit cell parameters for data integration. Following an exhaustive review of collected frames the resolution of the data set was judged. The data were integrated using the CrysAlisPro software with a narrow frame algorithm. The data were subsequently corrected for absorption by the program SCALE3 ABSPACK<sup>1</sup> scaling algorithm. These structures were solved by direct methods and refined by full-matrix least-squares refinement techniques on  $F^2$  using SHELXL 2016/4.<sup>2</sup> All calculations were carried out with the WinGx crystallographic package.<sup>3</sup> The atoms were located from iterative examination of

difference  $F$  maps following the least-squares refinements of the earlier models. The final model was refined anisotropically (if the number of data permitted) until full convergence was achieved. Hydrogen atoms were placed in calculated positions ( $C-H = 0.93 \text{ \AA}$ ) and included as riding atoms with isotropic displacement parameters 1.2–1.5 times the  $U_{eq}$  values of the attached C atoms. The modeling of electron density at 150 K within the unit cell did not lead to identification of recognizable solvent molecules in these structures, probably due to the highly disordered contents. This has generated alert level B in checkcif. An ORTEP III<sup>4</sup> view of the compound was drawn with 50% probability displacement ellipsoids.

**6.1.2.1. Crystal data of [PhC(N<sup>t</sup>Bu)<sub>2</sub>Si{N(SiMe<sub>3</sub>)<sub>2</sub>}→InCl<sub>3</sub>] (2.1):** C<sub>23</sub>H<sub>43</sub>Cl<sub>3</sub>In<sub>1</sub>N<sub>3</sub>O<sub>1</sub>Si<sub>3</sub>, M = 683.04, colorless block, monoclinic, space group  $P2_1/n$ ,  $a = 9.7808(4) \text{ \AA}$ ,  $b = 19.3556(6) \text{ \AA}$ ,  $c = 17.1218(6) \text{ \AA}$ ,  $\alpha = 90.00^\circ$ ,  $\beta = 91.013(2)^\circ$ ,  $\gamma = 90.00^\circ$ ,  $V = 3240.9(2) \text{ \AA}^3$ ,  $Z = 4$ ,  $T = 100.01 \text{ K}$ ,  $D_{calc} = 1.400 \text{ g cm}^{-3}$ ,  $F(000) = 1408$ ,  $\mu = 1.108 \text{ mm}^{-1}$ , 44314 reflections measured, 9877 unique ( $R_{int} = 0.0299$ ) reflections used,  $T_{min} = 0.767$ ,  $T_{max} = 0.792$ , absorption correction type none, 320 refined parameters, number of restraints 0, goodness of fit =  $S = 1.061$ ,  $R1 = 0.0294$ ,  $wR2 = 0.0737$  (all data  $R1 = 0.0357$ ,  $wR2 = 0.0774$ ),  $\Delta\rho_{max} = 1.732 \text{ e \AA}^{-3}$ ,  $\Delta\rho_{min} = -0.964 \text{ e \AA}^{-3}$ .

**6.1.2.2. Crystal data of [PhC(N<sup>t</sup>Bu)<sub>2</sub>Si{N(SiMe<sub>3</sub>)<sub>2</sub>}→InBr<sub>3</sub>] (2.2):** C<sub>21</sub>H<sub>41</sub>Br<sub>3</sub>In<sub>1</sub>N<sub>3</sub>Si<sub>3</sub>, M = 774.36, colorless plate, monoclinic, space group  $P2_1/n$ ,  $a = 10.0195(3) \text{ \AA}$ ,  $b = 19.2450(5) \text{ \AA}$ ,  $c = 17.3510(4) \text{ \AA}$ ,  $\alpha = 90.00^\circ$ ,  $\beta = 90.231(2)^\circ$ ,  $\gamma = 90.00^\circ$ ,  $V = 3345.68(15) \text{ \AA}^3$ ,  $Z = 4$ ,  $T = 150.01(10) \text{ K}$ ,  $D_{calc} = 1.537 \text{ g cm}^{-3}$ ,  $F(000) = 1536$ ,  $\mu = 4.410 \text{ mm}^{-1}$ , 9759 reflections measured, 5580 unique ( $R_{int} = 0.0351$ ) reflections used,  $T_{min} = 0.342$ ,  $T_{max} = 0.452$ , 292 refined parameters, absorption correction type multi scan, number of restraints 0, goodness of fit =  $S = 1.056$ ,  $R1 = 0.0325$ ,  $wR2 = 0.0848$  (all data  $R1 = 0.0431$ ,  $wR2 = 0.0885$ ),  $\Delta\rho_{max} = 0.688 \text{ e \AA}^{-3}$ ,  $\Delta\rho_{min} = -0.618 \text{ e \AA}^{-3}$ .

**6.1.2.3. Crystal data of [PhC(N<sup>t</sup>Bu)<sub>2</sub>Ge{N(SiMe<sub>3</sub>)<sub>2</sub>}→InCl<sub>3</sub>] (2.3):** C<sub>21</sub>H<sub>41</sub>Cl<sub>3</sub>Ge<sub>1</sub>In<sub>1</sub>N<sub>3</sub>Si<sub>2</sub>, M = 685.51, yellowish block, monoclinic, space group  $P2_1/n$ ,  $a = 10.0296(4) \text{ \AA}$ ,  $b = 20.3217(9) \text{ \AA}$ ,  $c = 16.6347(5) \text{ \AA}$ ,  $\alpha = 90.00^\circ$ ,  $\beta = 91.132(3)^\circ$ ,  $\gamma = 90.00^\circ$ ,  $V = 3389.8(2) \text{ \AA}^3$ ,  $Z = 4$ ,  $T = 191(50) \text{ K}$ ,  $D_{calc} = 1.373 \text{ g cm}^{-3}$ ,  $F(000) = 1392$ ,  $\mu = 1.887 \text{ mm}^{-1}$ , 13773 reflections measured, 5952 unique ( $R_{int} = 0.0559$ ) reflections used,  $T_{min} = 0.87363$ ,  $T_{max} = 1.000$ , 292 refined parameters, absorption correction type multi scan, number of restraints 0, goodness of fit =  $S = 1.051$ ,  $R1 = 0.0448$ ,  $wR2 = 0.1056$  (all data  $R1 = 0.0673$ ,  $wR2 = 0.1248$ ),  $\Delta\rho_{max} = 0.685 \text{ e \AA}^{-3}$ ,  $\Delta\rho_{min} = -0.994 \text{ e \AA}^{-3}$ .

**6.1.2.4. Crystal data of [PhC(N<sup>t</sup>Bu)<sub>2</sub>Ge{N(SiMe<sub>3</sub>)<sub>2</sub>}→InBr<sub>3</sub>] (2.4):** C<sub>21</sub>H<sub>41</sub>Br<sub>3</sub>Ge<sub>1</sub>In<sub>1</sub>N<sub>3</sub>Si<sub>2</sub>, M= 818.89, colorless block, monoclinic, space group *P*2<sub>1</sub>/*n*, *a* = 10.26830(10) Å, *b* = 20.1650(4) Å, *c* = 16.7774(3) Å,  $\alpha = 90.00^\circ$ ,  $\beta = 91.3540(10)^\circ$ ,  $\gamma = 90.00^\circ$ , *V* = 3472.96(10) Å<sup>3</sup>, *Z* = 4, *T* = 150.00(10) K, *D*<sub>calc</sub> = 1.566 g cm<sup>-3</sup>, *F*(000) = 1608,  $\mu = 5.063$  mm<sup>-1</sup>, 14453 reflections measured, 6100 unique (*R*<sub>int</sub> = 0.0322) reflections used, *T*<sub>min</sub> = 0.53843, *T*<sub>max</sub> = 1.000, 292 refined parameters, absorption correction type multi scan, number of restraints 0, goodness of fit = *S* = 0.663, *R*1 = 0.0365, *wR*2 = 0.1091 (all data *R*1 = 0.0500, *wR*2 = 0.1216),  $\Delta\rho_{\text{max}} = 0.750$  e Å<sup>-3</sup>,  $\Delta\rho_{\text{min}} = -0.505$  e Å<sup>-3</sup>.

### 6.1.3. Details of the DFT Calculations

(I) PBE/def-TZVP optimized geometries (in gas phase) for all the complexes 2.1-2.4 and 1c.

#### 2.1

72

In	7.313085	14.051985	7.615347
Cl	5.976244	13.206177	5.855759
Si	6.258115	13.441023	9.943633
Cl	9.594710	13.441026	7.539754
Si	5.454572	11.583383	12.327704
Cl	7.144848	16.430202	7.541603
Si	7.278927	10.579431	10.000788
N	4.685870	14.437696	10.039698
N	6.536100	14.924789	11.048120
N	6.239854	11.893672	10.729945
C	5.323291	15.416177	10.717672

---

C	4.790566	16.763519	11.041365
C	3.402033	14.427018	9.285609
C	7.703622	15.538367	11.736900
C	7.418498	15.642234	13.245706
H	6.547472	16.282280	13.442675
H	8.285965	16.088081	13.753095
H	7.239604	14.651209	13.686992
C	4.133603	16.961882	12.265310
H	4.012201	16.126671	12.957506
C	4.547849	13.094238	13.024237
H	5.200712	13.961912	13.167221
H	4.157008	12.798327	14.010366
H	3.695929	13.391220	12.400964
C	3.240112	12.989241	8.768685
H	4.049228	12.728140	8.069357
H	2.292188	12.896907	8.221777
H	3.233191	12.267409	9.598478
C	3.440715	15.397233	8.092878
H	3.519237	16.439509	8.426873
H	2.512481	15.295495	7.512159
H	4.283045	15.178509	7.424018

---

---

C	4.938239	17.828630	10.140849
H	5.472816	17.667350	9.202390
C	2.227746	14.778650	10.213903
H	2.173529	14.089421	11.068501
H	1.287444	14.694861	9.650737
H	2.302936	15.805265	10.594134
C	8.880035	14.578694	11.503725
H	8.644385	13.566781	11.864738
H	9.763608	14.936597	12.049765
H	9.148503	14.518612	10.438449
C	3.624874	18.222298	12.585160
H	3.112459	18.372769	13.537060
C	9.087437	10.878407	10.463407
H	9.467038	11.795895	9.990719
H	9.705860	10.043293	10.099253
H	9.224327	10.955174	11.551756
C	6.786781	11.118979	13.596945
H	7.379902	10.242372	13.304908
H	6.316838	10.899449	14.567852
H	7.481732	11.960119	13.741305
C	3.768671	19.283949	11.687565

---

---

H	3.368753	20.268091	11.938331
C	4.124835	10.237445	12.173777
H	3.534835	10.382007	11.256651
H	3.437575	10.320363	13.029705
H	4.526059	9.217349	12.162676
C	6.755345	8.869924	10.638416
H	6.807300	8.741967	11.727090
H	7.459860	8.150378	10.191779
H	5.746394	8.600474	10.297928
C	7.083749	10.509906	8.121451
H	6.066152	10.745246	7.781156
H	7.312531	9.481006	7.801559
H	7.788652	11.164340	7.590498
C	4.425208	19.084467	10.469376
H	4.544546	19.912194	9.768064
C	8.055847	16.922692	11.169705
H	8.153794	16.885626	10.076558
H	9.015082	17.249287	11.596644
H	7.300491	17.674433	11.430586

## 2.2

72

---

In	7.374672	4.275241	9.640253
Br	7.482683	6.807927	9.833397
Br	8.844859	3.343121	11.468579
Br	4.947346	3.604032	9.745843
Si	9.240664	1.892329	4.871586
Si	8.418236	3.715302	7.279696
Si	7.431376	0.827157	7.169453
N	8.101511	5.198493	6.183224
N	9.975879	4.737496	7.158526
N	8.451095	2.175704	6.473927
C	12.421998	5.156225	6.935240
C	11.496099	3.298743	8.349974
C	9.313422	5.705143	6.487169
C	6.916238	5.791168	5.506038
C	11.240412	5.681949	9.095717
C	10.120327	3.419643	4.177413
C	7.916455	1.414004	3.599182
C	5.620806	1.097182	6.696317
C	10.932291	8.515621	4.554325
C	9.827374	7.054887	6.141392
C	10.816754	9.579157	5.454029

---

---

C	5.753728	4.824016	5.774502
C	7.618660	0.716229	9.045725
C	10.595945	0.570282	5.011039
C	7.986968	-0.863317	6.506914
C	9.710173	8.121693	7.043867
C	11.279251	4.744231	7.877721
C	6.562863	7.180147	6.059884
C	10.439355	7.254219	4.894364
C	7.173259	5.874011	3.990853
C	10.205802	9.379024	6.695484
H	10.542460	6.418567	4.200122
H	11.410782	8.665530	3.584487
H	11.202927	10.564917	5.187037
H	10.108239	10.207717	7.399372
H	9.211191	7.962209	8.002002
H	12.476170	4.497316	6.057292
H	12.314966	6.192122	6.590525
H	13.375873	5.078293	7.475935
H	10.707132	2.990801	9.053266
H	11.513360	2.602031	7.499323
H	12.455106	3.221910	8.880371

---



---

H	11.111763	6.728195	8.790915
H	10.427866	5.413893	9.783214
H	12.188479	5.602694	9.647099
H	9.452449	4.275659	4.035209
H	10.968425	3.729870	4.799237
H	10.514046	3.129141	3.190633
H	7.349568	0.515431	3.875446
H	7.197843	2.237572	3.471769
H	8.390386	1.226096	2.623555
H	5.217922	1.999963	7.177441
H	5.489303	1.183644	5.607948
H	5.017889	0.244694	7.046047
H	5.991920	3.810593	5.419298
H	5.508476	4.772368	6.845792
H	4.855055	5.166897	5.243603
H	8.638440	0.934674	9.390909
H	6.920697	1.365623	9.591113
H	7.379607	-0.317274	9.342470
H	11.182067	0.712561	5.931046
H	10.214377	-0.457075	5.007132
H	11.282548	0.679577	4.157419

---

---

H	7.950880	-0.977571	5.416197
H	8.993797	-1.127300	6.858060
H	7.284710	-1.596787	6.934364
H	6.476214	7.155304	7.154361
H	7.312044	7.932695	5.783807
H	5.597377	7.497311	5.640129
H	8.027906	6.527359	3.767554
H	7.364264	4.878481	3.565014
H	6.288182	6.293149	3.490496

### 2.3

72

In	2.403037	15.996584	-1.133848
Ge	3.430229	16.586114	1.260261
Cl	3.854694	16.901104	-2.750855
Cl	2.544461	13.632112	-1.213286
Cl	0.158225	16.698020	-1.177873
Si	4.282155	18.377823	3.808946
Si	2.516729	19.517826	1.485897
N	5.044835	15.444095	1.447044
N	3.139720	14.983403	2.409324
N	3.517790	18.177812	2.192833

---

C	0.818021	15.396833	2.894655
H	1.098051	16.369286	3.326786
H	-0.084676	15.042295	3.410664
H	0.558686	15.543800	1.834943
C	4.346457	14.487235	2.086162
C	4.837100	13.117390	2.394788
C	6.273740	14.517131	-0.521363
H	6.109202	13.466459	-0.250409
H	7.222600	14.581622	-1.073683
H	5.468068	14.834068	-1.196697
C	1.952178	14.372386	3.057416
C	6.343223	15.414188	0.726700
C	5.476315	12.871705	3.619124
H	5.615889	13.688256	4.330301
C	7.477838	14.944674	1.653260
H	7.528589	15.559486	2.562871
H	8.436464	15.038040	1.122814
H	7.356386	13.894759	1.947025
C	4.667528	12.076376	1.470133
H	4.149986	12.273720	0.529098
C	5.141483	10.798678	1.772817

---

---

H	5.005681	9.990523	1.051875
C	5.131011	16.805015	4.434756
H	4.447530	15.952147	4.513827
H	5.516579	17.028204	5.441771
H	5.979349	16.516043	3.802733
C	2.227407	14.150762	4.555531
H	3.058742	13.448862	4.707141
H	1.334523	13.725351	5.035994
H	2.466573	15.098928	5.058346
C	6.603840	16.866013	0.293278
H	5.827604	17.213507	-0.406967
H	7.567427	16.932858	-0.229725
H	6.631056	17.540295	1.161423
C	2.947245	18.830417	5.081775
H	2.387272	19.736563	4.813445
H	3.406792	18.998374	6.067741
H	2.223517	18.007279	5.182571
C	1.536116	13.048932	2.393678
H	1.433075	13.170661	1.306941
H	0.567349	12.728249	2.803592
H	2.263831	12.251498	2.588531

---

---

C	5.780496	10.553371	2.991798
H	6.148736	9.552542	3.224139
C	5.650065	19.693582	3.750290
H	6.310579	19.519584	2.887836
H	6.260738	19.611732	4.662893
H	5.273293	20.721355	3.688969
C	5.945910	11.590341	3.914304
H	6.445366	11.403474	4.866490
C	3.054847	21.204242	2.169937
H	2.985577	21.301129	3.261220
H	2.375444	21.951917	1.731031
H	4.076739	21.458810	1.857045
C	0.692555	19.228290	1.898859
H	0.323773	18.312033	1.413811
H	0.081521	20.063467	1.523104
H	0.528283	19.143605	2.982888
C	2.736986	19.610963	-0.392844
H	3.761620	19.384560	-0.718841
H	2.506774	20.640257	-0.710368
H	2.044698	18.955921	-0.939841

## 2.4

72

---

In	7.804471	4.278032	-1.275701
Ge	6.802933	3.747428	1.159983
Br	6.270499	3.238715	-2.968734
Br	10.210944	3.571682	-1.285527
Br	7.650075	6.788197	-1.508052
Si	5.974599	2.020846	3.765937
Si	7.739300	0.817768	1.488003
N	5.182452	4.882405	1.361213
N	7.100848	5.368313	2.283566
C	8.010789	6.291403	4.400235
H	7.197341	7.020902	4.512924
H	8.912310	6.717177	4.864055
H	7.746301	5.376531	4.949554
C	5.140774	3.606264	4.380140
H	5.834640	4.450188	4.463484
H	4.745360	3.390299	5.384985
H	4.300740	3.904623	3.742082
C	2.741809	5.331262	1.614939
H	2.709920	4.697674	2.512566
H	1.777510	5.234198	1.095549

---

---

H	2.853140	6.376875	1.926672
C	8.290826	5.986848	2.917756
C	5.882187	5.849367	1.982811
N	6.737007	2.182701	2.143661
C	4.729368	7.437914	3.527130
H	4.606962	6.614832	4.233609
C	5.524045	8.261093	1.384694
H	6.039380	8.078449	0.439248
C	5.375486	7.211325	2.302497
C	3.869775	4.892058	0.665287
C	5.022540	9.527076	1.692957
H	5.139537	10.340356	0.974376
C	4.232179	8.707241	3.828462
H	3.726097	8.877210	4.780454
C	3.629614	3.437235	0.230727
H	4.397144	3.107927	-0.487493
H	2.656260	3.350560	-0.270829
H	3.635843	2.760790	1.097679
C	9.560395	1.108367	1.916023
H	9.942551	2.007594	1.410246
H	10.171736	0.258521	1.575405

---

---

H	9.709651	1.224313	2.999307
C	4.376551	9.752759	2.911840
H	3.985857	10.744273	3.148184
C	9.404535	4.932890	2.818384
H	9.104543	3.993089	3.305423
H	10.314039	5.299380	3.313156
H	9.660868	4.719519	1.768946
C	4.592640	0.719412	3.730399
H	4.001125	0.804852	4.655133
H	4.958455	-0.311423	3.657907
H	3.916997	0.902422	2.881528
C	7.529476	0.663876	-0.386284
H	6.496203	0.842753	-0.715311
H	7.797822	-0.364707	-0.674503
H	8.195913	1.327817	-0.953865
C	7.192499	-0.851170	2.209495
H	7.243753	-0.923590	3.303536
H	7.883263	-1.604510	1.798790
H	6.177926	-1.119980	1.884685
C	3.898196	5.798354	-0.577321
H	4.041265	6.851045	-0.301099

---



---

H	2.943257	5.714428	-1.116410
H	4.702101	5.506387	-1.265994
C	7.305260	1.579309	5.047927
H	8.055501	2.382381	5.110567
H	7.834360	0.644270	4.819879
H	6.844409	1.471011	6.041636
C	8.738001	7.265393	2.190504
H	8.871432	7.080587	1.115921
H	9.697086	7.603501	2.608966
H	8.010413	8.077770	2.314303

**1c**

40

In	0.033011	-0.029648	-0.360008
Si	1.288873	-0.265808	-2.671104
Si	-2.532785	0.590321	-0.376982
Si	1.372352	-0.422254	1.879070
C	-2.750705	2.485069	-0.559382
H	-2.276588	2.858871	-1.479193
H	-3.822008	2.739921	-0.604105
H	-2.310402	3.024972	0.291703
C	-3.425360	-0.238144	-1.853318

---

H	-3.003366	0.101411	-2.810792
H	-3.332707	-1.333796	-1.818628
H	-4.498919	0.010618	-1.846503
C	-3.420594	0.051237	1.229543
H	-4.483273	0.342795	1.204013
H	-3.373262	-1.039635	1.365513
H	-2.959514	0.516038	2.113348
C	2.614430	1.006090	2.169402
H	2.100682	1.973019	2.273860
H	3.186812	0.827358	3.094350
H	3.330951	1.091106	1.339310
C	2.375358	-2.048469	1.764507
H	2.966170	-2.205450	2.681570
H	1.715368	-2.919447	1.636765
H	3.069002	-2.024644	0.910842
C	0.237969	-0.529634	3.413954
H	-0.482720	-1.355586	3.319241
H	0.831311	-0.697596	4.327461
H	-0.336507	0.398881	3.546844
C	2.926178	-1.242250	-2.512456
H	3.619518	-0.738571	-1.822278

---

---

H	2.750905	-2.257611	-2.126298
H	3.423768	-1.332676	-3.491442
C	0.190363	-1.154862	-3.961031
H	0.717952	-1.242389	-4.924637
H	-0.080175	-2.168821	-3.631266
H	-0.744112	-0.600895	-4.133360
C	1.704674	1.468436	-3.370449
H	2.198791	1.374476	-4.351303
H	0.795776	2.072767	-3.507227
H	2.382277	2.022539	-2.704305

**(II) PBE/def-TZVP optimized geometries (in solvent phase) for all the complexes 2.1–2.4 and 1c.**

**2.1**

72

In	7.324203	14.045671	7.647551
Cl	6.052531	13.245216	5.808755
Si	6.250972	13.440022	9.959452
Cl	9.617752	13.444217	7.531892
Si	5.450280	11.579359	12.335487
Cl	7.190852	16.429228	7.514250
Si	7.275284	10.577691	10.002067

---

N	4.685767	14.439669	10.039297
N	6.536386	14.929068	11.046075
N	6.238053	11.892217	10.733000
C	5.323255	15.419897	10.717532
C	4.789492	16.766305	11.040190
C	3.399575	14.423613	9.289365
C	7.704589	15.540033	11.737799
C	7.417964	15.645746	13.245635
H	6.546624	16.285736	13.440995
H	8.285677	16.091601	13.752313
H	7.239067	14.655320	13.687891
C	4.134142	16.965008	12.265177
H	4.014027	16.132161	12.960205
C	4.547873	13.092264	13.029588
H	5.200597	13.959708	13.173966
H	4.158863	12.794657	14.016057
H	3.693867	13.389565	12.409078
C	3.236780	12.983436	8.780049
H	4.048640	12.715161	8.086176
H	2.290757	12.890410	8.230160
H	3.225565	12.265544	9.613044

---

---

C	3.438312	15.388448	8.092611
H	3.516706	16.432283	8.422148
H	2.510738	15.283522	7.511771
H	4.282548	15.165525	7.426817
C	4.933755	17.829971	10.136989
H	5.464949	17.670597	9.196609
C	2.227125	14.779965	10.217437
H	2.176627	14.096539	11.076649
H	1.286144	14.691372	9.656269
H	2.302430	15.809185	10.590491
C	8.878810	14.577613	11.506315
H	8.639988	13.566465	11.867147
H	9.762375	14.933662	12.053007
H	9.147865	14.517746	10.441077
C	3.623437	18.225366	12.583085
H	3.112034	18.376054	13.535508
C	9.084390	10.883447	10.457237
H	9.456334	11.809740	9.995977
H	9.704573	10.055529	10.080134
H	9.223786	10.947652	11.546108
C	6.787024	11.110212	13.595789

---

---

H	7.371481	10.228123	13.302567
H	6.317135	10.895430	14.567814
H	7.487336	11.947564	13.736268
C	3.764208	19.285964	11.683071
H	3.363954	20.270307	11.932639
C	4.120091	10.236726	12.176841
H	3.513227	10.398253	11.273574
H	3.450558	10.306799	13.048086
H	4.522397	9.217622	12.141466
C	6.758264	8.867074	10.634327
H	6.812378	8.737763	11.722735
H	7.466646	8.154029	10.183163
H	5.750067	8.595784	10.292891
C	7.069028	10.515143	8.121874
H	6.045565	10.743658	7.794263
H	7.301909	9.488475	7.797725
H	7.765093	11.175010	7.585967
C	4.419242	19.085880	10.463643
H	4.535838	19.912499	9.760529
C	8.059142	16.922539	11.168352
H	8.161351	16.882122	10.075706

---

---

H 9.016751 17.249025 11.598480

H 7.301998 17.674515 11.423060

## 2.2

72

In 7.373941 4.258694 9.618826

Br 7.453862 6.795421 9.854316

Br 8.785305 3.357664 11.521496

Br 4.937103 3.592663 9.785398

Si 9.243871 1.889711 4.864568

Si 8.424891 3.713988 7.266715

Si 7.436014 0.825303 7.167035

N 8.099688 5.202245 6.187293

N 9.975032 4.740341 7.161444

N 8.454069 2.174870 6.472276

C 12.422717 5.155217 6.933773

C 11.496970 3.296377 8.345616

C 9.313549 5.708118 6.489008

C 6.915857 5.793104 5.505022

C 11.243828 5.678548 9.096752

C 10.117709 3.419851 4.172465

C 7.914233 1.410791 3.599658

---

C	5.624982	1.100313	6.698263
C	10.932770	8.515523	4.552899
C	9.828199	7.056372	6.141124
C	10.819322	9.579494	5.452763
C	5.753650	4.825669	5.770981
C	7.626251	0.720077	9.045321
C	10.598360	0.568977	5.009926
C	7.989598	-0.864557	6.508328
C	9.711928	8.123709	7.043627
C	11.280952	4.742824	7.877040
C	6.561902	7.182345	6.057605
C	10.439196	7.254248	4.893181
C	7.174652	5.875825	3.990715
C	10.208547	9.380794	6.694970
H	10.541620	6.419723	4.197817
H	11.410197	8.664270	3.582808
H	11.206475	10.564440	5.185377
H	10.112271	10.209143	7.399085
H	9.214559	7.966422	8.002685
H	12.472484	4.499325	6.053427
H	12.316062	6.192933	6.593872

---



---

H	13.376416	5.072556	7.474127
H	10.704285	2.983805	9.043079
H	11.518513	2.601996	7.493500
H	12.453420	3.219196	8.879718
H	11.116589	6.725484	8.793004
H	10.429431	5.410053	9.782767
H	12.191740	5.596858	9.647890
H	9.448182	4.274822	4.030663
H	10.968497	3.731418	4.789733
H	10.507824	3.129780	3.184182
H	7.347997	0.511811	3.876495
H	7.197019	2.235924	3.472120
H	8.389701	1.222687	2.624796
H	5.226979	2.008129	7.174192
H	5.494821	1.183303	5.609459
H	5.021341	0.250155	7.052429
H	5.992344	3.812382	5.416268
H	5.506810	4.774797	6.841992
H	4.856146	5.168508	5.238837
H	8.649954	0.931714	9.383780
H	6.933298	1.375014	9.591077

---

---

H	7.380439	-0.311442	9.343790
H	11.188984	0.718019	5.926002
H	10.215784	-0.458230	5.013190
H	11.278830	0.674787	4.150960
H	7.948356	-0.979068	5.417883
H	8.998141	-1.125860	6.856484
H	7.287600	-1.594705	6.941939
H	6.472748	7.157059	7.152015
H	7.312839	7.933704	5.783326
H	5.597713	7.499307	5.635115
H	8.032410	6.525075	3.768248
H	7.360503	4.880141	3.563171
H	6.290942	6.299954	3.492941

### 2.3

72

In	2.412805	16.023148	-1.112993
Ge	3.438659	16.585043	1.274447
Cl	3.822148	16.922024	-2.783552
Cl	2.531542	13.654613	-1.251612
Cl	0.154532	16.707912	-1.206530
Si	4.285660	18.378924	3.813485

---

Si	2.515187	19.517989	1.488987
N	5.045246	15.438423	1.445775
N	3.139771	14.978781	2.407317
N	3.518126	18.177914	2.194088
C	0.819395	15.397612	2.896450
H	1.099476	16.369235	3.330543
H	-0.084049	15.042636	3.410478
H	0.562055	15.545001	1.836143
C	4.347126	14.481732	2.086565
C	4.837658	13.113016	2.396783
C	6.278407	14.515635	-0.520307
H	6.113804	13.464894	-0.249256
H	7.227646	14.581342	-1.071481
H	5.471965	14.832167	-1.195509
C	1.951705	14.371686	3.059658
C	6.345525	15.412336	0.728093
C	5.474485	12.867577	3.622525
H	5.612131	13.682080	4.336142
C	7.479512	14.944317	1.655502
H	7.529502	15.560722	2.563930
H	8.437769	15.037563	1.124614

---

---

H	7.357145	13.894787	1.950266
C	4.670618	12.072679	1.470724
H	4.156221	12.268147	0.527801
C	5.144418	10.794647	1.773049
H	5.010585	9.987174	1.050926
C	5.132979	16.804584	4.434885
H	4.449188	15.952171	4.516941
H	5.519639	17.028660	5.441371
H	5.981123	16.514783	3.802755
C	2.226518	14.151876	4.557882
H	3.058595	13.451369	4.711347
H	1.332504	13.726688	5.036407
H	2.463749	15.100749	5.060213
C	6.604316	16.864752	0.297258
H	5.824875	17.214978	-0.398304
H	7.565868	16.932832	-0.228973
H	6.634386	17.536965	1.166742
C	2.948131	18.833173	5.080971
H	2.394086	19.743460	4.813902
H	3.409848	18.995871	6.066888
H	2.221097	18.012289	5.177804

---

---

C	1.534733	13.048262	2.396467
H	1.429967	13.171072	1.309803
H	0.566568	12.728298	2.808005
H	2.263333	12.251107	2.589439
C	5.781689	10.549289	2.993591
H	6.151085	9.548728	3.225583
C	5.651369	19.694422	3.744051
H	6.310802	19.515688	2.881568
H	6.260923	19.615360	4.657703
H	5.271428	20.720870	3.678267
C	5.944646	11.586080	3.917517
H	6.442368	11.399832	4.870850
C	3.050581	21.204978	2.167702
H	2.983060	21.302324	3.259059
H	2.366157	21.947039	1.726652
H	4.071014	21.460856	1.850948
C	0.690993	19.225390	1.900297
H	0.323572	18.306062	1.419998
H	0.081218	20.060514	1.521980
H	0.528490	19.143726	2.984831
C	2.737478	19.607405	-0.390540

---

---

H 3.766176 19.389615 -0.710215

H 2.498862 20.634328 -0.709124

H 2.051337 18.946735 -0.938746

## 2.4

72

In 7.805722 4.260692 -1.243565

Ge 6.799716 3.748027 1.180327

Br 6.295418 3.235908 -2.980661

Br 10.219349 3.549769 -1.320150

Br 7.683477 6.773522 -1.522818

Si 5.965632 2.008620 3.767697

Si 7.740199 0.812770 1.489253

N 5.183206 4.883462 1.359847

N 7.098008 5.375601 2.287300

C 8.012023 6.278819 4.411749

H 7.187840 6.993373 4.539755

H 8.910646 6.712390 4.873765

H 7.766219 5.352036 4.949734

C 5.141307 3.597203 4.382686

H 5.836475 4.441494 4.450632

H 4.764128 3.385044 5.395406

---

H	4.289580	3.891901	3.758156
C	2.745607	5.356911	1.604172
H	2.715055	4.752580	2.521506
H	1.780768	5.245502	1.088933
H	2.860235	6.411734	1.882233
C	8.285797	6.000808	2.923159
C	5.878572	5.853243	1.983888
N	6.736228	2.177680	2.144878
C	4.744867	7.450027	3.534773
H	4.628045	6.633256	4.249320
C	5.509119	8.259213	1.375197
H	6.010456	8.072923	0.423271
C	5.370717	7.214841	2.301082
C	3.869729	4.887085	0.665609
C	5.020839	9.530109	1.685028
H	5.133354	10.339787	0.961677
C	4.259841	8.723994	3.837648
H	3.771710	8.901269	4.797658
C	3.616536	3.426412	0.260320
H	4.388753	3.070980	-0.440614
H	2.648104	3.342605	-0.251037

---

---

H	3.603782	2.768100	1.140658
C	9.560766	1.111331	1.912712
H	9.933687	2.022628	1.421838
H	10.175283	0.270321	1.555800
H	9.710479	1.211024	2.997598
C	4.396488	9.764996	2.914027
H	4.016790	10.760220	3.152477
C	9.414243	4.965383	2.801109
H	9.132083	4.014661	3.277850
H	10.320898	5.339391	3.295484
H	9.666768	4.770658	1.747106
C	4.581058	0.712332	3.713284
H	3.989205	0.789801	4.638654
H	4.945586	-0.318150	3.629259
H	3.908388	0.908623	2.864973
C	7.527477	0.657339	-0.385306
H	6.487383	0.810592	-0.705884
H	7.819847	-0.364796	-0.673262
H	8.174803	1.336393	-0.957054
C	7.196891	-0.855480	2.210257
H	7.241707	-0.922813	3.304838

---



---

H	7.892987	-1.607089	1.805048
H	6.184656	-1.125802	1.879326
C	3.907956	5.767742	-0.595128
H	4.069280	6.823151	-0.340248
H	2.950231	5.687936	-1.129605
H	4.705609	5.448650	-1.279552
C	7.294837	1.554656	5.044757
H	8.030145	2.369107	5.132390
H	7.840418	0.634584	4.796009
H	6.826721	1.413194	6.031010
C	8.708239	7.296884	2.212395
H	8.834110	7.129855	1.133840
H	9.666422	7.641133	2.627421
H	7.970583	8.096512	2.356305
<b>1c</b>			
40			
In	0.031938	-0.031895	-0.359344
Si	1.287800	-0.265293	-2.670770
Si	-2.532083	0.590143	-0.377125
Si	1.371984	-0.421878	1.878587
C	-2.751649	2.485037	-0.559178

---

---

H	-2.275912	2.856672	-1.479107
H	-3.823402	2.739177	-0.603365
H	-2.309039	3.023514	0.292100
C	-3.426724	-0.238063	-1.853194
H	-3.001998	0.102160	-2.809519
H	-3.332315	-1.333757	-1.816394
H	-4.500133	0.012433	-1.845918
C	-3.421249	0.051346	1.229292
H	-4.483768	0.343710	1.202641
H	-3.371837	-1.039832	1.363748
H	-2.958299	0.517264	2.111925
C	2.615276	1.005978	2.170324
H	2.099519	1.972431	2.272515
H	3.187884	0.826276	3.095163
H	3.329772	1.089882	1.337813
C	2.375611	-2.048829	1.765672
H	2.966877	-2.204103	2.682995
H	1.714193	-2.918746	1.636290
H	3.068741	-2.023834	0.911274
C	0.237906	-0.529596	3.414843
H	-0.482618	-1.355547	3.317788

---

---

H	0.832326	-0.698095	4.327732
H	-0.336589	0.399713	3.545929
C	2.926252	-1.241888	-2.513162
H	3.618356	-0.737831	-1.821730
H	2.749229	-2.256907	-2.126401
H	3.423839	-1.331046	-3.492678
C	0.190595	-1.155948	-3.962267
H	0.719378	-1.241735	-4.925763
H	-0.079181	-2.169515	-3.629650
H	-0.743462	-0.599813	-4.132465
C	1.705637	1.468726	-3.371666
H	2.199921	1.373940	-4.352587
H	0.795221	2.071804	-3.506951
H	2.381499	2.021682	-2.702168

## 6.2: Chapter 3 experimental details, crystallographic data and details of theoretical calculations

### 6.2.1. Synthesis and experimental details of compounds 3.1-3.8

#### 6.2.1.1. Synthesis and characterization of compound 3.1

A solution of <sup>n</sup>BuLi in *n*-hexane (3.93 mL, 6.29 mmol, 1.6 M) was added drop wise to a stirred solution of **L1** (2,6-diisopropyl-N-((2Z,4E)-4-((pyridin-2-ylmethyl)imino)pent-2-en-2-yl)aniline) (2.0 g, 5.72 mmol, in THF 20 mL) at -78 °C, over a period of 10 min. The suspension was allowed

to warm up to room temperature and stirred for another 8 h. Next, the solution of  $\text{GeCl}_2 \cdot \text{dioxane}$  (1.39 g, 6.0 mmol) in THF was added drop by drop to the above suspension at  $-30\text{ }^\circ\text{C}$  via cannula. The reaction mixture was further warmed to room temperature and stirred for additional 15 h. Subsequently, all volatiles were removed in vacuo and the residue was extracted into toluene (30 mL). The resultant toluene solvent was concentrated to 10–12 mL and stored at  $-30\text{ }^\circ\text{C}$  in a freezer, which afforded colorless crystals of **3.1** within one day.

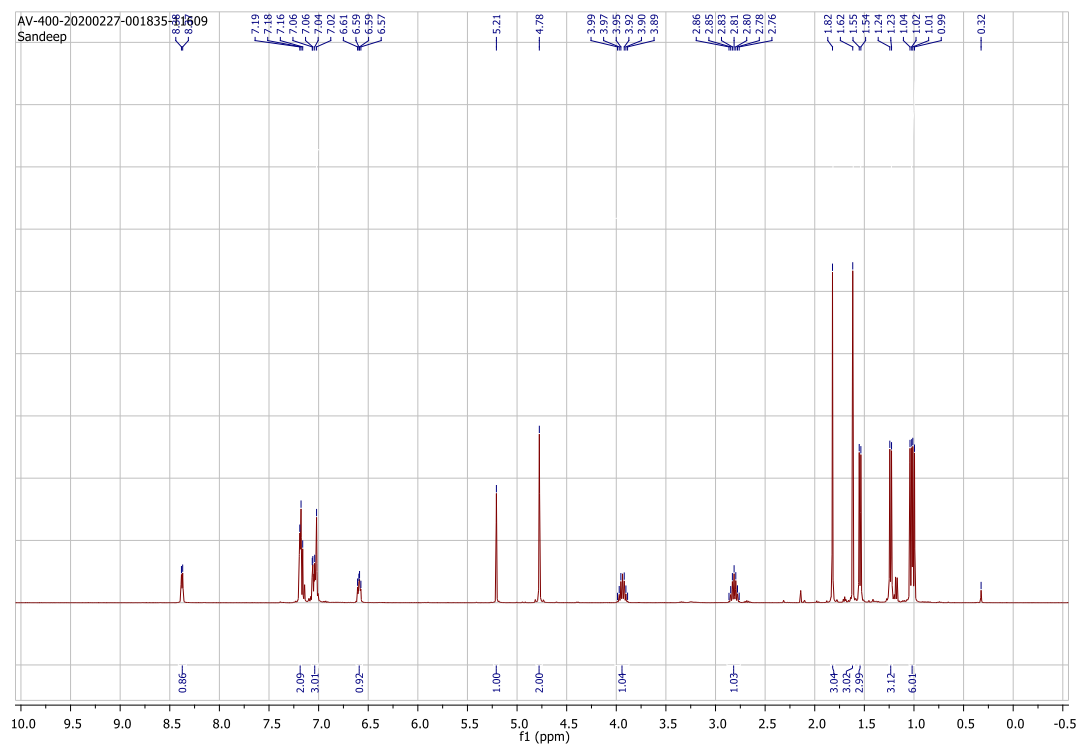
**Yield:** 2.57 g (98 %).

**Mp:** 218  $^\circ\text{C}$ .

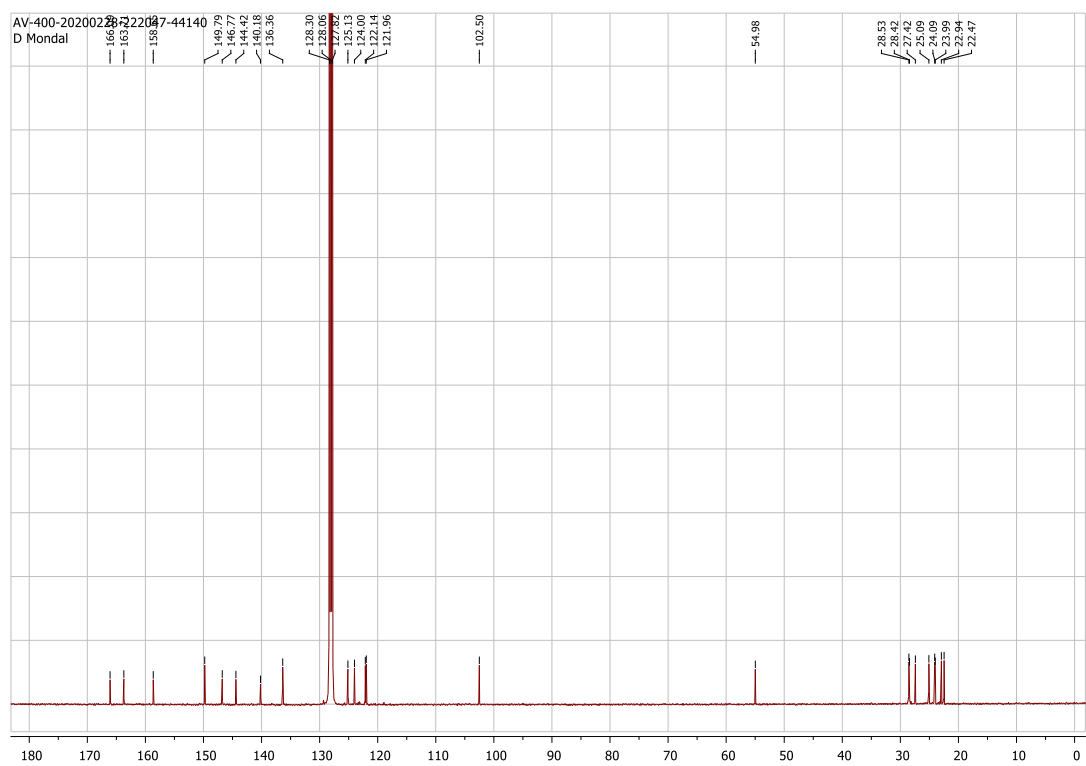
**NMR:**  $^1\text{H}$  NMR (400 MHz,  $\text{C}_6\text{D}_6$ , 298 K):  $\delta$  8.38 (d,  $J = 4.9$  Hz, 1H), 7.18 (d,  $J = 4.9$  Hz, 2H), 7.05 (dd,  $J = 12.4, 4.9$  Hz, 3H), 6.59 (dd,  $J = 8.1, 5.4$  Hz, 1H), 5.21 (s, 1H), 4.78 (s, 2H), 4.01 – 3.87 (m, 1H), 2.81 (hept,  $J = 6.9$  Hz, 1H), 1.82 (s, 3H), 1.62 (s, 3H), 1.54 (d,  $J = 6.6$  Hz, 3H), 1.23 (d,  $J = 6.9$  Hz, 3H), 1.02 (dd,  $J = 11.3, 6.9$  Hz, 6H) ppm.  $^{13}\text{C}$  NMR (100.56 MHz,  $\text{C}_6\text{D}_6$ , 298 K);  $\delta$  166.09, 163.71, 158.65, 149.79, 146.77, 144.42, 140.18, 136.36, 125.13, 124.00, 122.14, 121.96, 102.50, 54.98, 28.53, 28.42, 27.42, 25.09, 24.09, 23.99, 22.94, 22.47 ppm.

**LC-MS:** Calcd: 456.59, found: 456.1696.

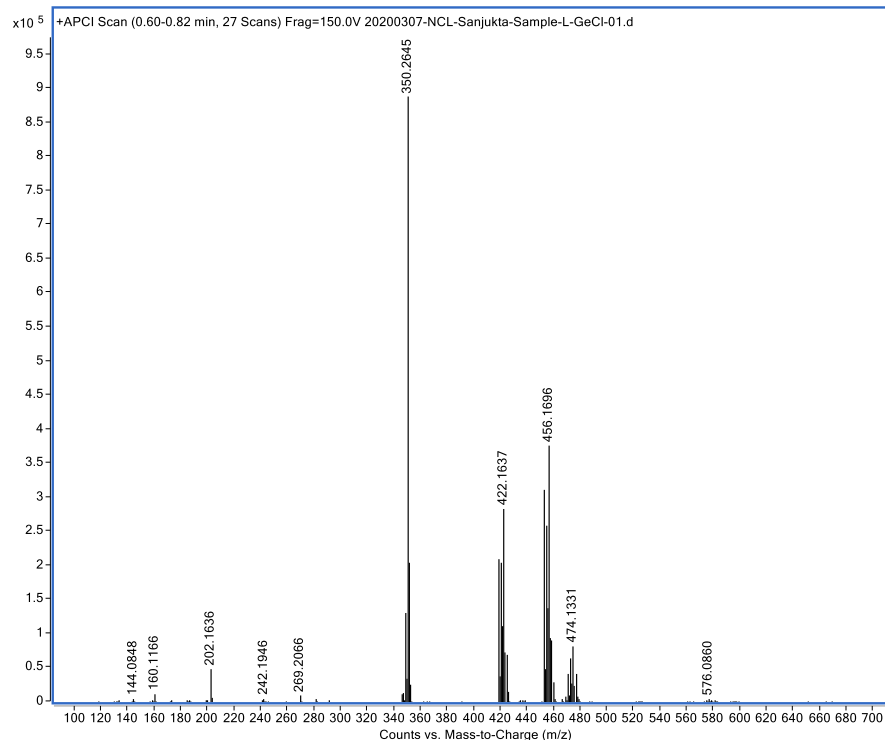
**a)  $^1\text{H}$  NMR of compound 3.1:**



b)  $^{13}\text{C}$  NMR of compound 3.1:



c) LC-MS data of compound 3.1:



### 6.2.1.2. Synthesis and characterization of compound 3.2 and 3.3

To a stirred solution of **3.1** (0.457 g, 1.0 mmol, in THF 10 mL) at  $-78\text{ }^{\circ}\text{C}$  was added drop wise  $\text{GeCl}_2$ -dioxane in THF (0.243 g, 1.05 mmol) over a period of 5 min. The solution was allowed to come to room temperature and stirred for 15 h. All volatiles were removed under reduced pressure and the residue was extracted with toluene of about 15 mL. The solvent was concentrated to 5-8 mL and stored at  $-30\text{ }^{\circ}\text{C}$  in a freezer overnight to afford colorless crystals of **3.2** suitable for X-ray analysis.

**Yield:** 0.148 g (53 %).

**Mp:**  $186\text{ }^{\circ}\text{C}$ .

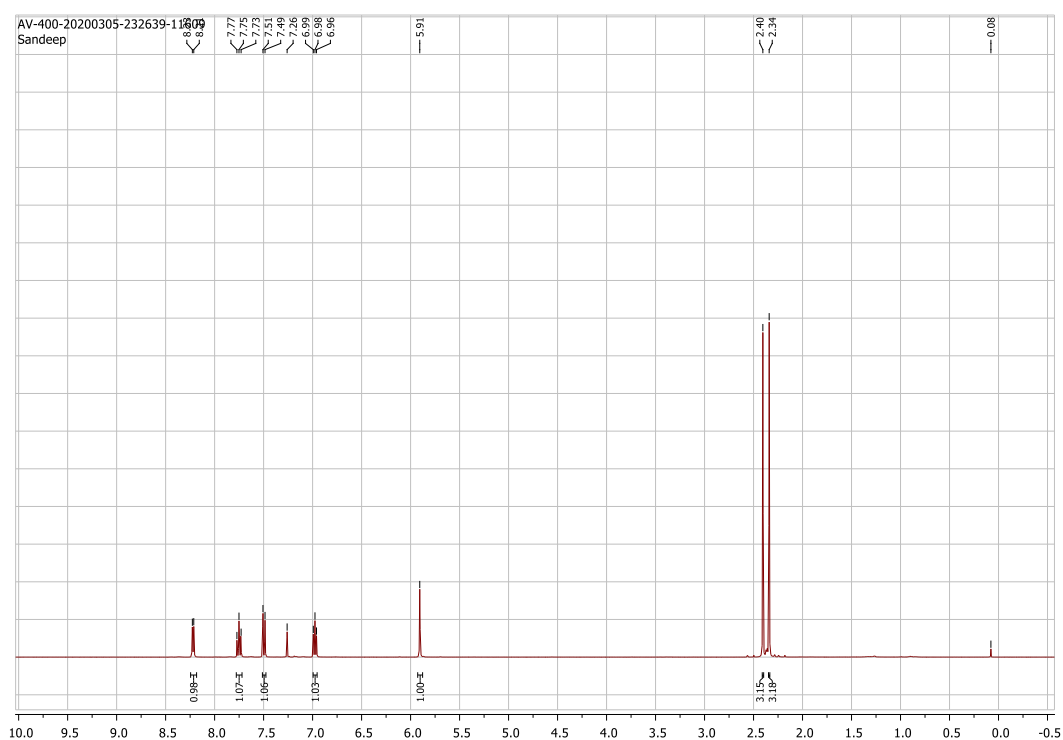
**NMR:**  $^1\text{H}$  NMR (400 MHz,  $\text{CDCl}_3$ , 298 K):  $\delta$  8.22 (d,  $J = 5.8$  Hz, 1H), 7.75 (t,  $J = 8.6$  Hz, 1H), 7.50 (d,  $J = 8.5$  Hz, 1H), 6.98 (t,  $J = 6.5$  Hz, 1H), 5.91 (s, 1H), 2.40 (s, 3H), 2.34 (s, 3H) ppm.  $^{13}\text{C}$  NMR (101 MHz,  $\text{CDCl}_3$ , 298 K);  $\delta$  151.50, 143.39, 141.10, 140.23, 130.07, 126.67, 118.23, 117.87, 116.01, 15.10, 13.23 ppm.

**LC-MS:** Calcd: 279.30, found: 279.0006.

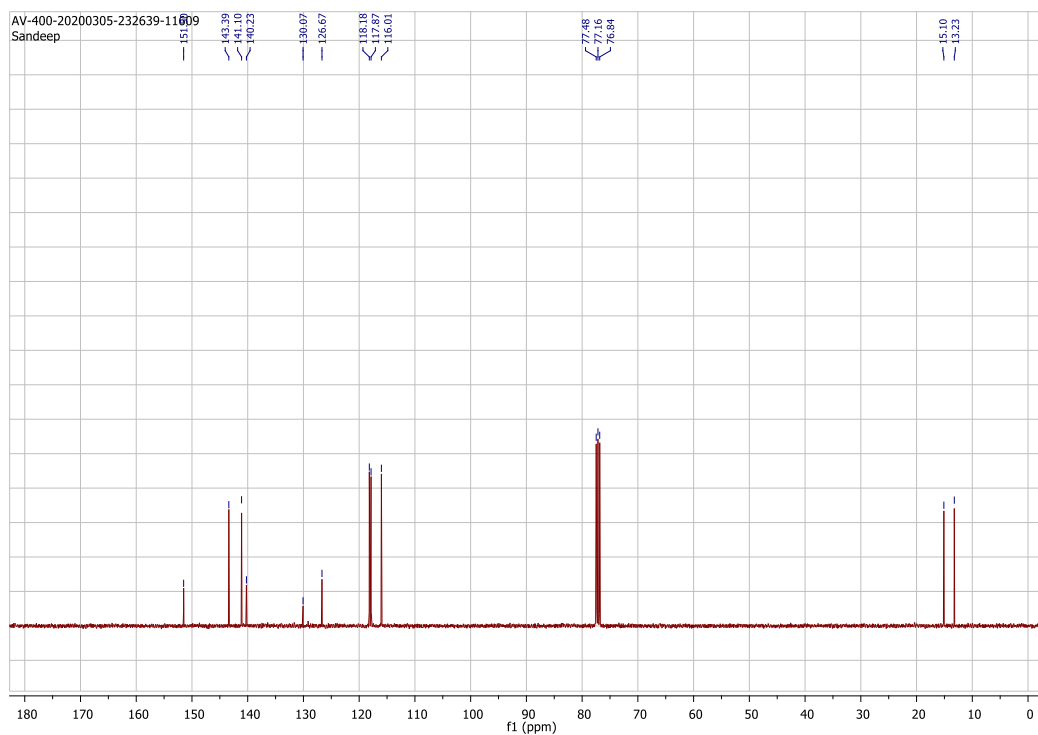
The undissolved part remained in toluene was further extracted with THF ( $2 \times 10$  mL), the solvent was then reduced to 10 mL and stored at  $-30$  °C in a freezer overnight to grow the suitable colorless crystals for X-ray analysis of compound **3.3**. The low solubility of **3.3** in most of the organic solvents prevents NMR spectroscopic measurement.

**Mp:** 145 °C.

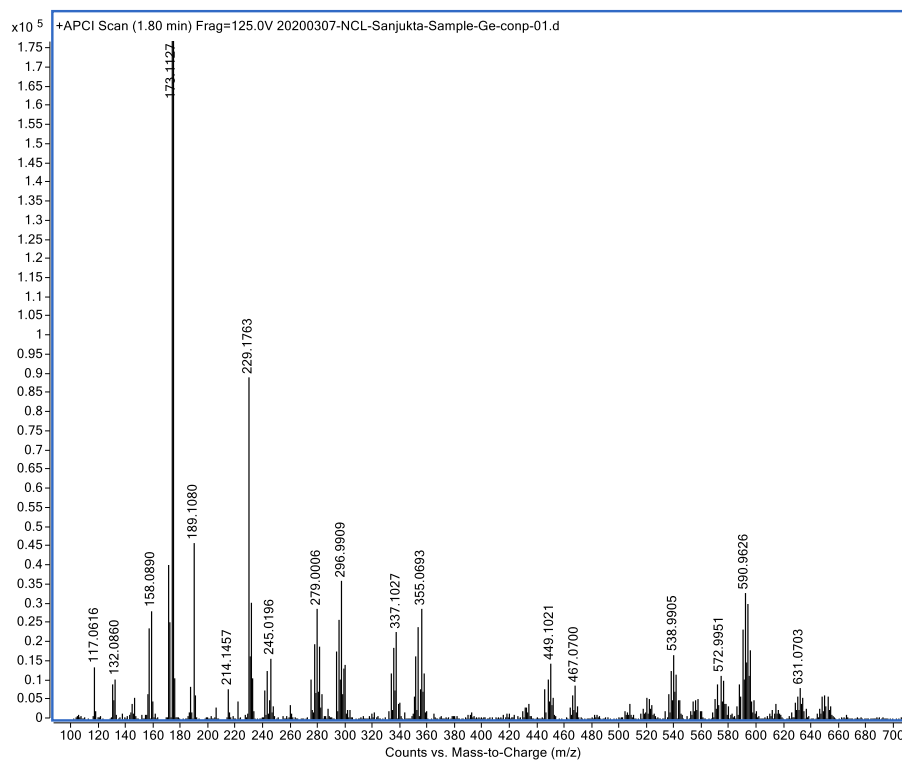
**a)  $^1\text{H}$  NMR of compound 3.2:**



**b)  $^{13}\text{C}$  NMR of compound 3.2:**



### c) LC-MS data of compound 3.2:



### 6.2.1.3. Synthesis and characterization of compound 3.4



The THF solution of SnCl<sub>2</sub> (0.200 g, 1.05 mmol, THF 10 mL) was slowly added to a stirred solution of **3.1** (0.457 g, 1.0 mmol) in THF (10 mL) at -78 °C over a period of 5 min. The solution was warmed to room temperature and stirred for 18 h. All volatiles were removed under reduced pressure and extracted with toluene (2 × 15 mL). The solvent was reduced to 5 mL and stored at -30 °C in a freezer overnight to obtain the yellow crystals of **3.4** suitable for X-ray analysis.

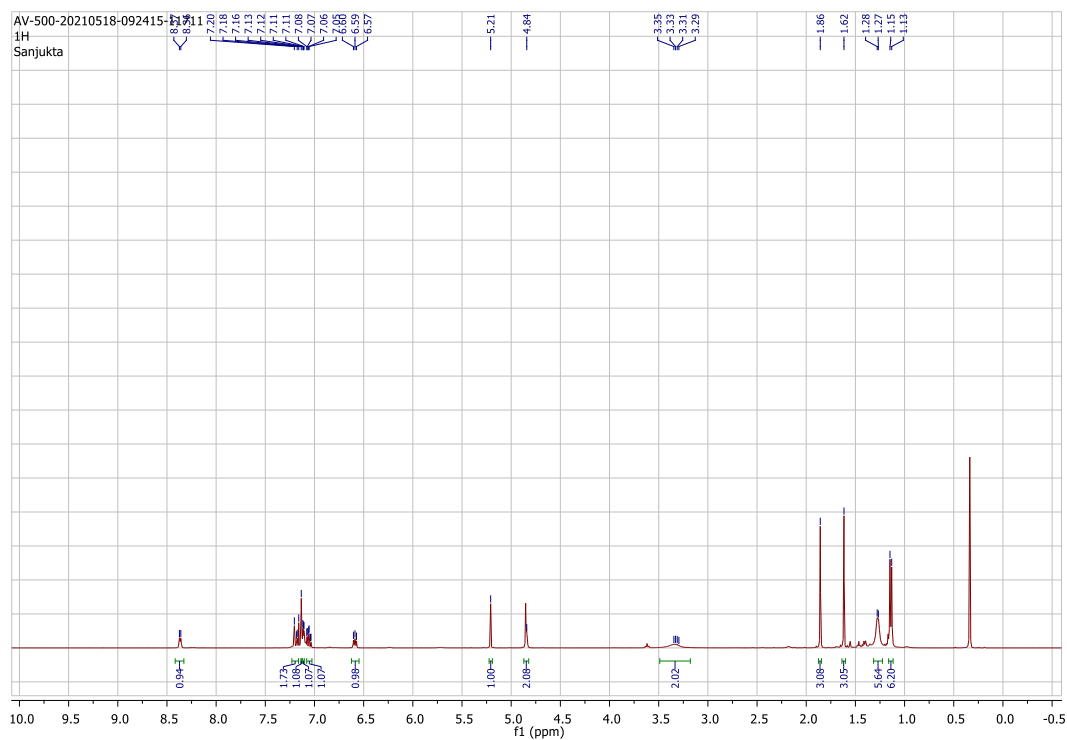
**Yield:** 0.425 g (84 %).

**Mp:** 179.8 °C.

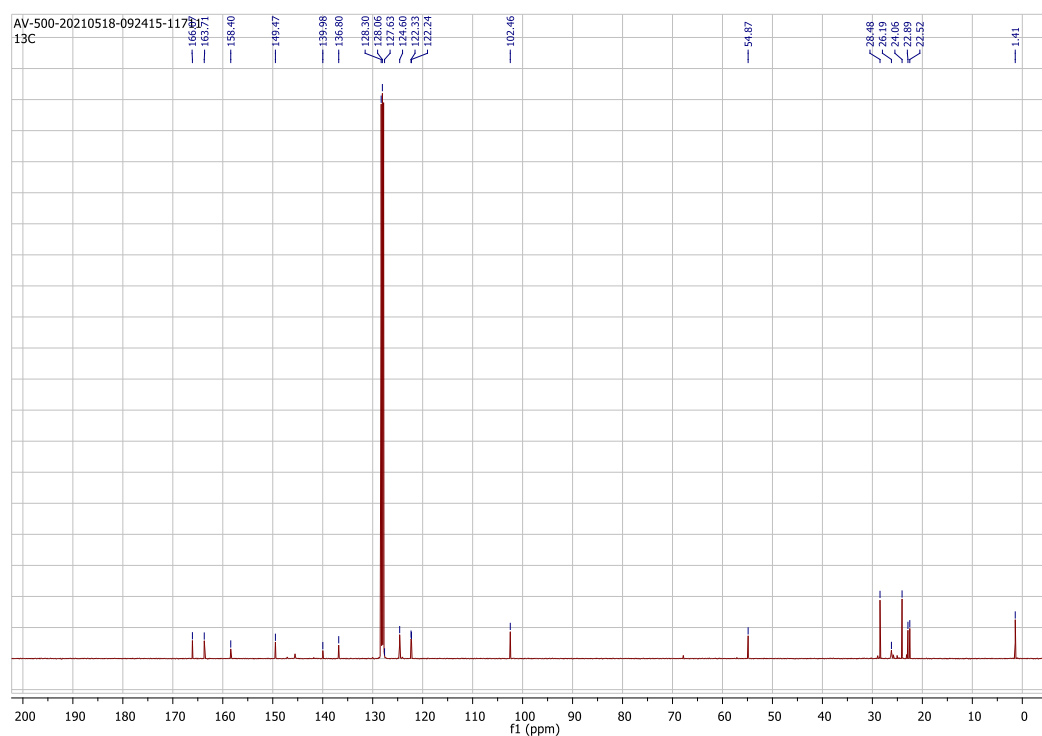
**NMR:** <sup>1</sup>H NMR (400 MHz, CDCl<sub>3</sub>, 298 K): δ 8.37 (1 H, d, *J* = 5.7 Hz), 7.23 – 7.16 (2 H, m), 7.13 (1 H, s), 7.12 – 7.10 (1 H, m), 7.06 (1 H, td, *J* = 7.6, 1.7 Hz), 6.62 – 6.55 (1 H, m), 5.21 (1 H, s), 4.84 (2 H, s), 3.32 (2 H, dq, *J* = 13.6, 6.8 Hz), 1.86 (3 H, s), 1.62 (3 H, s), 1.27 (6 H, d, *J* = 4.8 Hz), 1.14 (6 H, d, *J* = 6.9 Hz) ppm. <sup>13</sup>C NMR (101 MHz, CDCl<sub>3</sub>, 298 K): δ 166.07 (s), 163.71 (s), 158.40 (s), 149.47 (s), 136.80 (s), 139.98 (s), 124.60 (s), 122.33 (s), 122.24 (s), 102.46 (s), 54.87 (s), 28.48 (s), 26.19 (s), 24.06 (s), 22.89 (s), 22.52 (s), 1.41 (s) ppm. <sup>119</sup>Sn NMR (149 MHz, CDCl<sub>3</sub>, 298 K): δ -301.83 ppm.

**HRMS:** Calcd: 503.12, found: 504.0860.

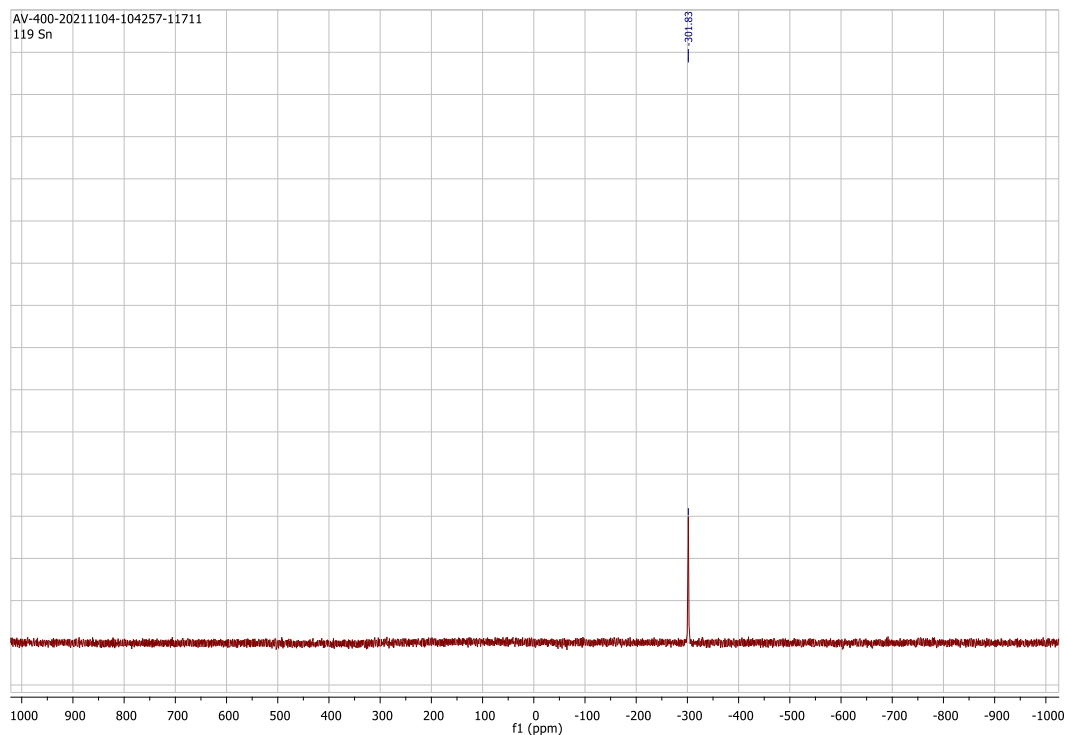
**a) <sup>1</sup>H NMR of compound 3.4:**



**b)  $^{13}\text{C}$  NMR of compound 3.4:**

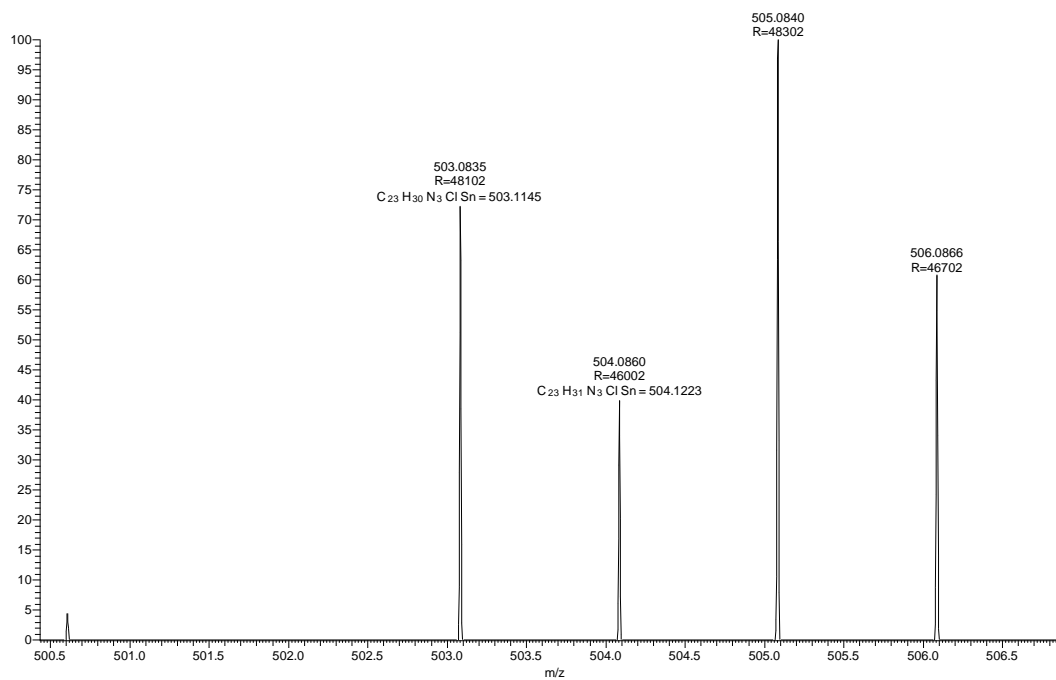


**c)  $^{119}\text{Sn}$  NMR of compound 3.4:**



#### d) HRMS data of compound 3.4:

SP-01\_210505165317 #895 RT: 4.84 AV: 1 NL: 2.52E5  
T: FTMS + p ESI Full ms [100.0000-1500.0000]



#### 6.2.1.4. Synthesis and characterization of compound 3.5

To a stirred solution of **3.1** (0.457 g, 1.0 mmol) in THF (10 mL) at  $-78\text{ }^{\circ}\text{C}$  was added drop wise  $\text{AlCl}_3$  (0.140 g, 1.05 mmol, THF 10 mL) over a period of 5 min. The solution was warmed to room temperature and stirred for 15 h. All volatiles were removed under reduced pressure and extracted with *n*-hexane ( $2 \times 15\text{ mL}$ ). The solvent was reduced to 5 mL and stored at  $-30\text{ }^{\circ}\text{C}$  in a freezer overnight to obtain the yellow crystals of **3.5** suitable for X-ray analysis.

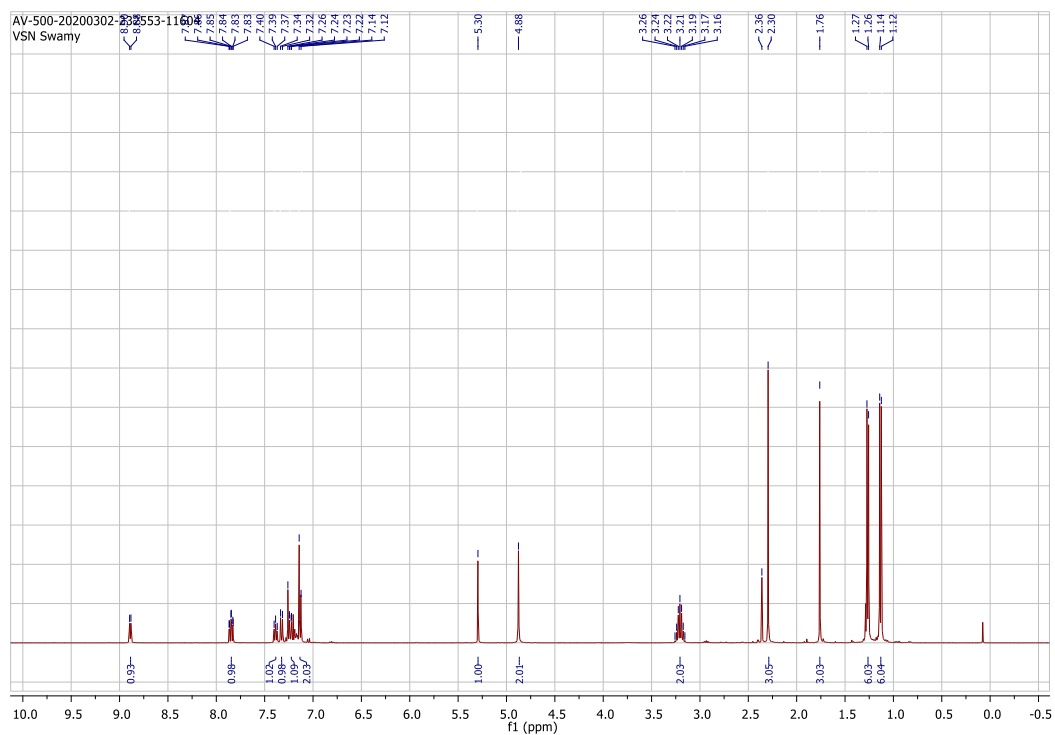
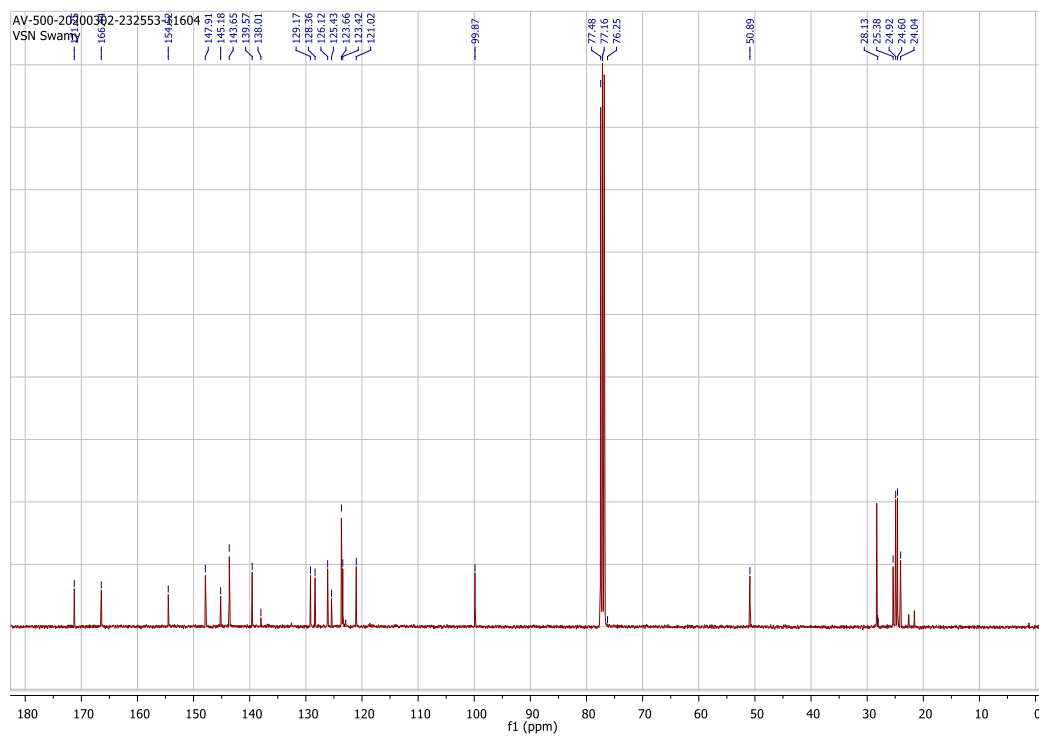
**Yield:** 0.42 g (94 %).

**Mp:**  $267\text{ }^{\circ}\text{C}$ .

**NMR:**  $^1\text{H}$  NMR (400 MHz,  $\text{CDCl}_3$ , 298 K):  $\delta$  8.89 (d,  $J = 4.6\text{ Hz}$ , 1H), 7.85 (t,  $J = 8.5\text{ Hz}$ , 1H), 7.39 (t,  $J = 6.4\text{ Hz}$ , 1H), 7.33 (d,  $J = 7.9\text{ Hz}$ , 1H), 7.24 –7.20 (m, 1H), 7.18 (d,  $J = 7.0\text{ Hz}$ , 1H), 7.13 (d,  $J = 7.1\text{ Hz}$ , 2H), 5.30 (s, 1H), 4.88 (s, 2H), 3.22 (dq,  $J = 13.6, 6.8\text{ Hz}$ , 2H), 2.30 (s, 3H), 1.76 (s, 3H), 1.27 (d,  $J = 6.8\text{ Hz}$ , 6H), 1.13 (d,  $J = 6.9\text{ Hz}$ , 6H) ppm.  $^{13}\text{C}$  NMR (101 MHz,  $\text{CDCl}_3$ , 298 K):  $\delta$  171.25, 166.44, 154.52, 147.91, 145.18, 143.65, 139.57, 138.01, 129.17, 128.36, 126.12, 125.43, 123.66, 123.42, 121.02, 99.87, 50.89, 28.29, 25.38, 24.92, 24.60, 24.04 ppm.

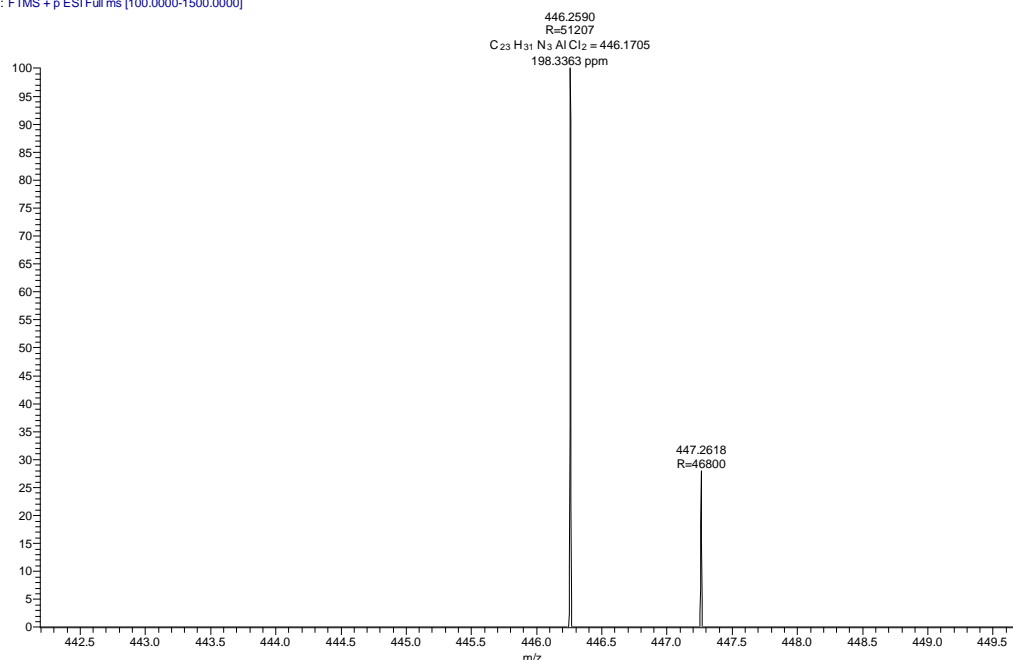
**HRMS:** Calcd.: 446.1705, found: 446.2590.

**d)  $^1\text{H}$  NMR of compound 3.5:**

e)  $^{13}\text{C}$  NMR of compound 3.5:

## f) HRMS data of compound 3.5:

L-ACI2\_200227150413 #386 RT: 2.14 AV: 1 NL: 4.05E6  
T: FTMS + p ESI Full ms [100.0000-1500.0000]



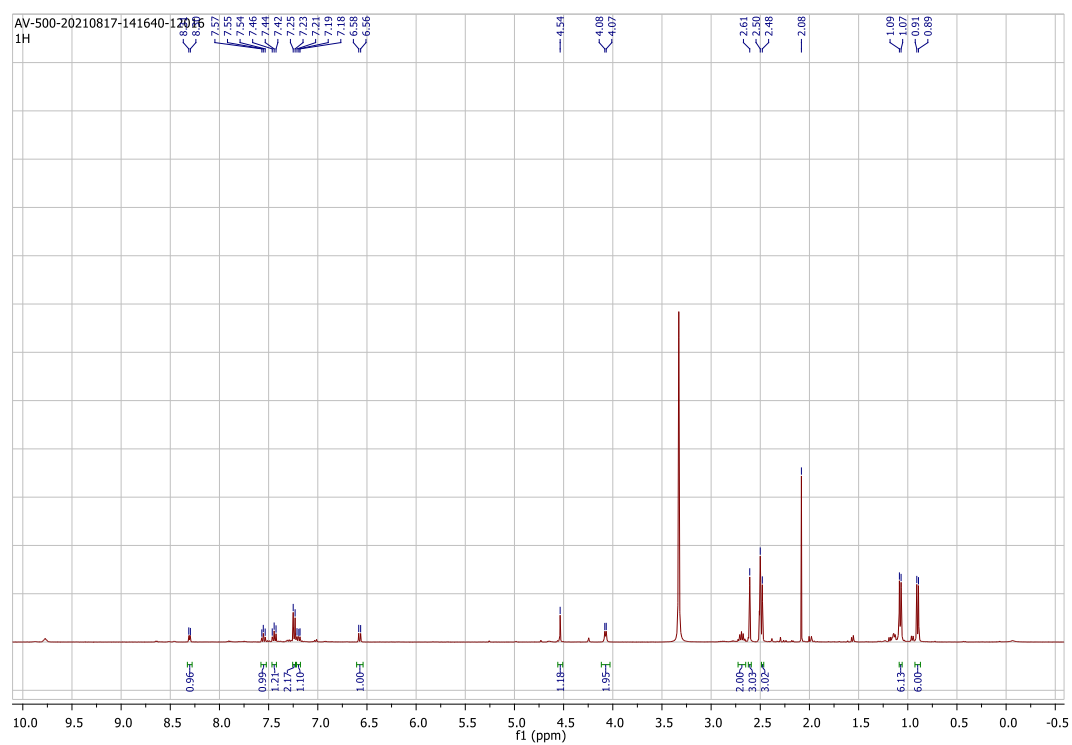
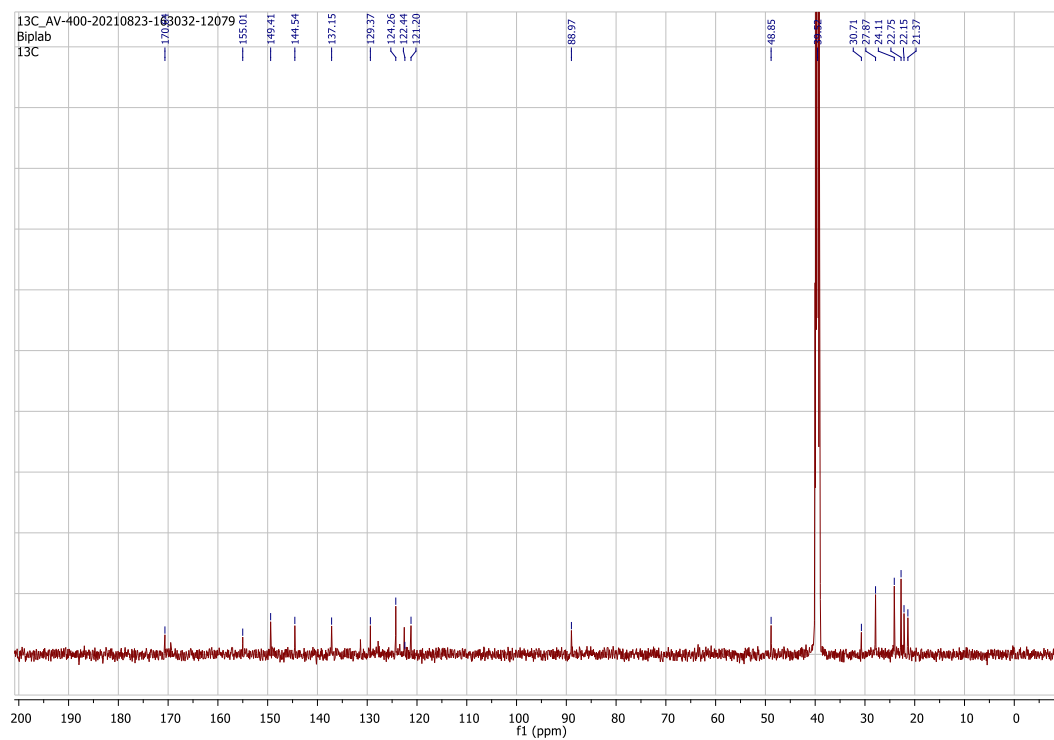
## 6.2.1.5. Synthesis and characterization of compound 3.6

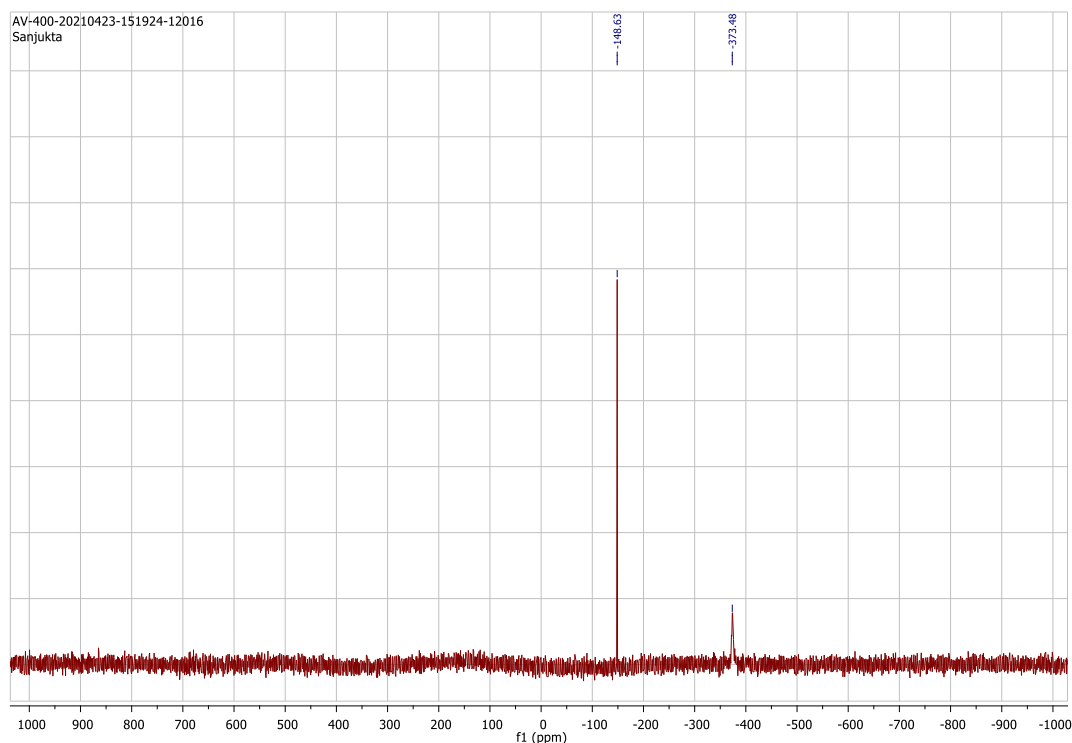
The THF solution of  $\text{SnCl}_2$  (0.200 g, 1.05 mmol, THF 10 mL) was slowly added to a stirred THF solution of **3.4** (0.500 g, 1.0 mmol) at  $-78\text{ }^\circ\text{C}$  over a period of 5 min. The solution was warmed to room temperature and stirred for 10-12 h. All volatiles were removed under reduced pressure and extracted with toluene (10 mL). The solvent was reduced to 5 mL and stored at  $-30\text{ }^\circ\text{C}$  in a freezer for 6-7 days to obtain the yellow crystals of **3.6** suitable for X-ray analysis.

**Yield:** 0.425 g (84 %).

**Mp:**  $168.2\text{ }^\circ\text{C}$ .

**NMR:**  $^1\text{H}$  NMR (400 MHz,  $\text{DMSO-d}_6$ , 298 K):  $\delta$  8.30 (1 H, d,  $J = 6.5$  Hz), 7.55 (1 H, t,  $J = 6.8$  Hz), 7.44 (1 H, t,  $J = 7.7$  Hz), 7.24 (2 H, d,  $J = 7.8$  Hz), 7.22 – 7.18 (1 H, m), 6.58 (1 H, d,  $J = 7.8$  Hz), 4.54 (1 H, s), 4.07 (2 H, d,  $J = 5.8$  Hz), 2.68 (2 H, dt,  $J = 13.7, 6.8$  Hz), 2.61 (3 H, s), 2.48 (3 H, s), 1.08 (6 H, d,  $J = 6.8$  Hz), 0.90 (6 H, d,  $J = 6.9$  Hz) ppm.  $^{13}\text{C}$  NMR (101 MHz,  $\text{CDCl}_3$ , 298 K):  $\delta$  170.64 (s), 155.01 (s), 149.41 (s), 144.54 (s), 137.15 (s), 129.37 (s), 124.26 (s), 122.44 (s), 121.20 (s), 88.97 (s), 48.85 (s), 30.71 (s), 27.87 (s), 24.11 (s), 22.75 (s), 22.15 (s), 21.37 (s) ppm.  $^{119}\text{Sn}$  NMR (149 MHz,  $\text{CDCl}_3$ , 298 K):  $\delta$  -148.63 and -373.48 ppm.

a)  $^1\text{H}$  NMR of compound 3.6:b)  $^{13}\text{C}$  NMR of compound 3.6:

c)  $^{119}\text{Sn}$  NMR of compound **3.6**:6.2.1.6. Synthesis and characterization of compound **3.7**

A toluene solution of  $\text{AlH}_3 \cdot \text{NMe}_2\text{Et}$  (4.80 mL, 2.40 mmol, 0.5 M) was cooled down to  $-78\text{ }^\circ\text{C}$  and was added drop by drop to a stirred solution of the toluene solution (10 mL) of the ligand **L1** (0.70 g, 2.00 mmol), *via* cannula at  $-78\text{ }^\circ\text{C}$ . The reaction mixture was allowed to warm to room temperature and left for stirring overnight. The solution was removed under reduced pressure and washed the residue with *n*-hexane ( $2 \times 10\text{ mL}$ ) and extracted with toluene (20 mL). The toluene was reduced to 10 mL and *n*-hexane (4 mL) was added to it drop by drop till the solution becomes turbid. The solution was kept at  $-30\text{ }^\circ\text{C}$  in a freezer for two days to obtain colourless crystals of **3.7**.

**Yield:** 1.26 g (84 %).

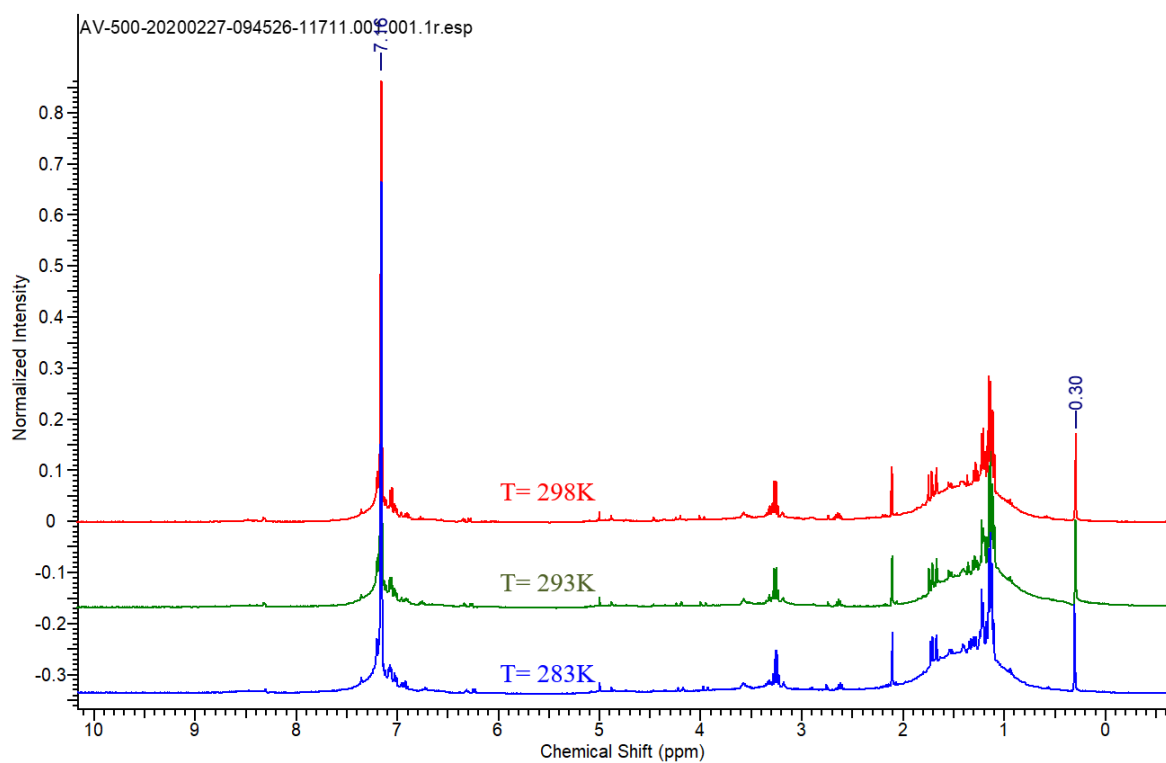
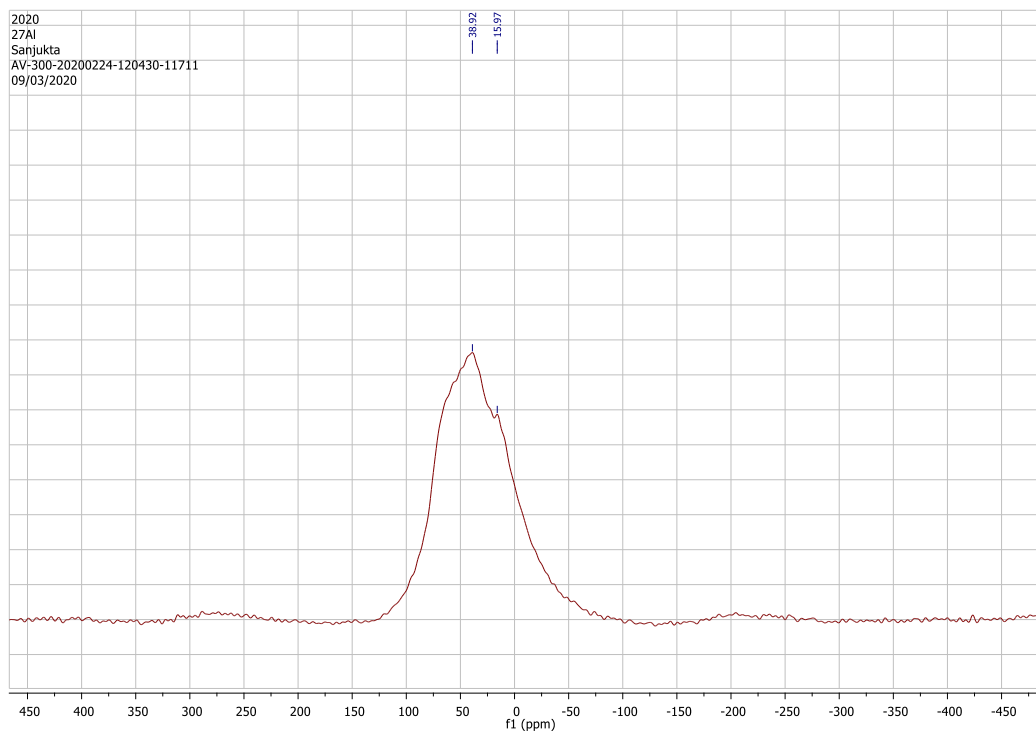
**Mp:**  $234\text{ }^\circ\text{C}$ .

**HRMS:** Calcd: 750.45, found: 375.2787 (Half fragment).

**IR (Nujol, mull,  $\text{cm}^{-1}$ ):** 1693 and 1743 (Al–H).

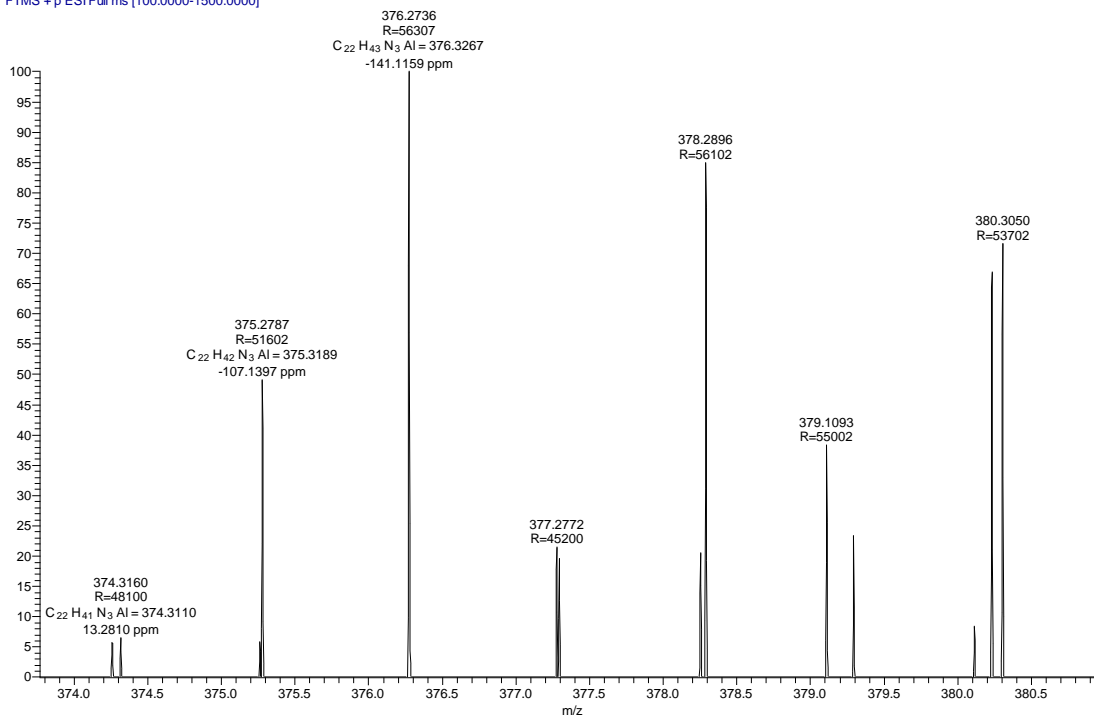
**NMR:** The clean resonance for the  $^1\text{H}$  NMR could not be observed due to the insolubility of **3.7** in common organic solvents and also could be due to the partial decomposition into an unidentified mixture within a few days at room temperature.  $^{27}\text{Al}$  NMR (400 MHz,  $\text{CDCl}_3$ ,  $25\text{ }^\circ\text{C}$ ):  $\delta$  38.92 ppm.



**a) Variable temperature NMR of 3.7 (in C<sub>6</sub>D<sub>6</sub>):****b) <sup>27</sup>Al NMR of compound 3.7:**

## c) HRMS data of compound 3.7:

L-AIH3\_200227151010 #242 RT: 1.30 AV: 1 NL: 5.31E6  
T: FTMS + p ESI Full ms [100.0000-1500.0000]



## 6.2.1.7. Synthesis and characterization of compound 3.8

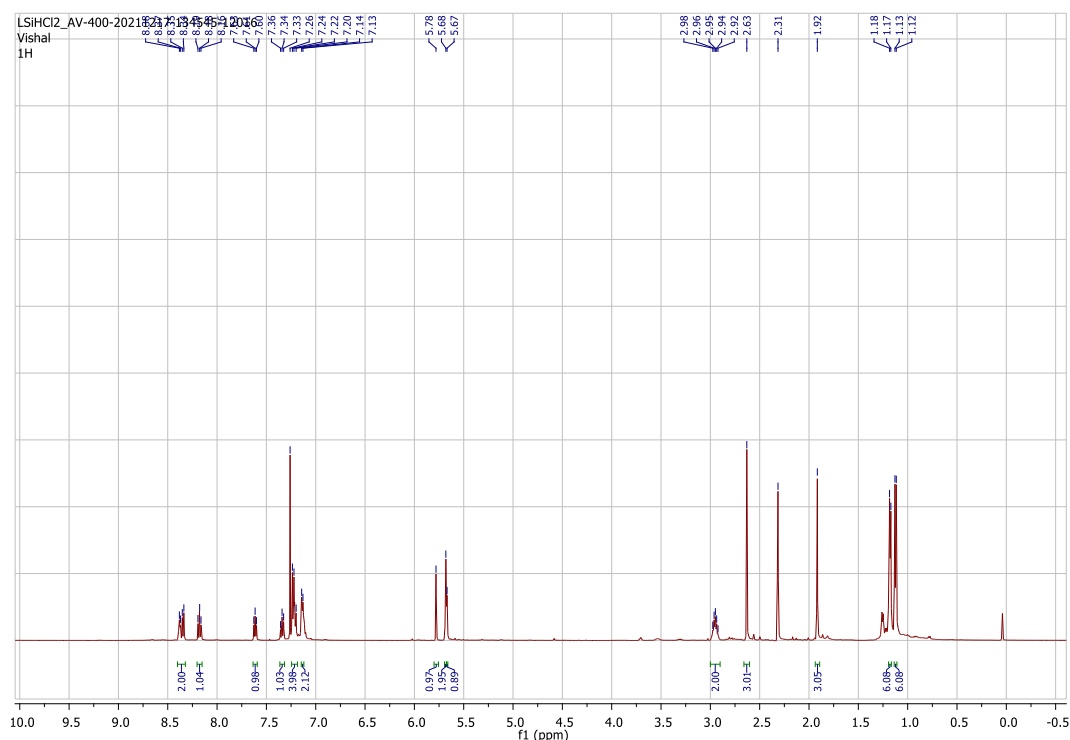
A solution of *n*BuLi in *n*-hexane (3.93 mL, 6.29 mmol, 1.6 M) was added drop wise to a stirred solution of **L1** (2,6-diisopropyl-N-((2Z,4E)-4-((pyridin-2-ylmethyl)imino)pent-2-en-2-yl)aniline) (2.0 g, 5.72mmol, in THF 20 mL) at  $-78\text{ }^{\circ}\text{C}$ , over a period of 10 min. The suspension was allowed to warm up to room temperature and stirred for another 8 h. Next, HSiCl<sub>3</sub> (0.6 mL, 6.0 mmol) was added drop by drop to the above suspension at  $-30\text{ }^{\circ}\text{C}$  via cannula. The reaction mixture was further warmed to room temperature and stirred for additional 15 h. Subsequently, all volatiles were removed in vacuo and the residue was extracted into toluene (30 mL). The resultant toluene solvent was concentrated to 10–12 mL and stored at  $-30\text{ }^{\circ}\text{C}$  in a freezer, which afforded colorless crystals of **3.8** within 2-3 days.

**Yield:** 2.19 g (84 %).

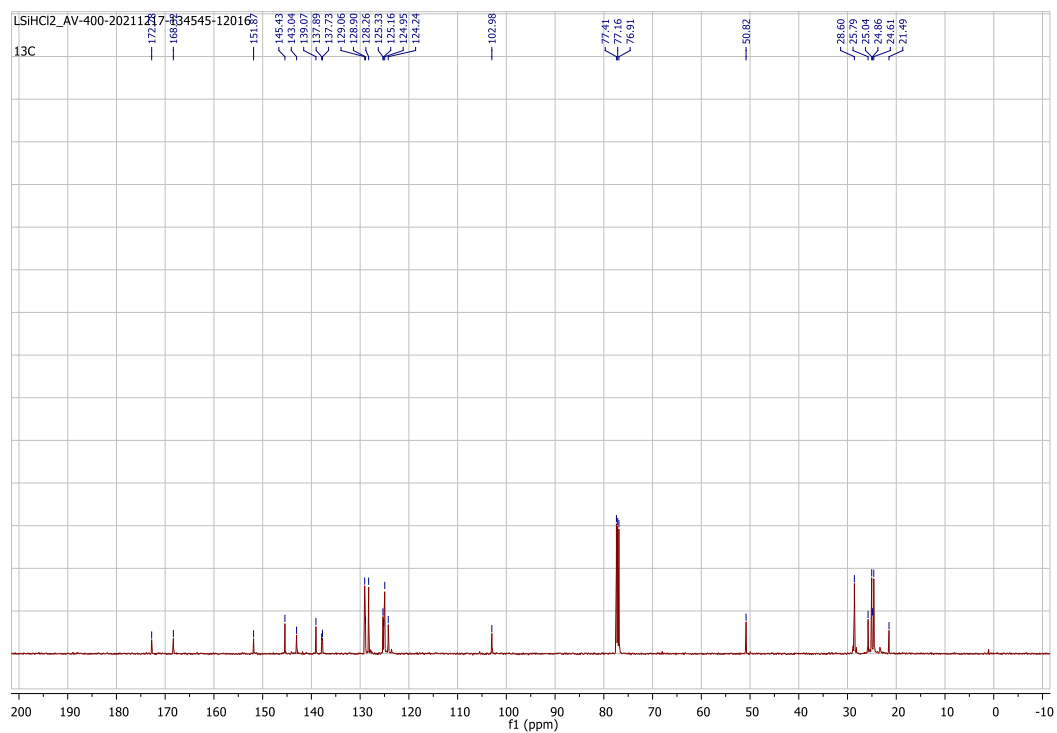
**Mp:** 191.2  $^{\circ}\text{C}$ .

**NMR:**  $^1\text{H}$  NMR (500MHz,  $\text{CDCl}_3$ , 298 K):  $\delta$  8.36 (2 H, dd,  $J = 16.2, 6.6$  Hz), 8.18 (1 H, t,  $J = 7.7$  Hz), 7.61 (1 H, t,  $J = 6.6$  Hz), 7.34 (1 H, t,  $J = 7.7$  Hz), 7.24 – 7.18 (4 H, m), 7.14 (2 H, d,  $J = 6.5$  Hz), 5.78 (1 H, s), 5.68 (2 H, s), 5.67 (1 H, s), 2.95 (2 H, dt,  $J = 13.3, 6.6$  Hz), 2.63 (3 H, s), 1.92 (3 H, s), 1.18 (6 H, d,  $J = 6.6$  Hz), 1.12 (6 H, d,  $J = 6.8$ ) ppm.  $^{13}\text{C}$  NMR (126 MHz,  $\text{CDCl}_3$ , 298 K):  $\delta$  172.78 (s), 168.32 (s), 151.87 (s), 145.43 (s), 143.04 (s), 139.07 (s), 137.89 (s), 137.73 (s), 124.95 (s), 124.24 (s), 102.98 (s), 50.82 (s), 28.60 (s), 25.79 (s), 25.04 (s), 24.86 (s), 24.61 (s) ppm.  $^{29}\text{Si}$  NMR (99 MHz,  $\text{CDCl}_3$ ):  $\delta$  -102.62 (s) ppm.

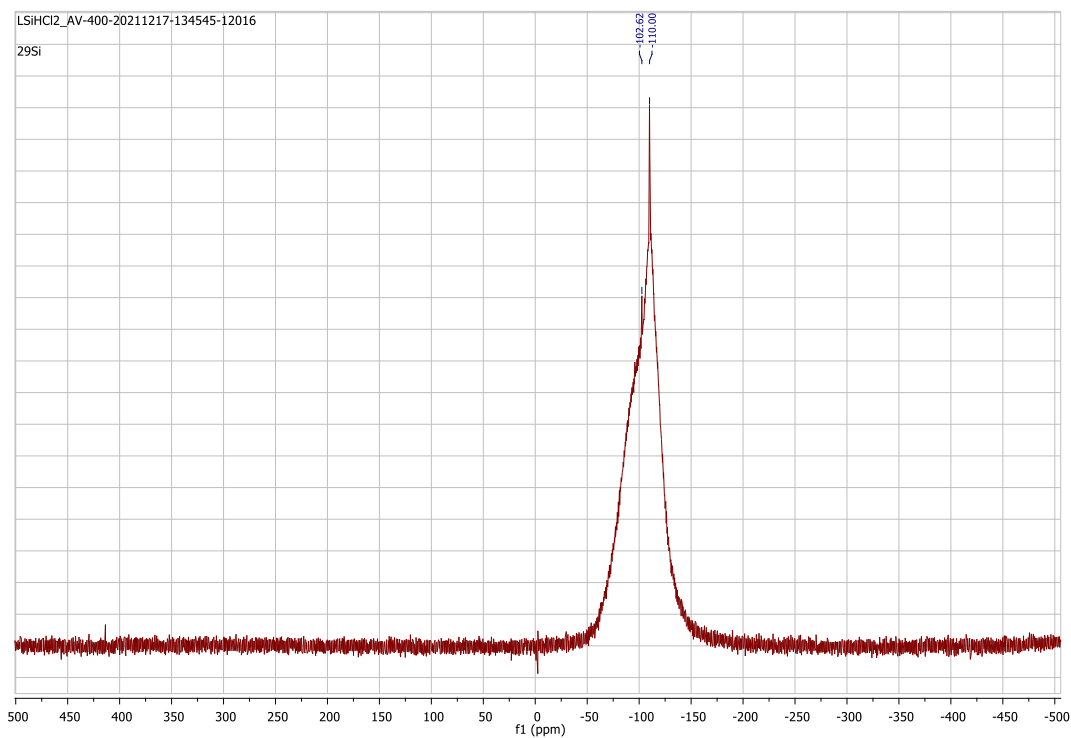
**a)  $^1\text{H}$  NMR of compound 3.8:**



**b)  $^{13}\text{C}$  NMR of compound 3.8:**



c)  $^{29}\text{Si}$  NMR of compound 3.8:



6.2.2. Crystallographic data for the structural analysis of compounds 3.1-3.8

**6.2.2.1. Crystal data of compound 3.1:**  $C_{23}H_{30}N_3Ge_1Cl_1$ ,  $M = 456.54$ ,  $0.36 \times 0.28 \times 0.16 \text{ mm}^3$ , monoclinic, space group ' $P2_1/n$ ',  $a = 10.7669(4)\text{\AA}$ ,  $b = 11.2877(4)\text{\AA}$ ,  $c = 18.6038(7)\text{\AA}$ ,  $\alpha = 90^\circ$ ,  $\beta = 96.881(2)^\circ$ ,  $\gamma = 90^\circ$ , Volume =  $2244.7(14)\text{\AA}^3$ ,  $Z = 4$ ,  $T = 105(2)$ ,  $D_{calc} (\text{g cm}^{-3}) = 1.351$ ,  $F(000) = 952$ ,  $\mu (\text{mm}^{-1}) = 0.098$ , 33365 reflections collected, 3954 unique reflections ( $R_{int} = 0.0383$ ), 3576 observed ( $I > 2\sigma(I)$ ) reflections, multi-scan absorption correction,  $T_{min} = 0.578$ ,  $T_{max} = 0.787$ , 260 refined parameters,  $S = 1.038$ ,  $R1 = 0.0249$ ,  $wR2 = 0.0674$  (all data  $R = 0.0292$ ,  $wR2 = 0.0595$ ), maximum and minimum residual electron densities;  $\Delta\rho_{max} = 1.732$ ,  $\Delta\rho_{min} = -0.964 (\text{e}\text{\AA}^{-3})$ .

**6.2.2.2. Crystal data of compound 3.2:**  $C_{11}H_{11}N_2Ge_1Cl_1$ ,  $M = 279.28$ ,  $0.36 \times 0.28 \times 0.16 \text{ mm}^3$ , triclinic, space group ' $P-1$ ',  $a = 7.9051(3)\text{\AA}$ ,  $b = 8.8862(4)\text{\AA}$ ,  $c = 9.0373(4)\text{\AA}$ ,  $\alpha = 67.589(2)^\circ$ ,  $\beta = 74.175(2)^\circ$ ,  $\gamma = 77.444(2)^\circ$ , Volume =  $560.04(4)\text{\AA}^3$ ,  $Z = 2$ ,  $T = 100(2)$ ,  $D_{calc} (\text{g cm}^{-3}) = 1.656$ ,  $F(000) = 280$ ,  $\mu (\text{mm}^{-1}) = 2.939$ , 8276 reflections collected, 1979 unique reflections ( $R_{int} = 0.0292$ ), 1928 observed ( $I > 2\sigma(I)$ ) reflections, multi-scan absorption correction,  $T_{min} = 0.334$ ,  $T_{max} = 0.589$ , 139 refined parameters,  $S = 1.082$ ,  $R1 = 0.0178$ ,  $wR2 = 0.0451$  (all data  $R = 0.0183$ ,  $wR2 = 0.0454$ ), maximum and minimum residual electron densities;  $\Delta\rho_{max} = 0.288$ ,  $\Delta\rho_{min} = -0.263 (\text{e}\text{\AA}^{-3})$ .

**6.2.2.3. Crystal data of compound 3.3:**  $C_{12}H_{19}N_1Ge_1Cl_2$ ,  $M = 320.77$ ,  $0.38 \times 0.28 \times 0.16 \text{ mm}^3$ , triclinic, space group ' $P-1$ ',  $a = 8.8999(6)\text{\AA}$ ,  $b = 9.3908(7)\text{\AA}$ ,  $c = 9.8279(7)\text{\AA}$ ,  $\alpha = 91.216(2)^\circ$ ,  $\beta = 109.977(2)^\circ$ ,  $\gamma = 110.198(2)^\circ$ , Volume =  $715.42(9)\text{\AA}^3$ ,  $Z = 2$ ,  $T = 296(2)$ ,  $D_{calc} (\text{g cm}^{-3}) = 1.498$ ,  $F(000) = 328$ ,  $\mu (\text{mm}^{-1}) = 2.490$ , 26002 reflections collected, 2523 unique reflections ( $R_{int} = 0.00445$ ), 2355 observed ( $I > 2\sigma(I)$ ) reflections, multi-scan absorption correction,  $T_{min} = 0.451$ ,  $T_{max} = 0.691$ , 222 refined parameters,  $S = 1.061$ ,  $R1 = 0.0169$ ,  $wR2 = 0.0383$  (all data  $R = 0.0206$ ,  $wR2 = 0.0399$ ), maximum and minimum residual electron densities;  $\Delta\rho_{max} = 0.338$ ,  $\Delta\rho_{min} = -0.220 (\text{e}\text{\AA}^{-3})$ .

**6.2.2.4. Crystal data of compound 3.4:**  $C_{23}H_{30}Cl_1N_3Sn_1$ ,  $M = 503.12$ , Yellow, Block,  $0.32 \times 0.3 \times 0.29 \text{ mm}^3$ , triclinic, space group ' $P-1$ ',  $a = 13.843(5)\text{\AA}$ ,  $b = 15.770(6)\text{\AA}$ ,  $c = 21.088(7)\text{\AA}$ ,  $\alpha = 89.939(14)^\circ$ ,  $\beta = 89.967(15)^\circ$ ,  $\gamma = 89.962(13)^\circ$ , Volume =  $4604(3)\text{\AA}^3$ ,  $Z = 2$ ,  $T = 100(2)$ ,  $D_{calc} (\text{g cm}^{-3}) = 1.446$ ,  $F(000) = 2040$ ,  $\mu (\text{mm}^{-1}) = 1.238$ , 287107 reflections collected, 28100 unique reflections ( $R_{int} = 0.0534$ ), 22835 observed ( $I > 2\sigma(I)$ ) reflections, multi-scan absorption correction,  $T_{min} = 0.6373$ ,  $T_{max} = 0.7461$ , 699 refined parameters,  $S = 1.056$ ,  $R1 = 0.0874$ ,  $wR2 = 0.2135$  (all data  $R = 0.1055$ ,  $wR2 = 0.2308$ ), maximum and minimum residual electron densities;  $\Delta\rho_{max} = 5.74$ ,  $\Delta\rho_{min} = -4.58 (\text{e}\text{\AA}^{-3})$ .

**6.2.2.5. Crystal data of compound 3.5:**  $C_{23}H_{30}N_3AlCl_2 \cdot 2(C_6H_6)$ ,  $M = 602.60$ ,  $0.32 \times 0.28 \times 0.12$  mm<sup>3</sup>, monoclinic, space group 'P2<sub>1</sub>/c',  $a = 17.2631(13)\text{\AA}$ ,  $b = 10.6231(7)\text{\AA}$ ,  $c = 18.1589(13)\text{\AA}$ ,  $\alpha = 90^\circ$ ,  $\beta = 103.330(3)^\circ$ ,  $\gamma = 90^\circ$ , Volume =  $3240.4(4)\text{\AA}^3$ ,  $Z = 4$ ,  $T = 100(2)$ ,  $D_{calc}$  (g cm<sup>-3</sup>) = 1.235,  $F(000) = 1280$ ,  $\mu$  (mm<sup>-1</sup>) = 0.256, 140823 reflections collected, 5699 unique reflections ( $R_{int} = 0.0788$ ), 4941 observed ( $I > 2\sigma(I)$ ) reflections, multi-scan absorption correction,  $T_{min} = 0.921$ ,  $T_{max} = 0.970$ , 377 refined parameters,  $S = 1.052$ ,  $R1 = 0.0323$ ,  $wR2 = 0.0793$  (all data  $R = 0.0406$ ,  $wR2 = 0.0862$ ), maximum and minimum residual electron densities;  $\Delta\rho_{max} = 0.856$ ,  $\Delta\rho_{min} = -0.224$  (e $\text{\AA}^{-3}$ ).

**6.2.2.6. Crystal data of compound 3.6:**  $C_{23}H_{30}Cl_3N_3Sn_2$ , (C<sub>7</sub>H<sub>8</sub>),  $M = 784.42$ , Yellow, Plate,  $0.32 \times 0.31 \times 0.28$  mm<sup>3</sup>, monoclinic, space group 'P2<sub>1</sub>/n',  $a = 24.474(2)\text{\AA}$ ,  $b = 9.8854(11)\text{\AA}$ ,  $c = 27.378(3)\text{\AA}$ ,  $\alpha = 90^\circ$ ,  $\beta = 95.371(4)^\circ$ ,  $\gamma = 90^\circ$ , Volume =  $6594.5(12)\text{\AA}^3$ ,  $Z = 4$ ,  $T = 100(2)$ ,  $D_{calc}$  (g cm<sup>-3</sup>) = 1.580,  $F(000) = 3120$ ,  $\mu$  (mm<sup>-1</sup>) = 1.781, 417386 reflections collected, 20176 unique reflections ( $R_{int} = 0.0263$ ), 17974 observed ( $I > 2\sigma(I)$ ) reflections, multi-scan absorption correction,  $T_{min} = 0.571$ ,  $T_{max} = 0.607$ , 699 refined parameters,  $S = 1.145$ ,  $R1 = 0.0263$ ,  $wR2 = 0.0556$  (all data  $R = 0.0321$ ,  $wR2 = 0.0577$ ), maximum and minimum residual electron densities;  $\Delta\rho_{max} = 0.74$ ,  $\Delta\rho_{min} = -0.92$  (e $\text{\AA}^{-3}$ ).

**6.2.2.7. Crystal data of compound 3.7:**  $C_{46}H_{58}N_6Al_2$ ,  $M = 748.94$ ,  $0.36 \times 0.26 \times 0.16$  mm<sup>3</sup>, triclinic, space group 'P-1',  $a = 8.8257(6)\text{\AA}$ ,  $b = 15.7134(10)\text{\AA}$ ,  $c = 17.6385(11)\text{\AA}$ ,  $\alpha = 82.476(2)^\circ$ ,  $\beta = 76.292(2)^\circ$ ,  $\gamma = 75.862(2)^\circ$ , Volume =  $2297.5(3)\text{\AA}^3$ ,  $Z = 2$ ,  $T = 100(2)$ ,  $D_{calc}$  (g cm<sup>-3</sup>) = 1.167,  $F(000) = 868$ ,  $\mu$  (mm<sup>-1</sup>) = 0.105, 95322 reflections collected, 8597 unique reflections ( $R_{int} = 0.0649$ ), 7467 observed ( $I > 2\sigma(I)$ ) reflections, multi-scan absorption correction,  $T_{min} = 0.978$ ,  $T_{max} = 0.991$ , 626 refined parameters,  $S = 1.073$ ,  $R1 = 0.0485$ ,  $wR2 = 0.1112$  (all data  $R = 0.0594$ ,  $wR2 = 0.1165$ ), maximum and minimum residual electron densities;  $\Delta\rho_{max} = 0.681$ ,  $\Delta\rho_{min} = -0.241$  (e $\text{\AA}^{-3}$ ).

**6.2.2.8. Crystal data of compound 3.8:**  $C_{23}H_{31}Cl_2N_3Si$ ,  $M = 448.50$ , Yellow, Block,  $0.38 \times 0.28 \times 0.18$  mm<sup>3</sup>, triclinic, space group 'P-1',  $a = 13.726(5)\text{\AA}$ ,  $b = 14.735(15)\text{\AA}$ ,  $c = 15.236(9)\text{\AA}$ ,  $\alpha = 91.48(4)^\circ$ ,  $\beta = 110.39(4)^\circ$ ,  $\gamma = 95.25(5)^\circ$ , Volume =  $2871(4)\text{\AA}^3$ ,  $Z = 4$ ,  $T = 100(2)$ ,  $D_{calc}$  (g cm<sup>-3</sup>) = 1.038,  $F(000) = 952$ ,  $\mu$  (mm<sup>-1</sup>) = 0.280, 51057 reflections collected, 13545 unique reflections ( $R_{int} = 0.0755$ ), 6865 observed ( $I > 2\sigma(I)$ ) reflections, multi-scan absorption correction,  $T_{min} = 0.901$ ,  $T_{max} = 0.951$ , 699 refined parameters,  $S = 1.059$ ,  $R1 = 0.0855$ ,  $wR2 = 0.1983$  (all data  $R = 0.1496$ ,  $wR2 = 0.2328$ ), maximum and minimum residual electron densities;  $\Delta\rho_{max} = 1.27$ ,  $\Delta\rho_{min} = -1.50$  (e $\text{\AA}^{-3}$ ).

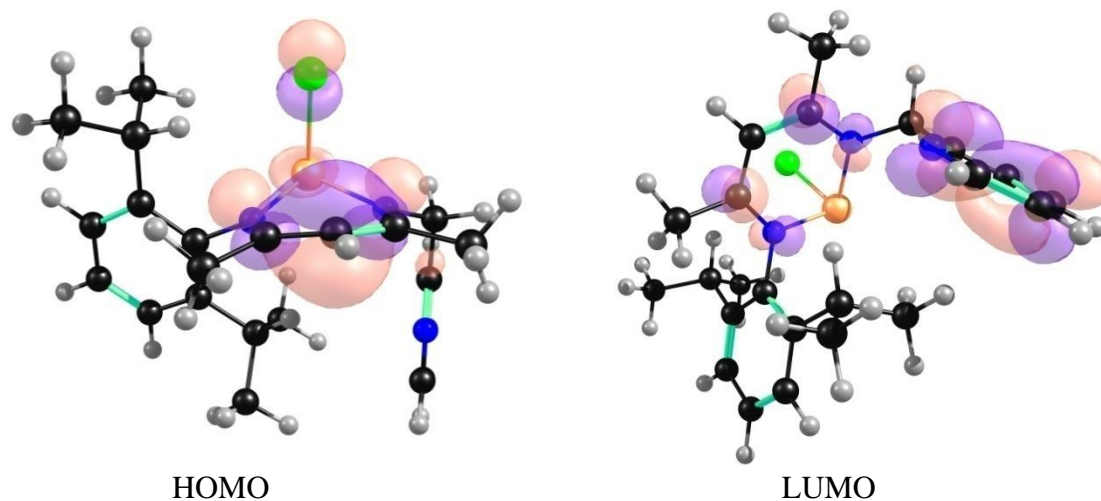
### 6.2.3. Details of theoretical calculations

All the geometry optimization in this study have been performed with density functional theory (DFT), with the aid of the Turbomole 7.1 suite of programs,<sup>5</sup> using the PBE functional.<sup>6</sup> The TZVP<sup>7</sup> basis set has been employed. The resolution of identity (RI),<sup>8</sup> along with the multipole accelerated resolution of identity (marij)<sup>9</sup> approximations have been employed for an accurate and efficient treatment of the electronic Coulomb term in the DFT calculations. Dispersion correction (disp3) and solvent correction were incorporated with optimization calculations using the COSMO model,<sup>10</sup> with toluene ( $\epsilon = 2.38$ ) as the solvent. Harmonic frequency calculations were performed for all stationary points to confirm them as a local minimum. The single point energy calculation of all the PBE/TZVP optimized compounds have been performed with M06-2X/6-311+G(d) level of theory using Gaussian09<sup>11</sup> software packages.

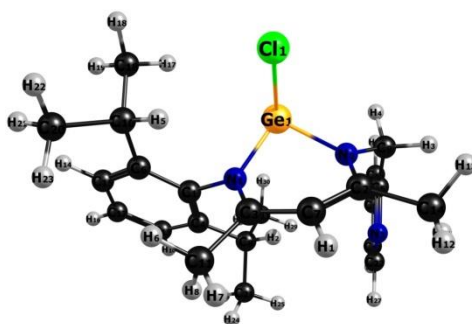
The nature of germanium-ligand and aluminium-ligand interaction in compound **3.2** and compound **3.7** was investigated with the natural bond orbitals (NBO) analysis procedures as implemented in the Gaussian 09 program. The analyses were performed at the PBE/TZVP optimized geometry using the M06-2X density functional together with the all-electron 6-311+g(d) basis set. In order to gain insight into the interaction of the carbon and nitrogen donor ligand with the central germanium and aluminium atom, the intermolecular charge transfer in the complex has been analysed with the natural bond orbital (NBO) analysis. The energetic estimate of donor (i) – acceptor (j) orbital interactions can be obtained by the second order perturbation theory analysis of the Fock matrix in the NBO basis. The donor–acceptor interaction energy  $E(2)$  is given by,

$$E(2) = \Delta E(i,j) = \frac{q(i,j)F(i,j)^2}{\{\epsilon(i) - \epsilon(j)\}}$$

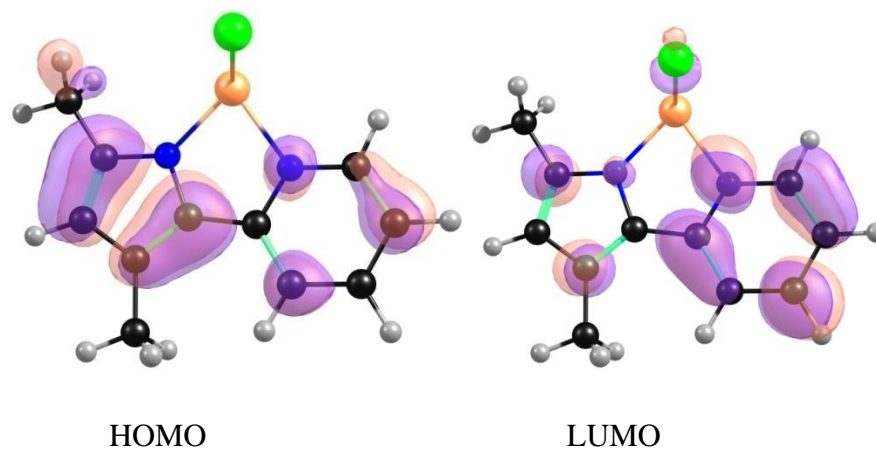
where  $q(i)$  is the donor orbital occupancy,  $\epsilon(i)$  and  $\epsilon(j)$  are the diagonal elements (orbital energies), and  $F(i,j)$  is the off-diagonal NBO Fock matrix element. In the present investigation, the important interactions between the central germanium and aluminium with the ligands have been analyzed. With the NBO analysis we have also performed NLMO and WBI bond order analysis.



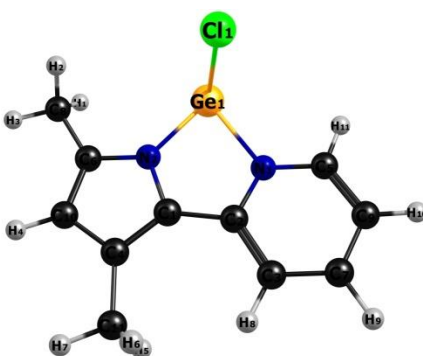
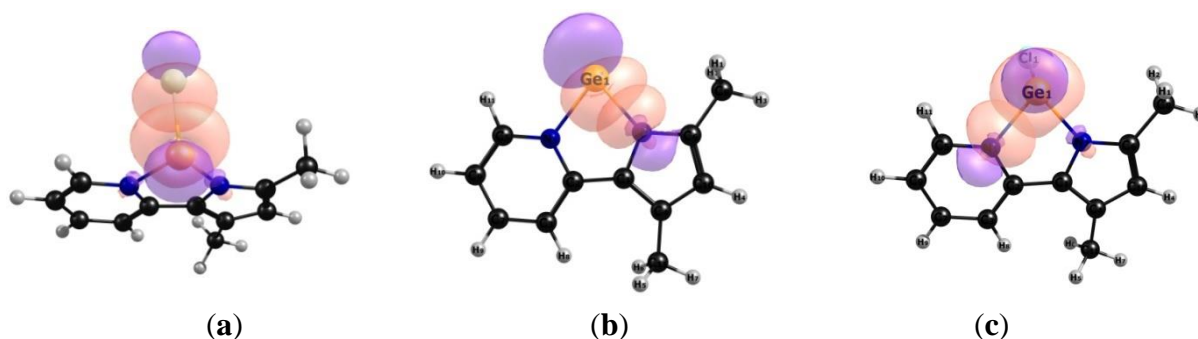
**Fig. 6.1:** HOMO and LUMO of Compound 3.1. HOMO-LUMO energy gap 6.48 eV



**Fig. 6.2:** PBE/TZVP optimized geometry of compound 3.1. Bond lengths (Å) and bond angles (°) Ge1-Cl1 2.31; Ge1-N1 1.99; Ge1-N2 1.98; N1-Ge1-N2 88.0; N1-Ge1-Cl1 94.8; N2-Ge1-Cl1 95.0.

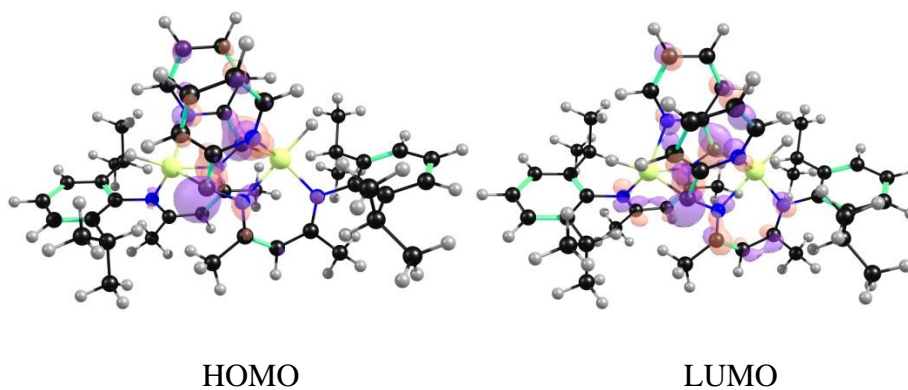




**Fig. 6.3:** HOMO and LUMO of Compound **3.2**. HOMO-LUMO energy gap 5.48 eV**Fig. 6.4:** PBE/TZVP optimized geometry of compound **3.2**. Bond lengths (Å) and bond angles (°) Ge1-Cl1 2.29; Ge1-N1 2.12; Ge1-N2 1.99; N2-C5 1.39; N1-C4 1.37; C4-C5 1.42; N1-Ge1-Cl1 92.9; N2-Ge1-Cl1 96.2; N1-Ge1-N2 78.1.**Table 6.1.** Results of the NBO analysis for the compound **3.2** computed at the M06-2X/6-311+G(d) Level of Theory: natural occupation and natural charges at germanium (Q in e), stabilization energies ( $\Delta E(2)$  in kcal/mol) associated with the most important donor-acceptor interactions, WBI and NLMO bond orders

Compound	Ge natural occupation				$Q_{\text{NBO}}$	charge transfer			bond order			
	4s	4p	4d	5s		donor	occu.	acceptor	occu	E(2)	WBI	NLMO
<b>3.2</b>	1.70	1.20	0.01	0.01	1.08	N3	1.77	Ge1	0.22	61.8	0.35	0.38
						N4	1.73	Ge1	0.27	84.0	0.45	0.48
						Cl2	1.63	Ge1	0.44	178.6	0.71	0.59

**Fig. 6.5:** Selective natural bonding orbital interaction in compound **3.2**. (a) LP (4)Cl $\rightarrow$ LP\*(2) Ge, (b) LP (1) N $\rightarrow$ LP\*(4) Ge, (c) LP (1) N $\rightarrow$ LP\*(3) Ge.



**Fig. 6.6:** HOMO and LUMO of Compound **3.7** with a HOMO-LUMO energy gap 2.72 eV.



**Fig. 6.7:** PBE/TZVP optimized geometry of compound **3.7**. Bond lengths (Å) and bond angles (°)  
 Al1-N2 1.99; Al1-C8 2.22; Al1-H53 1.62; Al1-N1 1.97; Al1-N4 1.93; Al2-N3 2.17; Al2-C7 2.00;  
 Al2-H54 1.61; Al2-N6 2.06; Al2-N5 2.00; N3-C8 1.45; N2-C7 1.32

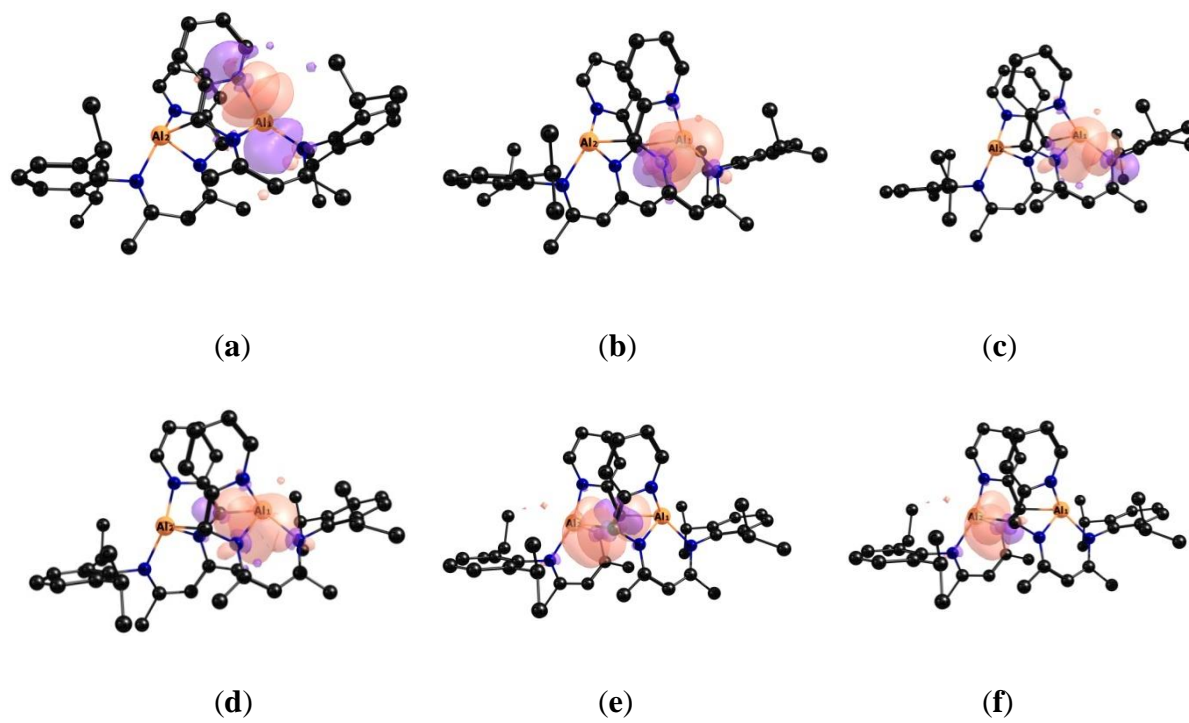
Compound	Al natural occupation				Q <sub>NBO</sub>	charge transfer				bond order			
	3s	3p	3d	4s		donor	occu.	acceptor	occu	E(2)	WBI	NLMO	
<b>3.7</b>	Al15	0.54	0.80	0.02	0.01	1.64	N1	1.82	Al15	0.21	60.2	0.26	0.36
							N17	1.82	Al15	0.31	89.4	0.24	0.35
							N19	1.80	Al15	0.31	58.5	0.30	0.39
							C22	1.69	Al15	0.31	25.7	0.37	0.44
Al16		0.58	0.80	0.02	0.01	1.59	N18	1.80	Al16	0.39	33.0	0.21	0.29
							N20	1.82	Al16	0.17	50.8	0.24	0.34
							N104	1.84	Al16	0.25	34.5	0.21	0.30
							C21	1.64	Al16	0.39	134.1	0.53	0.60

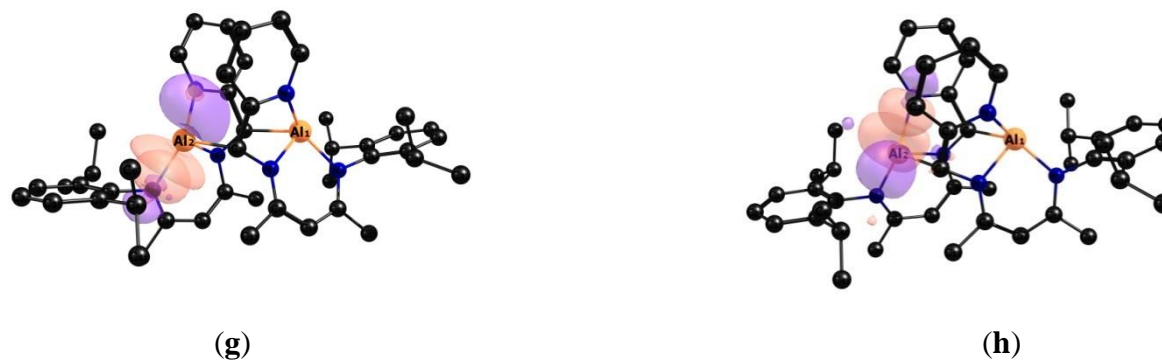
**Table 6.2.** Results of the NBO analysis for the compound **3.7** computed at the M06-2X/6-311+G(d) Level of Theory: natural occupation and natural charges at aluminium (Q in e), stabilization energies ( $\Delta E(2)$  in kcal/mol) associated with the most important donor-acceptor interactions, WBI and NLMO bond orders.

**(I) Further Analysis of Compound 3.2.** The difference in donation between the pyrrole and pyridine nitrogen donors can be ascribed to the nature of the donor atom and to the Ge–N bond distance. In compound **3.2**, the two Ge–N bond distances for pyrrole and the pyridine ligands are 1.98 Å and 2.07 Å and the N1–Ge1–N2 bond angle is 78.7°, which is consistent with the X-ray crystal data. In the above explained bonding interaction, the lone pair on the nitrogen and chloride donors, with an occupancy of more than 1.60e, have interactions with the Ge with occupancies less than 0.5e, which indicates strong donor-acceptor interactions between ligands and the metal centre. We have also computed the NLMO and WBI bond orders (Table S.1) analysis, the values (~0.4 for Ge-N and ~0.7 for Ge-Cl) of which suggest that the Ge-Cl bond has some covalent character but in Ge-N bonds there are ionic or dative type interactions present. Furthermore, DFT calculations reveal that in **3.2**, both the HOMO and LUMO are localized over the five and six membered rings and both of them are pi in nature. The HOMO–LUMO energy gap for **3.2** has been determined to be 5.48 eV.

**(II) Analysis of Compound 3.7.** The NBO analysis of **3.7** revealed that the contribution of the 3d orbital of the Al centre towards the bonding is very small: the natural occupation in the 3d shell of the two Al centres is equal to 0.02; thus the total 3d population is distinctly smaller than that required for a formal  $sp^3d$  hybridization (Table S.2). A stabilizing electronic effect responsible for the formation of chemical bonds is the transfer of charge from the ligands to the metal ion. The NBO charges of the two Al atoms are 1.59e and 1.64e. The dominant ionic character of the Al–ligand bonds is also evident in the localized Lewis-like description of the bonding pattern. In the Lewis structure of **3.7**, no localized electron pair for bonding between the Al and the coordinated ligands was found. From the NBO data, the “non-Lewis” occupancy suggests that large charge-transfer interactions take place where the ligand lone-pair orbital effectively donates its electron density to an unoccupied orbital on the metal. From the NBO analysis, the second order perturbation energy for the two Al centres with the surrounding ligands span between 25.7

kcal/mol and 134.2 kcal/mol. The interactions energies of one of the Al centres with one carbon donor and three nitrogen donor ligands are 25.7 kcal/mol, 60.2 kcal/mol, 58.5 kcal/mol and 89.4 kcal/mol respectively (Table S.2). On the other hand, the interaction energies of the other Al centre with the same donor ligands are 134.2 kcal/mol, 34.5 kcal/mol, 50.8 kcal/mol and 33.1 kcal/mol respectively (Table S.2). It has been observed that for the penta-coordinated neutral Al complex, the donation of one of the nitrogen atoms is generally higher than the donation from the other nitrogen atoms. The difference in donation can be ascribed to the nature of the donor atom and to the Al–N bond distance. In the compound **3.7**, the two Al–N bond distances in the six membered ring are larger (1.99 Å and 2.17 Å) than for the other two Al–N bonds (1.93 and 2.00 Å). This is consistent with the crystal structure. In all the cases, the lone pair on the nitrogen and carbon donors, with an occupancy of more than 1.70e, has interactions with the Al with occupancies less than 0.3e, which indicates strong donor-acceptor interactions between ligands and the metal centre. We have also computed the NLMO and WBI bond orders (Table S.2) that further confirm these results. It has been found that the NLMO and WBI bond orders are low ( $>0.4$ ), which indicate that the covalent bonding of the Al with the coordinated ligand is weak. Only in the case of Al–H does the bond order ( $\sim 0.7$ ) indicate covalency.





**Fig. 6.8:** Selective natural bonding orbital interaction in compound **3.7**. (a) LP(1)N→LP\*(2)Al, (b) LP(1)N→LP\*(1)Al, (c) LP(1)N→LP\*(1)Al, (d) LP(1)C→LP\*(1)Al, (e) LP(1)C→LP\*(1)Al, (f) LP(1)N→LP\*(1)Al, (g) LP(1)N→LP\*(3)Al, (h) LP(1)N→LP\*(2)Al.

### PBE/TZVP optimized geometries for all the compounds

#### Compound 3.1

Ge	5.94009400	6.76945900	12.15996200
Cl	7.99082600	7.53295900	13.02305500
N	5.53006500	8.45448700	11.25992800
N	4.96126800	7.35540400	13.75261200
N	2.18455300	7.05074900	13.77791600
C	5.37809300	8.38066600	9.81854500
C	4.84130400	8.62752800	14.12127000
C	5.35008200	9.61576600	11.89842900
C	4.09910600	8.15254100	9.29381800
C	2.89592000	6.05099700	14.31058500
C	6.51193200	8.48191600	8.99700900
C	5.17502300	9.69195800	13.27590700

---

H	5.29264500	10.54384100	13.68058000
C	2.87030500	7.97961400	10.18313900
H	3.16431100	8.06280400	11.13544200
C	4.37620000	6.26964000	14.55198500
H	4.51511400	6.47123800	15.51093700
H	4.85880500	5.42938400	14.34918700
C	7.90872900	8.67008200	9.56440100
H	7.81932700	8.85858700	10.54256100
C	5.28221800	10.89353400	11.10552100
H	6.05393000	10.94568300	10.50377500
H	5.29377900	11.65906500	11.71724100
H	4.45559700	10.90843300	10.57950100
C	0.21964300	5.68809800	13.93989600
H	-0.71403100	5.59418400	13.79509300
C	3.96851100	8.05941800	7.90636700
H	3.10994000	7.91380600	7.52644300
C	4.28267800	8.98500900	15.47418200
H	3.32500100	8.77957300	15.49616200
H	4.41660700	9.94107700	15.64022600
H	4.74414500	8.46577500	16.16476800
C	6.32065300	8.37321600	7.61546800
H	7.07007600	8.43642700	7.03514700
C	2.31356200	4.85551700	14.67887300

---

---

H	2.84078000	4.16177500	15.05658000
C	5.06401300	8.17568100	7.08132100
H	4.95373500	8.11924300	6.13936100
C	8.73381800	7.38847700	9.40629900
H	8.29660500	6.65635700	9.88873000
H	9.63174500	7.53115300	9.77237100
H	8.80118600	7.15865900	8.45547400
C	0.95116000	4.67423700	14.49472900
H	0.53274900	3.86039300	14.74998200
C	8.62889200	9.86206300	8.91962000
H	8.74033100	9.69613400	7.96048300
H	9.50884600	9.97606900	9.33648300
H	8.09739900	10.67477800	9.05020200
C	1.82816200	9.07192400	9.91292600
H	2.22238900	9.95123600	10.09005100
H	1.05422700	8.93760100	10.50008100
H	1.54065900	9.02451600	8.97632200
C	0.87164900	6.83921700	13.60116000
H	0.35965400	7.54018400	13.21329400
C	2.26231400	6.59878900	10.00010300
H	1.97634100	6.48929900	9.06867100
H	1.48775600	6.50171500	10.59243000
H	2.92924600	5.91588400	10.21934000

---

**Compound 3.2**

Ge	9.50280000	7.79220000	5.46070000
Cl	7.58560000	8.96060000	6.02210000
N	8.53110000	6.00720000	5.61050000
N	9.01750000	7.50770000	3.60440000
C	8.38220000	6.31780000	3.29820000
C	8.05440000	5.50130000	4.43590000
C	7.29940000	4.31970000	4.43510000
C	8.14220000	6.26040000	1.91940000
C	8.29860000	5.37160000	6.78250000
C	9.18760000	8.21750000	2.45030000
C	7.03940000	3.68830000	5.64720000
C	9.81580000	9.56950000	2.44950000
C	7.55360000	4.21770000	6.83890000
C	8.65850000	7.46440000	1.39910000
C	7.45880000	5.16560000	1.14430000
H	10.08027386	9.84049364	3.45025773
H	9.12289504	10.28451087	2.05765543
H	10.69510691	9.55386175	1.84001267
H	7.82923795	8.01558266	1.00740862
H	7.15936908	4.38735469	1.81480381
H	6.59636990	5.56276609	0.65097107
H	8.13493628	4.76855303	0.41622484



---

H	6.92963372	3.91073161	3.51808432
H	6.44646996	2.79789332	5.66978133
H	7.36969533	3.73280058	7.77482287
H	8.70404445	5.77661467	7.68609168

**Compound 3.7**

N	8.26485800	7.44828800	2.16386100
C	7.46051300	6.43596900	2.64601600
C	6.72060000	5.63531500	1.74278500
H	6.13240900	4.81135400	2.14887800
C	6.75803600	5.91722000	0.38860700
H	6.16857900	5.32485000	-0.31361200
C	7.56860600	6.97578600	-0.07838700
H	7.61858200	7.22588500	-1.13815400
C	8.32000300	7.69181000	0.83840300
H	9.00980200	8.48569900	0.54015600
C	4.27543900	3.38679800	5.01223500
H	4.67643900	3.06471300	4.04101400
H	3.81219200	4.37662400	4.88284800
H	3.48015400	2.68613600	5.30926700
Al	9.63996300	8.08187600	3.52717700
Al	8.36774900	4.34622600	4.36934500
N	8.05103300	7.35865900	4.66358500
N	10.02915300	5.44014400	4.98933500

---

N	9.80477300	9.61271900	4.79057500
N	8.31191000	3.46999000	6.15896200
C	7.46342600	6.23879400	4.07674800
C	10.54972800	6.21853500	3.95667800
C	7.82249900	7.65987000	5.95399600
C	8.46299800	8.72754900	6.59859000
H	8.18125100	8.89322000	7.63806500
C	9.32414200	9.69333500	6.04053400
C	6.77703000	6.89036700	6.71689300
H	5.82662900	6.89300500	6.16370600
H	6.62314000	7.30940800	7.71893700
H	7.07289900	5.83774000	6.81759000
C	9.66064900	10.88653500	6.90423500
H	10.69740800	11.21499000	6.75234700
H	9.50005600	10.65198600	7.96394200
H	9.01884800	11.74360000	6.64720800
C	10.46234400	10.77487500	4.24928500
C	9.67861100	11.87397800	3.82329700
C	10.33773600	13.00044000	3.31526900
H	9.75194000	13.85983400	2.98334300
C	11.72813100	13.04070300	3.21684900
H	12.22385000	13.93261200	2.82792100
C	12.48011200	11.93030600	3.59483700

---

---

H	13.56656200	11.95511000	3.48711600
C	11.86678800	10.77530400	4.09787600
C	8.15592100	11.80648700	3.81290600
H	7.84143800	11.01554600	4.50942700
C	7.66928400	11.38854600	2.41165700
H	7.93325100	12.15481700	1.66623500
H	6.57677000	11.25564300	2.40086700
H	8.13316100	10.44297300	2.09704700
C	7.47873400	13.10902500	4.26294600
H	7.84303200	13.43635300	5.24819000
H	6.39035400	12.96461800	4.33272500
H	7.65292900	13.93040200	3.55172700
C	12.70377200	9.56292600	4.47448700
H	12.02016700	8.70473800	4.56714300
C	13.71549000	9.18955600	3.38165000
H	13.20841900	9.07621000	2.41316900
H	14.20178000	8.23445000	3.63133400
H	14.50760800	9.94625800	3.27227500
C	13.39740200	9.75696900	5.83355300
H	13.97914500	8.86231100	6.10385700
H	12.66964600	9.94131800	6.63699200
H	14.08730200	10.61480600	5.80205100
C	10.36700500	5.67885100	6.26850500

---

---

C	9.79502200	4.97519100	7.33825000
H	10.16687000	5.23378300	8.32923300
C	8.89761300	3.88985000	7.29115200
C	11.46070000	6.66982300	6.57015300
H	12.35412800	6.44205700	5.97106800
H	11.71858900	6.66877100	7.63630200
H	11.14798700	7.68349900	6.28587800
C	8.64360500	3.15999000	8.58941800
H	7.60084500	2.82453400	8.66621700
H	8.88830000	3.80180300	9.44473800
H	9.26940400	2.25633600	8.65470900
C	7.61920200	2.20680600	6.18876400
C	8.37188100	1.00743000	6.19668000
C	7.67881400	-0.20942400	6.23319400
H	8.23944000	-1.14642100	6.24087400
C	6.28511300	-0.24704900	6.24938100
H	5.76335000	-1.20560400	6.28826900
C	5.56120900	0.94211500	6.19479000
H	4.46999300	0.90594200	6.17773000
C	6.20745300	2.18404900	6.14390200
C	9.89006900	1.02133800	6.06413700
H	10.25350200	2.01228000	6.37225100
C	10.28170700	0.84228500	4.58513200

---

---

H	9.95807700	-0.14310800	4.21662200
H	11.37237600	0.92001500	4.45704500
H	9.80730100	1.60724000	3.95419300
C	10.59320200	-0.01876200	6.94791100
H	10.28767100	0.07002000	8.00128900
H	11.68377800	0.11663900	6.89614100
H	10.37755100	-1.04766900	6.62273400
C	5.39755700	3.46835400	6.05644700
H	6.07696600	4.26480800	5.71519900
C	4.84696600	3.87990300	7.43257200
H	4.16897900	3.10782800	7.82901600
H	4.28362900	4.82293800	7.36013700
H	5.65405200	4.02634000	8.16498400
H	10.51116700	8.81482600	2.35758800
H	7.42483900	3.21619000	3.66703800
C	10.44991700	5.45846100	2.73240500
N	9.63009300	4.34841900	2.76491500
C	9.48025100	3.58972600	1.65994300
H	8.78523800	2.75187600	1.76154300
C	10.14732900	3.86325100	0.47727500
H	10.02253300	3.20615600	-0.38346900
C	10.97082300	5.00934000	0.41206600
H	11.49398900	5.25885100	-0.51276500

---

---

C	11.10438700	5.81519200	1.52879600
H	11.70465600	6.72582300	1.52065800

### 6.3: Chapter 4 experimental details and crystallographic data

#### 6.3.1. Synthesis and experimental details of compounds 4.1–4.4

##### 6.3.1.1. Synthesis of compound 4.1

THF (20 mL) was added to a mixture of **3.4** (0.500 g, 1 mmol) and Ni(COD)<sub>2</sub> (0.275 g, 1 mmol) at ambient temperature. The solution turned yellow to black with the formation of a precipitate, and the resulting suspension was stirred for 12 h. The supernatant solvent was filtered and was reduced to 5 mL and stored at –30 °C in a freezer overnight to obtain the black crystals of **4.1** suitable for X-ray analysis.

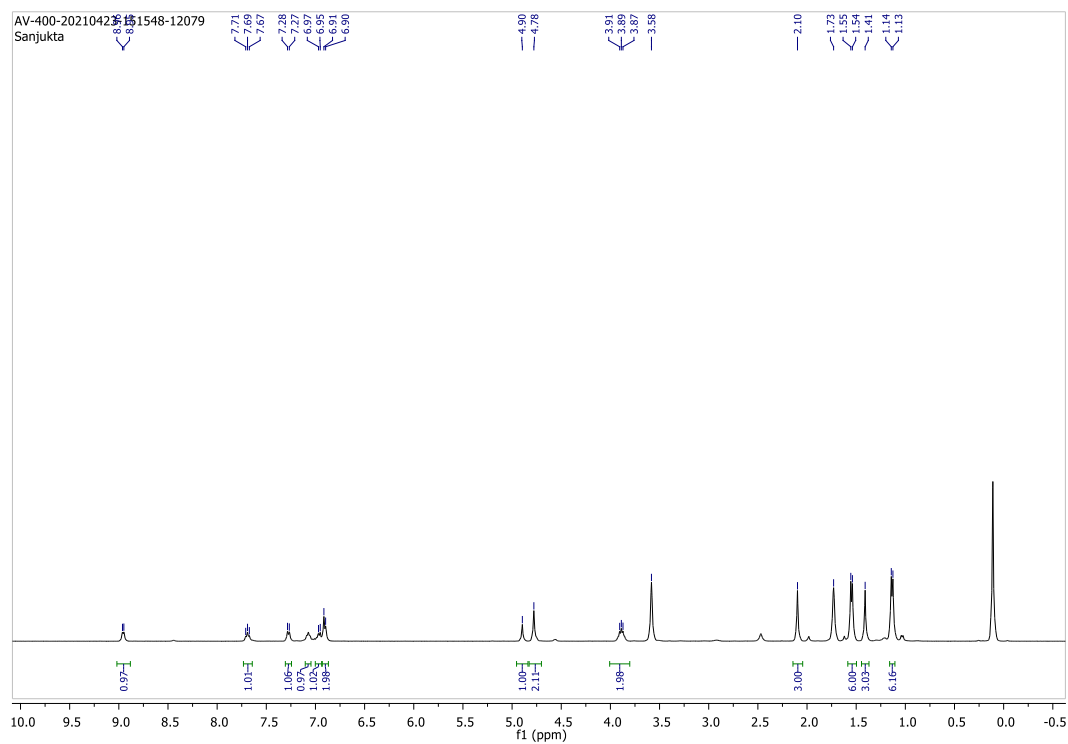
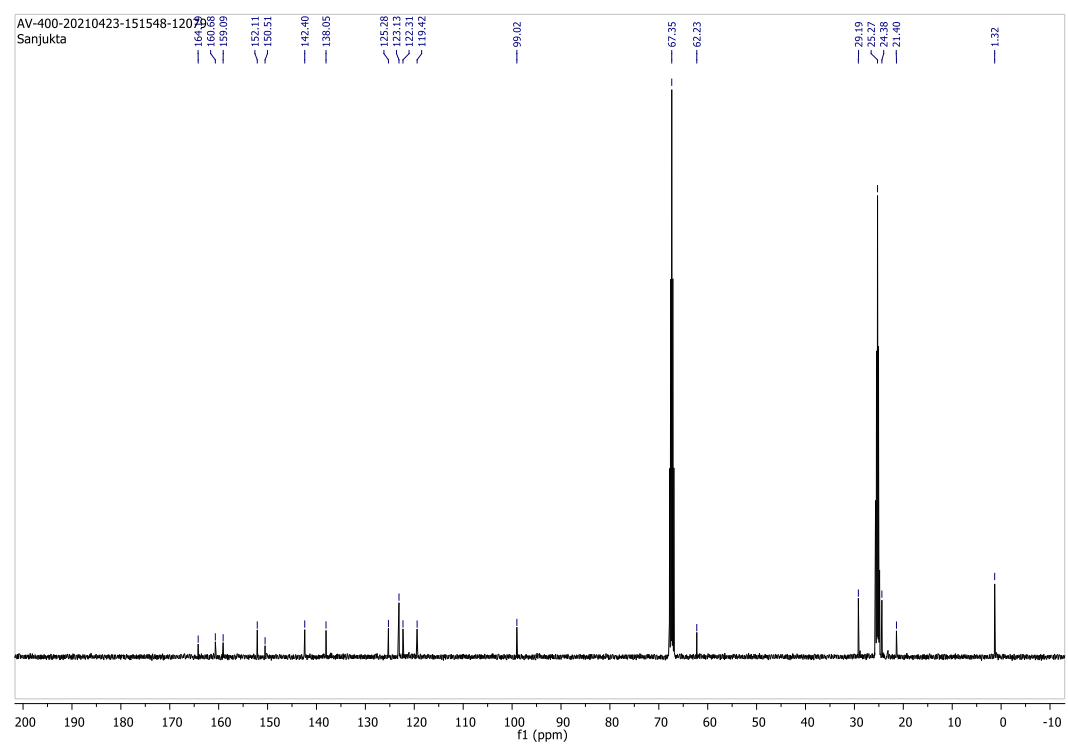
**Yield:** 0.403 g (92 %).

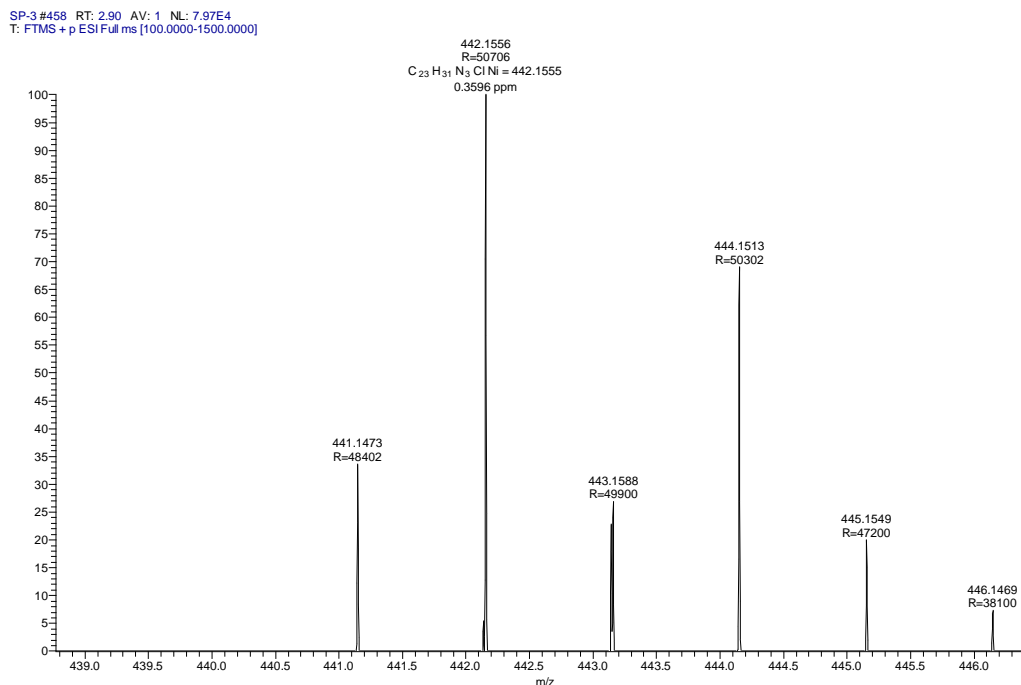
**Mp:** 206.9 °C.

**NMR:** <sup>1</sup>H NMR (400 MHz, THF-d<sub>8</sub>, 298 K): δ 8.96 (1 H, d, *J* = 5.6 Hz), 7.69 (1 H, t, *J* = 7.4 Hz), 7.28 (1 H, d, *J* = 7.4 Hz), 7.07 (1 H, t, *J* = 6.3 Hz), 6.96 (1 H, d, *J* = 7.1 Hz), 6.91 (2 H, d, *J* = 7.0 Hz), 4.90 (1 H, s), 4.78 (2 H, s), 4.01 – 3.80 (2 H, m), 2.10 (3 H, s), 1.55 (6 H, d, *J* = 6.6 Hz), 1.41 (3 H, s), 1.13 (6 H, d, *J* = 6.6 Hz) ppm. <sup>13</sup>C NMR (400 MHz, THF-d<sub>8</sub>, 298 K): δ 164.19 (s), 160.68 (s), 159.09 (s), 152.11 (s), 150.51 (s), 142.40 (s), 138.05 (s), 125.28 (s), 123.13 (s), 122.31 (s), 119.42 (s), 99.02 (s), 62.23 (s), 29.19 (s), 24.38 (s), 21.40 (s), 1.32 (s) ppm.

**HRMS:** Calcd: 441.15, found: 442.1556.

##### a) <sup>1</sup>H NMR of compound 4.1:

**b)  $^{13}\text{C}$  NMR of compound 4.1:****c) HRMS data of compound 4.1:**



### 6.3.1.2. Synthesis of compound 4.2

THF (20 mL) was added to a mixture of **3.4** (0.500 g, 1 mmol) and Copper(I) chloride (0.100 g, 1 mmol) at ambient temperature. The solution turned yellow to red with the formation of a white precipitate, and the resulting suspension was stirred for 12 h. The supernatant solvent was filtered and was reduced to 5 mL and stored at  $-30\text{ }^{\circ}\text{C}$  in a freezer overnight to obtain the red crystals of **4.2** suitable for X-ray analysis.

**Yield:** 0.417g (94 %).

**Mp:** 89.3  $^{\circ}\text{C}$ .

### 6.3.1.3. Synthesis of compound 4.3

A solution of K-selectride (1 equiv, 0.23 mL, 0.226 mmol) in THF (5 mL) was added to a solution of complex **4.1** (100 mg, 0.226 mmol) in THF (5 mL) and Et<sub>2</sub>O (5 mL) solvent mixture. The mixture was stirred for 2 h at RT and the solvent was removed in vacuo. The residue was extracted with Et<sub>2</sub>O (10 mL) and evaporation of the solvent to reduce it to 5 mL and stored at  $-30\text{ }^{\circ}\text{C}$  in a freezer overnight yielded the brown-red crystals of **4.3** suitable for X-ray analysis.

**Yield:** 0.069 g (75 %).

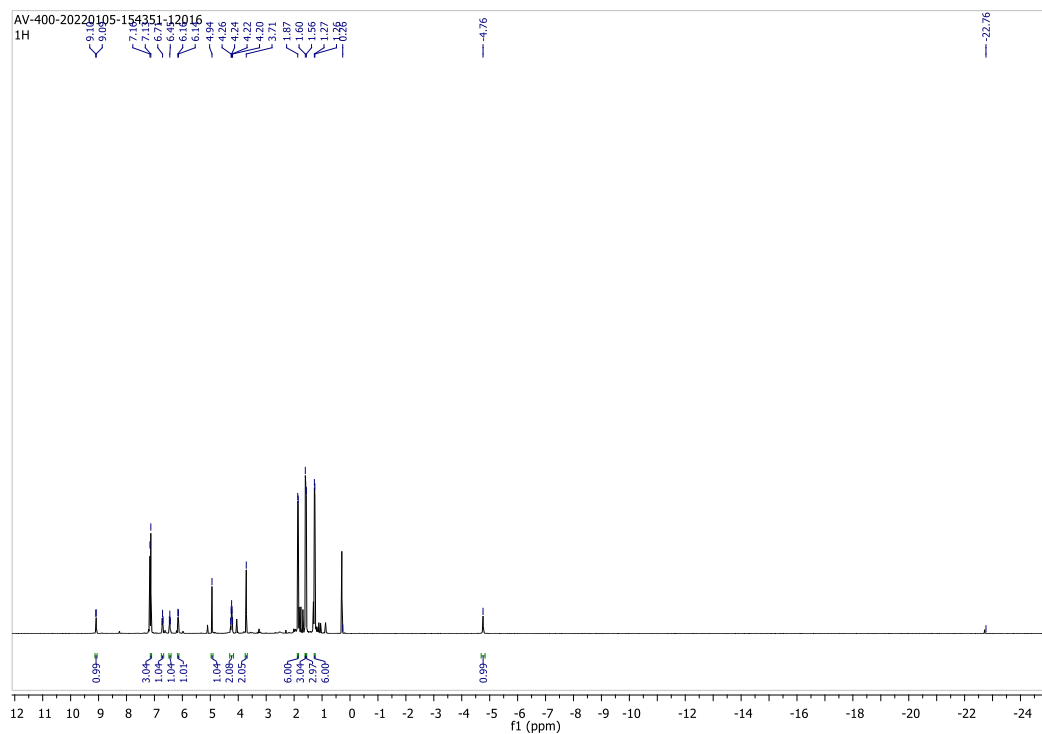
**Mp:** 191.2  $^{\circ}\text{C}$ .

**NMR:**  $^1\text{H}$  NMR (400 MHz, C<sub>6</sub>D<sub>6</sub>, 298 K):  $\delta$  9.09 (1 H, d,  $J = 5.7$  Hz), 7.13 (3 H, s), 6.71 (1 H, t,  $J = 7.5$  Hz), 6.45 (1 H, t,  $J = 6.5$  Hz), 6.15 (1 H, d,  $J = 7.7$  Hz), 4.94 (1 H, s), 4.24 (2 H, dt,  $J =$

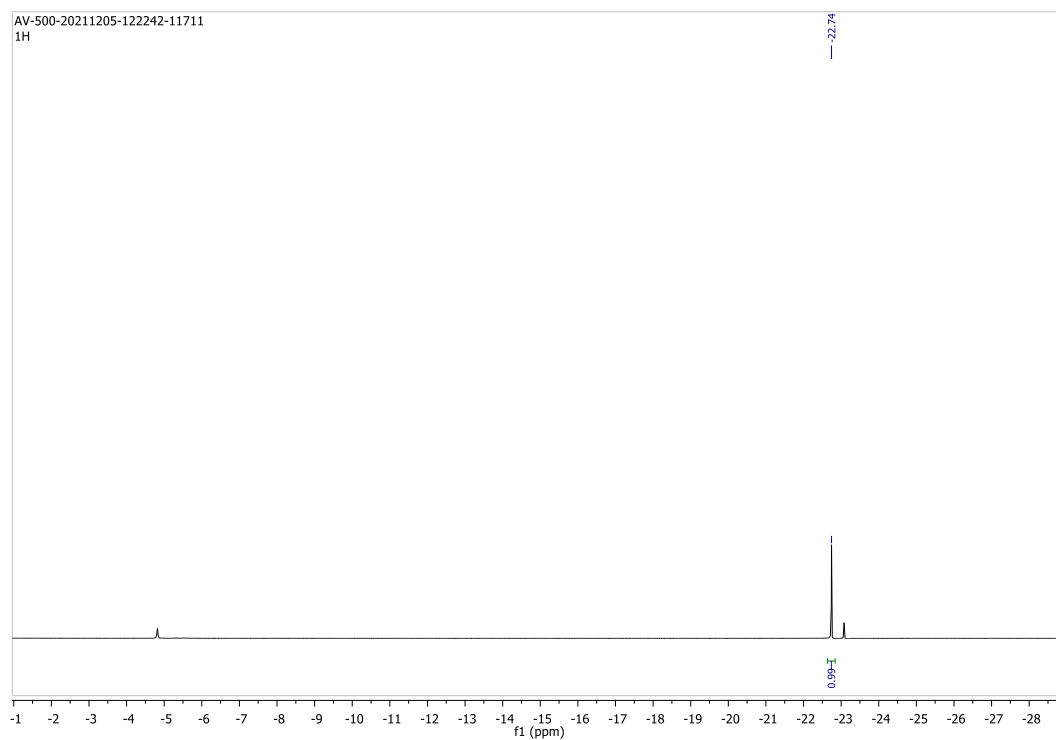


13.7, 6.9 Hz), 3.71 (2 H, s), 1.86 (6 H, d,  $J = 6.8$  Hz), 1.60 (3 H, s), 1.56 (3 H, s), 1.27 (6 H, d,  $J = 7.0$  Hz), -22.74 (1 H, s) ppm.  $^{13}\text{C}$ NMR (400 MHz,  $\text{C}_6\text{D}_6$ , 298 K):  $\delta$  164.56 (s), 158.76 (s), 157.86 (s), 156.82 (s), 155.17 (s), 139.97 (s), 133.68 (s), 124.67 (s), 123.23 (s), 122.23 (s), 119.25 (s), 98.04 (s), 58.94 (s), 28.49 (s), 24.03 (s), 23.65 (s), 22.86 (s) ppm.

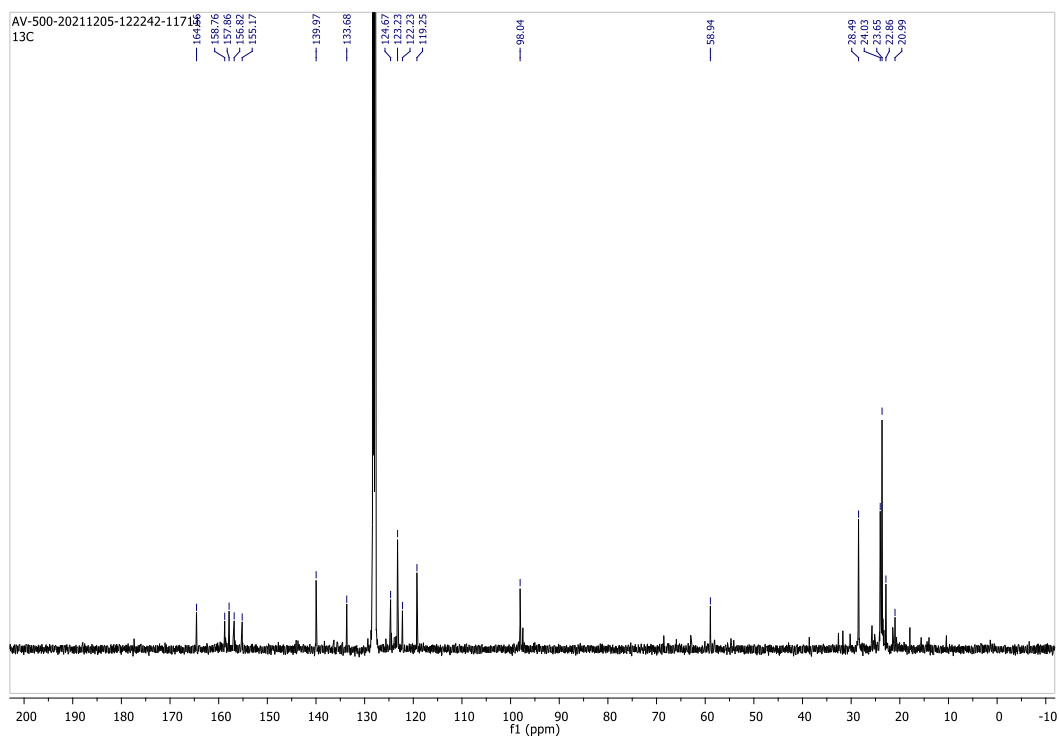
**a)  $^1\text{H}$  NMR of compound 4.3:**



**b) Expansion of  $^1\text{H}$  NMR of compound 4.3:**



**c)  $^{13}\text{C}$  NMR of compound 4.3:**



**6.3.1.4. Synthesis of compound 4.4**

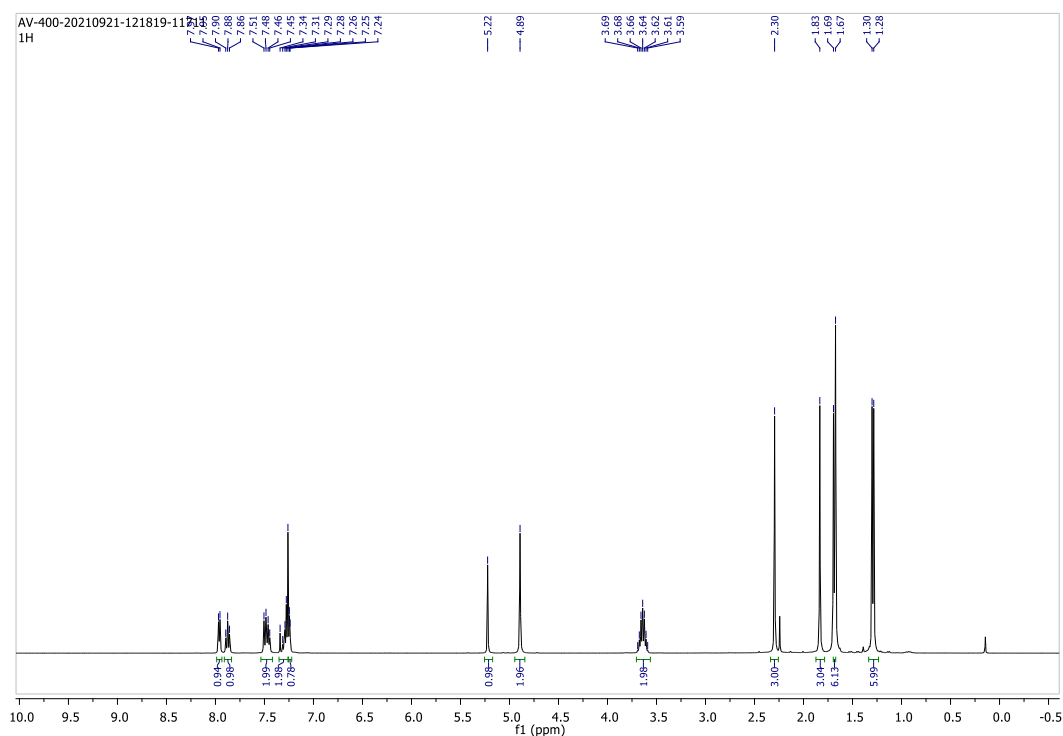
Acetonitrile (12-15 mL) was added to a mixture of **4.1** (0.100 g, 1 mmol) and AgSbF<sub>6</sub> (0.078 g, 1 mmol) at ambient temperature. The solution turned black to green with the formation of a white precipitate, and the resulting suspension was stirred for 2 h. The supernatant solvent was filtered and was reduced to 5 mL and stored at -30 °C in a freezer overnight to obtain the green crystals of **4.4** suitable for X-ray analysis.

**Yield:** 0.131 g (83 %).

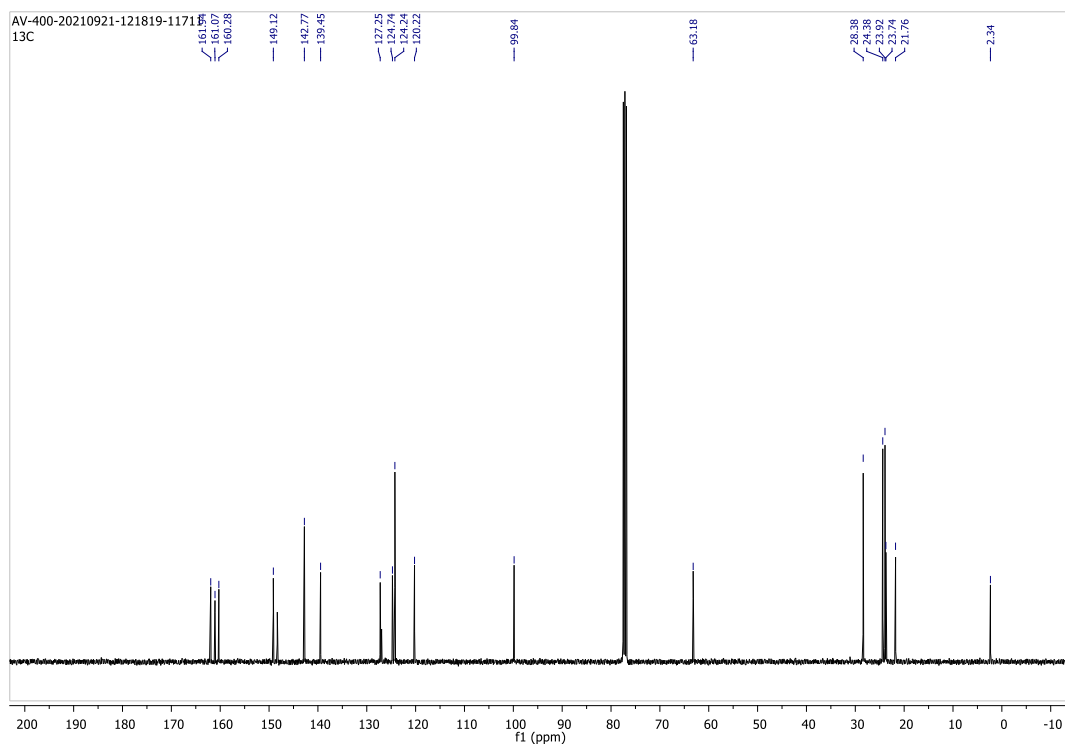
**Mp:** 211.4 °C.

**NMR:** <sup>1</sup>H NMR (400 MHz, CDCl<sub>3</sub>, 298 K): δ 7.96 (1 H, d, *J* = 5.9 Hz), 7.88 (1 H, t, *J* = 7.6 Hz), 7.47 (2 H, dd, *J* = 16.1, 7.5 Hz), 7.35 – 7.26 (2 H, m), 7.24 (1 H, d, *J* = 2.9 Hz), 5.22 (1 H, s), 4.89 (2 H, s), 3.70 – 3.56 (2 H, m), 2.30 (3 H, s), 1.83 (3 H, s), 1.68 (6 H, d, *J* = 8.3 Hz), 1.29 (6 H, d, *J* = 6.9 Hz) ppm. <sup>13</sup>C NMR (400 MHz, CDCl<sub>3</sub>, 298 K): δ 161.94 (s), 161.07 (s), 160.28 (s), 149.12 (s), 142.77 (s), 139.45 (s), 127.25 (s), 124.74 (s), 124.24 (s), 120.22 (s), 99.84 (s), 63.18 (s), 28.38 (s), 24.38 (s), 23.83 (d, *J* 18.8), 21.76 (s), 2.34 (s) ppm.

**a) <sup>1</sup>H NMR of compound 4.4:**



**b) <sup>13</sup>C NMR of compound 4.4:**



### 6.3.2. Crystallographic data for the structural analysis of compounds 4.1-4.4

**6.3.2.1. Crystal data of compound 4.1:**  $C_{23}H_{30}N_3Ni_1Cl_1$ ,  $M = 442.64$ , Black, Block,  $0.27 \times 0.30 \times 0.32 \text{ mm}^3$ , monoclinic, space group ' $P2_1/c$ ',  $a = 18.9083(17)\text{\AA}$ ,  $b = 14.9499(12)\text{\AA}$ ,  $c = 15.5831(14)\text{\AA}$ ,  $\alpha = 90^\circ$ ,  $\beta = 98.975(3)^\circ$ ,  $\gamma = 90^\circ$ , Volume =  $4351.1(7) \text{\AA}^3$ ,  $Z = 8$ ,  $T = 100.0$ ,  $D_{calc} (\text{g cm}^{-3}) = 1.351$ ,  $F(000) = 1872$ ,  $\mu (\text{mm}^{-1}) = 1.028$ , 86719 reflections collected, 7669 unique reflections ( $R_{int} = 0.0491$ ), 5410 observed ( $I > 2\sigma(I)$ ) reflections, multi-scan absorption correction,  $T_{min} = 0.895$ ,  $T_{max} = 0.940$ , 517 refined parameters,  $S = 1.094$ ,  $R1 = 0.0491$ ,  $wR2 = 0.1089$  (all data  $R = 0.0904$ ,  $wR2 = 0.1341$ ), maximum and minimum residual electron densities;  $\Delta\rho_{max} = 0.48$ ,  $\Delta\rho_{min} = -0.67 (\text{e}\text{\AA}^{-3})$ .

**6.3.2.2. Crystal data of compound 4.2:**  $C_{23}H_{31}N_3Cu_1Cl_1$ ,  $M = 448.51$ , Red, Block,  $0.30 \times 0.31 \times 0.26 \text{ mm}^3$ , monoclinic, space group ' $P2_1/n$ ',  $a = 16.039(2)\text{\AA}$ ,  $b = 13.9925(17)\text{\AA}$ ,  $c = 23.716(3)\text{\AA}$ ,  $\alpha = 90^\circ$ ,  $\beta = 103.307(4)^\circ$ ,  $\gamma = 90^\circ$ , Volume =  $5179.6(11) \text{\AA}^3$ ,  $Z = 4$ ,  $T = 100(2)$ ,  $D_{calc} (\text{g cm}^{-3}) = 1.148$ ,  $F(000) = 1880$ ,  $\mu (\text{mm}^{-1}) = 0.958$ , 90757 reflections collected, 9138 unique reflections ( $R_{int} = 0.0863$ ), 6503 observed ( $I > 2\sigma(I)$ ) reflections, multi-scan absorption correction, 517 refined

parameters,  $S = 1.135$ ,  $R1 = 0.0863$ ,  $wR2 = 0.2041$  (all data  $R = 0.1188$ ,  $wR2 = 0.2303$ ), maximum and minimum residual electron densities;  $\Delta\rho_{\max} = 1.44$ ,  $\Delta\rho_{\min} = -2.12$  ( $\text{e}\text{\AA}^{-3}$ ).

**6.3.2.3. Crystal data of compound 4.3:**  $\text{C}_{23}\text{H}_{31}\text{N}_3\text{Ni}_1$ ,  $M = 408.22$ , Red, Block,  $0.30 \times 0.28 \times 0.25$   $\text{mm}^3$ , monoclinic, space group ' $P2_1/n$ ',  $a = 11.647(7)\text{\AA}$ ,  $b = 13.213(6)\text{\AA}$ ,  $c = 14.134(7)\text{\AA}$ ,  $\alpha = 90^\circ$ ,  $\beta = 94.12(2)^\circ$ ,  $\gamma = 90^\circ$ , Volume =  $2169(2) \text{\AA}^3$ ,  $Z = 4$ ,  $T = 293(2)$ ,  $D_{\text{calc}}$  ( $\text{g cm}^{-3}$ ) =  $1.250$ ,  $F(000) = 872$ ,  $\mu$  ( $\text{mm}^{-1}$ ) =  $0.906$ , 126678 reflections collected, 4434 unique reflections ( $R_{\text{int}} = 0.0372$ ), 3762 observed ( $I > 2\sigma(I)$ ) reflections, multi-scan absorption correction,  $T_{\text{min}} = 0.7053$ ,  $T_{\text{max}} = 0.7429$ , 250 refined parameters,  $S = 1.061$ ,  $R1 = 0.0372$ ,  $wR2 = 0.0907$  (all data  $R = 0.0476$ ,  $wR2 = 0.0959$ ), maximum and minimum residual electron densities;  $\Delta\rho_{\max} = 0.34$ ,  $\Delta\rho_{\min} = -0.45$  ( $\text{e}\text{\AA}^{-3}$ ).

**6.3.2.4. Crystal data of compound 4.4:**  $\text{C}_{25}\text{H}_{33}\text{N}_4\text{F}_6\text{Ni}_1\text{Sb}_1$ ,  $M = 684.01$ , Green, Block,  $0.34 \times 0.31 \times 0.28$   $\text{mm}^3$ , monoclinic, space group ' $P2_1/c$ ',  $a = 11.3589(17)\text{\AA}$ ,  $b = 11.5323(17)\text{\AA}$ ,  $c = 23.206(3)\text{\AA}$ ,  $\alpha = 90^\circ$ ,  $\beta = 98.162(5)^\circ$ ,  $\gamma = 90^\circ$ , Volume =  $3009.1(8) \text{\AA}^3$ ,  $Z = 4$ ,  $T = 100(2)$ ,  $D_{\text{calc}}$  ( $\text{g cm}^{-3}$ ) =  $3.500$ ,  $F(000) = 2856$ ,  $\mu$  ( $\text{mm}^{-1}$ ) =  $10.490$ , 145149 reflections collected, 9241 unique reflections ( $R_{\text{int}} = 0.0585$ ), 8921 observed ( $I > 2\sigma(I)$ ) reflections, multi-scan absorption correction, 362 refined parameters,  $S = 1.316$ ,  $R1 = 0.0585$ ,  $wR2 = 0.1857$  (all data  $R = 0.0616$ ,  $wR2 = 0.1953$ ), maximum and minimum residual electron densities;  $\Delta\rho_{\max} = 2.16$ ,  $\Delta\rho_{\min} = -1.52$  ( $\text{e}\text{\AA}^{-3}$ ).

## 6.4: Chapter 5 experimental details, crystallographic data and General procedure for catalytic hydroboration

### 6.4.1. Synthesis and experimental details of Ligand L2 and compounds 5.1-5.6

#### 6.4.1.1. Synthesis and experimental details of ligand (L2): (3,5-dimethyl-2-(2-pyridyl)pyrrole)

One equiv of both the 2,4-pentanedione (244 mg, 2.4 mmol) and 2-(aminomethyl)pyridine (296 mg, 2.7 mmol) along with a catalytic amount of *p*-toluene sulfonic acid (56 mg, 0.3 mmol) were added in 20 mL of xylenes into a round bottom flask,. The reaction flask was fitted nicely with a Dean-Stark apparatus (xylenes, 2 mL) and a reflux condenser. The trap was flushed with argon and stirred the reaction mixture at room temperature for 30 min. The mixture was then heated to reflux at  $170^\circ\text{C}$  for 10-12 h. After cooling the reaction mixture, the solvent was evaporated in

vacuum and purified through column chromatography (silica gel, hexanes/ethyl acetate 5:1, 3% Et<sub>3</sub>N). The removal of solvent afforded ligand **L2** as a white crystalline solid.

**Yield:** 309 mg (74%).

#### 6.4.1.2. High yield synthesis of compound 3.2

A solution of <sup>n</sup>BuLi (7.25 mL, 14.51 mmol, 2M) in n-hexane was added drop by drop to a stirred solution of 2-(3,5-dimethyl-1H-pyrrol-2-yl)pyridine (2.0 g, 11.61 mmol, in THF 20 mL) at -78 °C over a period of 20 min. The suspension was allowed to warm up to room temperature and stirred for 6 h. After that, the THF (20 mL) solution of GeCl<sub>2</sub>·dioxane (2.82 g, 12.19 mmol) was added drop by drop to the above suspension at -30 °C via cannula. The reaction mixture was further warmed to room temperature and stirred for another 15 h. Subsequently, all volatiles were removed in vacuo and the residue was extracted with toluene (30 mL). The resultant toluene solvent was concentrated to 10–12 mL and stored at -30 °C in a freezer, which afforded yellow crystals of **3.2** within one day.

**Yield:** 3.04 g (93 %).

All the spectroscopic data have been compared with the reported data in chapter 3.<sup>12</sup>

#### 6.4.1.3. Synthesis and characterization of compound 5.1

A solution of SnCl<sub>2</sub> (0.70 g, 3.65 mmol) in THF (20 mL) was added drop by drop to a stirred solution of **3.2** (1.0 g, 3.58 mmol, in THF 20 mL) at -78 °C, over a period of 20 min. The suspension was allowed to warm up to room temperature and stirred for 15 h. Subsequently, all volatiles were removed in vacuo and the residue was extracted with THF (30 mL). The resultant THF solvent was concentrated to 8-10 mL and stored at -30 °C in a freezer, which afforded yellow crystals of **5.1**.

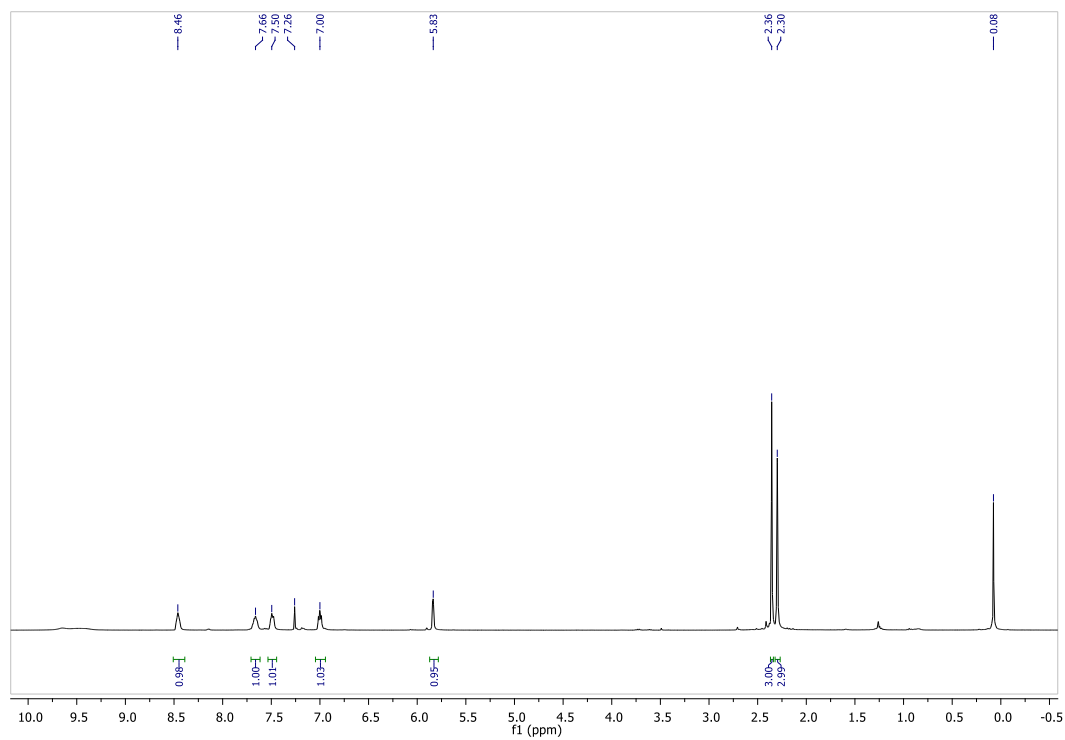
**Yield:** 0.998 g (86 %).

**Mp:** 213.2 °C.

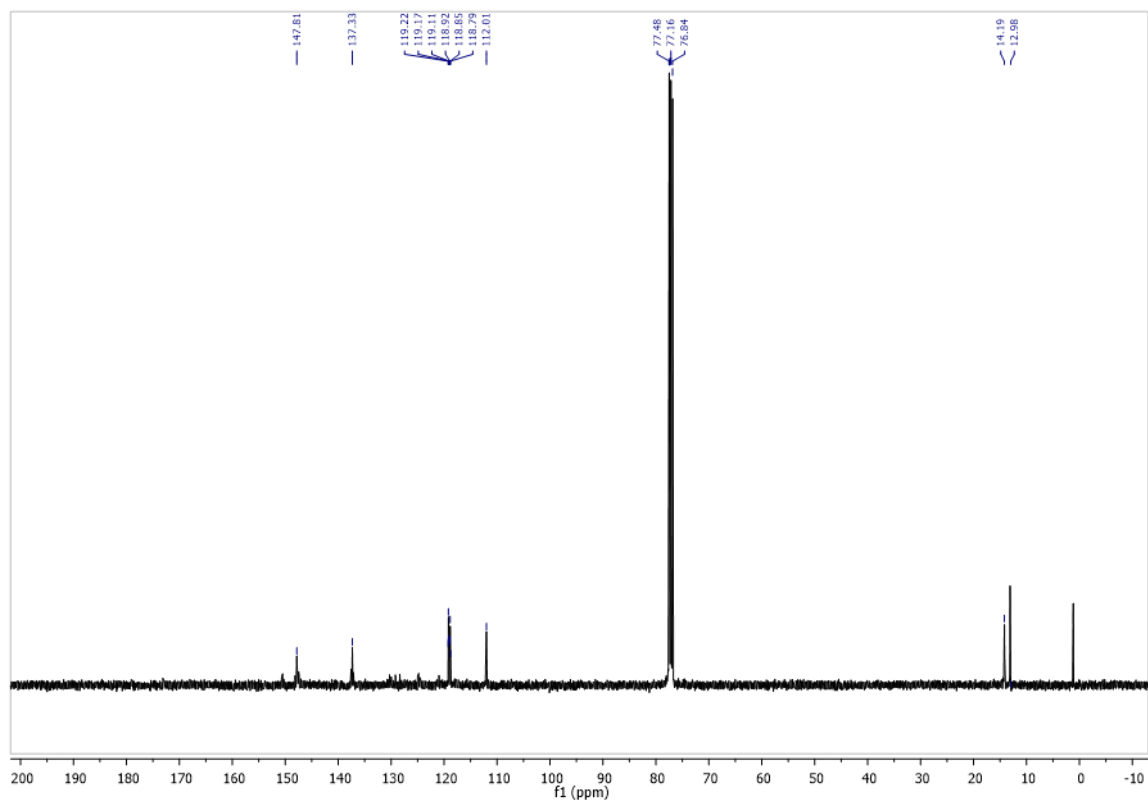
**NMR:** <sup>1</sup>H NMR (400 MHz, CDCl<sub>3</sub>, 298 K): δ 8.46 (s, 1H), 7.66 (s, 1H), 7.50 (s, 1H), 7.00 (s, 1H), 5.83 (s, 1H), 2.36 (s, 3H), 2.30 (s, 3H) ppm. <sup>13</sup>C NMR (101 MHz, CDCl<sub>3</sub>, 298 K): δ 147.81 (s), 137.33 (s), 119.42 (s), 119.17 (s), 119.11 (s), 118.92 (s), 118.85 (s), 118.79 (s), 112.01 (s), 14.19 (s), 12.98 (s) ppm. <sup>119</sup>Sn NMR (149 MHz, C<sub>6</sub>D<sub>6</sub>, 298 K): δ -151.86 ppm.

**HRMS:** Calcd: 325.96, found: 326.2407.

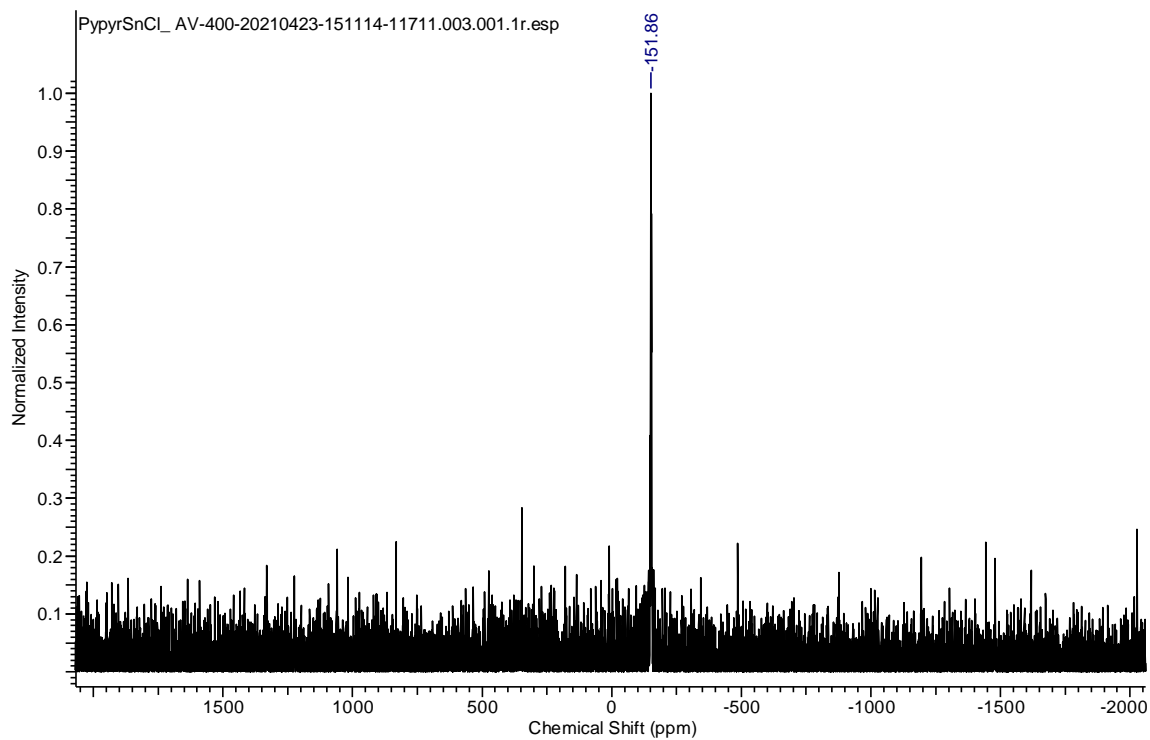
#### a) <sup>1</sup>H NMR of compound 5.1:



b) <sup>13</sup>C NMR of compound 5.1:

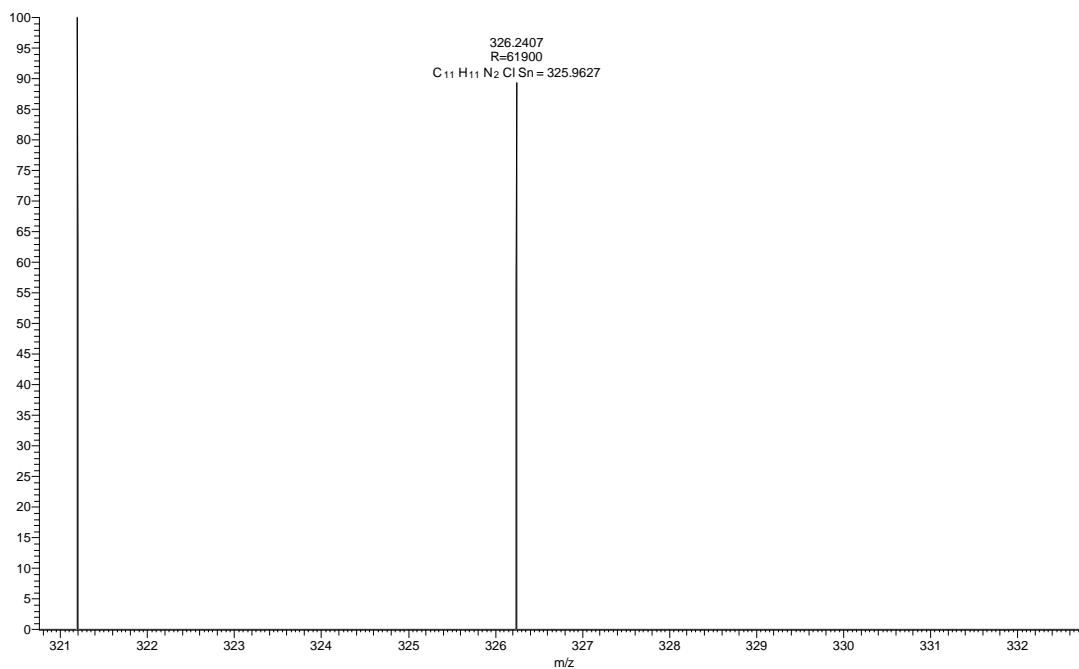


c) <sup>119</sup>Sn NMR of compound 5.1:



**d) HRMS data of compound 5.1:**

SP-02\_210505170411 #1160 RT: 6.17 AV: 1 NL: 1.37E5  
T: FTMS + p ESI Full ms [100.0000-1500.0000]



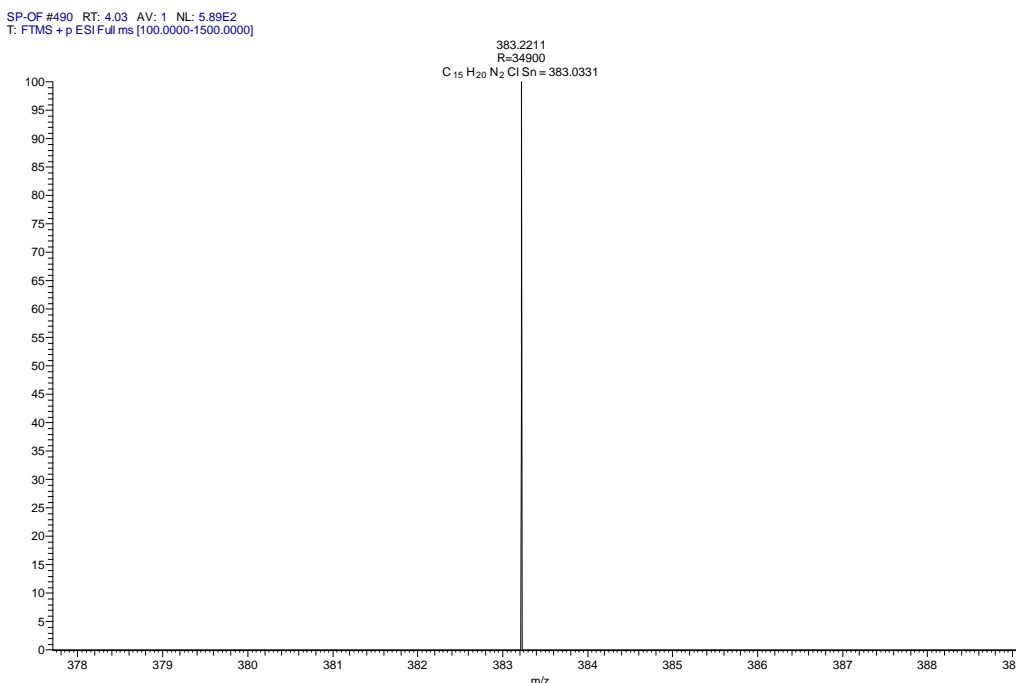
**6.4.1.4. Synthesis and characterization of compound 5.2**



A solution of <sup>n</sup>BuLi in n-hexane (6.38 mL, 12.77 mmol, 2M, 1.1 equiv.) was added drop wise to a stirred solution of 2-(3,5-dimethyl-1H-pyrrol-2-yl)pyridine (2.0 g, 11.61 mmol, in THF 20 mL) at -78 °C, over a period of 20 min. The suspension was allowed to warm up to room temperature and stirred for 6 h. Next, the solution of SnCl<sub>2</sub> (2.31 g, 12.19 mmol) in THF was added drop by drop to the above suspension at -30 °C via cannula. The reaction mixture was further warmed to room temperature and stirred for another 15 h. Subsequently, all volatiles were removed in vacuo and the residue was extracted into toluene (30 mL). The resultant toluene solvent was concentrated to 10–12 mL and stored at -30 °C in a freezer, which afforded yellow crystals of **5.1** and **5.2** within one day in the same flask. HRMS:

**HRMS:** Calcd: 382.03, found: 383.0331.

**a) HRMS data of compound 5.2:**



**6.4.1.5. Synthesis and characterization of compound 5.3**

A solution of potassium tert-butoxide (72.42 mg, 0.645 mmol in 10 mL toluene) was added to a stirred solution of compound **5.1** (200 mg, 0.614 mmol in 15 mL toluene) at -78 °C over a period of 10 min and the reaction mixture was allowed to warm up to room temperature and further stirred for 15 h. Subsequently, all volatiles were removed in vacuo and the residue was extracted into

toluene (15 mL). The resultant toluene was concentrated to 5-8 mL and stored at  $-30\text{ }^{\circ}\text{C}$  in a freezer, which afforded colorless crystals of **5.3** within one day.

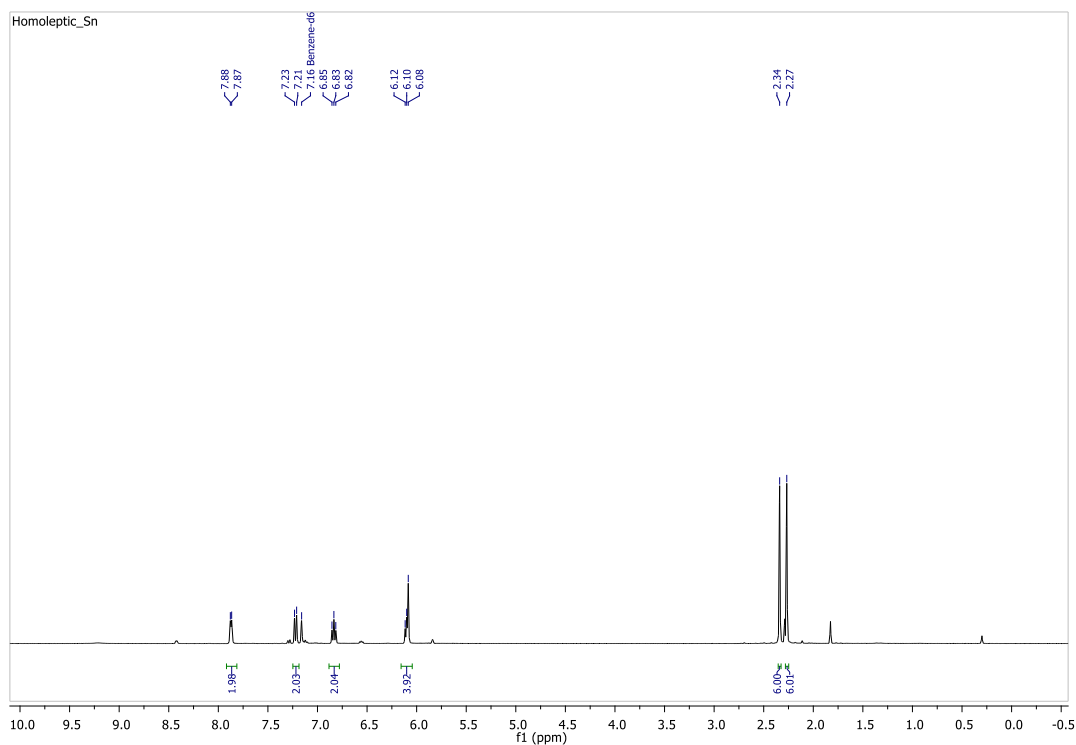
**Yield:** 0.257 g (90 %).

**Mp:** 164.6  $^{\circ}\text{C}$ .

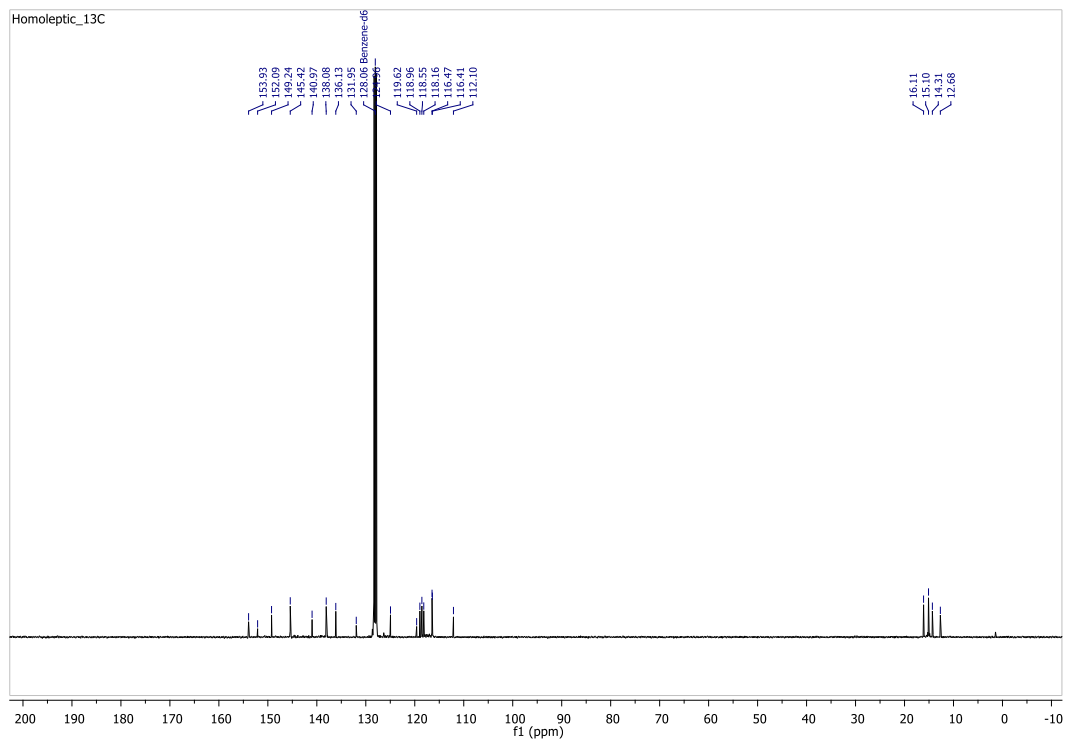
**NMR:**  $^1\text{H}$  NMR (400 MHz,  $\text{C}_6\text{D}_6$ , 298 K):  $\delta$  7.87 (d, 2H), 7.22 (d, 2H), 6.83 (t, 2H), 6.12 – 6.08 (m, 4H), 2.34 (s, 6H), 2.27 (s, 6H) ppm.  $^{13}\text{C}$  NMR (100.56 MHz,  $\text{C}_6\text{D}_6$ , 298 K);  $\delta$  153.93 (s), 152.09 (s), 149.24 (s), 145.42 (s), 140.97 (s), 138.08 (s), 136.13 (s), 131.95 (s), 124.96 (s), 119.62 (s), 118.96 (s), 118.55 (s), 118.16 (s), 116.47 (s), 116.41 (s), 112.10 (s), 16.11 (s), 15.10 (s), 14.31 (s), 12.68 (s) ppm.

**HRMS:** Calcd: 462.09, found: 463.2427.

a)  $^1\text{H}$  NMR of compound **5.3**:

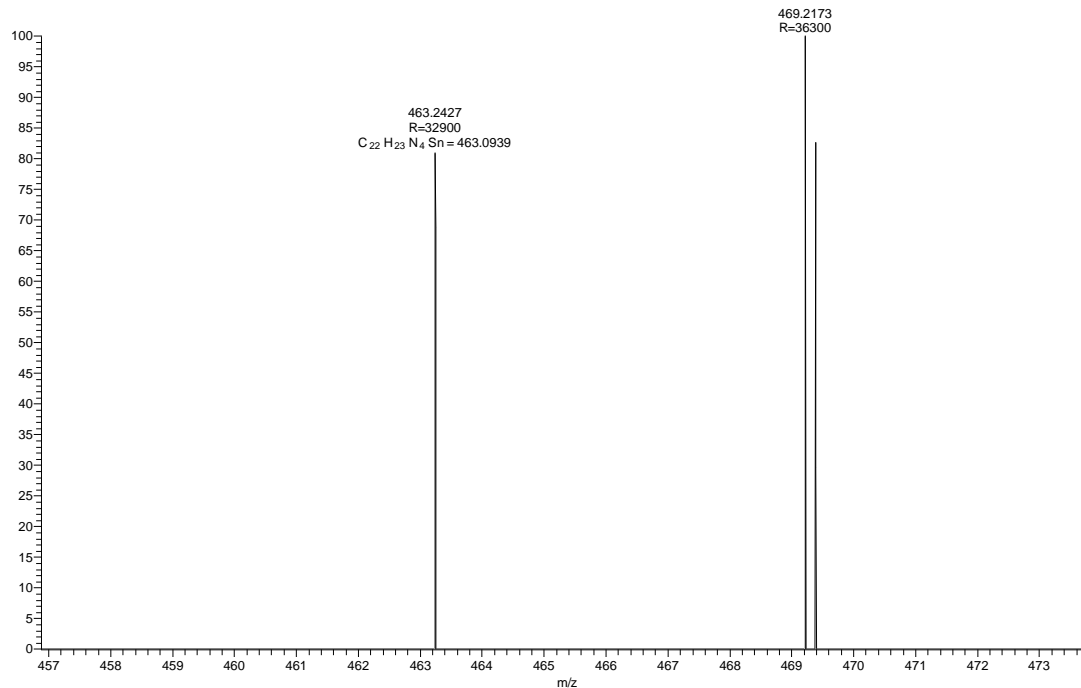


b)  $^{13}\text{C}$  NMR of compound **5.3**:



**c) HRMS data of compound 5.3:**

SP-OD #151 RT: 1.04 AV: 1 NL: 1.98E3  
T: FTMS + p ESI Full ms [100.0000-1500.0000]



**6.4.1.6. Synthesis and characterization of compound 5.4**

A solution of potassium tris(trimethylsilyl)silane (324.38 mg, 0.753 mmol in 10 mL toluene) was added to a solution of compound **3.2** (200 mg, 0.717 mmol in 15 mL toluene) at  $-78\text{ }^{\circ}\text{C}$  over a period of 15 min and the color changes slowly from pale yellow to deep red. Then the reaction mixture was allowed to warm up to room temperature and further stirred for 12 h. Subsequently, all volatiles were removed in vacuo and the residue was extracted into toluene (15 mL). The resultant toluene was concentrated to 5-8 mL and stored at  $-30\text{ }^{\circ}\text{C}$  in a freezer, which afforded colorless crystals of **5.4** within two-three days.

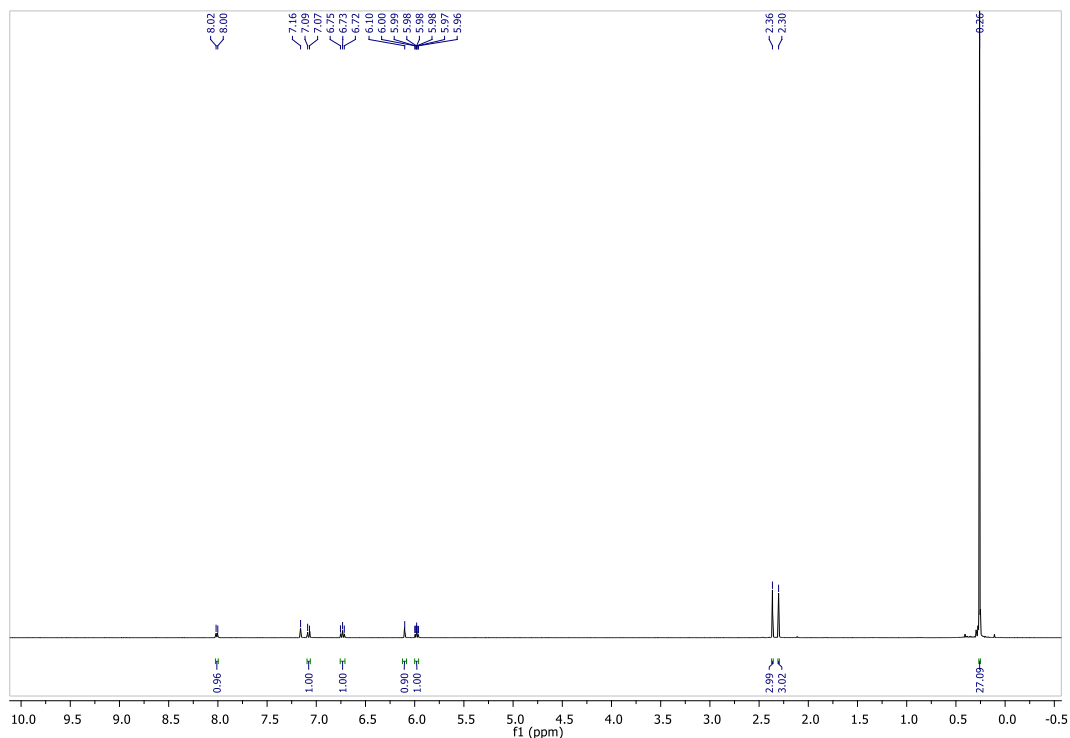
**Yield:** 330 mg (93 %).

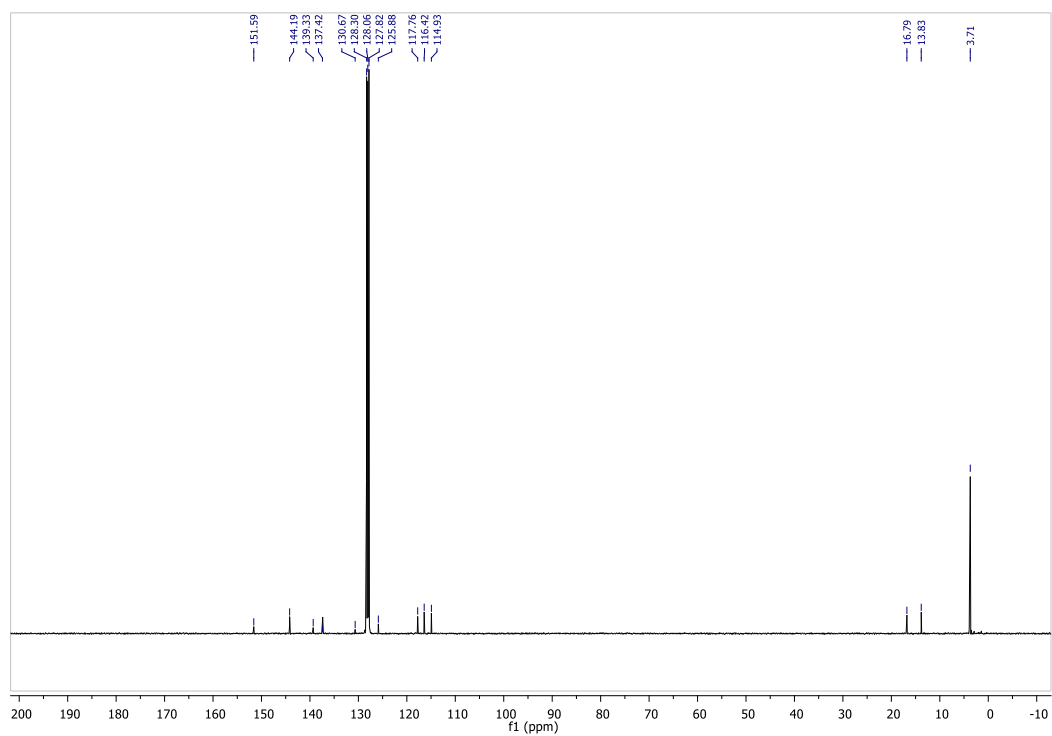
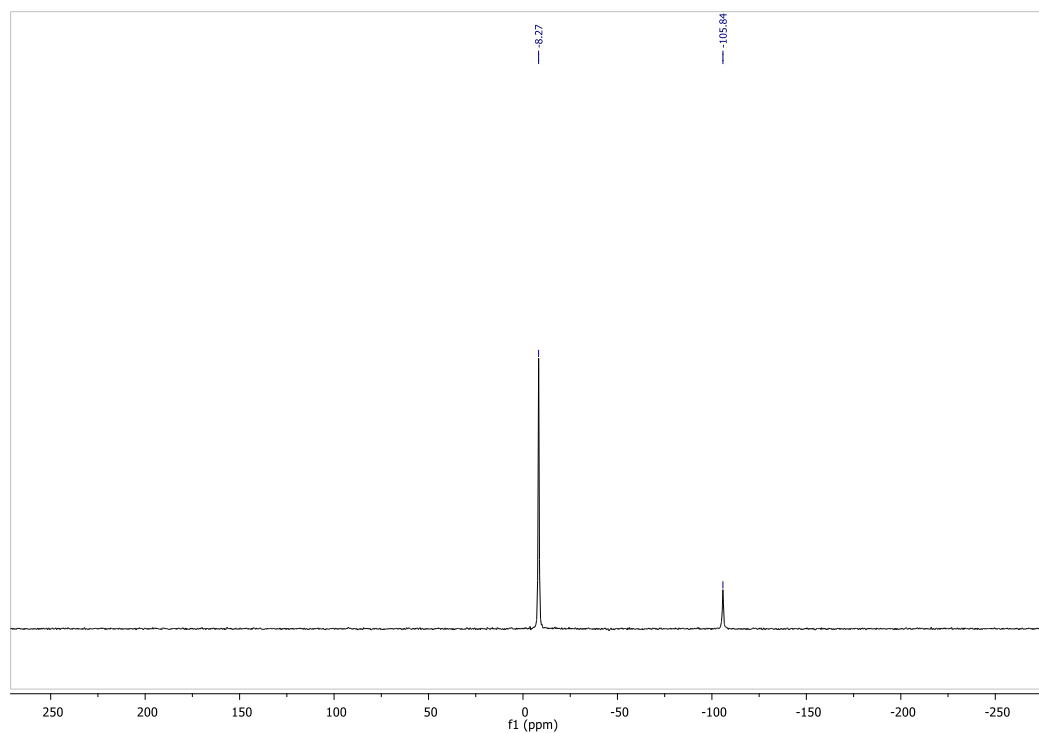
**Mp:** 128.3  $^{\circ}\text{C}$ .

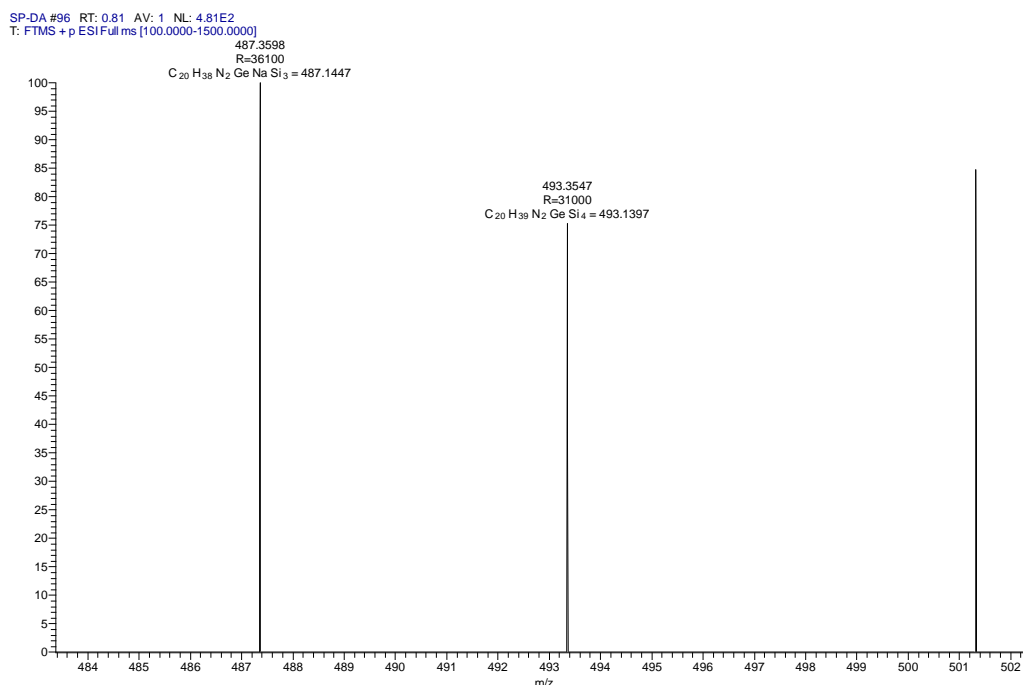
**NMR:**  $^1\text{H}$  NMR (400 MHz,  $\text{C}_6\text{D}_6$ , 298 K):  $\delta$  8.01 (d, 1H), 7.08 (d, 1H), 6.73 (t, 1H), 6.10 (s, 1H), 5.98 (dt, 1H), 2.36 (s, 3H), 2.30 (s, 3H), 0.26 (s, 27H) ppm.  $^{13}\text{C}$  NMR (100.56 MHz,  $\text{C}_6\text{D}_6$ , 298 K):  $\delta$  151.59 (s), 144.19 (s), 139.33 (s), 137.42 (s), 130.67 (s), 125.88 (s), 117.76 (s), 116.42 (s), 114.93 (s), 16.79 (s), 13.83 (s), 3.71 (s) ppm.  $^{29}\text{Si}$  CP/MAS NMR (298 K):  $\delta$  -105.84 ( $\text{Si}(\text{SiMe}_3)$ ), -8.27 ( $\text{Si}(\text{SiMe}_3)$ ) ppm.

**HRMS:** Calcd: 492.13, found: 493.3547.

**a)  $^1\text{H}$  NMR of compound 5.4:**



**b)  $^{13}\text{C}$  NMR of compound 5.4:****c) Solid state  $^{29}\text{Si}$  NMR (CP/MAS) of compound 5.4:****d) HRMS data of compound 5.4:**



#### 6.4.1.7. Synthesis and characterization of compound 5.5

A solution of potassium tris(trimethylsilyl)silane (277.97 mg, 0.645 mmol in 10 mL toluene) was added to a solution of compound **5.1** (200 mg, 0.614 mmol in 15 mL toluene) at  $-78\text{ }^{\circ}\text{C}$  over a period of 15-20 min and the reaction mixture was allowed to warm up to room temperature. The color of the reaction mixture changes slowly from yellow to deep red. Further, the reaction was stirred for additional 12 h. Subsequently, all volatiles were removed in vacuo and the residue was extracted into toluene (15 mL). The resultant toluene solvent was concentrated to 5-8 mL and stored at  $-30\text{ }^{\circ}\text{C}$  in a freezer, which afforded colorless crystals of **5.5** within two days.

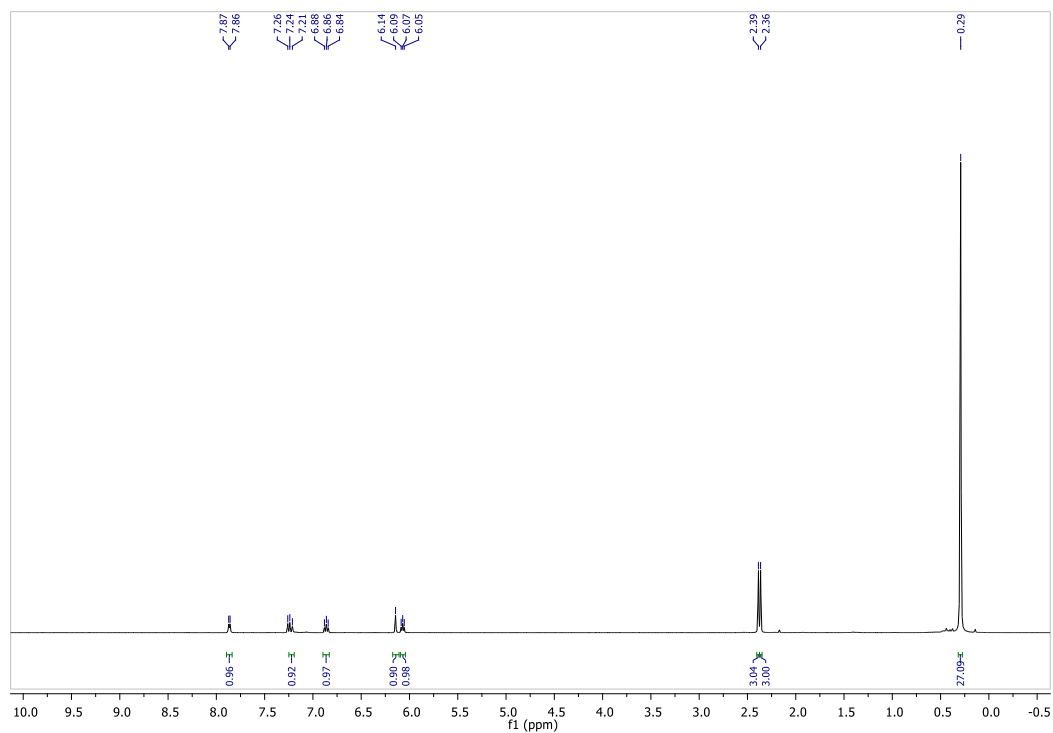
**Yield:** 312 mg (94 %).

**Mp:**  $138.9\text{ }^{\circ}\text{C}$ .

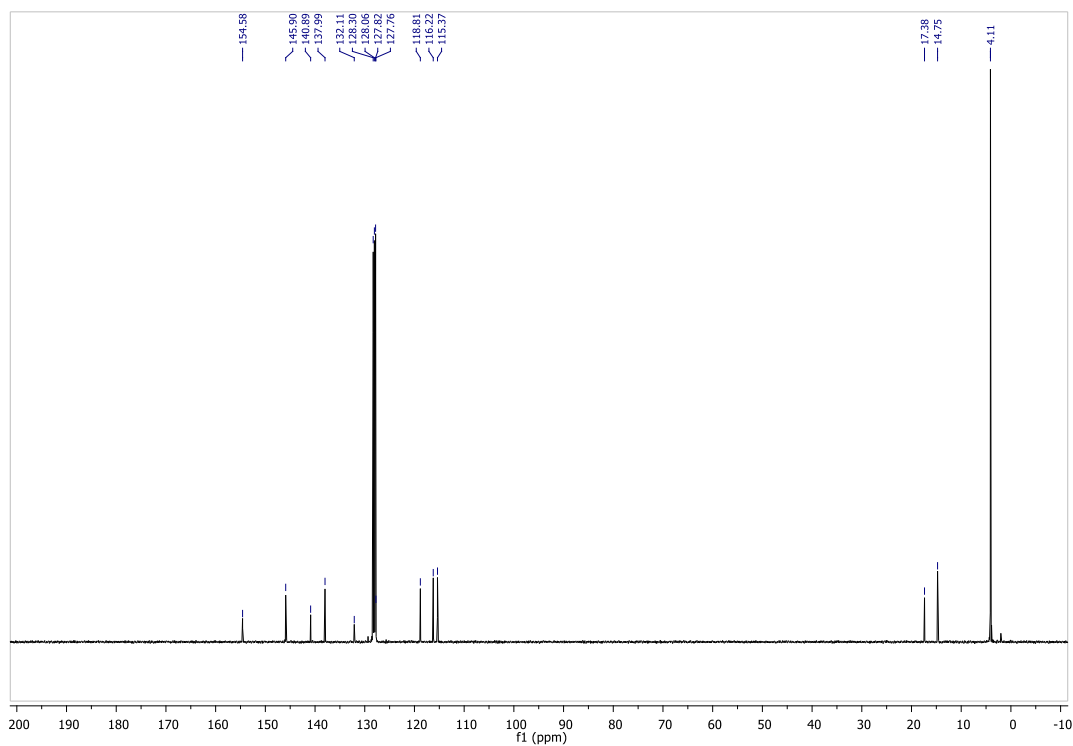
**NMR:**  $^1\text{H}$  NMR (400 MHz,  $\text{C}_6\text{D}_6$ , 298 K):  $\delta$  7.86 (d, 1H), 7.23 (d, 1H), 6.86 (t, 1H), 6.14 (s, 1H), 6.07 (t, 1H), 2.39 (s, 3H), 2.36 (s, 3H), 0.29 (s, 27H) ppm.  $^{13}\text{C}$  NMR (100.56 MHz,  $\text{C}_6\text{D}_6$ , 298 K):  $\delta$  154.58 (s), 145.90 (s), 140.89 (s), 137.99 (s), 132.11 (s), 128.30 (s), 127.76 (s), 118.81 (s), 116.22 (s), 115.37 (s), 17.38 (s), 14.75 (s), 4.11 (s) ppm.  $^{29}\text{Si}$  CP/MAS NMR (298 K):  $\delta$  -99.86 (Si(SiMe<sub>3</sub>)), -6.28 (Si(SiMe<sub>3</sub>)) ppm.

**HRMS:** Calcd: 538.11, found: 539.032.

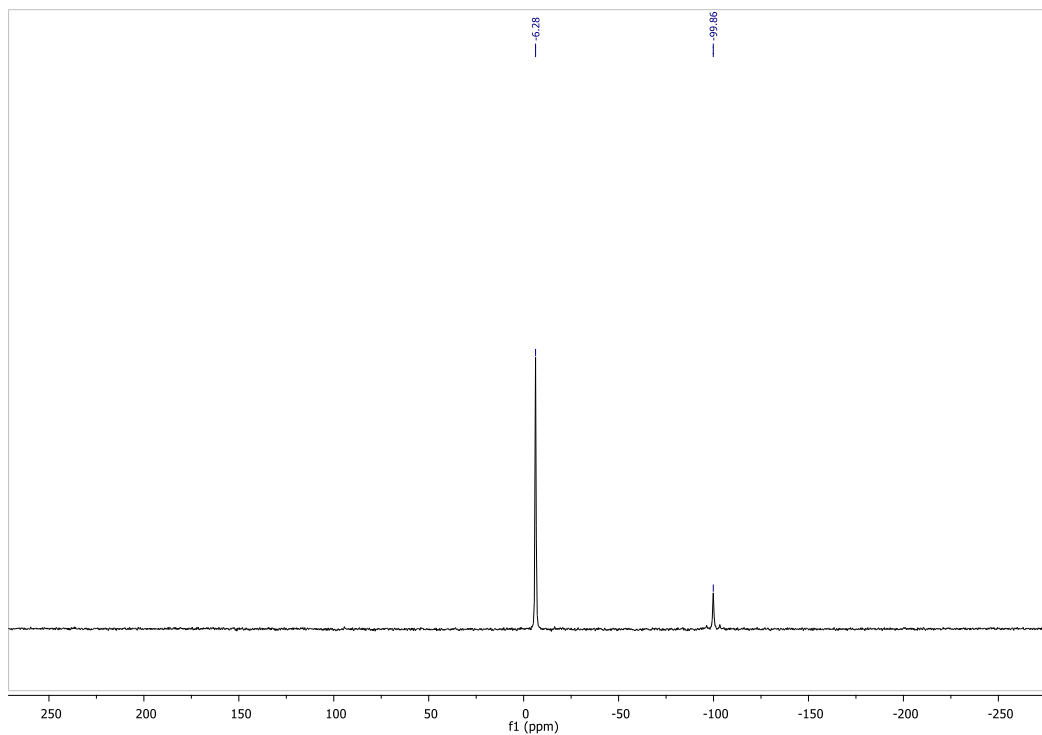
a)  $^1\text{H}$  NMR of compound **5.5**:



b) <sup>13</sup>C NMR of compound 5.5:

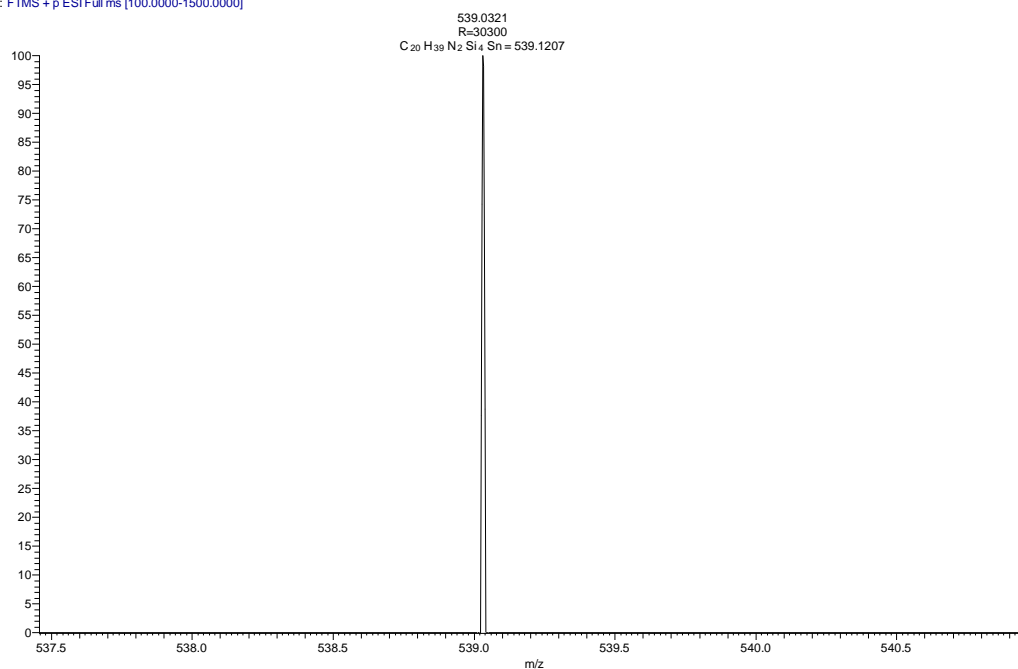


c) Solid state <sup>29</sup>Si NMR (CP/MAS) of compound 5.5:



**d) HRMS data of compound 5.5:**

SP-OE #206 RT: 1.68 AV: 1 NL: 5.27E3  
T: FTMS + p ESI Full ms [100.0000-1500.0000]



**6.4.1.8. Synthesis and characterization of compound 5.6**



A 10 mL toluene solution of pentafluoropyridine (70.07 mg, 0.415 mmol) was added to a solution of compound **5.4** (200 mg, 0.406 mmol in toluene 10 mL) at  $-30\text{ }^{\circ}\text{C}$  over a period of 10 min and the reaction mixture was allowed to warm up to room temperature and further stirred for 15 h. Subsequently, all volatiles were removed in vacuo and the residue was extracted into toluene (15 mL). The resultant toluene solvent was concentrated to 5-8 mL and stored at  $-30\text{ }^{\circ}\text{C}$  in a freezer, which afforded colorless crystals of **5.6** within a week.

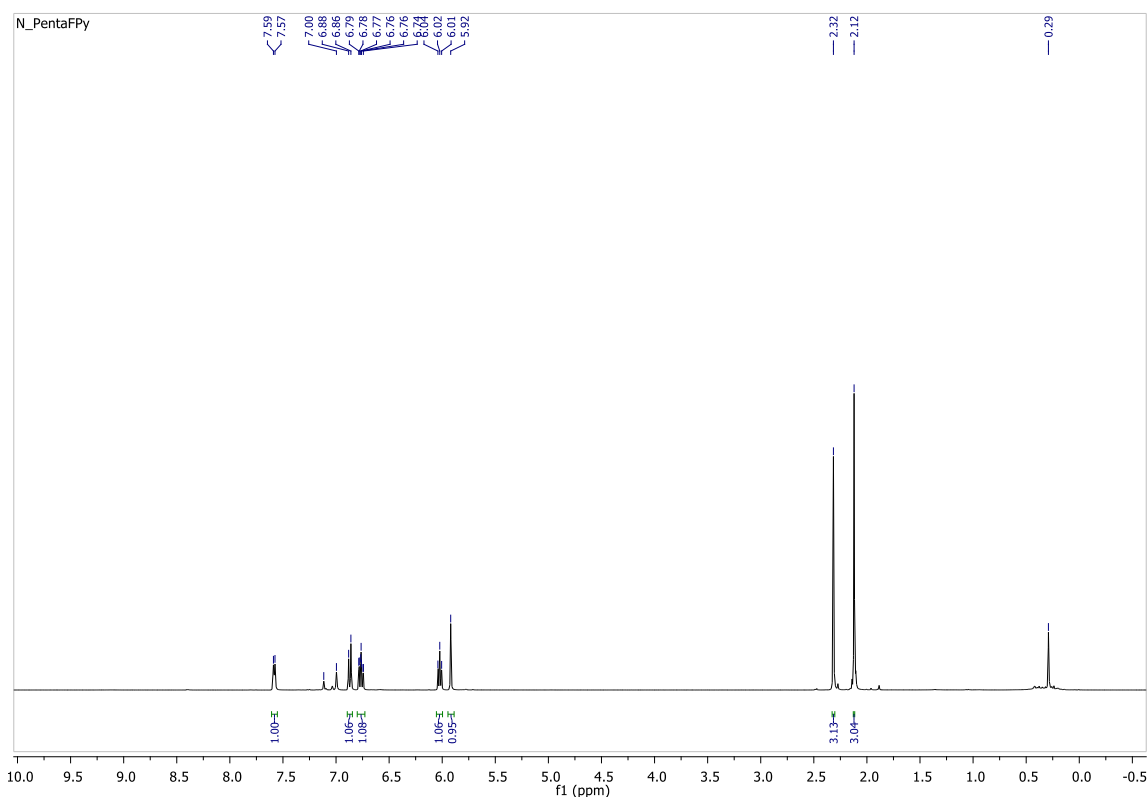
**Yield:** 148 mg (91 %).

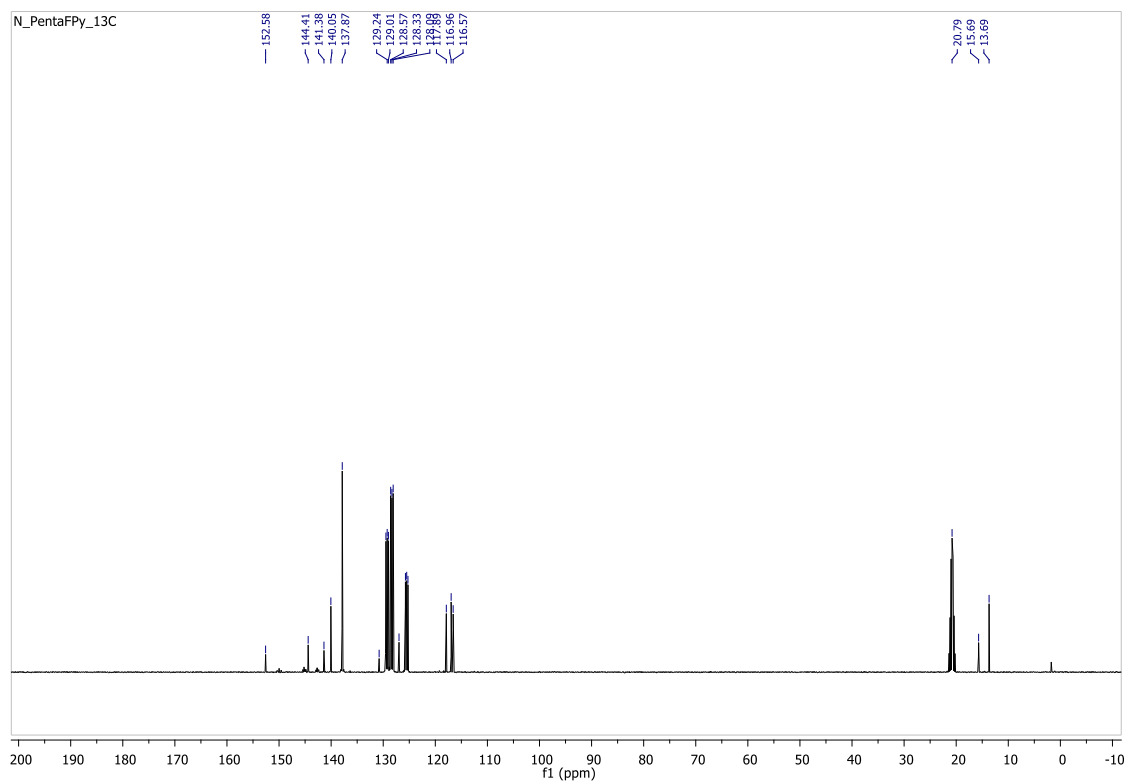
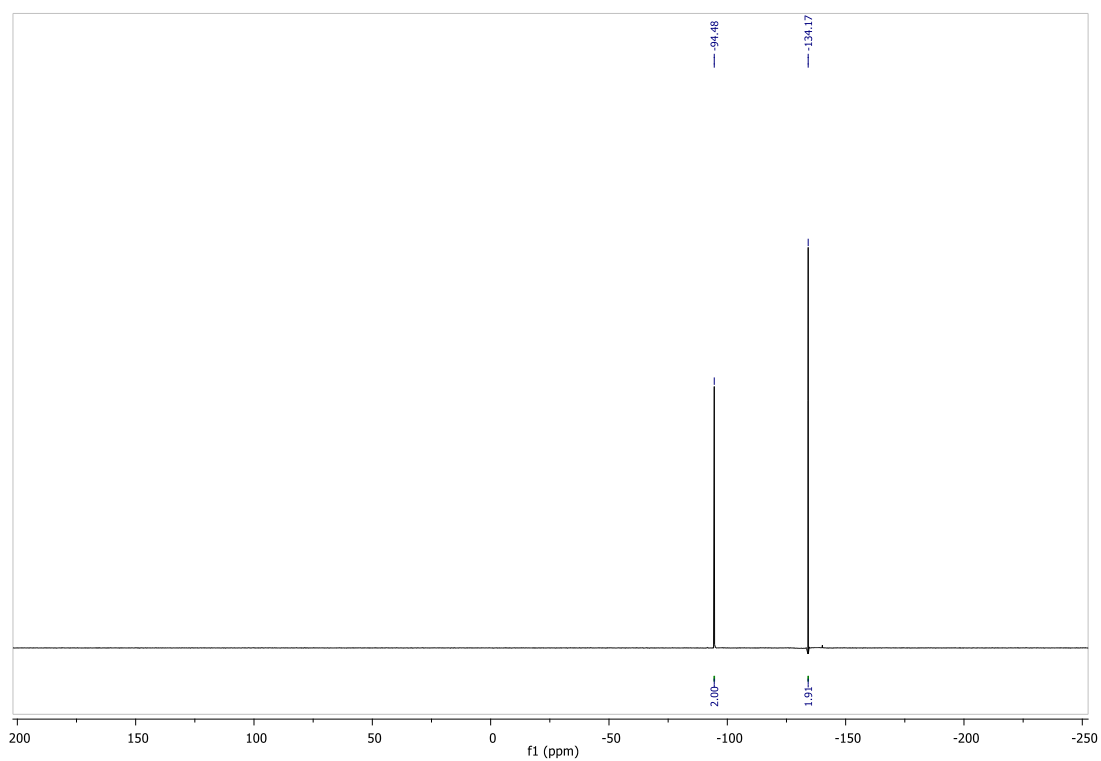
**Mp:** 155.6  $^{\circ}\text{C}$ .

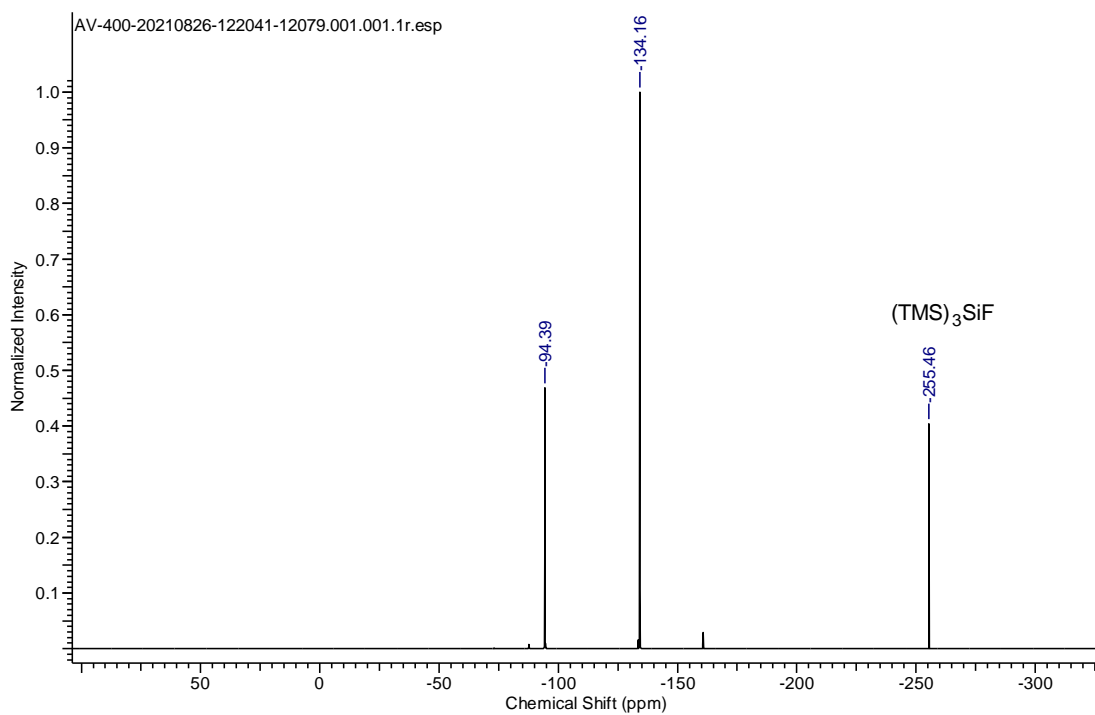
**NMR:**  $^1\text{H}$  NMR (400 MHz, toluene- $d_8$ , 298 K):  $\delta$  7.58 (1 H, d), 6.87 (d, 1H), 6.76 (dt, 1H), 6.02 (t, 1H), 5.92 (s, 1H), 2.32 (s, 3H), 2.12 (s, 3H) ppm.  $^{13}\text{C}$  NMR (100.56 MHz, toluene- $d_8$ , 298 K);  $\delta$  152.58 (s), 144.41 (s), 141.38 (s), 140.05 (s), 137.87 (s), 130.78 (s), 126.97 (s), 125.73 (s), 125.49 (s), 125.25 (s), 117.89 (s), 116.96 (s), 116.57 (s), 20.79 (s), 15.69 (s), 13.69 (s) ppm.  $^{19}\text{F}$  NMR (376 MHz, toluene- $d_8$ , 298 K):  $\delta$  -94.48 (*o*-F), -134.17 (*m*-F) ppm.

**HRMS:** Calcd: 395.01, found: 396.0174.

a)  $^1\text{H}$  NMR of compound **5.6**:

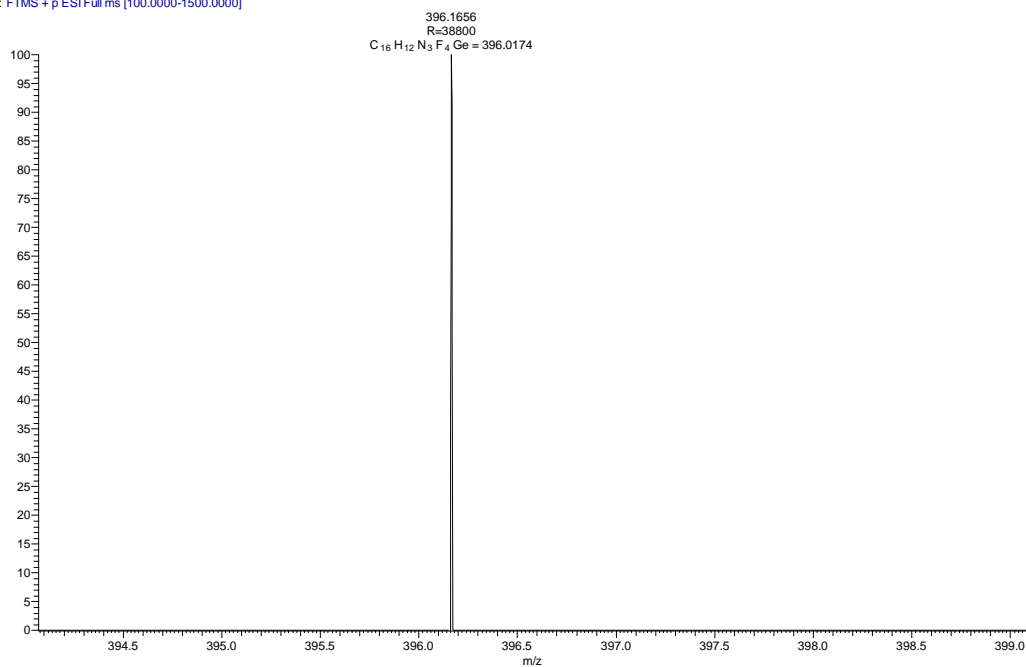


**b)  $^{13}\text{C}$  NMR of compound 5.6:****c)  $^{19}\text{F}$  NMR of compound 5.6:**

d)  $^{19}\text{F}$  NMR of reaction mixture:

## e) HRMS data of compound 5.6:

SP-OC #230 RT: 1.71 AV: 1 NL: 1.09E4  
T: FTMS + p ESI Full ms [100.0000-1500.0000]



## 6.4.2. Crystallographic data for the structural analysis of compounds 5.1-5.6

**6.4.2.1. Crystal data of compound 5.1:**  $C_{11}H_{11}ClSn$ ,  $M = 321.36$ , Colorless, block,  $0.15 \times 0.12 \times 0.08 \text{ mm}^3$ , triclinic, space group ' $P-1$ ',  $a = 8.05(5)\text{\AA}$ ,  $b = 9.04(6)\text{\AA}$ ,  $c = 9.04(7)\text{\AA}$ ,  $\alpha = 112.1(3)^\circ$ ,  $\beta = 105.4(2)^\circ$ ,  $\gamma = 97.0(3)^\circ$ , Volume =  $570(7)\text{\AA}^3$ ,  $Z = 2$ ,  $T = 100(2)$ ,  $D_{calc} (\text{g cm}^{-3}) = 1.872$ ,  $F(000) = 312$ ,  $\mu (\text{mm}^{-1}) = 2.437$ , 26604 reflections collected, 2339 unique reflections ( $R_{int} = 0.0699$ ), 2163 observed ( $I > 2\sigma(I)$ ) reflections, multi-scan absorption correction,  $T_{min} = 0.5829$ ,  $T_{max} = 0.7454$ , 138 refined parameters,  $S = 1.113$ ,  $R1 = 0.0282$ ,  $wR2 = 0.0760$  (all data  $R = 0.0320$ ,  $wR2 = 0.0779$ ), maximum and minimum residual electron densities;  $\Delta\rho_{max} = 1.01$ ,  $\Delta\rho_{min} = -0.71 (\text{e}\text{\AA}^{-3})$ .

**6.4.2.2. Crystal data of compound 5.2:**  $C_{15}H_{19}N_2SnCl$ ,  $M = 381.46$ , Colorless, block,  $0.12 \times 0.10 \times 0.08 \text{ mm}^3$ , monoclinic, space group ' $P2_1/n$ ',  $a = 8.713(4)\text{\AA}$ ,  $b = 14.390(6)\text{\AA}$ ,  $c = 12.347(5)\text{\AA}$ ,  $\alpha = 90^\circ$ ,  $\beta = 101.929(16)^\circ$ ,  $\gamma = 90^\circ$ , Volume =  $1514.7(11)\text{\AA}^3$ ,  $Z = 4$ ,  $T = 100(2)$ ,  $D_{calc} (\text{g cm}^{-3}) = 1.637$ ,  $F(000) = 760$ ,  $\mu (\text{mm}^{-1}) = 1.852$ , 69227 reflections collected, 2655 unique reflections ( $R_{int} = 0.0582$ ), 2497 observed ( $I > 2\sigma(I)$ ) reflections, multi-scan absorption correction,  $T_{min} = 0.5704$ ,  $T_{max} = 0.7464$ , 175 refined parameters,  $S = 1.360$ ,  $R1 = 0.0281$ ,  $wR2 = 0.0873$  (all data  $R = 0.0321$ ,  $wR2 = 0.1000$ ), maximum and minimum residual electron densities;  $\Delta\rho_{max} = 0.96$ ,  $\Delta\rho_{min} = -1.22 (\text{e}\text{\AA}^{-3})$ .

**6.4.2.3. Crystal data of compound 5.3:**  $C_{22}H_{22}N_4Sn$ ,  $M = 461.15$ , Yellow, Plate,  $0.31 \times 0.28 \times 0.27 \text{ mm}^3$ , triclinic, space group ' $P-1$ ',  $a = 11.9136(7)\text{\AA}$ ,  $b = 12.1859(7)\text{\AA}$ ,  $c = 13.5673(8)\text{\AA}$ ,  $\alpha = 91.477(2)^\circ$ ,  $\beta = 103.126(2)^\circ$ ,  $\gamma = 90.790(2)^\circ$ , Volume =  $1917.18(19)\text{\AA}^3$ ,  $Z = 4$ ,  $T = 100(2)$ ,  $D_{calc} (\text{g cm}^{-3}) = 1.598$ ,  $F(000) = 928$ ,  $\mu (\text{mm}^{-1}) = 1.347$ , 41117 reflections collected, 8809 unique reflections ( $R_{int} = 0.0585$ ), 7299 observed ( $I > 2\sigma(I)$ ) reflections, multi-scan absorption correction,  $T_{min} = 0.665$ ,  $T_{max} = 0.695$ , 504 refined parameters,  $S = 1.268$ ,  $R1 = 0.0491$ ,  $wR2 = 0.1004$  (all data  $R = 0.0633$ ,  $wR2 = 0.1004$ ), maximum and minimum residual electron densities;  $\Delta\rho_{max} = 0.96$ ,  $\Delta\rho_{min} = -0.90 (\text{e}\text{\AA}^{-3})$ .

**6.4.2.4. Crystal data of compound 5.4:**  $C_{20}H_{38}GeN_2Si_4$ ,  $M = 491.49$ , Orange, Block,  $0.36 \times 0.32 \times 0.29 \text{ mm}^3$ , triclinic, space group ' $P-1$ ',  $a = 8.7746(3)\text{\AA}$ ,  $b = 9.7135(4)\text{\AA}$ ,  $c = 17.1214(7)\text{\AA}$ ,  $\alpha = 77.682(1)^\circ$ ,  $\beta = 83.909(1)^\circ$ ,  $\gamma = 69.398(1)^\circ$ , Volume =  $1333.75(9)\text{\AA}^3$ ,  $Z = 2$ ,  $T = 100.0$ ,  $D_{calc} (\text{g cm}^{-3}) = 1.224$ ,  $F(000) = 520$ ,  $\mu (\text{mm}^{-1}) = 1.337$ , 26560 reflections collected, 8173 unique reflections ( $R_{int} = 0.0281$ ), 7294 observed ( $I > 2\sigma(I)$ ) reflections, multi-scan absorption correction,  $T_{min} = 0.624$ ,  $T_{max} = 0.679$ , 256 refined parameters,  $S = 1.024$ ,  $R1 = 0.0281$ ,  $wR2 = 0.0718$  (all data

$R = 0.0324$ ,  $wR2 = 0.0743$ ), maximum and minimum residual electron densities;  $\Delta\rho_{\max} = 0.69$ ,  $\Delta\rho_{\min} = -0.52$  ( $\text{e}\text{\AA}^{-3}$ ).

**6.4.2.5. Crystal data of compound 5.5:**  $\text{C}_{20}\text{H}_{38}\text{N}_2\text{Si}_4\text{Sn}$ ,  $M = 537.57$ , Red, Block,  $0.12 \times 0.09 \times 0.08$   $\text{mm}^3$ , triclinic, space group ' $P-1$ ',  $a = 8.930(3)\text{\AA}$ ,  $b = 9.723(3)\text{\AA}$ ,  $c = 17.277(5)\text{\AA}$ ,  $\alpha = 78.349(14)^\circ$ ,  $\beta = 84.063(9)^\circ$ ,  $\gamma = 68.696(11)^\circ$ , Volume =  $1368.0(7)\text{\AA}^3$ ,  $Z = 2$ ,  $T = 293.15$ ,  $D_{\text{calc}}$  ( $\text{g cm}^{-3}$ ) =  $1.305$ ,  $F(000) = 556$ ,  $\mu$  ( $\text{mm}^{-1}$ ) =  $1.117$ , 75997 reflections collected, 6779 unique reflections ( $R_{\text{int}} = 0.0566$ ), 6418 observed ( $I > 2\sigma(I)$ ) reflections, multi-scan absorption correction,  $T_{\min} = 0.6602$ ,  $T_{\max} = 0.7457$ , 255 refined parameters,  $S = 1.231$ ,  $R1 = 0.0196$ ,  $wR2 = 0.0548$  (all data  $R = 0.0226$ ,  $wR2 = 0.0636$ ), maximum and minimum residual electron densities;  $\Delta\rho_{\max} = 0.90$ ,  $\Delta\rho_{\min} = -0.82$  ( $\text{e}\text{\AA}^{-3}$ ).

**6.4.2.6. Crystal data of compound 5.6:**  $\text{C}_{16}\text{H}_{11}\text{F}_4\text{GeN}_3$ ,  $M = 393.89$ , Yellow, Plate,  $0.34 \times 0.32 \times 0.29$   $\text{mm}^3$ , triclinic, space group ' $P-1$ ',  $a = 7.8354(7)\text{\AA}$ ,  $b = 11.7342(10)\text{\AA}$ ,  $c = 16.9181(16)\text{\AA}$ ,  $\alpha = 83.968(3)^\circ$ ,  $\beta = 84.442(3)^\circ$ ,  $\gamma = 75.253(2)^\circ$ , Volume =  $1491.9(2)\text{\AA}^3$ ,  $Z = 4$ ,  $T = 100(2)$ ,  $D_{\text{calc}}$  ( $\text{g cm}^{-3}$ ) =  $1.754$ ,  $F(000) = 784$ ,  $\mu$  ( $\text{mm}^{-1}$ ) =  $2.101$ , 85931 reflections collected, 9196 unique reflections ( $R_{\text{int}} = 0.0339$ ), 7369 observed ( $I > 2\sigma(I)$ ) reflections, multi-scan absorption correction,  $T_{\min} = 0.494$ ,  $T_{\max} = 0.544$ , 437 refined parameters,  $S = 1.045$ ,  $R1 = 0.0339$ ,  $wR2 = 0.0722$  (all data  $R = 0.0503$ ,  $wR2 = 0.0800$ ), maximum and minimum residual electron densities;  $\Delta\rho_{\max} = 0.81$ ,  $\Delta\rho_{\min} = -0.74$  ( $\text{e}\text{\AA}^{-3}$ ).

### 6.4.3. General procedure for catalytic hydroboration

Substrate (0.25 mmol), pinacolborane (0.25 mmol), catalyst **5.5** (5 mol%) were charged in Schlenk tube inside glove box. The reaction mixture was allowed to run at room temperature in neat condition. The progress of the reaction was monitored by  $^1\text{H}$  NMR, which indicated the completion of the reaction by the appearance of a new  $\text{CH}_2$  (aldehyde and alkene)/ $\text{CH}$  (ketone and alkyne) peak. Upon completion of reaction mesitylene (0.25 mmol) as internal standard, was added while making the NMR in  $\text{CDCl}_3$ .

#### 6.4.3.1. Spectroscopic data for hydroborated products

**2-(benzyloxy)-pinacolborane (1a):**  $^1\text{H}$  NMR (400 MHz,  $\text{CDCl}_3$ , 298 K):  $\delta$  7.32 – 7.16 (5 H, m), 6.74 (3 H, s), 4.87 (2 H, s), 2.21 (9 H, s), 1.20 (12 H, s) ppm;  $^{13}\text{C}$  NMR (101 MHz,  $\text{CDCl}_3$ , 298 K):  $\delta$  137.74 (s), 128.35 (s), 127.43 (s), 126.99 (s), 83.14 (s), 66.75 (s), 25.09 (s) ppm.

**2-((4-methylbenzyl)oxy)-pinacolborane (1b):**  $^1\text{H}$  NMR (400 MHz,  $\text{CDCl}_3$ , 298 K):  $\delta$  7.35 (2 H, d), 6.93 (2 H, d), 6.87 (3 H, s), 4.93 (2 H, s), 3.83 (3 H, s), 2.35 (9 H, s), 1.33 (12 H, s) ppm;  $^{13}\text{C}$  NMR (101 MHz,  $\text{CDCl}_3$ , 298 K):  $\delta$  137.56 (s), 131.43 (s), 128.48 (s), 126.88 (s), 82.78 (s), 66.40 (s), 55.07 (s), 24.54 (s), 21.13 (s) ppm.

**2-(4-dimethylaminobenzyloxy)-pinacolborane (1c):**  $^1\text{H}$  NMR (400 MHz,  $\text{CDCl}_3$ , 298 K):  $\delta$  7.70 (2 H, d), 7.15 (2 H, d), 5.29 (2 H, s), 3.49 (1 H, s), 3.37 (6 H, s), 2.74 (9H, s), 1.72 (12 H, s) ppm;  $^{13}\text{C}$  NMR (101 MHz,  $\text{CDCl}_3$ , 298 K):  $\delta$  137.63 (s), 128.36 (s), 126.81 (s), 82.81 (s), 66.66 (s), 40.50 (s), 24.52 (s), 21.08 (s) ppm.

**2-(4-bromobenzyloxy)-pinacolborane (1d):**  $^1\text{H}$  NMR (400 MHz,  $\text{CDCl}_3$ , 298 K):  $\delta$  7.51 (2 H, d), 7.31 – 7.25 (2 H, m), 6.86 (3 H, s), 4.93 (2 H, s), 2.35 (9 H, s), 1.33 (12 H, s) ppm;  $^{13}\text{C}$  NMR (101 MHz,  $\text{CDCl}_3$ , 298 K):  $\delta$  137.95 (s), 137.26 (s), 131.04 (s), 128.07 (s), 126.59 (s), 120.87 (s), 82.69 (s), 65.61 (s), 24.26 (s) ppm.

**2-(4-nitrobenzyloxy)-pinacolborane (1e):**  $^1\text{H}$  NMR (400 MHz,  $\text{CDCl}_3$ , 298 K):  $\delta$  8.20 (2 H, d), 7.51 (2 H, d), 6.81 (3 H, s), 5.04 (2 H, s), 2.29 (9 H, s), 1.30 (12 H, d) ppm;  $^{13}\text{C}$  NMR (101 MHz,  $\text{CDCl}_3$ , 298 K):  $\delta$  137.43 (s), 126.68 (s), 126.66(s), 123.35 (s), 83.06 (s), 24.35 (s), 20.97 (s) ppm.

**2-(benzhydryloxy)-pinacolborane (1f):**  $^1\text{H}$  NMR (400 MHz,  $\text{CDCl}_3$ , 298 K):  $\delta$  7.47 (5 H, d), 7.36 (4 H, t, ), 7.29 (2 H, d), 6.87 (3 H, s), 6.28 (1 H, s), 2.35 (9 H, s), 1.33 (6 H, s), 1.27 (12 H, s) ppm;  $^{13}\text{C}$  NMR (101 MHz,  $\text{CDCl}_3$ , 298 K):  $\delta$  143.51 (s), 137.99 (s), 128.59 (s), 127.65 (s), 127.28 (s), 126.86 (s), 83.30 (s), 78.29 (s), 25.23 (s), 24.86 (s), 21.55 (s) ppm.

**2-(2-chlorobenzhydryloxy)-pinacolborane (1g):**  $^1\text{H}$  NMR (400 MHz,  $\text{CDCl}_3$ , 298 K):  $\delta$  7.68 (1 H, d), 7.40 (2 H, d), 7.20 (6 H, ddd), 6.78 (3 H, s), 6.57 (1 H, s), 2.25 (9 H, s), 1.24 (6 H, s), 1.17 (12 H, s) ppm;  $^{13}\text{C}$  NMR (101 MHz,  $\text{CDCl}_3$ , 298 K):  $\delta$  140.59 (s), 137.71 (s), 129.35 (s), 128.60 (s), 128.18 (d), 127.60 (s), 127.20 – 126.88 (m), 83.12 (s), 74.49 (s), 24.94 (s), 24.54 (d), 21.25 (s) ppm.

**2-(1-phenylethoxy)-pinacolborane (1h):**  $^1\text{H}$  NMR (400 MHz,  $\text{CDCl}_3$ , 298 K):  $\delta$  7.51 (2 H, d), 7.31 – 7.25 (2 H, m), 6.86 (3 H, s), 4.93 (2 H, s), 2.35 (9 H, s), 1.33 (12 H, s) ppm;  $^{13}\text{C}$  NMR (101 MHz,  $\text{CDCl}_3$ , 298 K):  $\delta$  138.02 (s), 128.56 (s), 127.29 (s), 125.70 (s), 83.07 (s), 73.05 (s), 25.82 (s), 24.87 (s), 21.55 (s) ppm.

**2-(1-(4-fluorophenyl)ethoxy)-pinacolborane (1i) :**  $^1\text{H}$  NMR (400 MHz,  $\text{CDCl}_3$ , 298 K):  $\delta$  7.39 (2 H, dd), 7.10 (2 H, d), 6.86 (3 H, s), 5.29 (1 H, q), 2.62 (1 H, s), 2.33 (9 H, s), 1.53 (3 H, d), 1.30

(12 H, s) ppm;  $^{13}\text{C}$  NMR (101 MHz,  $\text{CDCl}_3$ , 298 K):  $\delta$  C (101 MHz,  $\text{CDCl}_3$ , 298 K)  $\delta$  160.91 (s), 140.51 (s), 137.82 (s), 131.09 (d), 127.07 (s), 115.00 (s), 72.18 (s), 25.55 (s), 24.63 (s), 21.32 (s) ppm.

**2-(1-(4-nitrophenyl)ethoxy)-pinacolborane (1j):**  $^1\text{H}$  NMR (400 MHz,  $\text{CDCl}_3$ , 298 K):  $\delta$  8.37 – 8.05 (2 H, m), 7.54 (2 H, d), 6.82 (3 H, s), 5.35 (1 H, q), 2.67 (1 H, s), 2.30 (9 H, s), 1.53 (2 H, d), 1.29 (12 H, s), 1.26 (6 H, d) ppm;  $^{13}\text{C}$  NMR (101 MHz,  $\text{CDCl}_3$ , 298 K):  $\delta$  137.64 (s), 126.91 (s), 126.11 (s), 123.57 (s), 83.10 (s), 25.27 (s), 24.52 (s), 21.17 (s) ppm.

**4,4,5,5-tetramethyl-2-phenethyl-1,3,2-dioxaborolane (2a):**  $^1\text{H}$  NMR (400 MHz,  $\text{CDCl}_3$ , 298 K):  $\delta$  7.34 – 7.12 (5 H, m), 6.83 (3 H, s), 2.80 (2 H, t), 2.31 (9 H, s), 1.30 (6 H, s), 1.25 (6 H, s), 1.19 (2 H, t) ppm;  $^{13}\text{C}$  NMR (101 MHz,  $\text{CDCl}_3$ , 298 K):  $\delta$  138.02 (s), 128.39 (s), 127.30 (s), 125.88 (s), 83.41 (s), 30.37 (s), 25.25 (s), 21.56 (s) ppm.

**4,4,5,5-tetramethyl-2-(4-methylphenethyl)-1,3,2-dioxaborolane (2b):**  $^1\text{H}$  NMR (400 MHz,  $\text{CDCl}_3$ , 298 K):  $\delta$  7.20 (4 H, dd), 6.91 (3 H, s), 2.87 – 2.79 (2 H, t), 2.41 (3 H, s), 2.39 (9 H, s), 1.37 (6 H, s), 1.33 (6 H, s), 1.27 – 1.21 (2 H, t) ppm;  $^{13}\text{C}$  NMR (101 MHz,  $\text{CDCl}_3$ , 298 K):  $\delta$  138.00 (s), 129.24 (s), 128.24 (s), 127.30 (s), 83.38 (s), 29.92 (s), 25.20 (d), 24.90 (s), 21.55 (s) ppm.

**2-(4-methoxyphenethyl)-4,4,5,5-tetramethyl-1,3,2-dioxaborolane (2c):**  $^1\text{H}$  NMR (400 MHz,  $\text{CDCl}_3$ , 298 K):  $\delta$  7.21 (2 H, d), 6.90 (2 H, s), 6.87 (3 H, s), 3.83 (3 H, s), 2.83 – 2.75 (2 H, t), 2.36 (9 H, s), 1.35 (6 H, s), 1.30 (6 H, s), 1.24 – 1.17 (2 H, t) ppm;  $^{13}\text{C}$  NMR (101 MHz,  $\text{CDCl}_3$ , 298 K):  $\delta$  157.66 (s), 137.70 (s), 136.59 (s), 128.92 (s), 126.97 (s), 83.06 (s), 55.18 (s), 29.14 (s), 24.85 (s), 21.23 (s) ppm.

**2-(4-(tert-butoxy)phenethyl)-4,4,5,5-tetramethyl-1,3,2-dioxaborolane (2d):**  $^1\text{H}$  NMR (400 MHz,  $\text{CDCl}_3$ , 298 K):  $\delta$  7.15 (2 H, d), 6.93 (2 H, d), 6.84 (3 H, s), 2.77 (2 H, t), 2.32 (9 H, s), 1.36 (6 H, s), 1.31 (6 H, s), 1.26 (9 H, d), 1.22 – 1.15 (2 H, t) ppm;  $^{13}\text{C}$  NMR (101 MHz,  $\text{CDCl}_3$ , 298 K):  $\delta$  153.08 (s), 139.28 (s), 137.72 (s), 128.40 (s), 126.98 (s), 124.08 (s), 83.29 (s), 83.06 (s), 81.95 (s), 28.89 (s), 24.89 (d), 24.58 (s), 22.78 (s), 21.25 (s) ppm.

**4,4,5,5-tetramethyl-2-styryl-1,3,2-dioxaborolane (3a):**  $^1\text{H}$  NMR (400 MHz,  $\text{CDCl}_3$ , 298 K):  $\delta$  7.53 – 7.22 (5 H, m), 6.78 (3 H, s), 6.18 (1 H, d), 2.26 (9 H, s), 1.34 – 1.20 (14 H, m) ppm;  $^{13}\text{C}$  NMR (101 MHz,  $\text{CDCl}_3$ , 298 K):  $\delta$  149.63 (s), 137.74 (s), 128.97 (s), 128.65 (s), 127.07 (d), 83.39 (s), 24.89 (s), 22.80 (s), 21.27 (s) ppm.

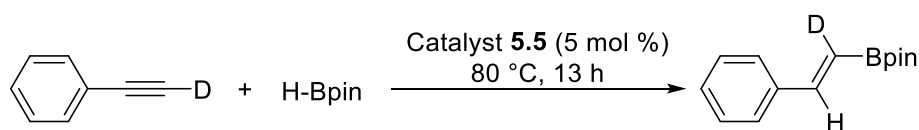
**4,4,5,5-tetramethyl-2-(4-methylstyryl)-1,3,2-dioxaborolane (3b):**  $^1\text{H}$  NMR (400 MHz,  $\text{CDCl}_3$ , 298 K):  $\delta$  7.51 – 7.13 (4 H, m), 6.85 (3 H, s), 6.18 (1 H, d), 2.39 (3 H, s), 2.33 (9 H, s), 1.46 (1 H, d), 1.38 – 1.28 (12 H, d) ppm;  $^{13}\text{C}$  NMR (101 MHz,  $\text{CDCl}_3$ , 298 K):  $\delta$  149.93 (s), 138.11 (s), 129.72 (s), 127.40 (d), 83.67 (s), 25.23 (s), 21.61 (s) ppm.

**2-(4-bromostyryl)-4,4,5,5-tetramethyl-1,3,2-dioxaborolane (3c):**  $^1\text{H}$  NMR (400 MHz,  $\text{CDCl}_3$ , 298 K):  $\delta$  7.36 – 7.17 (3 H, m), 7.10 (1 H, s), 6.68 (3 H, s), 6.04 (1 H, d), 3.00 (1 H, s), 2.16 (9 H, s), 1.29 -1.20 (6 H, d) 1.15 (12 H, s) ppm;  $^{13}\text{C}$  NMR (101 MHz,  $\text{CDCl}_3$ , 298 K):  $\delta$  148.20 (s), 137.71 (s), 133.59 (s), 131.81 (s), 128.57 (s), 126.98 (s), 83.28 (s), 78.50 (s), 24.90 (d), 21.26 (s) ppm.

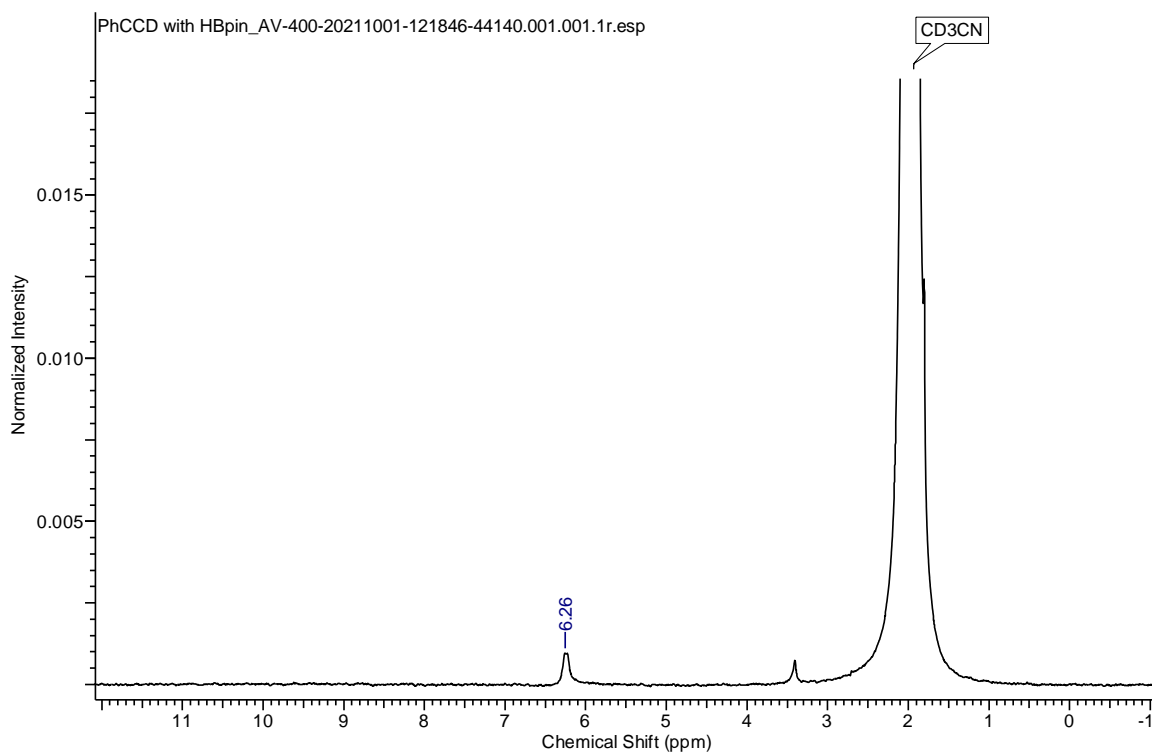
**4,4,5,5-tetramethyl-2-(oct-1-en-1-yl)-1,3,2-dioxaborolane (3d):**  $^1\text{H}$  NMR (400 MHz,  $\text{CDCl}_3$ , 298 K):  $\delta$  6.86 (3 H, s), 6.71 (2 H, d), 5.50 (1 H, d), 2.34 (9H, s), 2.24-2.19 (2 H, quat), 1.45 (3 H, s), 1.33-1.29 (20 H, m), 0.95 (3 H, s) ppm;  $^{13}\text{C}$  NMR (101 MHz,  $\text{CDCl}_3$ , 298 K):  $\delta$  154.82 (s), 137.71 (s), 126.99 (s), 82.98 (s), 81.95 (s), 35.93 (s), 31.83 (s), 29.02 (s), 24.87 (s), 24.72 (d), 22.74 (d), 21.24 (s), 14.17 (s) ppm.

#### 6.4.3.2. Regioselectivity studies

Phenylacetylene-d1 (25.7 mg, 0.25 mmol), pinacolborane (35.5 mg, 0.27 mmol) and catalyst **5.5** (5.0 mol%) were charged in a screw cap NMR tube inside the glove box. The reaction mixture was heated at 80 °C for 13 h. The progress of the reaction was monitored by the  $^2\text{H}$  NMR. After dissolving in  $\text{CD}_3\text{CN}$ , the spectrum shows a peak at  $\delta = 6.26$  ppm, which indicates a *cis* orientation of deuterium and phenyl group.

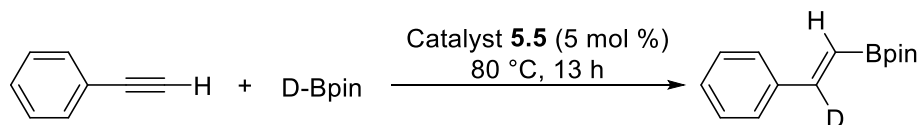


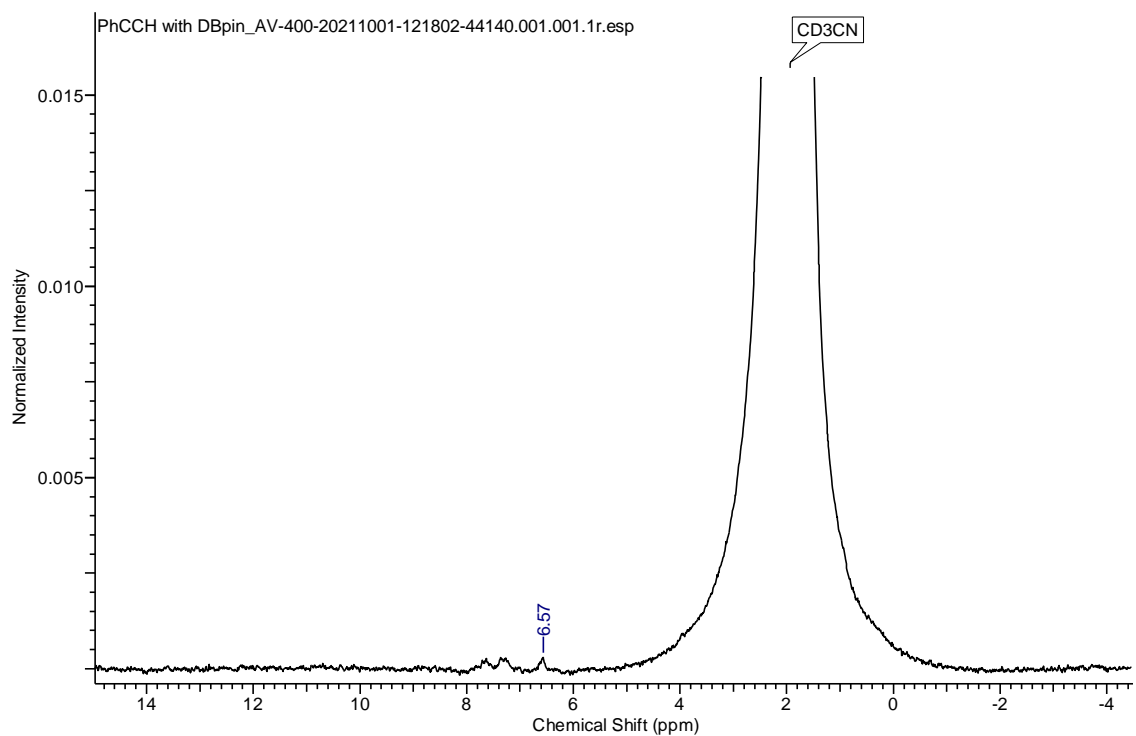




<sup>2</sup>H NMR spectrum of the reaction of PhC≡CD with HBpin in presence of catalyst **5.5**  
(CD<sub>3</sub>CN, 76.77 MHz, 298 K)

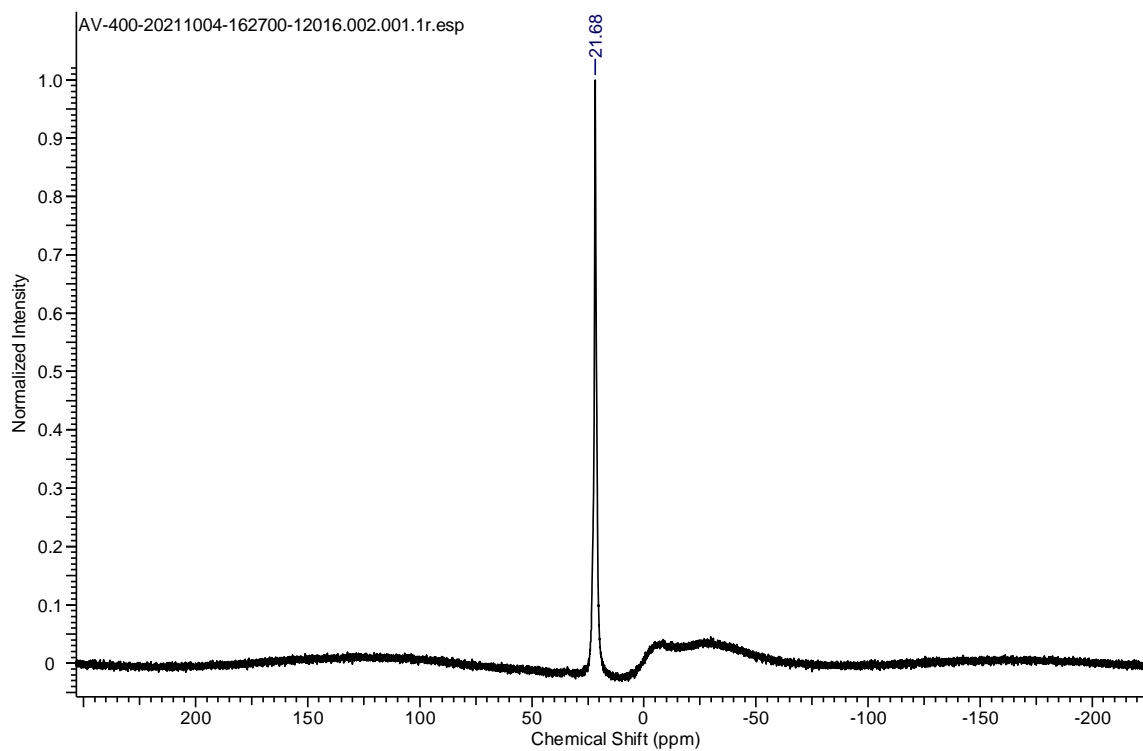
Phenylacetylene (25.5 mg, 0.25 mmol), pinacolborane-d<sub>1</sub> (50 mg, 0.27 mmol) and catalyst **5.5** (5.0 mol%) were charged in a screw cap NMR tube inside the glove box. The reaction mixture was heated at 80 °C for 13 h. The progress of the reaction was monitored by <sup>2</sup>H NMR after dissolving in CD<sub>3</sub>CN, which indicated the peak at  $\delta = 6.57$  ppm, due to the *cis* orientation of deuterium and Bpin unit.

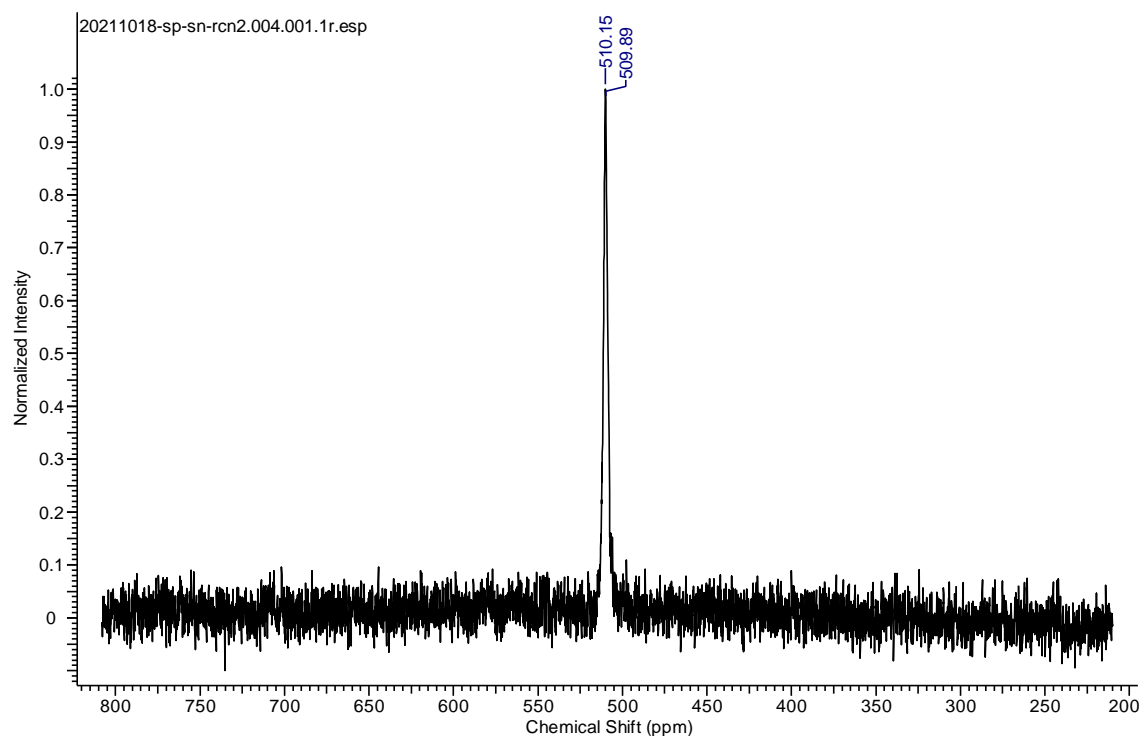




$^2\text{H}$  NMR spectrum of the reaction of  $\text{PhC}\equiv\text{CH}$  with DBpin in presence of catalyst **5.5**  
( $\text{CD}_3\text{CN}$ , 76.77 MHz, 298 K)

### 6.4.3.3. Mechanistic studies



**$^{11}\text{B}$  NMR for reaction of 5.5 with HBpin** **$^{119}\text{Sn}$  NMR for the reaction of 5.5 with HBpin****6.5: References**

1. CrysAlisPro, Version 1.171.33.66; Oxford Diffraction Ltd.: Abingdon, U.K., 2010.
2. G. M. Sheldrick, *Acta Crystallogr., Sect. A.*, 2008, **64**, 112–122.
3. L. J. Farrugia, WinGx, v. 2014.1, An Integrated System of Windows Programs for the Solution, Refinement and Analysis of Single-Crystal X-ray Diffraction Data; Department of Chemistry, University of Glasgow, Glasgow, U.K., 2014.
4. L. J. Farrugia, *J. Appl. Crystallogr.*, 1997, **30**, 565–565.
5. R. Ahlrichs, M. Bar, M. Häser, H. Horn and C. Kölmel, *Chem. Phys. Lett.*, 1989, **162**, 165–169.
6. J. P. Perdew, K. Burke and M. Ernzerhof, *Phys. Rev. Lett.*, 1996, **77**, 3865–3868.
7. S. Ansgar, H. Christian and A. Reinhart, *J. Chem. Phys.*, 1994, **100**, 5829–5835.
8. K. Eichkorn, O. Treutler, H. Öhm, M. Häser and R. Ahlrichs, *Chem. Phys. Lett.*, 1995, **240**, 283–289.

- 
9. M. Sierka, A. Hogekamp and R. Ahlrichs, *J. Chem. Phys.*, 2003, **118**, 9136-9148.
  10. A. Klamt and G. Schuurmann, *J. Chem. Soc., Perkin Trans.*, 1993, **2**, 799–805.
  11. Gaussian 09, Revision **E.01**; M. J. Frisch , G. W. Trucks, H. B. Schlegel, G. E. Scuseria, M. A. Robb, J. R. Cheeseman, G. Scalmani, V. Barone, B. Mennucci, G. A. Petersson, H. Nakatsuji, M. Caricato, X. Li, H. P. Hratchian, A. F. Izmaylov, J. Bloino, G. Zheng, J. L. Sonnenberg, M. Hada, M. Ehara, K. Toyota, R. Fukuda, J. Hasegawa, M. Ishida, T. Nakajima, Y. Honda, O. Kitao, H. Nakai, T. Vreven, J. A. Montgomery, Jr., J. E. Peralta, F. Ogliaro, M. Bearpark, J. J. E. Heyd, K. N. B. Kudin, V. N. Staroverov, R. Kobayashi, J. K. Raghavachari, A. Rendell, J. C. Burant, S. S. Iyengar, J. Tomasi, M. Cossi, N. Rega, J. M. Millam, M. Klene, J. E. Knox, J. B. Cross, V. Bakken, C. Adamo, J. Jaramillo, R. Gomperts, R. E. Stratmann, O. Yazyev, A. J. Austin, R. Cammi, C. Pomelli, J. W. Ochterski, R. L. Martin, K. Morokuma, V. G. Zakrzewski, G. A. Voth, P. Salvador, J. J. Dannenberg, S. Dapprich, A. D. Daniels, Ö. Farkas, J. B. Foresman, J. V. Ortiz, J. Cioslowski, D. J. Fox, Gaussian, Inc., *Wallingford CT*, **2009**.
  12. S. Pahar, V. S. V. S. N. Swamy, T. Das, R. G. Gonnade, K. Vanka and S. S. Sen, *Chem. Commun.*, 2020, **56**, 11871–11874.

---

**Abstract**

---

**Name of the Student:** Sanjukta Pahar**Registration No.:** 10CC16A26009**Faculty of Study:** Chemical Science**Year of Submission:** 2022**AcSIR academic centre/CSIR Lab:****Name of the Supervisor:** Dr. Sakya S. SenCSIR-National Chemical Laboratory,  
Pune**Title of the thesis:** “Donor–Acceptor Stabilization of Compounds with Low Coordinate Group 13 and 14 Elements”

---

Small molecules like H<sub>2</sub>, CO, CO<sub>2</sub>, NH<sub>3</sub> are ubiquitous and relatively cheap synthons for building many complex molecules and produced in large scales in industrial processes. As most of the homogeneous catalytic cycles involve such small molecules, so, it is deemed desirable to use them in syntheses of value-added chemical products. The activation of such relatively inert bonds usually requires a catalyst. The typical catalysts feature late transition metals due to their amenability to be in a variety of oxidation states, to coordinate to a substrate, and to be a good source/sink for electrons depending on the nature of the transition state. We have aimed to develop new ligand systems to stabilize the low-coordinated, low-valent main group compounds and explore them as alternative resources to transition metal complexes for activation of small molecules as well as important organic transformations, and to evolve the new ways for the sustainable production of metal-free catalytic systems. In this context, in our 1<sup>st</sup> working chapter (Chapter 2), we have described the silylene–indium and germylene–indium donor-acceptor complex which is still remained elusive presumably due to the low solubility of the indium halides in the majority of the organic solvents. The single-crystal X-ray studies, in combination with the DFT calculations, endorsed the classical donor–acceptor nature of the Si–In and the Ge–In bonds. The 2<sup>nd</sup> working chapter (Chapter 3) illustrates the unprecedented reactivities along with the unusual transmetallation of chlorogermylene featuring the unsymmetrical nacaac-based tridentate ligand (**L**) containing a pyridyl-methyl group. In 3<sup>rd</sup> working chapter (Chapter 4), we have expanded our transmetallation methodology from *p*- to *d*- block nickel and copper which afforded analogous ligand (**L**) supported nickel and copper halide. Tri-coordinated cationic nickel complex and nickel hydride have been prepared and characterized by single-crystal XRD and spectroscopic state of art. In our last chapter (Chapter 5), we have introduced pyridylpyrrolide ligand and prepared a series of low-valent monomeric germanium and tin compounds. The hypersilyl group substituted germylene has utilized for the C–F bond activation of C<sub>5</sub>F<sub>5</sub>N and afforded a tetrafluoropyridyl germylene via the elimination of (Me<sub>3</sub>Si)<sub>3</sub>SiF. On the other way, hypersilyl stannylene has been explored as an efficient catalyst for the hydroboration of aldehydes, ketones, alkenes, and alkynes.

---

**List of publication(s) in SCI Journal(s) (published & accepted) emanating from  
the thesis work, with complete bibliographic details**

1. **S. Pahar**, S. Karak, M. Pait, K. V. Raj, K. Vanka and S. S. Sen, *Organometallics*, 2018, **37**, 1206 – 1213.
2. **S. Pahar**, V. S. V. S. N. Swamy, T. Das, R. G. Gonnade, K.Vanka and S. S. Sen, *Chem. Commun.*, 2020, **56**, 11871 – 11874.
3. **S. Pahar**, V. Sharma, S. Tothadi, and S. S. Sen, *Dalton Trans.*, 2021, **50**, 16678 – 16684.

**Other publications:**

1. **S. Pahar**, G. Kundu and S. S. Sen, *ACS Omega*, 2020, **5**, 25477 – 25484.
2. G. Kundu, **S. Pahar**, S. Tothadi and S. S. Sen, *Organometallics*, 2020, **39**, 4696 – 4703.
3. S. Yadav, **S. Pahar** and S. S. Sen, *Chem. Commun.*, 2017, **53**, 4562–4564.
4. M. K. Bisai, **S. Pahar**, T. Das, K. Vanka and S. S. Sen, *Dalton Trans.*, 2017, **46**, 2420–2424.

**List of papers with abstract presented (oral/poster) at national/international conferences/seminars with complete details**

1. Poster presentation on ‘**ChemSci 2021: Leaders in Field Symposium**’ at JNCASR (Virtual mode: Twitter) (13-15<sup>th</sup> December 2021)  
**Title:** "Unusual Access to flexible  $\beta$ -diketiminato and Pyridylpyrrolido ligand Based Germanium and Tin Chemistry"
2. Poster presentation on ‘**International Conference on Main-group Molecules to Materials-II (MMM-II)**’ (Virtual mode: Twitter) (13-15<sup>th</sup> December 2021)  
**Title:** "Unusual Access to flexible  $\beta$ -diketiminato and Pyridylpyrrolido ligand Based Germanium and Tin Chemistry"
3. Oral presentation on ‘**NCL – RF Annual Students’ Conference**’ (29<sup>th</sup> & 30<sup>th</sup> November 2021)  
**Title:** "Unusual Access to flexible  $\beta$ -diketiminato and Pyridylpyrrolido ligand Based Germanium and Tin Chemistry"
4. Poster presentation on ‘**Inorganic Ireland Symposium 2021**’ (Virtual mode) (14<sup>th</sup> May 2021)  
**Title:** Reactivity, bonding and structural elucidation of pendant methyl-pyridinato  $\beta$ -diketiminato ligand moiety
5. Poster presentation on ‘**#RSC Poster Twitter Conference 2021**’ (Virtual mode: Twitter) (2-3<sup>rd</sup> March 2021).  
**Title:** “Access to Structurally Diverse Germynes and Six-membered Dialane with a Flexible  $\beta$ -diketiminato Scaffold”
6. Poster presentation on ‘**LatinXChem 2020**’ (Virtual mode: Twitter) (7<sup>th</sup> September 2020)  
**Title:** “Convenient Access to Silicon(II) and Germanium (II)- Indium complexes”
7. Poster presentation at ‘**Global Inorganic Discussion Weekday (GIDW)**’ (Virtual mode: Twitter) (9-10<sup>th</sup> July 2020)  
**Title:** “Convenient Access to Germanium and Aluminium Compounds Using the Pendant Power of Methyl-pyridinato Ligand”

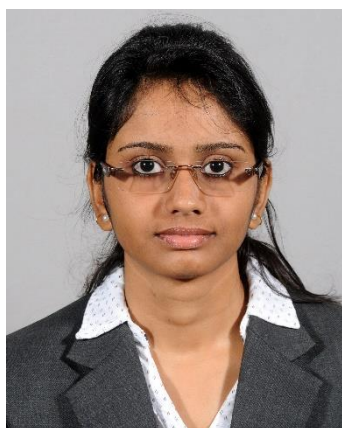
8. Presented a research poster at ‘**CEFMC-2020, 2nd International Conference on Crystal Engineering: From Molecule to Crystal, a Virtual Meeting**’ 19 – 20<sup>th</sup> June 2020.  
**Title:** “Reactivity, bonding and structural elucidation of pendant methylpyridinato  $\beta$ -diketiminato ligand moiety”
9. Presented a poster at ‘**National Science Day**’ at CSIR-NCL (February- 2020, Pune).  
**Title:** “Convenient Access to Germanium and Aluminium compounds using methyl pyridinato ligand”
10. Presented a poster at ‘**MODERN TRENDS IN INORGANIC CHEMISTRY- XVIII (MTIC-XVIII)**’ at Indian Institute of Technology, Guwahati (December- 2019).  
**Title:** “Access to Silicon(II)- and Germanium(II)-Indium Complexes”
11. Presented a poster at ‘**International Conference on Structural and Inorganic Chemistry-II (ICSIC-II)**’ at IISER, Pune (March- 2019).  
**Title:** “Access to Silicon(II)- and Germanium(II)-Indium Complexes”
12. Presented a poster at ‘**National Science Day**’ at CSIR-NCL, Pune (February- 2019).  
**Title:** “Access to Silicon(II)- and Germanium(II)-Indium Complexes”

**List of Conference Attended with Details**

1. ‘**MODERN TRENDS IN INORGANIC CHEMISTRY- XVIII (MTIC-XVIII)**’ at Indian Institute of Technology, Guwahati (December- 2019).
2. ‘**International Conference on Structural and Inorganic Chemistry-II (ICSIC-II)**’ at IISER, Pune (March- 2019).
3. ‘**MODERN TRENDS IN INORGANIC CHEMISTRY- XVII (MTIC-XVII)**’ at CSIR-NCL, Pune (December- 2017).



## About the author



Ms. Sanjukta Pahar, daughter of Subrata Pahar and Sova Pahar, was born in Dhanyakuria, a village of North 24 Parganas district, West Bengal, India, in 1993. She completed her B.Sc. in Chemistry from Asutosh College, University of Calcutta (2010-2013). She obtained her master's degree from IIT Madras (2013-2015). Sanjukta then undertook a project as project assistant (2015-2016) with Dr. Amitava Das at National Chemical Laboratory (NCL-Pune), India. Formerly she received "DST-INSPIRE Fellowship, Govt. of India" and joined immediately as a research scholar with Dr. Sakya Singha Sen in July, 2016. Her area of research work lies on "Donor-Acceptor Stabilization of Compounds with Low Coordinate Group 13 and 14 Elements". She has been awarded and completed the Short-Term Research Internship program entitled as "Newton-Bhabha PhD Placement Programme 2019-2020" with the supervision of Dr. Rebecca L. Melen in Cardiff University, UK.

### Education and Research Experience:

- Doctoral fellow at National Chemical Laboratory, Pune, India from July, 2016 to present (Supervisor: **Dr. Sakya Singha Sen**) (Area of Research: "Donor-Acceptor Stabilization of Compounds with Low Coordinate Group 13 and 14 Elements")
- Newton Bhabha PhD Internship experience from 15<sup>th</sup> October, 2020 to 15<sup>th</sup> February, 2021 at Cardiff university, Wales, United Kingdom (UK) (Supervisor: **Dr. Rebecca L. Melen**) (Research experience: "Selective Diazo Cross-Coupling reaction: Using B(C<sub>6</sub>F<sub>5</sub>)<sub>3</sub> as an efficient catalyst")
- Project Assistant (PA II) at National Chemical Laboratory, Pune, India from April, 2016 to July, 2016 (Supervisor: **Dr. Sakya Singha Sen**).
- Project Assistant (PA II) at National Chemical Laboratory, Pune, India from September, 2015 to March, 2016 (Supervisor: **Dr. Amitava Das**).
- **M.Sc.:** (2013-2015) Chemistry, IIT Madras, India. MSc project from August, 2014 to April, 2015 at IIT Madras, Chennai, India (Supervisor: **Dr. Md. Mahiuddin Baidya**).

➤ **B.Sc.:** (2010-2013) Chemistry, Asutosh College, University of Calcutta.

### List of Scientific Contributions:

#### Publications

1. **S. Pahar**, V. Sharma, S. Tothadi, and S. S. Sen, *Dalton Trans.*, 2021, **50**, 16678 – 16684.
2. **S. Pahar**, V. S. V. S. N. Swamy, T. Das, R. G. Gonnade, K. Vanka and S. S. Sen, *Chem. Commun.*, 2020, **56**, 11871 – 11874.
3. **S. Pahar**, G. Kundu and S. S. Sen, *ACS Omega*, 2020, **5**, 25477 – 25484.
4. G. Kundu, **S. Pahar**, S. Tothadi and S. S. Sen, *Organometallics*, 2020, **39**, 4696 – 4703.
5. **S. Pahar**, S. Karak, M. Pait, K. V. Raj, K. Vanka and S. S. Sen, *Organometallics*, 2018, **37**, 1206 – 1213.
6. S. Yadav, **S. Pahar** and S. S. Sen, *Chem. Commun.*, 2017, **53**, 4562–4564.
7. M. K. Bisai, **S. Pahar**, T. Das, K. Vanka and S. S. Sen, *Dalton Trans.*, 2017, **46**, 2420–2424.

#### Symposia Attended

National conferences:	2 (Poster Presentation)
	1 (Oral Presentation)
International conferences:	1 (Participation)
	2 (Poster presentation)
	6 (Poster Presentation, Virtual mode)

## Access to Silicon(II)– and Germanium(II)–Indium Compounds

Sanjukta Pahar,<sup>†,‡</sup> Suvendu Karak,<sup>‡,§</sup> Moumita Pait,<sup>†</sup> K. Vipin Raj,<sup>§</sup> Kumar Vanka,<sup>‡,§</sup> and Sakya S. Sen<sup>\*,†,‡,§</sup>

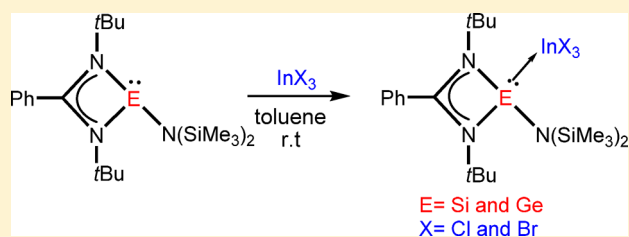
<sup>†</sup>Inorganic Chemistry and Catalysis Division, CSIR-National Chemical Laboratory, Dr. Homi Bhabha Road, Pashan, Pune 411008, India

<sup>‡</sup>Academy of Scientific and Innovative Research (AcSIR), New Delhi 110020, India

<sup>§</sup>Physical and Material Chemistry Division, CSIR-National Chemical Laboratory, Dr. Homi Bhabha Road, Pashan, Pune 411008, India

### S Supporting Information

**ABSTRACT:** Despite the remarkable ability of N-heterocyclic silylene to act as a Lewis base and form stable Lewis adducts with group 13 elements such as boron, aluminum, and gallium, there has been no such comparable investigation with indium and the realization of a stable silylene–indium complex has still remained elusive. Similarly, a germylene–indium complex is also presently unknown. We describe herein the reactions of  $[\text{PhC}(\text{N}t\text{Bu})_2\text{SiN}(\text{SiMe}_3)_2]$  (**1**) and  $[\text{PhC}(\text{N}t\text{Bu})_2\text{GeN}(\text{SiMe}_3)_2]$  (**4**) with  $\text{InCl}_3$  and  $\text{InBr}_3$  that have resulted in the first silylene–indium complexes,  $[\text{PhC}(\text{N}t\text{Bu})_2\text{Si}\{\text{N}(\text{SiMe}_3)_2\}\rightarrow\text{InCl}_3]$  (**2**) and  $[\text{PhC}(\text{N}t\text{Bu})_2\text{Si}\{\text{N}(\text{SiMe}_3)_2\}\rightarrow\text{InBr}_3]$  (**3**), as well as the first germylene–indium complexes,  $[\text{PhC}(\text{N}t\text{Bu})_2\text{Ge}\{\text{N}(\text{SiMe}_3)_2\}\rightarrow\text{InCl}_3]$  (**5**) and  $[\text{PhC}(\text{N}t\text{Bu})_2\text{Ge}\{\text{N}(\text{SiMe}_3)_2\}\rightarrow\text{InBr}_3]$  (**6**). The solid-state structures of all species have been validated by single-crystal X-ray diffraction studies. Note that **5** and **6** are the first structurally characterized organometallic compounds that feature a Ge–In single bond (apart from the compounds in Zintl phases). Theoretical calculations reveal that the Si(II)→In bonds in **2** and **3** and the Ge(II)→In bonds in **5** and **6** are dative bonds.



## INTRODUCTION

The concept of chemical bonding that the combination of a Lewis base and a Lewis acid results in the formation of a Lewis adduct has just celebrated its centenary anniversary<sup>1</sup> and is still growing stronger. With the advent of stable N-heterocyclic carbenes (NHCs) and their higher homologues, N-heterocyclic silylenes (NHSis), we have entered into a new era of neutral Lewis bases. The realization of NHC and NHSi complexes of main-group elements has seen a flurry of research activity into their bonding properties and reactivity in recent years.<sup>2,3</sup> However, there are a few main-group halides for which the coordination chemistry of NHC and NHSi either has been explored only cursorily or has not been developed at all. Indium halide is one prominent example of such a halide. In fact, the organometallic chemistry of indium is, by far, significantly less developed in comparison to its lighter congeners such as boron, aluminum, and gallium. This is partially due to the low solubility of indium halides in a majority of organic solvents. Nevertheless, on adoption of a salt elimination methodology between  $\text{InCl}_3$  and lithiated ligands, quite a few indium derivatives have been isolated.<sup>4</sup> Very recently, Braunschweig and co-workers reported the formation of a metal-only Lewis pair (MOLP)<sup>5</sup> between indium halides and electron-rich coordinatively unsaturated zerovalent platinum compounds.<sup>6</sup> They have also demonstrated that a dynamic equilibrium exists between MOLPs and their oxidative addition products.<sup>6</sup> The N-heterocyclic carbene

(NHC) chemistry of indium has also come to the fore in recent years. The advances made in this field have mainly come from the group of Jones and co-workers, who isolated coordination complexes between NHC and indium halides.<sup>7a,b</sup> Subsequently, their trimethyl complexes with NHCs have also been realized.<sup>7c</sup> Thorough quantum mechanical calculations on the structures and stabilities of NHC–indium adducts have also been reported.<sup>8</sup>

The use of indium compounds in electronics (indium is becoming one of the most important dopant species for silicon crystals used in photovoltaics, for instance)<sup>9</sup> has provided renewed interest in the chemistry of silicon and indium. Early works by Götze,<sup>10</sup> Cowley,<sup>11</sup> Weidlein,<sup>12</sup> and, to a large extent, by Wiberg<sup>13</sup> have led to the isolation of a variety of silyl–indium compounds, where the formal oxidation state of silicon is +4. However, in recent years, attention has shifted to silicon compounds, where the formal oxidation state of silicon is +2, popularly known as silylenes.<sup>14</sup> Examples of carbonyl-free silylene complexes of 3d transition metals in the formal oxidation state +2 are now too frequent to be comprehensively listed, thanks to extensive investigations by the groups of H. Roesky, P. Roesky, Stalke, Driess, Tacke, Inoue, Khan, and many others.<sup>15–26</sup> The coverage of the s and p blocks is also expanding

Received: February 13, 2018

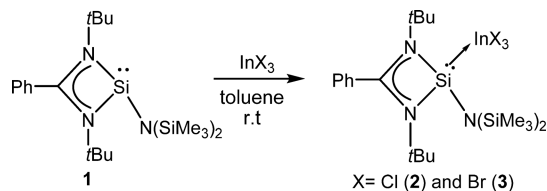
Published: March 21, 2018

and is supplemented by examples of bonding to s-/p-block Lewis acids such as boron,<sup>27</sup> aluminum,<sup>27</sup> calcium,<sup>28</sup> germanium,<sup>29</sup> tin,<sup>30</sup> and lead.<sup>30</sup> However, when it comes to indium, there has only been one reaction reported between a Si(II) compound and an indium derivative. Jutzi and co-workers reported the reaction of decamethylsilicocene with  $\text{InMe}_3$  that led to the disilyl indium compound  $[\text{Cp}^*\text{Si}(\text{Me})_2]_2\text{InMe}$  in place of a stable silylene–indium adduct, resulting from the insertion of the silylene moiety into two In–C bonds.<sup>31</sup> Therefore, a typical silylene–indium adduct is still inaccessible. In light of the extensive coordination chemistry of  $[\text{PhC}(\text{N}t\text{Bu})_2\text{SiN}(\text{SiMe}_3)_2]$  (**1**)<sup>32</sup> toward main-group halides, we have investigated the reactions of **1** with indium halides. The reaction scope has also been extended to the analogous Ge(II) amide  $[\text{PhC}(\text{N}t\text{Bu})_2\text{GeN}(\text{SiMe}_3)_2]$  (**4**)<sup>33</sup> with indium halides as, to the best of our knowledge, no compound with a Ge–In single bond has been structurally characterized. The report of a Ge–In single bond has only been found in Zintl compounds such as  $\text{La}_3\text{In}_4\text{Ge}$  and  $\text{La}_3\text{InGe}$ .<sup>34</sup> We now report the first silylene–indium and germylene–indium complexes and their isolation, structural elucidation, and bonding properties.

## RESULTS AND DISCUSSION

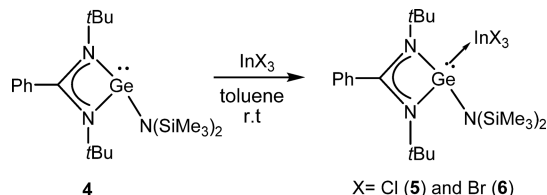
**Synthesis.** When **1** was reacted with an equimolar amount of  $\text{InCl}_3$  or  $\text{InBr}_3$  in toluene, monomeric compounds of composition  $[\text{PhC}(\text{N}t\text{Bu})_2\text{Si}\{\text{N}(\text{SiMe}_3)_2\} \rightarrow \text{InCl}_3]$  (**2**) and  $[\text{PhC}(\text{N}t\text{Bu})_2\text{Si}\{\text{N}(\text{SiMe}_3)_2\} \rightarrow \text{InBr}_3]$  (**3**) (Scheme 1) were

**Scheme 1.** Reactions of Si(II) Amide with Indium Halides



obtained as colorless precipitates. The removal of toluene and subsequent workup in THF resulted in the colorless crystals of **2** and **3**. The same synthetic strategy was followed for the preparation of germylene–indium complexes,  $[\text{PhC}(\text{N}t\text{Bu})_2\text{Ge}\{\text{N}(\text{SiMe}_3)_2\} \rightarrow \text{InCl}_3]$  (**5**) and  $[\text{PhC}(\text{N}t\text{Bu})_2\text{Ge}\{\text{N}(\text{SiMe}_3)_2\} \rightarrow \text{InBr}_3]$  (**6**), from **4** (Scheme 2). As expected, the adducts are

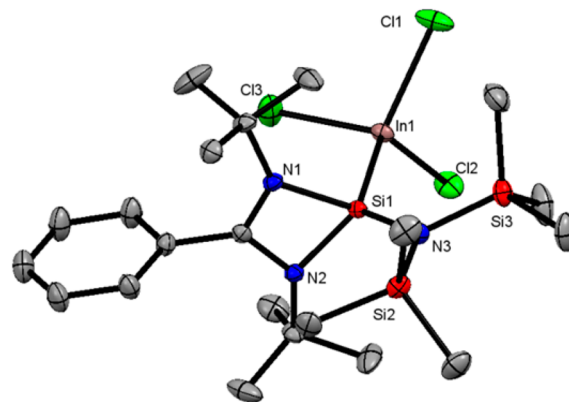
**Scheme 2.** Reactions of Ge(II) Amide with Indium Halides



insoluble in most of solvents and marginally soluble in THF and  $\text{CHCl}_3$ . Moreover, they show a tendency toward decomposition, resulting in a grayish precipitate, which is most probably elemental indium. The partial solubility of the adducts in  $\text{CDCl}_3$  allowed us to record the  $^1\text{H}$  NMR spectra. The  $^1\text{H}$  NMR spectra of **2**, **3**, **5**, and **6** show typical signals for the *t*Bu protons in the amidinate ligand ( $\delta$  1.42 (**2**), 1.35 (**3**), 1.23 (**5**), and 1.24 (**6**) ppm). We could not obtain any resonance in the solution-state  $^{29}\text{Si}$  NMR spectrum presumably due to the low solubility of the adducts and gradual decomposition to elemental indium.

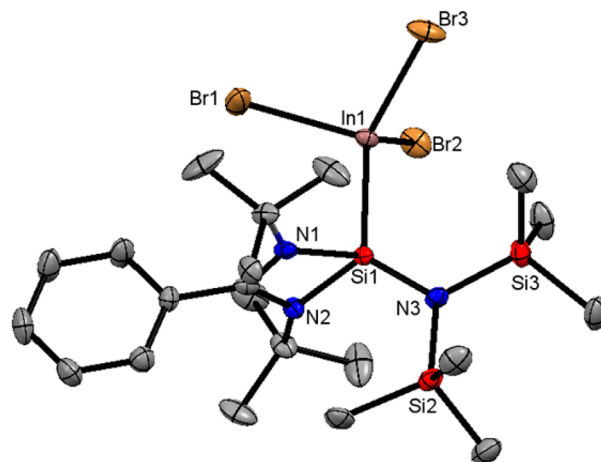
However, in the solid state, the  $^{29}\text{Si}$  NMR chemical shift of **3** appears at  $\delta$   $-31.7$  ppm, while **2** shows a broad signal ranging from  $-54.4$  to  $-84.3$  ppm, which are in good accordance with silylene adducts reported by Khan, Tacke, and others.<sup>25,26,27a</sup> The appearance of two signals for the trimethylsilyl groups in  $^1\text{H}$  (**2**,  $\delta$  0.56 and 0.65 ppm; **3**, 0.50 and 0.60 ppm) as well as  $^{29}\text{Si}$  NMR of **2** and **3** indicates that they are not equivalent, resulting from the hindered rotation due to the presence of the bulky substituents around the Si(II) atom. Akin to **2** and **3**, both **5** and **6** show two signals for the  $\text{SiMe}_3$  moieties in their respective  $^1\text{H}$  NMR spectra (**5**,  $\delta$  0.43 and 0.62 ppm; **6**, 0.42 and 0.63 ppm). The molecular ion peaks were observed with the highest relative intensity in the ESI-MS spectrum at  $m/z$  676.1 (**2**), 784.9 (**3**), 700.0 (**5**), and 830.9 (**6**).

**Structural Elucidation.** The molecular structures of compounds **2** and **3** are depicted in Figures 1 and 2, respectively.



**Figure 1.** Molecular structure of **2**. Anisotropic displacement parameters are depicted at the 50% probability level. Hydrogen atoms are omitted for clarity. Selected bond lengths and angles are given in Table 1.

The selected bond lengths of **2** and **3** are given in Table 1. Both crystallize in the monoclinic space group  $P2_1/n$ .<sup>35</sup> The structural parameters of **2** and **3** are very much alike, and the noticeable alterations of the bond lengths and angles are attributed to the halide atoms being different. The Si(II) atoms in **2** and **3** are four-coordinate and exhibit a slightly distorted tetrahedral geometry.



**Figure 2.** Molecular structure of **3**. Anisotropic displacement parameters are depicted at the 50% probability level. Hydrogen atoms have been omitted for clarity. Selected bond lengths and angles are given in Table 1.

Table 1. Structural Parameters of 2, 3, 5, and 6

param	2	3	5	6
Si–In, Å	2.5804(5)	2.5840(12)		
Ge–In, Å			2.6167(6)	2.6241(6)
In–Cl, Å	2.3806(5), 2.3845(5), 2.3977(6)		2.3567(14), 2.3611(15), 2.3690(16)	
In–Br, Å		2.5278(6), 2.5174(5), 2.5167(5)		2.4932(7), 2.5019(8), 2.5011(6)
Si–N(SiMe <sub>3</sub> ) <sub>2</sub> , Å	1.6946(16)	1.697(4)		
Ge–N(SiMe <sub>3</sub> ) <sub>2</sub> , Å			1.811(4)	1.814(4)
∠Si–In–Cl, deg	119.566(17), 117.018(18), 105.085(17)			
∠Si–In–Br, deg		105.90(3), 117.70(3), 118.42(3)		
∠Ge–In–Cl, deg			115.73(4), 113.48(4), 105.26(4)	
∠Ge–In–Br, deg				116.35(2), , and 111.41(2)
∠In–Si–N(SiMe <sub>3</sub> ) <sub>2</sub> , deg	124.43(6)	124.27(13)		
∠In–Ge–N(SiMe <sub>3</sub> ) <sub>2</sub> , deg			128.79(13)	128.49(13)

The Si–N(SiMe<sub>3</sub>)<sub>2</sub> bond distances in **2** and **3** are 1.6946(16) and 1.697(4) Å, respectively, which are shorter than that in the parent silylene **2** (1.769(7) Å). The respective Si(II)–In bond lengths in **2** and **3** are 2.5804(5) and 2.5840(12) Å, respectively, which are marginally longer than the sum of their covalent radii (2.55 Å). Although, to the best of our knowledge, Si(II)–In bond lengths have not been reported previously, the value is very close to that in the doubly chloride bridged complex [ $\{(Me_3Si)_3Si\}_2In(\mu-Cl)_2Li(thf)_2$ ] (2.591(7) Å) reported by Cowley and co-workers,<sup>11</sup> but substantially shorter than those in the previously reported complexes  $In_8(Si^tBu_3)_6$  (2.615(1)–2.683(1) Å)<sup>13b</sup> and  $In_{12}(Si^tBu_3)_8$  (2.668(3)–2.685(3) Å).<sup>13c</sup> The geometry around the indium atom in **2** and **3** is distorted tetrahedral. The average In–Cl distance observed in **2** is 2.3869 Å, which is marginally longer than the average In–Cl bond length in IMes–InCl<sub>3</sub> (2.352 Å).<sup>6</sup> Similarly, the average In–Br bond length (2.5206 Å) is slightly longer than that in Jones' [ $InBr_3\{CN(iPr)_2CMe_2N(iPr)\}$ ] (2.500 Å).<sup>5</sup>

To the best of our knowledge, structural authentication of a compound with a Ge–In single bond has no precedence (apart from those in Zintl phases). Rösch et al. reported that  $In(GeEt_3)_3$  could not be isolated as a pure compound, and no preparative details are available.<sup>36</sup> It were characterized only by IR spectroscopy.<sup>37</sup> Single-crystal X-ray studies confirm the identity of **5** and **6**, which are the first structurally authenticated compounds having a Ge–In single bond (Figures 3 and 4). Both **5** and **6** crystallize in the monoclinic space group  $P2_1/n$ . The structural features of **5** and **6** are very similar to those of **2** and **3**. Both Ge atoms in **5** and **6** are four-coordinated and adopt a distorted-tetrahedral geometry. The Ge–In bonds were determined to be 2.6167(6) (**5**) and 2.6241(6) (**6**) Å, which are shorter than the sum of the germanium and indium covalent radii (2.72 Å)<sup>38a</sup> and expectedly longer than those reported for [ $(tBu_2MeSi)_2GeInGe(SiMe^tBu_2)_2$ ][Li(thf)<sub>4</sub>] (2.5453(4) and 2.5387(4) Å), where the Ge–In bonds possess some double-bond character.<sup>38b</sup> The Ge–N<sub>amidinate</sub> bond lengths are comparable with those in **4** and previously reported amidinato gerymlene chloride [ $PhC(N^tBu)_2GeCl$ ].<sup>39</sup> The geometry of the In atoms in **5** and **6** is close to tetrahedral, as observed from the mean Ge–In–Cl (111.5°) and Ge–In–Br (111.29°) bond angles. The In–Cl and In–Br bonds in **5** and **6** are comparable to those of **2** and **3**.

**Theoretical Studies.** As silylene– and gerymlene–indium complexes have not been reported in the literature before, we

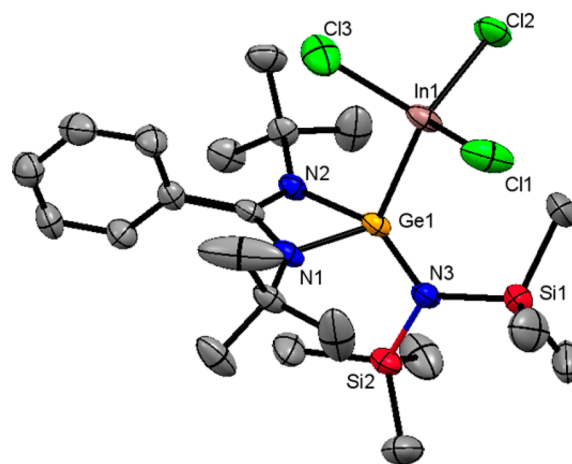


Figure 3. Molecular structure of **5**. Anisotropic displacement parameters are depicted at the 50% probability level. Hydrogen atoms have been omitted for clarity. Selected bond lengths and angles are given in Table 1.

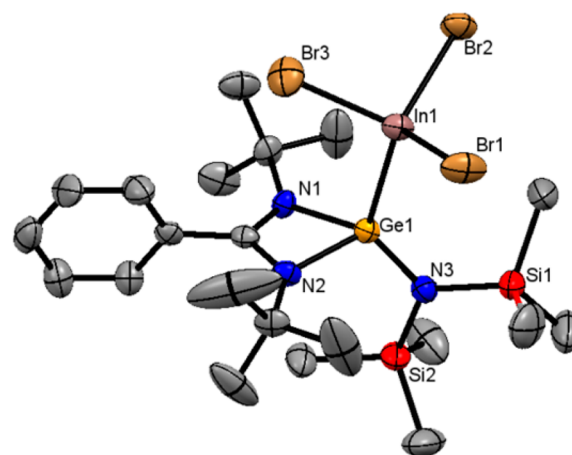
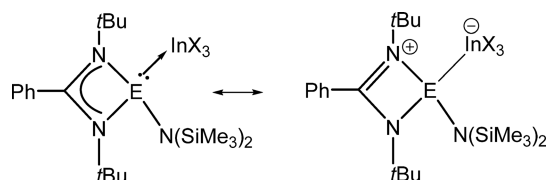


Figure 4. Molecular structure of **6**. Anisotropic displacement parameters are depicted at the 50% probability level. Hydrogen atoms have been omitted for clarity. Selected bond lengths and angles are given in Table 1.

were intrigued to gain insight into the nature of the Si–In and Ge–In bonds in these complexes. The dative bonding in main-

group compounds has recently created heated debate in the literature.<sup>40–42</sup> In order to gain more insight into the bonding in silylene–indium and germylene–indium complexes, density functional theory (DFT) calculations have been performed at the def-TZVP/PBE level of theory (for further details and corresponding references, please see the [Supporting Information](#)).

The Si–In or Ge–In bond can be interpreted either as a classical donor–acceptor bond between the In(III) species and a silylene or germylene or as an ion pair consisting of a silyl or germyl cation with a Si–In or Ge–In single bond (see [Figure 5](#)).



**Figure 5.** Possible bonding interpretation for the complexes **2**, **3**, **5**, and **6**. E is Ge or Si, and X is Br or Cl.

We have chosen as a standard tris(trimethylsilyl)indium species  $\text{In}(\text{SiMe}_3)_3$  (**7**),<sup>10</sup> a molecule with a Si–In single bond. We have also performed calculations on the model silylene–indium compound with a three-coordinate silicon center bearing a Si–In bond such as the diaminosilylene–indium complexes  $(\text{Me}_2\text{N})_2\text{Si}:\rightarrow\text{InX}_3$  (X = Cl (**8**), Br (**9**)). The nature of the Si–In bond has been analyzed on the basis of four parameters: (a) bond dissociation energy (BDE), (b) shared electron number (SEN), which is an indicator of covalent bond strength, (c) Wiberg bond index (WBI), and (d) bond length. The results of the calculations are shown in [Table 2](#). A dative bond can be distinguished from an electron-sharing bond by the nature of dissociation of the bond. The former favors heterolytic dissociation while the latter prefers homolytic dissociation.<sup>40</sup> Calculations suggest that both **2** and **3** prefer heterolytic cleavage (BDEs of 42.2 and 38.7 kcal/mol, respectively) over homolytic cleavage (BDEs of 122.1 and 117.3 kcal/mol, respectively), similar to those in **8** and **9** (heterolytic cleavage (BDE of 23.7 and 21.7 kcal/mol respectively) vs homolytic cleavage (BDE of 134.0 and 130.7 kcal/mol respectively)), while the standard molecule **7**, with a Si–In single bond, prefers homolytic cleavage (BDE of 46.0 kcal/mol) over heterolytic cleavage (BDE of 149.9 kcal/mol). This indicates dative bond character in the Si–In bond in complexes **2** and **3**. Even though the Si–In bond lengths in **2**, **3**, and **7** do not show significant differences, both SEN and WBI values obtained from calculations for **2** and **3** are less than the values obtained for **7** (see [Table 2](#)) but are in good agreement with those obtained for **8** and **9**, indicating the dative bond character of the Si–In bond in **2** and **3**.

Natural bond orbital (NBO) analysis has also been done in order to obtain more evidence for the dative bond character of

the Si–In bond in complexes **2** and **3**. The general NBO criterion to distinguish a dative bond from a covalent bond is the change in the formal charge on the atoms. The calculated atomic charges  $Q_A(\text{dat})$  and  $Q_B(\text{dat})$  for a dative-bonded pair deviate markedly from the charges ( $Q_A(\text{sep})$  and  $Q_B(\text{sep})$ ) in the dissociated species by about equal and opposite amounts for A and B.<sup>42</sup> In complex **3**, the charge differences ( $\Delta Q$ ) calculated (see [Table 3](#)) as described above are  $-0.369$  for In and  $+0.400$  for Si. A similar trend is seen in complex **2**, with a charge difference of  $-0.381$  for In and of  $+0.376$  for Si. These data are in good accordance with those obtained for **8** and **9**. However, such a trend is not observed in the standard molecule **7**, due to its covalent bond character. All of these results clearly indicate that the bond between Si and In is a classical donor–acceptor bond.

To the best of our knowledge, there has been no compound reported so far with a Ge–In single bond. It is therefore not possible to directly compare the SEN, WBI, and bond length values of complexes **5** and **6** (provided in [Table 2](#)) with those of a standard molecule. However, calculations suggest that both **5** and **6** prefer heterolytic cleavage (BDEs of 29.8 and 27.1 kcal/mol, respectively) over homolytic cleavage (BDEs of 124.3 and 120.3 kcal/mol, respectively), which indicates the dative bond character of the Ge–In bond in complexes **5** and **6**. The NBO analysis, done and discussed earlier for complexes **2** and **3**, was also conducted for complexes **5** and **6**. It was found that the charge difference ( $\Delta Q$ ) is  $+0.268$  for Ge and  $-0.339$  for In in complex **6** (see [Table 3](#)). The same trend is found in the case of complex **5** as well: a charge difference of  $+0.250$  for Ge and  $-0.345$  for In. These results suggest that the Ge–In bond in **5** and **6** is a classical donor–acceptor bond.

In order to understand the influence of solvent effects, we have performed solvent-phase calculations as well. For further details, please see the [Supporting Information](#). Even though the exact values obtained from these calculations are changed due to the effect of the solvent (see [Tables S1 and S2](#) in the [Supporting Information](#)), the trends in the values as well as the conclusions are still the same as in the case of the gas-phase calculations. Hence, the conclusions reached with regard to the nature of the bonding in the silicon and germanium complexes are not altered when solvent effects are taken into account.

## CONCLUSIONS

In conclusion, we have prepared and characterized the first silylene complexes of indium **2** and **3**, by the reactions of  $[\text{PhC}(\text{N}t\text{Bu})_2\text{SiN}(\text{SiMe}_3)_2]$  (**1**) with  $\text{InCl}_3$  and  $\text{InBr}_3$ , respectively. The methodology has been extended to prepare the first germylene complexes of indium, **5** and **6**. The compositions of **2**, **3**, **5**, and **6** were authenticated by single-crystal X-ray studies that confirmed the monomeric nature of the adducts. The X-ray studies, in combination with DFT calculations, suggest that the Si–In and the Ge–In bonds are of the donor–acceptor type. Overall, this study underpins the high synthetic potential of the

**Table 2.** Bond Dissociation Energies (BDEs), Shared Electron Numbers (SENs), Wiberg Bond Indices (WBIs), and Bond Distances for Complexes **2**, **3**, and **5–9**

	<b>2</b>	<b>3</b>	<b>5</b>	<b>6</b>	<b>7</b>	<b>8</b>	<b>9</b>
BDE for homolytic cleavage ( $\Delta G$ , kcal/mol)	122.1	117.3	124.3	120.3	46.0	134.0	130.7
BDE for heterolytic cleavage ( $\Delta G$ , kcal/mol)	42.2	38.7	29.8	27.1	149.9	23.7	21.7
SEN (In–A)	0.995	0.984	1.005	0.991	1.217	0.981	0.987
WBI (In–A)	0.739	0.745	0.671	0.675	0.823	0.677	0.691
In–A (Å)	2.63	2.64	2.67	2.69	2.64	2.68	2.68

Table 3. Natural Charges for Si, Ge, and In Atoms in Complexes 2, 3, and 5–9 and the Corresponding Separated Fragments

charge	2		3		5		6	
	Si	In	Si	In	Ge	In	Ge	In
Q(dat)	1.495	1.010	1.519	0.774	1.338	1.046	1.356	0.804
Q(sep)	1.119	1.391	1.119	1.143	1.088	1.391	1.088	1.143
$\Delta Q$ (Q(dat) – Q(sep))	0.376	–0.381	0.400	–0.369	0.250	–0.345	0.268	–0.339
charge	7		8		9			
	Si	In	Si	In	Si	In		
Q(dat)	1.015	0.400	1.337	1.003	1.359	0.750		
Q(sep)	1.204	0.369	1.001	1.391	1.001	1.143		
$\Delta Q$ (Q(dat) – Q(sep))	–0.189	0.031	0.336	–0.388	0.358	–0.393		

donor-stabilized silylenes and germlyenes for the preparation of novel higher-coordinate tetrel(II) compounds.

## EXPERIMENTAL SECTION

All experiments were carried out under an inert atmosphere of argon applying standard Schlenk techniques or in a glovebox. The solvents used were purified by an MBRAUN MB SPS-800 solvent purification system. All chemicals purchased from Sigma-Aldrich were used without further purification. Compounds 1<sup>32</sup> and 4<sup>33</sup> were prepared according to the literature procedure. <sup>1</sup>H and <sup>13</sup>C NMR spectra were recorded in CDCl<sub>3</sub> using a Bruker Avance DPX 200 or a Bruker Avance DRX 400 spectrometer and were referenced to external SiMe<sub>4</sub>. Solid state NMR was measured at CSIR-NCL using JEOL 400 using the internal standard TSPA. LC-mass spectra were obtained using an Agilent Technologies 6120 instrument. Elemental analyses were performed at the CSIR-National Chemical Laboratory, Pune, India. Melting points were measured in a sealed glass tube on a Stuart SMP-30 melting point apparatus and were uncorrected.

**Synthesis of 2.** Toluene (20 mL) was added to a mixture of 1 (0.419 g, 1 mmol) and InCl<sub>3</sub> (0.221 g, 1 mmol) at ambient temperature. The solution turned yellow to colorless with the formation of a white precipitate, and the resulting suspension was stirred for 12 h. The supernatant solvent was removed by using cannula filtration, and the precipitate obtained was dried under vacuum and was further dissolved in 10 mL of THF. Then the solution was supersaturated and kept at –35 °C to give single crystals of 2 suitable for X-ray analysis. Yield: 0.519 g (79.0%). Mp: 176.8 °C. <sup>1</sup>H NMR (400 MHz, CDCl<sub>3</sub>, 25 °C):  $\delta$  7.70–7.62 (m, 5 H), 1.42 (s, 18 H), 0.65 (s, 9 H), 0.56 (s, 9 H) ppm. <sup>13</sup>C NMR (400 MHz, CDCl<sub>3</sub>, 25 °C):  $\delta$  174.34, 131.97, 129.16, 128.36, 127.18, 56.83, 31.69, 29.28, 5.64, 4.84 ppm. <sup>29</sup>Si CP/MAS NMR (25 °C):  $\delta$  11.4 (SiMe<sub>3</sub>), 4.3 (SiMe<sub>3</sub>), –54.4 to –84.3 (SiN(SiMe<sub>3</sub>)<sub>2</sub>). HRMS (CH<sub>3</sub>CN):  $m/z$  calcd for C<sub>22</sub>H<sub>43</sub>N<sub>3</sub>Cl<sub>3</sub>InSi<sub>3</sub> + Na<sup>+</sup> [M + Na]<sup>+</sup> 676.0761, found 676.0833.

**Synthesis of 3.** Toluene (20 mL) was added to a mixture of 1 (0.419 g, 1 mmol) and InBr<sub>3</sub> (0.354 g, 1 mmol) at ambient temperature. The solution turned yellow to pale orange with the formation of an orange precipitate, and the resulting suspension was stirred for 12 h. The supernatant solvent was removed by using cannula filtration, and the precipitate obtained was dried under vacuum; subsequently, 10 mL of THF was added to the precipitate. The solution was kept at –35 °C in a freezer to get single crystals of 3 suitable for X-ray analysis. Yield: 0.583 g (74%). Mp: 175.9 °C. <sup>1</sup>H NMR (400 MHz, CDCl<sub>3</sub>, 25 °C):  $\delta$  7.62–7.54 (m, 5 H), 1.35 (s, 18 H), 0.60 (s, 9 H), 0.50 (s, 9 H) ppm. <sup>13</sup>C solid state NMR (25 °C):  $\delta$  175.21, 136.67, 131.57, 129.4, 124.77, 57.73, 32.49, 23.18, 7.29 ppm. <sup>29</sup>Si CP/MAS NMR (25 °C):  $\delta$  14.1 (SiMe<sub>3</sub>), 10.9 (SiMe<sub>3</sub>), –31.7 (SiN(SiMe<sub>3</sub>)<sub>2</sub>). HRMS (CH<sub>3</sub>CN):  $m/z$  calcd for C<sub>22</sub>H<sub>42</sub>N<sub>3</sub>Br<sub>3</sub>InSi<sub>3</sub> + H<sup>+</sup> [M + H]<sup>+</sup> 784.9348, found 784.9966.

**Synthesis of 5.** To a mixture of 1 (0.465 g, 1 mmol) and InCl<sub>3</sub> (0.221 g, 1 mmol) in a Schlenk flask was added toluene (20 mL) at ambient temperature. The solution turned colorless with concomitant formation of a white precipitate. The resulting suspension was stirred for 12 h. The reaction mixture was filtered, and the filtrate was concentrated and kept at –35 °C in a freezer to afford a white crystals of 5 suitable for X-ray analysis. Yield: 0.450 g (64%). Mp: 136.9 °C. <sup>1</sup>H NMR (400 MHz,

CDCl<sub>3</sub>, 25 °C):  $\delta$  7.13–7.06 (m, 5 H), 1.23 (s, 18 H), 0.62 (s, 9 H), 0.43 (s, 9 H) ppm. <sup>13</sup>C solid state NMR (25 °C):  $\delta$  164.54, 133.14, 130.97, 129.49, 60.19, 57.0, 31.62, 30.08, 5.93 ppm. HRMS (CH<sub>3</sub>CN):  $m/z$  calcd for C<sub>22</sub>H<sub>43</sub>N<sub>3</sub>Cl<sub>3</sub>GeInSi<sub>2</sub> + H<sup>+</sup> [M + H]<sup>+</sup> 700.0384, found 700.0634.

**Synthesis of 6.** A mixture of 1 (0.465 g, 1 mmol) and InBr<sub>3</sub> (0.354 g, 1 mmol) was placed in a Schlenk flask, and toluene (20 mL) was added to it at ambient temperature. The solution turned colorless with simultaneous formation of a white precipitate. The reaction mixture was filtered after 12 h, and the filtrate was kept at –35 °C in a freezer to afford a white crystal of 6 suitable for X-ray analysis. Yield: 0.598 g (72%). Mp: 162.8 °C. <sup>1</sup>H NMR (400 MHz, CDCl<sub>3</sub>, 25 °C):  $\delta$  7.10–7.05 (m, 5 H), 1.24 (s, 18 H), 0.63 (s, 9 H), 0.42 (s, 9 H) ppm. <sup>13</sup>C solid state NMR (25 °C):  $\delta$  172.75, 136.69, 130.43, 129.29, 125.17, 57.43, 32.71, 23.25, 7.15 ppm. HRMS (CH<sub>3</sub>CN):  $m/z$  calcd for C<sub>22</sub>H<sub>42</sub>N<sub>3</sub>Br<sub>3</sub>GeInSi<sub>2</sub> + H<sup>+</sup> [M + H]<sup>+</sup> 830.8791, found 830.9405.

**Crystal Structure Determination.** A good-quality single crystal was hand-picked under a polarized optical microscope and then mounted in the diffractometer. The data collection was done at 100–150 K. The crystals were mounted on a Super Nova Dual source X-ray diffractometer system (Agilent Technologies) equipped with a CCD area detector and operated at 250 W power (50 kV, 0.8 mA) to generate Mo K $\alpha$  radiation ( $\lambda$  = 0.71073 Å) and Cu K $\alpha$  radiation ( $\lambda$  = 1.54178 Å) at 100–150 K. Initial scans of each specimen were performed to obtain preliminary unit cell parameters and to assess the mosaicity (breadth of spots between frames) of the crystal to select the required frame width for data collection. The CrysAlisPro program software suite was employed to carry out overlapping  $\phi$  and  $\omega$  scans at detector ( $2\theta$ ) settings ( $2\theta$  = 28°). Following data collection, reflections were sampled from all regions of the Ewald sphere to redetermine unit cell parameters for data integration. Following an exhaustive review of collected frames the resolution of the data set was judged. The data were integrated using the CrysAlisPro software with a narrow frame algorithm. The data were subsequently corrected for absorption by the program SCALE3 ABSPACK<sup>43</sup> scaling algorithm. These structures were solved by direct methods and refined by full-matrix least-squares refinement techniques on  $F^2$  using SHELXL-2016/4.<sup>44</sup> All calculations were carried out with the WinGx crystallographic package.<sup>45</sup> The atoms were located from iterative examination of difference  $F$  maps following the least-squares refinements of the earlier models. The final model was refined anisotropically (if the number of data permitted) until full convergence was achieved. Hydrogen atoms were placed in calculated positions (C–H = 0.93 Å) and included as riding atoms with isotropic displacement parameters 1.2–1.5 times the  $U_{eq}$  values of the attached C atoms. The modeling of electron density at 150 K within the unit cell did not lead to identification of recognizable solvent molecules in these structures, probably due to the highly disordered contents. This has generated alert level B in checkcif. An ORTEP III<sup>46</sup> view of the compound was drawn with 50% probability displacement ellipsoids.

**Crystal data of 2:** CCDC 1821424.  $M_r$  = 683.04, colorless block, monoclinic, space group  $P2_1/n$ ,  $a$  = 9.7808(4) Å,  $b$  = 19.3556(6) Å,  $c$  = 17.1218(6) Å,  $\alpha$  = 90.00°,  $\beta$  = 91.013(2)°,  $\gamma$  = 90.00°,  $V$  = 3240.9(2) Å<sup>3</sup>,  $Z$  = 4,  $T$  = 100.01 K,  $D_{calc}$  = 1.400 g cm<sup>–3</sup>,  $F(000)$  = 1408,  $\mu$  = 1.108 mm<sup>–1</sup>, 44314 reflections measured, 9877 unique ( $R_{int}$  = 0.0299) reflections used,  $T_{min}$  = 0.767,  $T_{max}$  = 0.792, absorption correction type

none, 320 refined parameters, number of restraints 0, goodness of fit =  $S = 1.061$ ,  $R_1 = 0.0294$ ,  $wR_2 = 0.0737$  (all data  $R_1 = 0.0357$ ,  $wR_2 = 0.0774$ ),  $\Delta\rho_{\max} = 1.732 \text{ e } \text{Å}^{-3}$ ,  $\Delta\rho_{\min} = -0.964 \text{ e } \text{Å}^{-3}$ .

**Crystal data of 3:** CCDC 1821425.  $M_r = 774.36$ , colorless plate, monoclinic, space group  $P2_1/n$ ,  $a = 10.0195(3) \text{ Å}$ ,  $b = 19.2450(5) \text{ Å}$ ,  $c = 17.3510(4) \text{ Å}$ ,  $\alpha = 90.00^\circ$ ,  $\beta = 90.231(2)^\circ$ ,  $\gamma = 90.00^\circ$ ,  $V = 3345.68(15) \text{ Å}^3$ ,  $Z = 4$ ,  $T = 150.01(10) \text{ K}$ ,  $D_{\text{calc}} = 1.537 \text{ g cm}^{-3}$ ,  $F(000) = 1536$ ,  $\mu = 4.410 \text{ mm}^{-1}$ , 9759 reflections measured, 5580 unique ( $R_{\text{int}} = 0.0351$ ) reflections used,  $T_{\text{min}} = 0.342$ ,  $T_{\text{max}} = 0.452$ , 292 refined parameters, absorption correction type multiscan, number of restraints 0, goodness of fit =  $S = 1.056$ ,  $R_1 = 0.0325$ ,  $wR_2 = 0.0848$  (all data  $R_1 = 0.0431$ ,  $wR_2 = 0.0885$ ),  $\Delta\rho_{\max} = 0.688 \text{ e } \text{Å}^{-3}$ ,  $\Delta\rho_{\min} = -0.618 \text{ e } \text{Å}^{-3}$ .

**Crystal data of 5:** CCDC 1821426.  $M_r = 685.51$ , yellowish block, monoclinic, space group  $P2_1/n$ ,  $a = 10.0296(4) \text{ Å}$ ,  $b = 20.3217(9) \text{ Å}$ ,  $c = 16.6347(5) \text{ Å}$ ,  $\alpha = 90.00^\circ$ ,  $\beta = 91.132(3)^\circ$ ,  $\gamma = 90.00^\circ$ ,  $V = 3389.8(2) \text{ Å}^3$ ,  $Z = 4$ ,  $T = 191(50) \text{ K}$ ,  $D_{\text{calc}} = 1.373 \text{ g cm}^{-3}$ ,  $F(000) = 1392$ ,  $\mu = 1.887 \text{ mm}^{-1}$ , 13773 reflections measured, 5952 unique ( $R_{\text{int}} = 0.0559$ ) reflections used,  $T_{\text{min}} = 0.87363$ ,  $T_{\text{max}} = 1.000$ , 292 refined parameters, absorption correction type multiscan, number of restraints 0, goodness of fit =  $S = 1.051$ ,  $R_1 = 0.0448$ ,  $wR_2 = 0.1056$  (all data  $R_1 = 0.0673$ ,  $wR_2 = 0.1248$ ),  $\Delta\rho_{\max} = 0.685 \text{ e } \text{Å}^{-3}$ ,  $\Delta\rho_{\min} = -0.994 \text{ e } \text{Å}^{-3}$ .

**Crystal data of 6:** CCDC 1821427.  $M_r = 818.89$ , colorless block, monoclinic, space group  $P2_1/n$ ,  $a = 10.26830(10) \text{ Å}$ ,  $b = 20.1650(4) \text{ Å}$ ,  $c = 16.7774(3) \text{ Å}$ ,  $\alpha = 90.00^\circ$ ,  $\beta = 91.3540(10)^\circ$ ,  $\gamma = 90.00^\circ$ ,  $V = 3472.96(10) \text{ Å}^3$ ,  $Z = 4$ ,  $T = 150.00(10) \text{ K}$ ,  $D_{\text{calc}} = 1.566 \text{ g cm}^{-3}$ ,  $F(000) = 1608$ ,  $\mu = 5.063 \text{ mm}^{-1}$ , 14453 reflections measured, 6100 unique ( $R_{\text{int}} = 0.0322$ ) reflections used,  $T_{\text{min}} = 0.53843$ ,  $T_{\text{max}} = 1.000$ , 292 refined parameters, absorption correction type multiscan, number of restraints 0, goodness of fit =  $S = 0.663$ ,  $R_1 = 0.0365$ ,  $wR_2 = 0.1091$  (all data  $R_1 = 0.0500$ ,  $wR_2 = 0.1216$ ),  $\Delta\rho_{\max} = 0.750 \text{ e } \text{Å}^{-3}$ ,  $\Delta\rho_{\min} = -0.505 \text{ e } \text{Å}^{-3}$ .

## ■ ASSOCIATED CONTENT

### Supporting Information

The Supporting Information is available free of charge on the ACS Publications website at DOI: 10.1021/acs.organomet.8b00093.

Complete computational details and representative NMR spectra (PDF)

Cartesian coordinates for the calculated structures (XYZ)

### Accession Codes

CCDC 1821424–1821427 contain the supplementary crystallographic data for this paper. These data can be obtained free of charge via [www.ccdc.cam.ac.uk/data\\_request/cif](http://www.ccdc.cam.ac.uk/data_request/cif), or by emailing [data\\_request@ccdc.cam.ac.uk](mailto:data_request@ccdc.cam.ac.uk), or by contacting The Cambridge Crystallographic Data Centre, 12 Union Road, Cambridge CB2 1EZ, UK; fax: +44 1223 336033.

## ■ AUTHOR INFORMATION

### Corresponding Author

\*E-mail for S.S.S.: [ss.sen@ncl.res.in](mailto:ss.sen@ncl.res.in).

### ORCID

Moumita Pait: 0000-0001-7215-7048

K. Vipin Raj: 0000-0002-7178-264X

Kumar Vanka: 0000-0001-7301-7573

Sakya S. Sen: 0000-0002-4955-5408

### Notes

The authors declare no competing financial interest.

## ■ ACKNOWLEDGMENTS

This work was supported by a Ramanujan research grant (SB/S2/RJN-073/2014), Department of Science and Technology (DST), India. S.P. thanks the DST, of India for an INSPIRE Fellowship (IF160314). S.K. thanks the UGC of India for a research fellowship. M.P. is also thankful to the DST-SERB

NPDF (PDF/2016/002059) for providing financial assistance for this work. K.V. acknowledges “MSM” (CSC0129) and DST (EMR/2014/000013) for funding.

## ■ REFERENCES

- (1) Lewis, G. N. THE ATOM AND THE MOLECULE. *J. Am. Chem. Soc.* **1916**, *38*, 762–785.
- (2) Selected examples of carbene-supported main-group compounds: (a) Bourissou, D.; Guerret, O.; Gabbai, F. P.; Bertrand, G. Stable Carbenes. *Chem. Rev.* **2000**, *100*, 39–91. (b) Wang, Y.; Xie, Y.; Wei, P.; King, R. B.; Schaefer, H. F., III; Schleyer, P. v. R.; Robinson, G. H. A Stable Silicon(0) Compound with a Si=Si Double Bond. *Science* **2008**, *321*, 1069–1071. (c) Ghadwal, R. S.; Roesky, H. W.; Merkel, S.; Henn, J.; Stalke, D. Lewis Base Stabilized Dichlorosilylene. *Angew. Chem., Int. Ed.* **2009**, *48*, 5683–5686. (d) Filippou, A. C.; Chernov, O.; Schnakenburg, G. SiBr<sub>2</sub>(Idipp): A Stable N-Heterocyclic Carbene Adduct of Dibromosilylene. *Angew. Chem., Int. Ed.* **2009**, *48*, 5687–5690. (e) Al-Rafia, S. M. I.; Malcom, A. C.; McDonald, R.; Ferguson, M. J.; Rivard, E. Trapping the parent inorganic ethylenes H<sub>2</sub>SiGeH<sub>2</sub> and H<sub>2</sub>SiSnH<sub>2</sub> in the form of stable adducts at ambient temperature. *Angew. Chem., Int. Ed.* **2011**, *50*, 8354–8357. (f) Braunschweig, H.; Dewhurst, R. D.; Hammond, K.; Mies, J.; Radacki, K.; Vargas, A. Ambient-Temperature Isolation of a Compound with a Boron-Boron Triple Bond. *Science* **2012**, *336*, 1420–1422. (g) Mondal, K. C.; Roesky, H. W.; Schwarzer, M. C.; Frenking, G.; Niepötter, B.; Wolf, H.; Herbst-Irmer, R.; Stalke, D. A Stable Singlet Biradicaloid Siladibene: (L)<sub>2</sub>Si. *Angew. Chem., Int. Ed.* **2013**, *52*, 2963–2967. (h) Mondal, K. C.; Roesky, H. W.; Schwarzer, M. C.; Frenking, G.; Tkach, I.; Wolf, H.; Kratzert, D.; Herbst-Irmer, R.; Niepötter, B.; Stalke, D. Conversion of a Singlet Silylene to a stable Biradical. *Angew. Chem., Int. Ed.* **2013**, *52*, 1801–1805. (i) Xiong, Y.; Yao, S.; Inoue, S.; Epping, J. D.; Driess, M. A Cyclic Silylone (“Siladibene”) with an Electron-Rich Silicon(0) Atom. *Angew. Chem., Int. Ed.* **2013**, *52*, 7147–7150.
- (3) Alvarez-Rodriguez, L.; Cabeza, J. A.; Garcia-Alvarez, P.; Polo, D. Transition-Metal Chemistry of Amidinosilylenes, -Germynes and -Stannylenes. *Coord. Chem. Rev.* **2015**, *300*, 1–28.
- (4) (a) Einstein, F. W. B.; Gilbert, M. M.; Tuck, D. G. Cyclopentadienyl bridge. Crystal structure of tris(cyclopentadienyl)indium(III) at –100. deg. *Inorg. Chem.* **1972**, *11*, 2832–2836. (b) Beachley, O. T., Jr.; Blom, R.; Churchill, M. R.; Faegri, K., Jr.; Fettinger, J. C.; Pazik, J. C.; Victoriano, L. (Pentamethylcyclopentadienyl)indium(I) and -indium(III) compounds. Syntheses, reactivities, and x-ray diffraction and electron diffraction studies of In(C<sub>5</sub>Me<sub>5</sub>). *Organometallics* **1989**, *8*, 346–356. (c) Hawley, A. L.; Ohlin, C. A.; Fohlmeister, L.; Stasch, A. Heavier group 13 metal(I) heterocycles stabilized by sterically demanding diiminophosphinates: a structurally characterized monomer-dimer pair for gallium. *Chem. - Eur. J.* **2017**, *23*, 447–455. (d) Prashanth, B.; Bawari, D.; Singh, S. Heteroleptic Iminophosphonamide In(III) Complexes: Source of Mild Lewis Acid Indium Centers. *ChemistrySelect* **2017**, *2*, 2039–2043.
- (5) Selected references on MOLP: (a) Braunschweig, H.; Gruss, K.; Radacki, K. Interaction between d- and p-Block Metals: Synthesis and Structure of Platinum–Alane Adducts. *Angew. Chem., Int. Ed.* **2007**, *46*, 7782–7784. (b) Braunschweig, H.; Gruss, K.; Radacki, K. Reactivity of Pt<sup>0</sup> Complexes toward Gallium(III) Halides: Synthesis of a Platinum Gallane Complex and Oxidative Addition of Gallium Halides to Pt<sup>0</sup>. *Inorg. Chem.* **2008**, *47*, 8595–8597. (c) Hupp, F.; Ma, M.; Kroll, F.; Jimenez-Halla, J. O. C.; Dewhurst, R. D.; Radacki, K.; Stasch, A.; Jones, C.; Braunschweig, H. Platinum Complexes Containing Pyramidalized Germanium and Tin Dihalide Ligands Bound through  $\sigma, \sigma$  M = E Multiple Bonds. *Chem. - Eur. J.* **2014**, *20*, 16888–16898. (d) Braunschweig, H.; Celik, M. A.; Dewhurst, R. D.; Heid, M.; Hupp, F.; Sen, S. S. Stepwise isolation of low-valent, low-coordinate Sn and Pb mono- and dications in the coordination sphere of platinum. *Chem. Sci.* **2015**, *6*, 425–435. (e) Bauer, J.; Braunschweig, H.; Dewhurst, R. D. Metal-Only Lewis Pairs with Transition Metal Lewis Bases. *Chem. Rev.* **2012**, *112*, 4329–4346. (f) Braunschweig, H.; Cogswell, P.; Schwab, K. Synthesis,



structure and reactivity of complexes containing a transition metal-bismuth bond. *Coord. Chem. Rev.* **2011**, *255*, 101–117.

(6) Bertermann, R.; Böhnke, J.; Braunschweig, H.; Dewhurst, R. D.; Kupfer, T.; Muessig, J. H.; Pentecost, L.; Radacki, K.; Sen, S. S.; Vargas, A. Dynamic, Reversible Oxidative Addition of Highly Polar Bonds to a Transition Metal. *J. Am. Chem. Soc.* **2016**, *138*, 16140–16147.

(7) (a) Black, S. J.; Hibbs, D. E.; Hursthouse, M. B.; Jones, C.; Malik, K. M. A.; Smithies, N. A. Synthesis and characterisation of stable carbene-indium(III) halide complexes. *J. Chem. Soc., Dalton Trans.* **1997**, 4313–4320. (b) Abernethy, C. D.; Cole, M. L.; Jones, C. Preparation, Characterization, and Reactivity of the Stable Indium Trihydride Complex  $[\text{InH}_3\{\text{CN}(\text{Mes})\text{C}_2\text{H}_2\text{N}(\text{Mes})\}]$ . *Organometallics* **2000**, *19*, 4852–4857. (c) Wu, M. M.; Gill, A. M.; Yunpeng, L.; Yongxin, L.; Ganguly, R.; Falivene, L.; García, F. Aryl-NHC-group 13 trimethyl complexes: structural, stability and bonding insights. *Dalton Trans.* **2017**, *46*, 854–864.

(8) Holzmann, N.; Stasch, A.; Jones, C.; Frenking, G. Structures and Stabilities of Group 13 Adducts  $[(\text{NHC})(\text{EX}_3)]$  and  $[(\text{NHC})_2(\text{E}_2\text{X}_n)]$  ( $\text{E} = \text{B}$  to  $\text{In}$ ;  $\text{X} = \text{H}, \text{Cl}$ ;  $n = 4, 2, 0$ ;  $\text{NHC} = \text{N}$ -Heterocyclic Carbene) and the Search for Hydrogen Storage Systems: A Theoretical Study. *Chem. - Eur. J.* **2011**, *17*, 13517–13525.

(9) Karazhanov, S. Z. High- $\kappa$  gate dielectrics: Current status and materials properties considerations. *J. Appl. Phys.* **2001**, *89*, 4030–4036.

(10) Bürger, H.; Götze, U. Tris(trimethylsilyl)indium. *Angew. Chem., Int. Ed. Engl.* **1969**, *8*, 140–141.

(11) Arif, A. M.; Cowley, A. H.; Elkins, T. M.; Jones, R. A. Synthesis and structural characterisation of compounds with gallium-silicon and indium-silicon bonds. *J. Chem. Soc., Chem. Commun.* **1986**, 1776–1777.

(12) Wochele, R.; Schwarz, W.; Klinkhammer, K. W.; Locke, K.; Weidlein, J. Neue Hypersilanide der Erdmetalle Aluminium, Gallium und Indium. *Z. Anorg. Allg. Chem.* **2000**, *626*, 1963–1973.

(13) (a) Wiberg, N.; Amelunxen, K.; Nöth, H.; Schmidt, M.; Schwenk, H. Tetrasupersilyldiindium ( $\text{In-In}$ ) and Tetrasupersilyldithallium ( $\text{Tl-Tl}$ ):  $(\text{tBu}_3\text{Si})_2\text{M-M}(\text{Si}^i\text{tBu}_3)_2$  ( $\text{M} = \text{In}, \text{Tl}$ ). *Angew. Chem., Int. Ed. Engl.* **1996**, *35*, 65–67. (b) Wiberg, N.; Blank, T.; Purath, A.; Stösser, G.; Schnöckel, H. Hexasupersilyloctaindane  $(\text{tBu}_3\text{Si})_6\text{In}_8$  - A Compound with a Novel  $\text{In}_8$  Cluster Framework. *Angew. Chem., Int. Ed.* **1999**, *38*, 2563–2565. (c) Wiberg, N.; Blank, T.; Nöth, H.; Ponikvar, W. Dodecaindane  $(\text{tBu}_3\text{Si})_8\text{In}_{12}$ -A Compound with an  $\text{In}_{12}$  Deltapolyhedron Framework. *Angew. Chem., Int. Ed.* **1999**, *38*, 839–841.

(14) For reviews on silicon(II) compounds, please see: (a) Haaf, M.; Schmedake, T. A.; West, R. Stable Silylenes. *Acc. Chem. Res.* **2000**, *33*, 704–714. (b) Nagendran, S.; Roesky, H. W. The Chemistry of Aluminum(I), Silicon(II), and Germanium(II). *Organometallics* **2008**, *27*, 457–492. (c) Mizuhata, Y.; Sasamori, T.; Tokitoh, N. Stable Heavier Carbene Analogues. *Chem. Rev.* **2009**, *109*, 3479–3511. (d) Mandal, S. K.; Roesky, H. W. Interstellar molecules: guides for new chemistry. *Chem. Commun.* **2010**, *46*, 6016–6041. (e) Yao, S.; Xiong, Y.; Driess, M. Zwitterionic and Donor-Stabilized N-Heterocyclic Silylenes (NHSis) for Metal-Free Activation of Small Molecules. *Organometallics* **2011**, *30*, 1748–1767. (f) Asay, M.; Jones, C.; Driess, M. N-Heterocyclic Carbene Analogues with Low-Valent Group 13 and Group 14 Elements: Syntheses, Structures, and Reactivities of a New Generation of Multitalented Ligands. *Chem. Rev.* **2011**, *111*, 354–396. (g) Sen, S. S.; Khan, S.; Nagendran, S.; Roesky, H. W. Interconnected Bis-Silylenes: A New Dimension in Organosilicon Chemistry. *Acc. Chem. Res.* **2012**, *45*, 578–587. (h) Sen, S. S.; Khan, S.; Samuel, P. P.; Roesky, H. W. Chemistry of functionalized silylenes. *Chem. Sci.* **2012**, *3*, 659–682. (i) Ghadwal, R. S.; Azhakar, R.; Roesky, H. W. Dichlorosilylene: A High Temperature Transient Species to an Indispensable Building Block. *Acc. Chem. Res.* **2013**, *46*, 444–456. (j) Roesky, H. W. Chemistry of low valent silicon. *J. Organomet. Chem.* **2013**, *730*, 57–62. (k) Yadav, S.; Saha, S.; Sen, S. S. Compounds with Low-Valent p-Block Elements for Small Molecule Activation and Catalysis. *ChemCatChem* **2016**, *8*, 486–501 and references therein.

(15) Baus, J. A.; Muck, F. M.; Schneider, H.; Tacke, R. Iron(II), Cobalt(II), Nickel(II), and Zinc(II) Silylene Complexes: Reaction of the Silylene  $[\text{iPrNC}(\text{NiPr}_2)\text{NiPr}_2]\text{Si}$  with  $\text{FeBr}_2$ ,  $\text{CoBr}_2$ ,  $\text{NiBr}_2$ ,

$\text{MeOCH}_2\text{CH}_2\text{OMe}$ ,  $\text{ZnCl}_2$ , and  $\text{ZnBr}_2$ . *Chem. - Eur. J.* **2017**, *23*, 296–303.

(16) Muck, F. M.; Baus, J. A.; Ulmer, A.; Burschka, C.; Tacke, R. Reactivity of the Donor-Stabilized Guanidinatosilylene  $[\text{ArNC}(\text{NMe}_2)\text{-NAr}]\text{Si}[\text{N}(\text{SiMe}_3)_2]$  ( $\text{Ar} = 2,6\text{-Diisopropylphenyl}$ ). *Eur. J. Inorg. Chem.* **2016**, *2016*, 1660–1670.

(17) (a) Gallego, D.; Breck, A.; Irran, E.; Meier, F.; Kaupp, M.; Driess, M.; Hartwig, J. F. From Bis(silylene) and Bis(germylene) Pincer-Type Nickel(II) Complexes to Isolable Intermediates of the Nickel-Catalyzed Sonogashira Cross-Coupling Reaction. *J. Am. Chem. Soc.* **2013**, *135*, 15617–15626. (b) Breit, N. C.; Szilvási, T.; Suzuki, T.; Gallego, D.; Inoue, S. From a Zwitterionic Phosphasilene to Base Stabilized Silyliumylidene-Phosphide and Bis(silylene) Complexes. *J. Am. Chem. Soc.* **2013**, *135*, 17958–17968. (c) Wang, W.; Inoue, S.; Yao, S.; Driess, M. An Isolable Bis-Silylene Oxide (“Disilylenoxane”) and Its Metal Coordination. *J. Am. Chem. Soc.* **2010**, *132*, 15890–15892. (d) Tan, G.; Enthaler, S.; Inoue, S.; Blom, B.; Driess, M. Synthesis of Mixed Silylene-Carbene Chelate Ligands from N-Heterocyclic Silylcarbenes Mediated by Nickel. *Angew. Chem., Int. Ed.* **2015**, *54*, 2214–2218.

(18) (a) Gallego, D.; Inoue, S.; Blom, B.; Driess, M. Highly Electron-Rich Pincer-Type Iron Complexes Bearing Innocent Bis(metallylene)-pyridine Ligands: Syntheses, Structures, and Catalytic Activity. *Organometallics* **2014**, *33*, 6885–6897. (b) Blom, B.; Enthaler, S.; Inoue, S.; Irran, E.; Driess, M. Electron-Rich N-Heterocyclic Silylene (NHSi)-Iron Complexes: Synthesis, Structures, and Catalytic Ability of an Isolable Hydridosilylene-Iron Complex. *J. Am. Chem. Soc.* **2013**, *135*, 6703–6713.

(19) Wang, W.; Inoue, S.; Enthaler, S.; Driess, M. Bis(silylenyl)- and Bis(germylenyl)-Substituted Ferrocenes: Synthesis, Structure, and Catalytic Applications of Bidentate Silicon(II)-Cobalt Complexes. *Angew. Chem., Int. Ed.* **2012**, *51*, 6167–6171.

(20) Azhakar, R.; Ghadwal, R. S.; Roesky, H. W.; Hey, J.; Krause, L.; Stalke, D. Mixed valence  $\eta^6$ -arene cobalt(I) and cobalt(II) compound. *Dalton Trans.* **2013**, *42*, 10277–10281.

(21) (a) Schäfer, S.; Köppe, R.; Gamer, M. T.; Roesky, P. W. Zinc-silylene complexes. *Chem. Commun.* **2014**, *50*, 11401–11403. (b) Schäfer, S.; Köppe, R.; Roesky, P. W. Investigations of the Nature of  $\text{Zn}^{\text{II}}\text{-Si}^{\text{II}}$  Bonds. *Chem. - Eur. J.* **2016**, *22*, 7127–7133.

(22) Yadav, S.; Sangtani, E.; Dhawan, D.; Gonnade, R. G.; Ghosh, D.; Sen, S. S. Unprecedented solvent induced inter-conversion between monomeric and dimeric silylene-zinc iodide adducts. *Dalton Trans.* **2017**, *46*, 11418–11424.

(23) Khan, S.; Pal, S.; Kathewad, N.; Parameswaran, P.; De, S.; Purushothaman, I. Stepwise isolation of an unprecedented silylene supported dinuclear gold(I) cation with aurophilic interaction. *Chem. Commun.* **2016**, *52*, 3880–3882.

(24) Parvin, N.; Pal, S.; Khan, S.; Das, S.; Pati, S. K.; Roesky, H. W. Unique Approach to Copper(I) Silylene Chalcogenone Complexes. *Inorg. Chem.* **2017**, *56*, 1706–1712.

(25) Khan, S.; Ahirwar, S. K.; Pal, S.; Parvin, N.; Kathewad, N. Silicon(II) Bis(trimethylsilyl)amide  $(\text{LSiN}(\text{SiMe}_3)_2)$ ,  $\text{L} = \text{PhC}(\text{NtBu})_2$  Supported Copper, Silver, and Gold Complexes. *Organometallics* **2015**, *34*, 5401–5406.

(26) Parvin, N.; Dasgupta, R.; Pal, S.; Sen, S. S.; Khan, S. Strikingly diverse reactivity of structurally identical silylene and stannylene. *Dalton Trans.* **2017**, *46*, 6528–6532.

(27) (a) Mück, F. M.; Baus, J. A.; Bertermann, R.; Burschka, C.; Tacke, R. Lewis Acid/Base Reactions of the Bis(amidinato)silylene  $[\text{iPrNC}(\text{Ph})\text{NiPr}_2]\text{Si}$  and Bis(guanidinato)silylene  $[\text{iPrNC}(\text{NiPr}_2)\text{NiPr}_2]\text{Si}$  with  $\text{EIPh}_3$  ( $\text{E} = \text{B}, \text{Al}$ ). *Organometallics* **2016**, *35*, 2583–2588. (b) Junold, K.; Baus, J. A.; Burschka, C.; Fonseca Guerra, C.; Bickelhaupt, F. M.; Tacke, R. Bis $[\text{N,N}'\text{-diisopropylbenzamidinato}(-)]\text{-silicon(II)}$ : Lewis Acid/Base Reactions with Triorganylboranes. *Chem. - Eur. J.* **2014**, *20*, 12411–12415. (c) Ghadwal, R. S.; Roesky, H. W.; Merkel, S.; Stalke, D. Ambiphilicity of Dichlorosilylene in a Single Molecule. *Chem. - Eur. J.* **2010**, *16*, 85–88.

(28) Blom, B.; Klatt, G.; Gallego, D.; Tan, G.; Driess, M. Unprecedented silicon(II)→calcium complexes with N-heterocyclic silylenes. *Dalton Trans.* **2015**, *44*, 639–644.

(29) Chia, S.-P.; Xi, H.-W.; Li, Y.; Lim, K. H.; So, C.-W. A Base-Stabilized Lead(I) Dimer and an Aromatic Plumblydenide Anion. *Angew. Chem., Int. Ed.* **2013**, *52*, 6298–6301.

(30) Shan, Y.-L.; Leong, B.-X.; Xi, H.-W.; Ganguly, R.; Li, Y.; Lim, K. H.; So, C.-W. Reactivity of an amidinato silylene and germylene toward germanium(II), tin(II) and lead(II) halides. *Dalton Trans.* **2017**, *46*, 3642–3648.

(31) Kühler, T.; Jutzi, P.; Stammer, A.; Stammer, H.-G. Easy formation of indium–silicon bonds: reaction of decamethylsilococene with trimethylindium. *Chem. Commun.* **2001**, 539–540.

(32) Sen, S. S.; Hey, J.; Herbst-Irmer, R.; Roesky, H. W.; Stalke, D. Striking Stability of a Substituted Silicon(II) Bis(trimethylsilyl)amide and the Facile Si–Me Bond Cleavage without a Transition Metal Catalyst. *J. Am. Chem. Soc.* **2011**, *133*, 12311–12316.

(33) Samuel, P. P.; Singh, A. P.; Sarish, S. P.; Matussek, J.; Objartel, I.; Roesky, H. W.; Stalke, D. Oxidative Addition Versus Substitution Reactions of Group 14 Dialkylamino Metalylenes with Pentafluoropyridine. *Inorg. Chem.* **2013**, *52*, 1544–1549.

(34) Guloy, A. M.; Corbett, J. D. A remarkable hypoelectronic indium cluster in  $K_8In_{11}$ . *Inorg. Chem.* **1996**, *35*, 2616–2622.

(35) (a) Kottke, T.; Stalke, D. Crystal handling at low temperatures. *J. Appl. Crystallogr.* **1993**, *26*, 615–619. (b) Stalke, D. Cryo crystal structure determination and application to intermediates. *Chem. Soc. Rev.* **1998**, *27*, 171–178. (c) Schulz, T.; Meindl, K.; Leusser, D.; Stern, D.; Graf, J.; Michaelsen, C.; Ruf, M.; Sheldrick, G. M.; Stalke, D. A comparison of a microfocus X-ray source and a conventional sealed tube for crystal structure determination. *J. Appl. Crystallogr.* **2009**, *42*, 885–891. (d) Krause, L.; Herbst-Irmer, R.; Sheldrick, G. M.; Stalke, D. Comparison of silver and molybdenum microfocus X-ray sources for single-crystal structure determination. *J. Appl. Crystallogr.* **2015**, *48*, 3–10. (e) Krause, L.; Herbst-Irmer, R.; Stalke, D. An empirical correction for the influence of low-energy contamination. *J. Appl. Crystallogr.* **2015**, *48*, 1907–1913.

(36) Rösch, L. Formation of the Ge–In Bond. In *Inorganic Reactions and Methods: The Formation of Bonds to C, Si, Ge, Sn, Pb (Part 2)*; Zuckerman, J. J., Hagen, A. P., Eds.; Wiley: Hoboken, NJ, USA, 1989; Vol. 10.

(37) Vyazankin, N. S.; Razuvaev, G. A.; Kruglaya, O. A. Organometallic compounds with metal-metal bonds between different metals. *Organomet. Chem. Rev. A* **1968**, *3*, 323.

(38) (a) Emsley, J. *The Elements*, 3rd ed.; Oxford University Press: Oxford, U.K., 1998. (b) Nakata, N.; Izumi, R.; Lee, V. Y.; Ichinohe, M.; Sekiguchi, A. 1,3-Digerma-2-gallata- and -indataallenic Anions: The First Compounds with Ge=Ga or Ge=In Double Bonds. *Chem. Lett.* **2008**, *37*, 1146–1147.

(39) Nagendran, S.; Sen, S. S.; Roesky, H. W.; Koley, D.; Grubmüller, H.; Pal, A.; Herbst-Irmer, R. RGe(I)Ge(I)R Compound (R = PhC(NtBu)<sub>2</sub>) with a Ge–Ge Single Bond and a Comparison with the Gauche Conformation of Hydrazine. *Organometallics* **2008**, *27*, 5459–5463.

(40) Himmel, D.; Krossing, I.; Schnepf, A. Dative Bonds in Main-Group Compounds: A Case for Fewer Arrows! *Angew. Chem., Int. Ed.* **2014**, *53*, 370–374.

(41) Frenking, G. Dative Bonds in Main-Group Compounds: A Case for More Arrows! *Angew. Chem., Int. Ed.* **2014**, *53*, 6040–6046.

(42) Himmel, D.; Krossing, I.; Schnepf, A. Dative or Not Dative? *Angew. Chem., Int. Ed.* **2014**, *53*, 6047–6048.

(43) *CrysAlisPro, Version 1.171.33.66*; Oxford Diffraction Ltd.: Abingdon, U.K., 2010.

(44) Sheldrick, G. M. A short history of SHELX. *Acta Crystallogr., Sect. A* **2008**, *64*, 112–122.

(45) Farrugia, L. J. *WinGx, v. 2014.1, An Integrated System of Windows Programs for the Solution, Refinement and Analysis of Single-Crystal X-ray Diffraction Data*; Department of Chemistry, University of Glasgow, Glasgow, U.K., 2014.

(46) Farrugia, L. J. ORTEP-3 for Windows - a version of ORTEP-III with a Graphical User Interface (GUI). *J. Appl. Crystallogr.* **1997**, *30*, 565–565.


 Cite this: *Chem. Commun.*, 2020, 56, 11871

 Received 30th July 2020,  
 Accepted 25th August 2020

DOI: 10.1039/d0cc05202g

rsc.li/chemcomm

## Access to diverse germylenes and a six-membered dialane with a flexible $\beta$ -diketiminato†‡

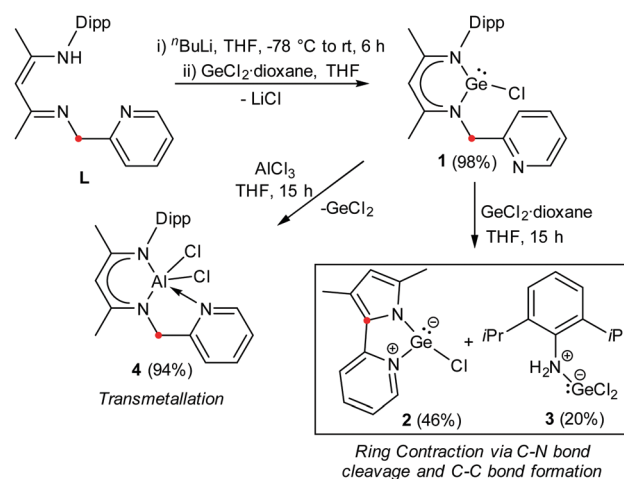
 Sanjukta Pahar,<sup>ab</sup> V. S. V. S. N. Swamy,<sup>ab</sup> Tamal Das,<sup>bc</sup> Rajesh G. Gonnade,<sup>id bc</sup> Kumar Vanka<sup>id bc</sup> and Sakya S. Sen<sup>id \*ab</sup>

A *nacnac*-based tridentate ligand containing a picolyl group (**L**) was employed to isolate chlorogermylene (**1**). The reaction of **1** with another equivalent of  $\text{GeCl}_2$ -dioxane surprisingly gave pyridylpyrrolide-based chlorogermylene (**2**) via C–N bond cleavage and C–C coupling, while with  $\text{AlCl}_3$ , it afforded a transmetalated product, **4**. The reaction of **L** with  $\text{AlH}_3\text{-NMe}_2\text{Et}$  led to an unusual cyclohexane type six-membered dialane heterocycle (**5**).

The *nacnac* supported chlorogermylene,  $[\text{CH}\{\text{CMe}\}(2,6\text{-iPr}_2\text{C}_6\text{H}_3\text{N})_2]\text{GeCl}$  (**A**),<sup>1</sup> from the Roesky group, has enjoyed substantial attention due to its utility as a synthon to prepare a series of germanium compounds.<sup>2</sup> The synthetic accomplishments would not have been possible without the use of a  $\beta$ -diketiminato ligand,<sup>3</sup> which provides adequate thermodynamic and/or kinetic stabilization. A less well-developed ligand system is a *nacnac* framework with a picolyl functionality (**L**), which is tridentate and has been used for the synthesis of iron, chromium, yttrium, and scandium complexes.<sup>4,5</sup> Recently, we have prepared magnesium and calcium complexes using this ligand and demonstrated their potential as catalysts for the hydroboration of aldehydes and ketones.<sup>6</sup> Hence, the ligand of choice has the potential to provide intramolecular stabilisation to the electron-deficient germylium-ylidenes. A further impetus comes from the recent report on pyridine functionalized silane, which shows unprecedented binding properties with Rh and Ir.<sup>7</sup> To our surprise, we did not obtain any germylium-ylidene species, but the presence of the picolyl functionality in **L** promoted

alternate reactivity such as smooth ring contraction *via* C–N bond cleavage, facile dehydrocoupling and a six membered Al-heterocycle formation, which are not observed for the *nacnac*-based systems. The work is another testimony to the fact that small variations in the ligand system can yield unprecedented outcomes.<sup>8</sup>

The reaction of the ligand (**L**) with  ${}^n\text{BuLi}$  and the subsequent addition of  $\text{GeCl}_2$ -dioxane at low temperature afforded the desired germylene monochloride (**1**) as a bright yellow solid (Scheme 1). Single crystal X-ray data revealed that, belying expectations, the Ge atom is tri-coordinate (Fig. 1) and displays a distorted trigonal-pyramidal geometry, and that the pyridine-*N* does not coordinate to the Ge center. Calculations with density functional theory (DFT) (see ESI† for details) show that the HOMO is located at the Ge center and throughout the six-membered *nacnac* ring, while the LUMO is spread over the pyridine ring (ESI,† Fig. S18). The HOMO–LUMO energy gap for **1** has been determined to be 6.48 eV, at the PBE/TZVP/M06-2X/6-311+G(d) level of theory (for further computational details, please see the ESI†).



**Scheme 1** Synthesis of **1–4**. The methylene carbon is highlighted in red (Dipp = 2,6-*iPr*<sub>2</sub>-C<sub>6</sub>H<sub>3</sub>).

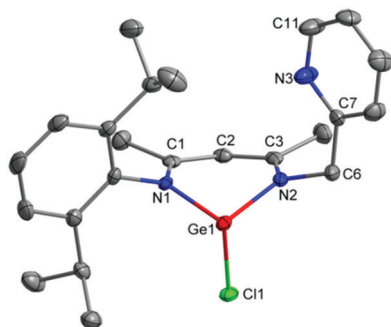
<sup>a</sup> *Inorganic Chemistry and Catalysis Division, CSIR-National Chemical Laboratory, Dr Homi Bhabha Road, Pashan, Pune 411008, India. E-mail: ss.sen@ncl.res.in*

<sup>b</sup> *Academy of Scientific and Innovative Research (AcSIR), Ghaziabad-201002, India*

<sup>c</sup> *Physical and Material Chemistry Division, CSIR-National Chemical Laboratory, Dr Homi Bhabha Road, Pashan, Pune 411008, India*

† Dedicated to Professor Sourav Pal on the occasion of his 65th birthday.

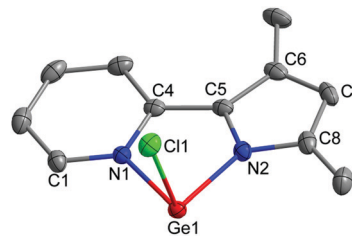
‡ Electronic supplementary information (ESI) available: Experimental & computational details, CIF files of **1–5**, and Checkcifs are given in the ESI. CCDC 2000072 (**1**), 2000154 (**2**), 2000073 (**3**), 2000071 (**4**) and 2002736 (**5**). For ESI and crystallographic data in CIF or other electronic format see DOI: 10.1039/d0cc05202g



**Fig. 1** Molecular structure of **1** with anisotropic displacement parameters depicted at the 50% probability level. Hydrogen atoms are not shown for clarity. Selected bond lengths (Å) and bond angles (°): Ge1–N1 1.9539(15), Ge1–N2 1.9591(16), Ge1–Cl1 2.3523(5); N1–Ge1–N2 90.67(6), N1–Ge1–Cl1 94.13(5), N2–Ge1–Cl1 92.30(5).

Subsequently, we sought to prepare the corresponding germylium ylide from **1** by abstracting the chloride ligand using another equivalent of  $\text{GeCl}_2$ -dioxane or  $\text{AlCl}_3$ . Surprisingly, the addition of another equivalent of  $\text{GeCl}_2$ -dioxane to a THF solution of **1** did not afford any  $\text{Ge}^{\text{II}} \rightarrow \text{Ge}^{\text{II}}$  donor–acceptor compound;<sup>9</sup> instead the cleavage of the C–N bond next to the Ge–heteroatom bond took place, leading to a new chlorogermylene (**2**) supported by the pyridylpyrrolide ligand, along with a  $\text{DippNH}_2 \cdot \text{GeCl}_2$  adduct (**3**) (Scheme 1). Schnepf and coworkers reported the reaction of a germylene,  $\text{R}_2\text{Ge}$  ( $\text{R} = (\text{SiMe}_3)_3\text{CS}$ ) with  $\text{GeCl}_2$ -dioxane, where also no  $\text{Ge}^{\text{II}} \rightarrow \text{Ge}^{\text{II}}$  donor–acceptor compound was formed, instead the  $\text{GeCl}_2$  moiety inserted into the C–S bond adjacent to the Ge–S bond.<sup>10</sup> X-ray diffraction analysis of the crystals obtained from the fractional crystallization of the reaction mixture confirmed the formation of **2** and **3**. Nucleophilic attack on the nacnac  $\beta$ -carbon and the subsequent ring contraction reaction has been recently reported, but it usually requires a strong reductant like alkali metals or the  $\text{Mg}(\text{i})$  dimer,<sup>11</sup> except for the report from Cui and coworkers, who demonstrated the ring contraction upon reacting a  $\beta$ -diketiminato  $\text{Al}(\text{i})$  compound,  $[\text{HC}\{(\text{C}t\text{Bu})_2(\text{NAr})_2\}]_2\text{Al}$  with an N-heterocyclic carbene (NHC).<sup>12</sup> Interestingly, pyridylpyrrolide (PyPyr) ligands have seen considerable recent research activity in transition metal chemistry due to the push–pull effect (pyrrolide  $\pi$  orbitals serve as donors, while pyridine  $\pi^*$  orbitals as acceptors).<sup>13</sup> Recently, Stalke and coworkers reported Ge–Pb compounds using a 2,5-bis-[(pyrrolidino)-methyl]-pyrrole pincer ligand, in order to study the main group metal–ligand interaction with the pyrrole  $\pi$ -system.<sup>14</sup> However, there is no literature present about the study of only the PyPyr moiety as a ligand for any heavier main group element. Our strategy serendipitously provides new access to PyPyr chlorogermylene, **2**.

The molecular structure of **2** has been derived from X-ray diffraction data (Fig. 2). The germanium atom is three coordinate, with a short Ge–N bond to the pyrrole (1.9408(15) Å) and a longer Ge–N bond (2.0401(14) Å) to the pyridine nitrogen atoms. The C–C bond lengths in the pyrrole ring are very close, with a slight increase in the C6–C7 bond length (1.408(3) Å). The small N1–Ge1–N2 bite angle of 79.77(1)° is consistent with

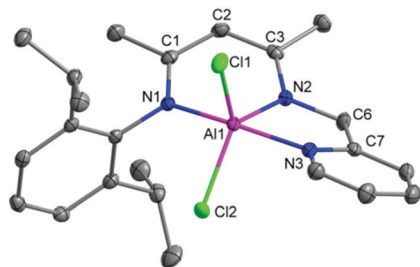


**Fig. 2** Molecular structure of **2** with anisotropic displacement parameters depicted at the 50% probability level. Hydrogen atoms are not shown for clarity. Selected bond lengths (Å) and bond angles (°): Ge1–N2 1.9408(15), Ge1–N1 2.0401(14), Ge1–Cl1 2.3141(4), N2–C8 1.366(2), N2–C5 1.384(2), N1–C1 1.348(2), N1–C4 1.367(2); N2–Ge1–N1 79.77(6), N2–Ge1–Cl1 95.75(4), N1–Ge1–Cl1 91.61(4).

the one in the late transition metal complexes supported by PyPyr.<sup>11</sup> The molecular structure of **3** is given in the ESI† (Fig. S17), which displays a Ge–N bond of 2.1674(14) Å, substantially longer than that in  $\text{DMAP} \rightarrow \text{GeCl}_2$  adduct (2.028(2) Å) reported by Rivard and coworkers.<sup>15</sup>

In order to understand the nature of the metal ligand interaction in the tri-coordinated germanium compound, we have further done natural bond orbital (NBO) analysis. The NBO analysis of **2** revealed that the contribution of the 4d orbital of the Ge centre towards the bonding is very small: the natural occupation in the 4d shell of the Ge centre is equal to 0.01 (ESI,† Table S1). A stabilizing electronic effect responsible for the formation of chemical bonds is the transfer of charge from the ligands to the metal ion. This is seen from the NBO analysis, which indicates that the “non-Lewis” occupancy in the orbitals comprising the Ge–ligand bonds in **2** is significant (see the column labeled “occupancy” in Table S1 in the ESI,† the deviation from the ideal value of 2.0 in the donor ligand orbitals indicates the transfer of electron density from the ligand orbitals to the germanium). This transfer of electron density gives rise to increased stability of the Ge–ligand bonds, which is evidenced from the high stabilization energies (in the range 60.0–180.0 kcal mol<sup>−1</sup>), seen from the donor–acceptor interactions (see the column labelled “E2” in Table S1 in the ESI,†). Consistent with the structural data, the pyrrole nitrogen interacts more strongly (84.0 kcal mol<sup>−1</sup>) than the pyridine nitrogen (61.8 kcal mol<sup>−1</sup>). The DFT calculations also reveal that in **2** both the HOMO and LUMO are localized over the five and six membered rings and both of them have pi symmetry. The HOMO–LUMO energy gap has been determined to be 5.48 eV (for more details please see the ESI,†).

The reaction of **1** with  $\text{AlCl}_3$  led to a transmetalated product, **4** along with the extrusion of  $\text{GeCl}_2$  (Scheme 1). Examples are scant for the transmetalation between two p-block elements.<sup>16</sup> Similarly,  $\text{GeCl}_2$  extrusion is also not very common.<sup>17</sup> Single crystal X-ray study reveals that the pyridine moiety coordinates to the aluminum center in **4** (Fig. 3), possibly due to the higher Lewis acidity of the latter in comparison to germanium. The Al–N<sub>ligands</sub> bonds are 1.9092(15) and 1.9783(15) Å, substantially shorter than the Al–N<sub>pyridine</sub> bond length [2.0641(15) Å]. The Al atom exhibits a distorted trigonal bipyramidal geometry with

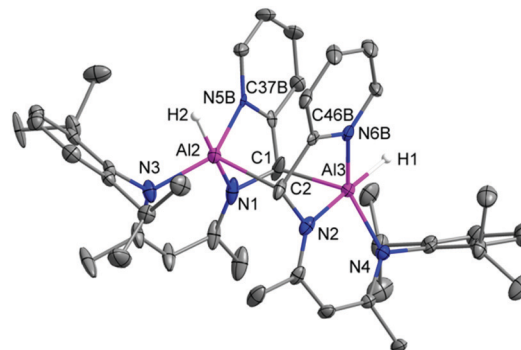


**Fig. 3** Molecular structure of **4** with anisotropic displacement parameters depicted at the 50% probability level. Hydrogen atoms are not shown for clarity. Selected bond lengths (Å) and bond angles (°): Al1–N2 1.9092(15), Al1–N1 1.9783(15), Al1–N3 2.0641(15); N2–Al1–N1 91.38(6), N2–Al1–N3 79.76(6), N1–Al1–N3 168.78(6), N2–Al1–Cl1 113.79(5), N1–Al1–Cl1 98.79(4), N3–Al1–Cl1 91.13(4), N2–Al1–Cl2 130.01(5), N1–Al1–Cl2 93.66(5), N3–Al1–Cl2 86.92(4), Cl1–Al1–Cl2 114.44(3).

N1 and N3 at the apical positions and N2, Cl1 and Cl2 are in the equatorial positions.

Soluble aluminum hydride compounds have been extensively used in recent years as the catalysts for the hydroboration of alkynes, aldehydes, ketones, esters, carbodimides, *etc.*<sup>18</sup> In order to prepare the analogous aluminum hydride from **4**, we have reacted **4** with several hydrogenating agents such as PhSiH<sub>3</sub>, Et<sub>3</sub>SiH, *l*-selectride, *etc.* without any success. Hence, we sought to prepare the aluminum hydride using a dehydrocoupling method by reacting the ligand with the alane. Surprisingly, the reaction of the ligand (**L**) with AlH<sub>3</sub>·NMe<sub>2</sub>Et at room temperature led to an unusual six-membered ring (**5**) consisting of two aluminum, two nitrogen and two carbon atoms (Scheme 2). Compounds containing an Al<sub>n</sub>C<sub>n</sub>N<sub>n</sub> framework are rare,<sup>19</sup> but a unique Al<sub>2</sub>Si<sub>4</sub> heterocycle has been recently reported by Roesky, Stalke, Koley and coworkers.<sup>20</sup>

The formation of **5** was made possible by the double dehydrocoupling between alane and N–H, as well as the sp<sup>3</sup> C–H bond of the methylene group. The Al–C dehydrocoupling is very important, as it is postulated as the first step for the alane catalyzed hydroboration of the terminal alkyne with HBpin.<sup>21</sup> The molecular structure of **5** is shown in Fig. 4. One can consider the core structure of **5** to be a tricyclo compound consisting of a six-membered Al<sub>2</sub>C<sub>2</sub>N<sub>2</sub> ring and two five-membered AlC<sub>2</sub>N<sub>2</sub> rings (Fig. 4). The six-membered ring is centrosymmetric with a twisted chair conformation. The coordination geometry of each Al atom can be described as trigonal bipyramidal. The two Al–N bond distances in the six-membered ring are 1.9801(17) and 1.9750(16) Å. The two Al–C bond

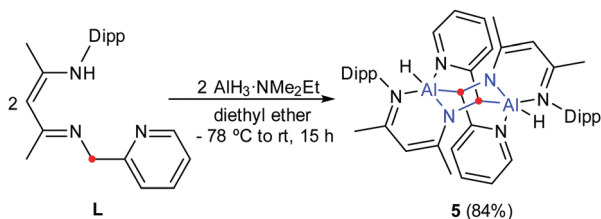


**Fig. 4** Molecular structure of **5** with anisotropic displacement parameters depicted at the 50% probability level. Hydrogen atoms (apart from those bound to Al) are not shown for clarity. Selected bond lengths (Å) and bond angles (°): Al2–N1 1.9801(17), Al2–C2 2.1542(18), Al2–H2 1.56(2), Al3–N2 1.9750(16), Al3–C1 2.1733(19), Al3–H1 1.55(2); N1–Al2–C2 90.44(7), N2–Al3–C1 90.02(7), C1–N1–Al2 110.80(14), C2–N2–Al3 110.90(12), N1–C1–Al3 113.05(12), N2–C2–Al2 113.14(11).

distances are 2.1542(18) and 2.1733(19) Å, which are longer than the Al(III)–C bonds in the dimer of Me<sub>3</sub>Al (2.145(7) and 2.146(8) Å),<sup>22</sup> presumably due to the higher coordination number in **5**. The Al–H bond lengths are 1.56(2) and 1.55(2) Å. Compound **5** has negligible solubility in common deuterated solvents once crystallized, so no meaningful solution state spectroscopic data could be acquired. Attempts were made to obtain solution state spectroscopic data before crystallization, but NMR data show unidentified product mixtures along with **5**. The <sup>27</sup>Al (*I* = 5/2) NMR of **5** shows a resonance at 38.9 ppm, which is in agreement with the presence of a penta-coordinated Al center.<sup>23</sup> In the IR spectrum, two sharp bands at 1693 and 1743 cm<sup>-1</sup> were noticed for the Al–H bond.

For understanding the nature of the aluminium ligand interactions in **5**, we have further performed NBO analysis.<sup>24</sup> From the NBO second order perturbation energy data, the values are high (>50.0 kcal mol<sup>-1</sup>) (see Table S2, ESI<sup>†</sup>). This, along with the results obtained from the WBI and NLMO bond order analysis, suggests that the covalent bonding of the Al atom with the coordinated ligand is weak. Only in the case of Al–H does the bond order (~0.7) indicate covalency. Most of the bonding is ionic in nature. For more details regarding the NBO analysis of compound **5**, please see the computational details section in the ESI.<sup>†</sup>

In summary, we have prepared a new chlorogermylene (**1**) bearing nacnac-based tridentate ligand containing a pyridylmethyl group. The ligand scaffold proved to be surprisingly flexible and allowed for the isolation of structurally different compounds under otherwise identical conditions. We have shown that the six-membered germylene **1** can be smoothly converted into a five-membered pyridylpyrrolide germylene **2** in the presence of another equivalent of GeCl<sub>2</sub>. On the other hand, **1** undergoes a transmetalation reaction with AlCl<sub>3</sub>. We have also reported the synthesis and molecular structure of an unexpected six-membered dialane heterocycle **5** resulting from the double dehydrocoupling of the ligand with AlH<sub>3</sub>. **5** can be viewed as an analogue of cyclohexane, where two C–C bonds



**Scheme 2** Dehydrocoupling mediated formation of a six-membered dialane.

have been replaced by isoelectronic Al–N bonds. The reactivity of **2** is already ongoing in our lab, which will be presented in a future publication.

The Science and Engineering Research Board (SERB), India (CRG/2018/000287) (SSS) is acknowledged for providing financial assistance. SP thanks DST, India for the INSPIRE fellowship (IF160314). VSVSNS and TD thank CSIR, India for their research fellowships. We thank Dr B. L. V. Prasad (CSIR-NCL) for the IR measurement. We are thankful to the referees for their critical inputs to improve the quality of the manuscript.

## Conflicts of interest

There are no conflicts to declare.

## Notes and references

- 1 Y. Ding, H. W. Roesky, M. Noltemeyer and H.-G. Schmidt, *Organometallics*, 2001, **20**, 1190–1194.
- 2 For selected references: (a) L. W. Pineda, V. Jancik, H. W. Roesky, D. Neculai and A. M. Neculai, *Angew. Chem., Int. Ed.*, 2004, **43**, 1419–1421; (b) L. W. Pineda, V. Jancik, K. Starke, R. B. Oswald and H. W. Roesky, *Angew. Chem., Int. Ed.*, 2006, **45**, 2602–2605; (c) M. Driess, S. Yao, M. Brym and C. van Wüllen, *Angew. Chem., Int. Ed.*, 2006, **45**, 4349–4352; (d) A. Jana, D. Ghoshal, H. W. Roesky, I. Objartel, G. Schwab and D. Stalke, *J. Am. Chem. Soc.*, 2009, **131**, 1288–1293; (e) S. P. Sarish, S. S. Sen, H. W. Roesky, I. Objartel and D. Stalke, *Chem. Commun.*, 2011, **47**, 7206–7208.
- 3 (a) L. Bourget-Marle, M. F. Lappert and J. R. Severn, *Chem. Rev.*, 2002, **102**, 3031–3066; (b) C. Camp and J. Arnold, *Dalton Trans.*, 2016, **45**, 14462–14498.
- 4 W. D. Morris, P. T. Wolczanski, J. Sutter, K. Meyer, T. R. Cundari and E. B. Lobkovsky, *Inorg. Chem.*, 2014, **53**, 7467–7484.
- 5 X. Xu, Y. Chen, G. Zou and J. Sun, *Dalton Trans.*, 2010, **39**, 3952–3958.
- 6 S. Yadav, R. Dixit, M. K. Bisai, K. Vanka and S. S. Sen, *Organometallics*, 2018, **37**, 4576–4584.
- 7 F. Kaiser, R. M. Reich, E. Rivard and F. E. Kühn, *Organometallics*, 2018, **37**, 136–144.
- 8 T. Kunz, C. Schrenk and A. Schnepf, *Inorg. Chem.*, 2020, **59**, 6279–6286.
- 9 (a) Z. Yang, X. Ma, R. B. Oswald, H. W. Roesky, C. Cui, H. Schmidt and M. Noltemeyer, *Angew. Chem., Int. Ed.*, 2006, **45**, 2277–2280; (b) S.-P. Chia, H.-W. Xi, Y. Li, K. H. Lim and C.-W. So, *Angew. Chem., Int. Ed.*, 2013, **52**, 6298–6301.
- 10 T. Kunz, C. Schrenk and A. Schnepf, *Chem. – Eur. J.*, 2019, **25**, 7210–7217.
- 11 (a) S. L. Choong, C. Schenk, A. Stasch, D. Dange and C. Jones, *Chem. Commun.*, 2012, **48**, 2504–2506; (b) W. D. Woodful, A. F. Richards, A. Stasch, M. Driess and C. Jones, *Organometallics*, 2010, **29**, 3655–3660.
- 12 J. Li, X. Li, W. Huang, H. Hu, J. Zhang and C. Cui, *Chem. – Eur. J.*, 2012, **18**, 15263–15266.
- 13 For selected references: (a) J. L. McBee, J. Escalada and T. D. Tilley, *J. Am. Chem. Soc.*, 2009, **131**, 12703–12713; (b) J. L. McBee and T. D. Tilley, *Organometallics*, 2009, **28**, 3947–3952; (c) D. Pucci, I. Aiello, A. Aprea, A. Bellusci, A. Crispini and M. Ghedini, *Chem. Commun.*, 2009, 1550–1552; (d) A. T. Luedtke and K. I. Goldberg, *Inorg. Chem.*, 2007, **46**, 8496–8498; (e) J. A. Flores, J. G. Andino, N. P. Tsvetkov, M. Pink, R. J. Wolfe, A. R. Head, D. L. Lichtenberger, J. Massa and K. G. Caulton, *Inorg. Chem.*, 2011, **50**, 8121–8131.
- 14 C. Maafß, D. M. Andrada, R. A. Mata, R. Herbst-Irmer and D. Stalke, *Inorg. Chem.*, 2013, **52**, 9539–9548.
- 15 A. K. Swarnakar, S. M. McDonald, K. C. Deutsch, P. Choi, M. J. Ferguson, R. McDonald and E. Rivard, *Inorg. Chem.*, 2014, **53**, 8662–8671.
- 16 (a) M. Oлару, R. Kather, E. Hupf, E. Lork, S. Mebs and J. Beckmann, *Angew. Chem., Int. Ed.*, 2018, **57**, 5917–5920; (b) M. Oлару, S. Krupke, E. Lork, S. Mebs and J. Beckmann, *Dalton Trans.*, 2019, **48**, 5585–5594.
- 17 B. Raghavendra, K. Bakthavachalam, T. Das, T. Roisnel, S. S. Sen, K. Vanka and S. Ghosh, *J. Organomet. Chem.*, 2020, **911**, 121142.
- 18 (a) W. Li, X. Ma, M. G. Walawalkar, Z. Yang and H. W. Roesky, *Coord. Chem. Rev.*, 2017, **350**, 14–29; (b) M. L. Shegavi and S. K. Bose, *Catal. Sci. Technol.*, 2019, **9**, 3307–3336; (c) N. Sarkar, S. Bera and S. Nembenna, *J. Org. Chem.*, 2020, **85**, 4999–5009.
- 19 (a) W. Zheng, A. Stasch, J. Prust, H. W. Roesky, F. Cimpoesu, M. Noltemeyer and H.-G. Schmidt, *Angew. Chem., Int. Ed.*, 2001, **40**, 3461–3464; (b) K. J. Blakeney, P. D. Martin and C. H. Winter, *Organometallics*, 2020, **39**, 1006–1013.
- 20 J. Li, M. Zhong, H. Keil, H. Zhu, R. Herbst-Irmer, D. Stalke, S. De, D. Koley and H. W. Roesky, *Chem. Commun.*, 2019, **55**, 2360–2363.
- 21 Z. Yang, M. Zhong, X. Ma, K. Nijesh, S. De, P. Parameswaran and H. W. Roesky, *J. Am. Chem. Soc.*, 2016, **138**, 2548–2551.
- 22 G. S. McGrady, J. S. Turner, R. M. Ibberson and M. Prager, *Organometallics*, 2000, **19**, 4398–4401.
- 23 R. Mondol and E. Otten, *Inorg. Chem.*, 2019, **58**, 6344–6355.
- 24 S. Milione, G. Milano and L. Cavallo, *Organometallics*, 2012, **31**, 8498–8504.



Cite this: DOI: 10.1039/d1dt03136h

# Pyridylpyrrolido ligand in Ge(II) and Sn(II) chemistry: synthesis, reactivity and catalytic application†

Sanjukta Pahar,<sup>a,b</sup> Vishal Sharma,<sup>a,b</sup> Srinu Tothadi <sup>c</sup> and Sakya S. Sen <sup>\*a,b</sup>

In our previous communication, we have reported the synthesis of a new chlorogermylene (**B**) featuring a pyridylpyrrolido ligand. This study details the preparation of a series of new germynes and stannylenes starting from **B**. A transmetalation reaction between **B** and SnCl<sub>2</sub> led to the analogous chlorostannylene (**1**) with the simultaneous elimination of GeCl<sub>2</sub>. This is a very unusual example of transmetalation between two elements of the same group. The preparation of **1** via lithiation led to the formation of **2** as a side product, where the *ortho* C–H bond of the pyridine ring was activated and functionalized with a <sup>n</sup>Bu moiety. Subsequently, **B** and **1** were used as precursors to generate germylene (**4**) and stannylene (**5**) featuring tris(trimethylsilyl)silyl (hypersilyl) moieties. We also prepared tetrafluoropyridyl germylene (**6**) by reacting **4** with C<sub>5</sub>F<sub>5</sub>N with the simultaneous elimination of (Me<sub>3</sub>Si)<sub>3</sub>SiF by utilizing the fluoride affinity of the silicon atom. As there is scarcity of Sn(II) compounds as single-site catalysts, we investigated **5** as a catalyst towards the hydroboration of aldehydes, ketones, alkenes and alkynes. All the compounds have been characterized by single-crystal X-ray diffraction and by state of the art spectroscopic studies.

Received 15th September 2021

Accepted 20th October 2021

DOI: 10.1039/d1dt03136h

rsc.li/dalton

## Introduction

For the enrichment and understanding of main-group chemistry, heavier congeners of carbenes have played a significant role along with the development of new sterically demanding monoanionic ligand scaffolds. To stabilize compounds with low-valent main-group elements, bidentate monoanionic bulky N,N'-ligands such as  $\beta$ -diketiminates, amidinates, guanidates, and recently two monoanionic ditopic ligands have been widely explored due to their straightforward synthesis, possibility for fine tuning the substituents, and occupying a second coordination site on the metal.<sup>1–5</sup> A very similar monoanionic bidentate ligand, the pyridylpyrrolido ligand (PyPyr), had found widespread applications in transition metal chemistry, thanks to pioneering works from the groups of Tilley, Goldberg, Pucci, Carty, Caulton and others apparently due to its push–pull nature.<sup>6–10</sup> The DFT calculations on *N*-methyl pyridyl-pyrrolido indicate that the HOMO is primarily located

on the pyrrolide site, while the LUMO is on the pyridyl moiety.<sup>11</sup> However, the chemistry of this ligand with main group elements has not been widely explored. This is somewhat surprising because the pyrrolide ligand is electron rich and the adjacent pyridyl motif may provide additional stability through donation. Recently, we have accessed a pyridylpyrrolido germylene (**B**)<sup>12</sup> serendipitously from a picolyl functionalized  $\beta$ -diketiminato chlorogermylene (Scheme 1). However, the yield of the germylene was less than 50%. Herein, we report a high yield synthesis of **B** and its reactivities. The corresponding stannylene chemistry has also been studied. Finally, the catalytic utility of a PyPyr-based hypersilyl stannylene towards hydroboration of alkenes, alkynes, aldehydes, and ketones has been examined.

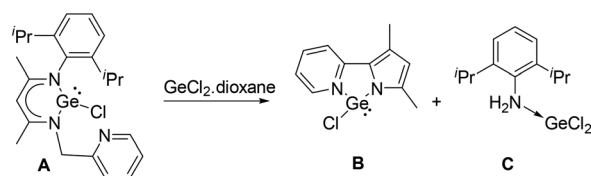
<sup>a</sup>Inorganic Chemistry and Catalysis Division, CSIR-National Chemical Laboratory, Dr Homi Bhabha Road, Pashan, Pune 411008, India. E-mail: ss.sen@ncl.res.in

<sup>b</sup>Academy of Scientific and Innovative Research (AcSIR), Ghaziabad-201002, India

<sup>c</sup>Organic Chemistry Division, CSIR-National Chemical Laboratory, Dr Homi Bhabha Road, Pashan, Pune 411008, India

† Electronic supplementary information (ESI) available: Synthesis, and spectroscopic and structural data of **1**–**6**. CCDC 2109664 (**1**), 2109665 (**2**), 2109666 (**3**), 2109667 (**4**), 2109668 (**5**) and 2109460 (**6**). For ESI and crystallographic data in CIF or other electronic format see DOI: 10.1039/d1dt03136h

### Our Previous Work



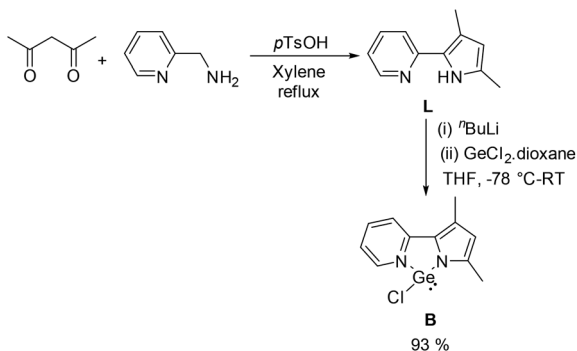
**Scheme 1** Rearrangement of picolyl substituted  $\beta$ -diketiminato chlorogermylene (**A**) to PyPyrchlorogermylene (**B**) upon addition of GeCl<sub>2</sub>-dioxane.<sup>12</sup>

## Results and discussion

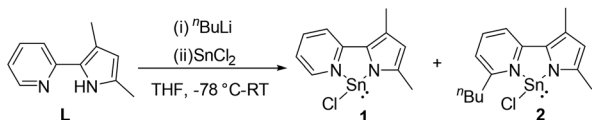
Scheme 2 shows the high yield synthesis of the PyPyr-based chlorogermylene used in this study. The pyridylpyrrole ligand was prepared according to a literature procedure<sup>13</sup> and the previously reported chlorogermylene **B** was prepared by reacting the ligand with <sup>n</sup>BuLi and GeCl<sub>2</sub>-dioxane in quantitative yields (Scheme 2).

Inspired by the high yield synthesis of **B**, we next endeavored to prepare the analogous stannylene. However, along with the formation of our desired stannylene (**1**), the reaction led to the formation of another stannylene (**2**), where the *ortho* C–H bond of the pyridine ring was activated and functionalized with a <sup>n</sup>Bu moiety (Scheme 3). Such direct C–H functionalization of pyridine was reported with excess <sup>t</sup>BuLi.<sup>14</sup> We could not prepare **2** in a scale that permits complete spectroscopic characterization even after using two equivalents of <sup>n</sup>BuLi and we always obtained a mixture of **1** and **2**. Hence, the identification of compound **2** was only supported by the solid-state single-crystal X-ray structure and HRMS data. An increase in the yield and purity of **1** could be achieved by lithiating **L** with Li(HMDS) with the subsequent addition of 1 equiv. of SnCl<sub>2</sub>.<sup>15b</sup>

The solid-state structure of **1** was derived from the X-ray diffraction data (Fig. 1). **1** crystallizes in the triclinic space group *P* $\bar{1}$ . The tri-coordinated tin atom contains a short Sn1–N1 bond to the pyrrole (2.15(2) Å) and a longer Sn1–N2 bond (2.25(1) Å) to the pyridine nitrogen atom. The two methyl groups attached with the pyrrole ring exhibit two singlets at  $\delta$  2.30 and 2.36 ppm in the <sup>1</sup>H NMR spectrum, whereas it resonates at –151.86 ppm in the <sup>119</sup>Sn NMR spectrum. The Sn–Cl bond length is 2.48(1) Å, which is in good agreement with the



Scheme 2 High yield synthesis of **B**.



Scheme 3 Synthesis of **1** and **2**.

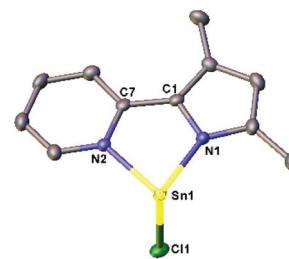


Fig. 1 The molecular structure of **1**. Anisotropic displacement parameters are depicted at the 50% probability level. Selected bond lengths [Å] and angles [°]: Sn1–N1 2.15(2), Sn1–N2 2.25(1), and Sn1–Cl1 2.48(1); N1–Sn1–N2 74.5(1), N1–Sn1–Cl1 93.6(1), and N2–Sn1–Cl1 90.16(9).

previously reported chlorostannylenes by the groups of Roesky, Stalke, Jones, Nakata, Nagendran, and others.<sup>15</sup>

Crystals of **2** suitable for X-ray structural analysis were obtained from a concentrated toluene solution at –30 °C. The single crystal X-ray study of **2** reveals that the pyridine moiety contains the <sup>n</sup>Bu group at the *ortho* position of pyridine N (Fig. 2). The tri-coordinated tin(II) chloride comprises a longer Sn1–N1 bond (2.251(3) Å) attached to the pyridine nitrogen atom and a relatively shorter Sn1–N2 bond (2.132(3) Å) attached to the pyrrole nitrogen atom. The Sn–Cl bond [2.3523(5) Å] in **2** is substantially shorter than that of **1**. The molecular ion peak of **2** was observed with the highest relative intensity in the HRMS spectrum at *m/z* 383.0331.

The reaction of an equimolar amount of SnCl<sub>2</sub> with **B** in THF led to the clean formation of **1** with concomitant removal of GeCl<sub>2</sub> (Scheme 4) in quantitative yields. There are limited examples of transmetalation between two p-block elements<sup>12,16</sup> and it is a rare transmetalation between two p-block elements from the same group. Storing the concentrated THF solution of **1** at –35 °C in a freezer afforded pale yellow crystals suitable for single crystal X-ray analysis. The formation of **1** was confirmed by comparing the NMR data as well as the unit cell value of a single crystal with the previously obtained sample.

Treatment of **1** with KO<sup>t</sup>Bu in toluene produced a homoleptic tin (**3**) (Scheme 4). Compound **3** was characterized by <sup>1</sup>H and <sup>13</sup>C NMR spectroscopy, HRMS and X-ray structural ana-

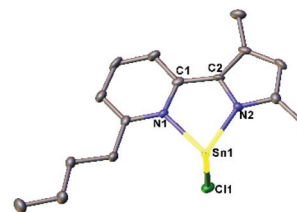
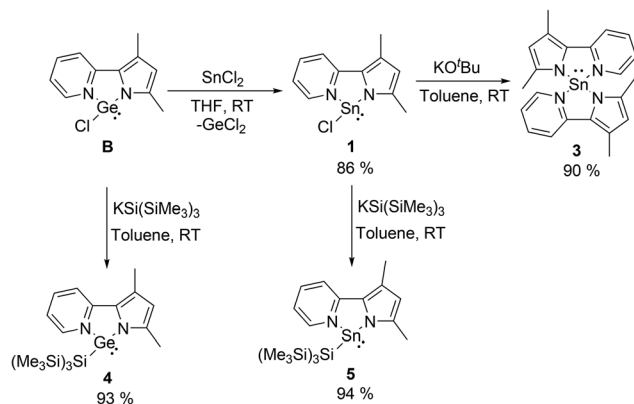


Fig. 2 The molecular structure of **2**. Anisotropic displacement parameters are depicted at the 50% probability level. Selected bond lengths [Å] and angles [°]: Sn1–N1 2.251(3), Sn1–N2 2.132(3), and Sn1–Cl1 2.3523(5); N1–Sn1–N2 74.7(1), N1–Sn1–Cl1 88.29(8), and N2–Sn1–Cl1 93.63(9).

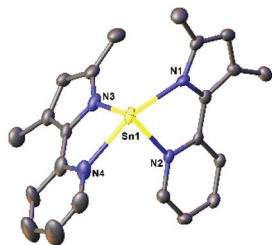




**Scheme 4** Alternative synthesis of chlorostannylene (**1**), and formation of homoleptic stannylene (**3**) and hypersilyl-germylene (**4**) and -stannylene (**5**). Yields are given for the respective steps.

lysis. However, the low solubility of **3** causes difficulties in recording the  $^{119}\text{Sn}$  NMR spectrum. The  $^1\text{H}$  NMR spectrum displays two singlets at  $\delta$  2.27 and 2.34 ppm, which were attributed to the methyl groups attached to the pyrrole ring. A toluene solution of **3** at  $-30^\circ\text{C}$  in a freezer afforded air-sensitive yellow crystals suitable for X-ray analysis. Compound **3** crystallizes in the triclinic space group  $P\bar{1}$  (Fig. 3). The coordination geometry around the Sn atom can be viewed as a distorted sawhorse-like structure. The Sn1–N bonds with pyrrole rings (2.197 (3) and 2.281 (4) Å) are shorter than the Sn1–N bonds (2.355(4) and 2.432 (5) Å) with pyridine nitrogen atoms.

Recent years have witnessed growth in the synthesis of tetraylene derivatives with electropositive hypersilyl moieties. The use of hypersilyl groups in compounds with main-group elements was dated back in 1981, when Brook uncovered that the photolysis of an acylsilane gave rise to the first well-defined compound with a Si=C double bond.<sup>17</sup> The advantages of the hypersilyl group are not only the good  $\sigma$ -donation or pronounced steric bulk but also the commercial readiness of the precursors and the possibility of further functionalization due to the presence of the  $\text{SiMe}_3$  moieties.



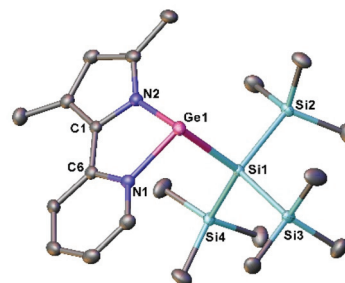
**Fig. 3** The molecular structure of **3**. Anisotropic displacement parameters are depicted at the 50% probability level. Selected bond lengths [Å] and angles [°]: Sn1–N1 2.281(4), Sn1–N2 2.355(4), Sn1–N3 2.197(3), and Sn1–N4 2.432(5); N1–Sn1–N2 70.0(1), N1–Sn1–N3 91.9(1), N2–Sn1–N4 80.1(1), and N3–Sn1–N4 71.1(1).

Subsequently, a significant research effort has been dedicated to using a hypersilyl moiety as a stabilizer for novel compounds with low-valent main-group elements with key contributions from the groups of Stalke,<sup>18</sup> Inoue,<sup>19</sup> Aldridge,<sup>20</sup> Rivard,<sup>21</sup> Leszczyńska,<sup>22</sup> Castel,<sup>23</sup> Marschner, Baumgartner, and others.<sup>24</sup> In our part, we have prepared benzamidinato silylene,<sup>25</sup> germylene,<sup>26</sup> and stannylene<sup>27</sup> with hypersilyl moieties and studied their reactivities.<sup>25,27–29</sup>

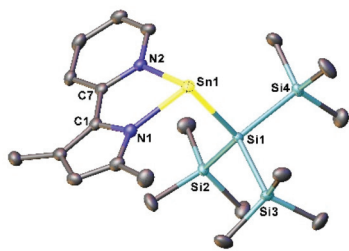
The reaction of **B** and **1** with  $\text{KSi}(\text{SiMe}_3)_3$  in toluene at room temperature smoothly afforded the hypersilyl germylene (**4**) and stannylene (**5**) derivatives (Scheme 4). **4** and **5** were isolated as red and orange crystals, respectively, from the concentrated toluene solution at a low temperature ( $-20^\circ\text{C}$ ) within 3–4 days. The  $^1\text{H}$  NMR spectra of **4** and **5** show resonance at 0.27 and 0.29 ppm, respectively, for the three  $\text{SiMe}_3$  groups. The two methyl groups attached to the pyrrole moiety show singlets at  $\delta$  2.30 and 2.36 ppm for **4**, whereas the same has been observed at  $\delta$  2.36 and 2.39 ppm for **5**. We could not obtain any resonance in the solution-state  $^{29}\text{Si}$  NMR (for **4** and **5**) as well as  $^{119}\text{Sn}$  NMR (for **5**) spectra due to the gradual decomposition of both compounds to ligands. However, in the solid state, the  $^{29}\text{Si}$  NMR chemical shift of **4** appears at  $\delta$   $-105.84$  ( $\text{Si}(\text{SiMe}_3)_3$ ) and  $-8.27$  ( $\text{Si}(\text{SiMe}_3)_3$ ) ppm, while **5** shows signals at  $\delta$   $-99.86$  ( $\text{Si}(\text{SiMe}_3)_3$ ) and  $-6.28$  ( $\text{Si}(\text{SiMe}_3)_3$ ) ppm.

The molecular structures of **4** and **5** are depicted in Fig. 4 and 5, respectively, with important bond lengths and angles. The tri coordinated Ge(II) and Sn(II) atoms in **4** and **5** exhibit a distorted trigonal-pyramidal geometry with an M–Si bond. The Ge–Si bond length in **4** (2.4900(4) Å) is shorter than those reported for other hypersilylgermylenes, such as  $[\text{PhC}(\text{NSiMe}_3)_2\text{GeSi}(\text{SiMe}_3)_3]$  (2.525(1) Å)<sup>23a</sup> and  $[\text{PhC}(\text{N}^t\text{Bu})_2\text{GeSi}(\text{SiMe}_3)_3]$  (2.5216(5) Å).<sup>26</sup> The Sn–Si bond length in **5** (2.6675(8) Å) is in good agreement with the Sn–Si bonds in the dimeric bis(hypersilyl)stannylene  $[\text{Sn}\{\text{Si}(\text{SiMe}_3)_3\}_2]$  (2.6667(11) Å).<sup>30</sup>

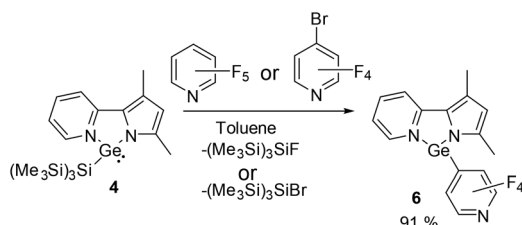
Due to our current interest in understanding the C–F bond activation by carbenes and its heavier analogues,<sup>31–35</sup> the reactivity of hypersilyl germylene **4** with pentafluoropyridine has been investigated. The strong affinity of silicon towards fluorine led to the elimination of  $(\text{Me}_3\text{Si})_3\text{SiF}$ , which was detected



**Fig. 4** The molecular structure of **4**. Anisotropic displacement parameters are depicted at the 50% probability level. Selected bond lengths [Å] and angles [°]: Ge1–Si1 2.4900(4), Si1–Si2 2.3488(5), Ge1–N1 2.039(1), and Ge1–N2 1.973(1); N1–Ge1–N2 79.54(5), N1–Ge1–Si1 94.66(3), and N2–Ge1–Si1 99.65(3).

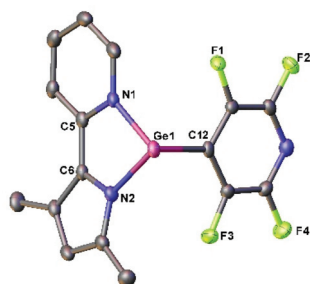


**Fig. 5** The molecular structure of **5**. Anisotropic displacement parameters are depicted at the 50% probability level. Selected bond lengths [Å] and angles [°]: Sn1–Si1 2.6675(8), Si1–Si2 2.347(1), Sn1–N1 2.170(2), and Sn1–N2 2.251(1); N1–Sn1–N2 74.09(5), N1–Sn1–Si1 97.64(4), and N2–Sn1–Si1 93.98(4).



**Scheme 5** Formation of perfluoroaryl germylene (**6**) from **4**.

at  $-255$  ppm in the  $^{19}\text{F}$  NMR spectrum and afforded tetrafluoroaryl germylene **6** (Scheme 5) (see the ESI† for the NMR of the reaction mixture). The  $^{19}\text{F}$  NMR spectrum of **6** shows two sharp resonances at  $-94.48$  (*o*-F) and  $-134.17$  (*m*-F) ppm. The analogous reaction with 4-bromo-2,3,5,6-tetrafluoropyridine did not lead to C–F bond activation; instead, the C–Br bond at the *para* position gets activated resulting in the formation of **6**. The activation of the *para*-F atom of  $\text{C}_5\text{F}_5\text{N}$  and the composition of **6** was confirmed by single crystal X-ray diffraction studies, which is illustrated in Fig. 6. The geometry around the germanium atom is distorted trigonal-pyramidal with a Ge(II)–C bond length of  $2.072(2)$  Å, which is comparable well with the previously reported Ge–C bond length.<sup>26,36</sup>



**Fig. 6** The molecular structure of **6**. Anisotropic displacement parameters are depicted at the 50% probability level. Selected bond lengths [Å] and angles [°]: Ge1–N1 2.050(1), Ge1–N2 1.956(2), Ge1–C12 2.072(2), N3–C16 1.310(3), N3–C14 1.312(3), C16–F4 1.344(3), C14–F2 1.342(2); N1–Ge1–N2 79.82(7), N1–Ge1–C12 91.37(7), and N2–Ge1–C12 93.69(7).

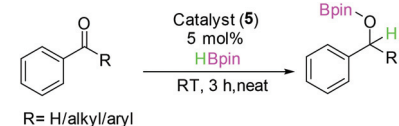
## Catalytic studies

The hydroboration of a series of aldehydes, ketones, alkynes, and alkenes with **5** has been investigated. These studies are centered on stannylenes systems, given the low cost of tin compared to germanium and the very limited focus on using tin(II) compounds as catalysts or pre-catalysts for hydroboration of organic substrates. Although there is an exponential number of publications on hydroboration using *p*-block compounds,<sup>37</sup> to the best of our knowledge there are only few reports on tin catalyzed hydroboration by the groups of Jones,<sup>38</sup> Wesemann,<sup>39</sup> Nagendran,<sup>15c</sup> Khan,<sup>40</sup> and recently by Nakata.<sup>41</sup> These examples are limited to only aldehydes and ketones. Our preliminary study on the catalytic application of **1**, **3**, and **5** revealed that they can catalyze benzaldehyde hydroboration with pinacolborane (HBpin) under mild conditions; however, the activities of **1** and **3** are poorer compared to **5** (see Table 1, entries 1–3).

Both benzaldehyde and acetophenone reductions in the presence of 5 mol% of **5** were completed in 3 hours at room temperature. It was observed that electron withdrawing groups such as *para*-F (Table 1, entry 11), *para*-Br (Table 1, entry 6) and *ortho*-Cl (Table 1, entry 9) and electron-donating groups such as *p*-OMe (Table 1, entry 4) and *p*-NMe<sub>2</sub> (Table 1, entry 5) have little effect on reactivity. However, the reaction was sluggish for benzaldehyde and acetophenone with NO<sub>2</sub> substituents (Table 1, entries 7 and 12).

In order to shed some light on the mechanism, several control experiments were carried out. We did not obtain any product from the reaction of **5** with aldehydes or ketones.<sup>38</sup> However, the reaction of **5** with HBpin presumably led to the formation of an unstable Sn(II) hydride. The  $^1\text{H}$  NMR spectrum is inconclusive but the  $^{119}\text{Sn}$  NMR spectrum of the reaction mixture shows a doublet at 509.9 ppm with  $J_{\text{Sn-H}} = 38.81$  Hz, which is in good agreement with the previously reported  $[\{\text{HC}(\text{CMe}(\text{NAr})_2)\}_2\text{SnH}]$  (45 Hz) ( $\text{Ar} = 2,6\text{-}i\text{-Pr}_2\text{C}_6\text{H}_3$ ).<sup>42</sup> The corresponding  $^{11}\text{B}$  NMR spectrum of the reaction mixture displays resonance at 21.68 ppm, reflecting a three-coordinated boron center.<sup>43</sup> The disappearance of the B–H proton also points towards the formation of the PyPyrSn(II) hydride. We surmise that the PyPyrSn(II) hydride reacts with aldehydes/ketones to form the corresponding metalla-alkoxides, which subsequently react with another molecule of HBpin to regenerate the hydride and form borate esters. A tentative mechanistic cycle is given in the ESI (please see Scheme S1†).

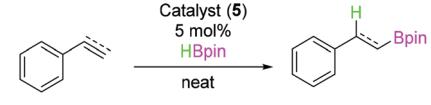
Subsequently, the hydroboration of styrene and phenylacetylene was studied. The catalytic activity of **5** was found to be lower for alkene (Table 2, entry 1) than that of alkyne (Table 2, entry 5). In fact, substituted alkenes and alkynes reacted sluggishly to form hydroboration products, giving very moderate yields. The intramolecularly base stabilized nature of **5** and the non-polar nature of alkenes and alkynes can be attributed to the sluggish nature of the hydroboration. To explain the regioselectivity of the products, we have performed a catalytic reaction using  $\text{PhC}\equiv\text{CD}$  and HBpin, where we observed resonance at 6.26 ppm in the  $^2\text{H}$  NMR spectrum,

**Table 1** Hydroboration of aldehydes and ketones catalyzed by **5** (unless otherwise mentioned in the legend)


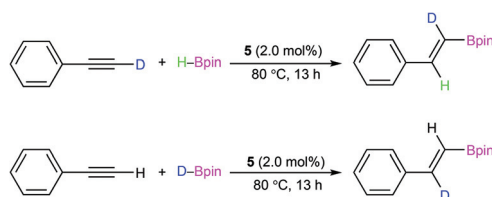
Entry	Substrates	Time/temperature	Yield (%)
1		3 h/RT	97
2		3 h/RT	87 <sup>a</sup> 75 <sup>b</sup>
3		3 h/RT	67 <sup>c</sup> 68 <sup>d</sup>
4		3 h/RT	98
5		3 h/RT	86
6		3 h/RT	96
7		3 h/RT	72
8		3 h/RT	99
9		3 h/RT	98
10		3 h/RT	99
11		3 h/RT	80
12		3 h/RT	42

All reactions were carried out under neat conditions at room temperature using 1 equiv. of HBpin. Yields were determined by the <sup>1</sup>H NMR integration relative to mesitylene (1 equiv.) as an internal standard and the identity of the product was confirmed by RCH<sub>2</sub>OBpin or RR<sup>1</sup>CHOBpin resonances. <sup>a</sup> Catalyst: 5 mol% **1**. <sup>b</sup> Catalyst: 10 mol% **1**. <sup>c</sup> Catalyst: 5 mol% **3**. <sup>d</sup> Catalyst: 10 mol% **3**.

suggesting a *cis* orientation of the deuterium and phenyl group. On the other hand, the product generated from the catalytic reaction of PhC≡CH with DBpin exhibits resonance at 6.57 ppm in the <sup>2</sup>H NMR spectrum, indicating the *cis*

**Table 2** Hydroboration of alkenes and alkynes catalyzed by **5**. Yields were determined by <sup>1</sup>H NMR integration relative to mesitylene (1 equiv.)


Entry	Substrates	Time/temperature	Yield (%)
1		13 h/100 °C	64
2		13 h/100 °C	53
3		13 h/100 °C	62
4		13 h/100 °C	42
5		13 h/80 °C	74
6		13 h/80 °C	58
7		13 h/80 °C	34
8		13 h/80 °C	58

**Scheme 6** Deuterium labelling experiment: hydroboration of phenylacetylene-D with HBpin (above) and hydroboration of phenylacetylene with DBpin (below).

arrangement of deuterium and the Bpin moiety (see Scheme 6). These results are in good agreement with previous works on alkyne hydroboration by us<sup>44</sup> as well as others.<sup>45</sup>

## Conclusions

A series of low-valent monomeric germanium and tin compounds featuring a pyridylpyrrolide ligand has been reported. Taking advantage of the nucleophilic substitution reactions using KSi(SiMe<sub>3</sub>)<sub>3</sub>, we synthesized hypersilyl germylene (**4**) and stannylene (**5**). The reaction of **4** with C<sub>5</sub>F<sub>5</sub>N led to a tetrafluoropyridyl germylene *via* the concomitant elimination of (Me<sub>3</sub>Si)<sub>3</sub>SiF through the C–F bond cleavage of C<sub>5</sub>F<sub>5</sub>N. Finally,

we used hypersilyl stannylene 5 as a catalyst for the hydroboration of aldehydes, ketones, alkenes, and alkynes. While the catalyst is efficient for aldehydes and ketones, the reduction of alkenes and alkynes was sluggish.

## Conflicts of interest

There are no conflicts to declare.

## Acknowledgements

Financial support from the Science and Engineering Research Board, SERB (Grant CRG/2018/000287), is acknowledged. S. P. thanks the DST Inspire (IF160314) and V. S. thanks the CSIR, India, for providing research fellowships. S. T. is grateful to CSIR-HRDG for an SRA fellowship (Pool No. 9119).

## Notes and references

- L. Bourget-Merle, M. F. Lappert and J. R. Severn, *Chem. Rev.*, 2002, **102**, 3031–3066.
- C. Camp and J. Arnold, *Dalton Trans.*, 2016, **45**, 14462–14498.
- M. Asay, C. Jones and M. Driess, *Chem. Rev.*, 2010, **111**, 354–396.
- (a) I. Koehne, N. Graw, T. Teuteberg, R. Herbst-Irmer and D. Stalke, *Inorg. Chem.*, 2017, **56**, 14968–14978; (b) I. Koehne, S. Bachmann, T. Niklas, R. Herbst-Irmer and D. Stalke, *Chem. – Eur. J.*, 2017, **23**, 13141–13149.
- R. Kretschmer, *Chem. – Eur. J.*, 2020, **26**, 2099–2119.
- J. L. McBee and T. D. Tilley, *Organometallics*, 2009, **28**, 3947–3952.
- A. T. Luedtke and K. I. Goldberg, *Inorg. Chem.*, 2007, **46**, 8496–8498.
- D. Pucci, I. Aiello, A. Aprea, A. Bellusci, A. Crispini and M. Ghedini, *Chem. Commun.*, 2009, 1550–1552.
- J.-L. Chen, C.-H. Lin, J.-H. Chen, Y. Chi, Y.-C. Chiu, P.-T. Chou, C.-H. Lai, G. Lee and A. J. Carty, *Inorg. Chem.*, 2008, **47**, 5154–5161.
- J. A. Flores, J. G. Andino, N. P. Tsvetkov, M. Pink, R. J. Wolfe, A. R. Head, D. L. Lichtenberger, J. Massa and K. G. Caulton, *Inorg. Chem.*, 2011, **50**, 8121–8131.
- K. Searles, A. K. Das, R. W. Buell, M. Pink, C.-H. Chen, K. Pal, D. G. Morgan, D. J. Mindiola and K. G. Caulton, *Inorg. Chem.*, 2013, **52**, 5611–5619.
- S. Pahar, V. S. V. S. N. Swamy, T. Das, R. G. Gonnade, K. Vanka and S. S. Sen, *Chem. Commun.*, 2020, **56**, 11871–11874.
- J. J. Klappa, A. E. Rich and K. McNeill, *Org. Lett.*, 2002, **4**, 435–437.
- F. V. Scalzi and N. F. Golob, *J. Org. Chem.*, 1971, **36**, 2541–2542.
- (a) S. S. Sen, M. P. Kritzler-Kosch, S. Nagendran, H. W. Roesky, T. Beck, A. Pal and R. Herbst-Irmer, *Eur. J. Inorg. Chem.*, 2010, 5304–5311; (b) C. Maaß, D. M. Andrada, R. A. Mata, R. Herbst-Irmer and D. Stalke, *Inorg. Chem.*, 2013, **52**, 9539–9548; (c) M. K. Sharma, M. Ansari, P. Mahawar, G. Rajaraman and S. Nagendran, *Dalton Trans.*, 2019, **48**, 664–672; (d) T. Chlupatý, Z. Padělková, F. DeProft, R. Willem and A. Růžička, *Organometallics*, 2012, **31**, 2203–2211; (e) C. Jones, R. P. Rose and A. Stasch, *Dalton Trans.*, 2008, 2871–2878; (f) N. Nakata, N. Hosoda, S. Takahashi and A. Ishii, *Dalton Trans.*, 2018, **47**, 481–490.
- (a) M. Oлару, R. Kather, E. Hupf, E. Lork, S. Mebs and J. Beckmann, *Angew. Chem., Int. Ed.*, 2018, **57**, 5917–5920; (b) M. Oлару, S. Krupke, E. Lork, S. Mebs and J. Beckmann, *Dalton Trans.*, 2019, **48**, 5585–5594.
- A. G. Brook, F. Abdesaken, B. Gutekunst, G. Gutekunst and R. K. Kallury, *J. Chem. Soc., Chem. Commun.*, 1981, 191–192.
- A. Heine and D. Stalke, *Angew. Chem., Int. Ed. Engl.*, 1994, **33**, 113–115.
- (a) D. Wendel, A. Porzelt, F. A. D. Herz, D. Sarkar, C. Jandl, S. Inoue and B. Rieger, *J. Am. Chem. Soc.*, 2017, **139**, 8134–8137; (b) D. Wendel, T. Szilvási, C. Jandl, S. Inoue and B. Rieger, *J. Am. Chem. Soc.*, 2017, **139**, 9156–9159.
- A. V. Protchenko, A. D. Schwarz, M. P. Blake, C. Jones, N. Kaltsoyannis, P. Mountford and S. Aldridge, *Angew. Chem., Int. Ed.*, 2013, **52**, 568–571.
- M. M. D. Roy, M. I. J. Ferguson, R. McDonald, Y. Zhou and E. Rivard, *Chem. Sci.*, 2019, **10**, 6476–6481.
- K. I. Leszczyńska, P. Deglmann, C. Präsang, V. Huch, M. Zimmer, D. Schweinfurth and D. Scheschkewitz, *Dalton Trans.*, 2020, **49**, 13218–13225.
- (a) D. Matioszek, N. Katir, S. Ladeira and A. Castel, *Organometallics*, 2011, **30**, 2230–2235; (b) N. Katir, D. Matioszek, S. Ladeira, J. Escudíe and A. Castel, *Angew. Chem., Int. Ed.*, 2011, **50**, 5352–5355.
- (a) H. Arp, J. Baumgartner, C. Marschner and T. Müller, *J. Am. Chem. Soc.*, 2011, **133**, 5632–5635; (b) H. Arp, C. Marschner, J. Baumgartner, P. Zark and T. Müller, *J. Am. Chem. Soc.*, 2013, **135**, 7949–7959; (c) H. Arp, J. Baumgartner and C. Marschner, *J. Am. Chem. Soc.*, 2012, **134**, 6409–6415.
- M. K. Bisai, V. S. V. S. N. Swamy, T. Das, K. Vanka, R. G. Gonnade and S. S. Sen, *Inorg. Chem.*, 2019, **58**, 10536–10542.
- M. K. Bisai, V. S. Ajithkumar, R. G. Gonnade and S. S. Sen, *Organometallics*, 2021, **40**, 2651–2657.
- M. K. Bisai, V. S. V. S. N. Swamy, K. V. Raj, K. Vanka and S. S. Sen, *Inorg. Chem.*, 2021, **60**, 1654–1663.
- M. K. Bisai, T. Das, K. Vanka, R. G. Gonnade and S. S. Sen, *Angew. Chem.*, 2021, **60**, 20706–20710.
- M. K. Bisai, V. Sharma, R. G. Gonnade and S. S. Sen, *Organometallics*, 2021, **40**, 2133–2138.
- K. W. Klinkhammer and W. Schwarz, *Angew. Chem., Int. Ed. Engl.*, 1995, **34**, 1334–1336.
- M. Pait, G. Kundu, S. Tothadi, S. Karak, S. Jain, K. Vanka and S. S. Sen, *Angew. Chem.*, 2019, **58**, 2804–2808.

- 32 G. Kundu, S. De, S. Tothadi, A. Das, D. Koley and S. S. Sen, *Chem. – Eur. J.*, 2019, **25**, 16533–16537.
- 33 G. Kundu, V. S. Ajithkumar, M. K. Bisai, S. Tothadi, T. Das, K. Vanka and S. S. Sen, *Chem. Commun.*, 2021, **57**, 4428–4431.
- 34 V. S. V. S. N. Swamy, N. Parvin, K. V. Raj, K. Vanka and S. S. Sen, *Chem. Commun.*, 2017, **53**, 9850–9853.
- 35 S. S. Sen and H. W. Roesky, *Chem. Commun.*, 2018, **54**, 5046–5057.
- 36 A. Jana, H. W. Roesky, C. Schulzke, A. Döring, T. Beck, A. Pal and R. Herbst-Irmer, *Inorg. Chem.*, 2009, **48**, 193–197.
- 37 M. L. Shegavi and S. K. Bose, *Catal. Sci. Technol.*, 2019, **9**, 3307–3336.
- 38 T. J. Hadlington, M. Hermann, G. Frenking and C. Jones, *J. Am. Chem. Soc.*, 2014, **136**, 3028–3031.
- 39 J. Schneider, C. P. Sindlinger, S. M. Freitag, H. Schubert and L. Wesemann, *Angew. Chem., Int. Ed.*, 2017, **56**, 333–337.
- 40 R. Dasgupta, S. Das, S. Hiwase, S. Pati and S. Khan, *Organometallics*, 2019, **38**, 1429–1435.
- 41 K. Nakaya, S. Takahashi, A. Ishii, K. Boonpalit, P. Surawatanawong and N. Nakata, *Dalton Trans.*, 2021, **50**, 14810–14819.
- 42 A. Jana, H. W. Roesky, C. Schulzke and A. Döring, *Angew. Chem., Int. Ed.*, 2009, **48**, 1106–1109.
- 43 M. K. Bisai, T. Das, K. Vanka and S. S. Sen, *Chem. Commun.*, 2018, **54**, 6843–6846.
- 44 M. K. Bisai, S. Yadav, T. Das, K. Vanka and S. S. Sen, *Chem. Commun.*, 2019, **55**, 11711–11714.
- 45 S. Mandal, P. K. Verma and K. Geetharani, *Chem. Commun.*, 2018, **54**, 13690–13693.